A MODIFIED TRIAXIAL PERMEAMETER FOR PHYSICAL CHARACTERIZATION OF PARAMETERS AFFECTING CONTAMINANT TRANSPORT THROUGH WETLAND DEPOSITS

by

William Bradford Ramsay

B.S. Business Administration, University of Vermont
Burlington, Vermont, 1986

B.S. Civil Engineering, University of Massachusetts
Amherst, Massachusetts, 1994

Submitted to the Department of Civil and Environmental Engineering
in partial fulfillment of the requirements for the degree of

Master of Science in Civil and Environmental Engineering

at the

MASSACHUSETTS INSTITUTE OF TECHNOLOGY
May 1996

© 1996 Massachusetts Institute of Technology
All Rights Reserved

Signature of Author: ...   .
                    Department of Civil and Environmental Engineering, May 24, 1996

Certified by: ...   .
                    Professor Patricia J. Culligan-Hensley, Thesis Co-Supervisor

Certified by: ....
                                        Dr. John T. Co... ·   Thesis Co-Supervisor

Accepted by: ....
                                                    Joseph M. Sussman
......, ... Committee on Graduate Studies

A MODIFIED TRIAXIAL PERMEAMETER FOR PHYSICAL CHARACTERIZATION OF PARAMETERS AFFECTING CONTAMINANT TRANSPORT THROUGH WETLAND DEPOSITS

by

William Bradford Ramsay

ABSTRACT

The Wells G and H Superfund site, located in the Aberjona watershed in Woburn, Massachusetts, has been studied by a number of MIT research groups since 1987. Initial research conducted to characterize the hydraulic properties of the wetland deposits, did not indicate the classical trend linking changes in hydraulic conductivity to changes in total porosity. It was hypothesized, therefore, that hydraulic conductivity was changing in response to changes in the effective porosity of the deposits.

Equipment was developed to enable measurement of hydraulic conductivity, as well as the measurement of breakthrough curves resulting from pulses of a conservative tracer solution, while controlling the flow rate and effective stress acting on a soil specimen. The breakthrough curves (concentration vs. time data) could then be analyzed with a curve fitting package to obtain estimates of the hydrodynamic dispersion coefficient, effective porosity, and the mass transfer coefficient governing the transport of contaminants between the mobile and immobile regions in the soil.

A preliminary set of experiments was performed using two specimens of uniform silica sand, followed by two specimens of the Aberjona wetland deposits. While there were not enough data to confirm the presence or absence of the anticipated trends, the suitability of the equipment for use in obtaining the hydrologic properties of the wetland deposits was established.

Thesis Co-Supervisor: Dr. Patricia J. Culligan-Hensley
Title: Assistant Professor of Civil and Environmental Engineering

Thesis Co-Supervisor: Dr. John T. Germaine
Title: Principle Research Associate in Civil and Environmental Engineering

ACKNOWLEDGMENTS

TABLE OF CONTENTS

List of Tables

List of Figures

CHAPTER 1

INTRODUCTION AND BACKGROUND

1.1 INTRODUCTION

The City of Woburn, Massachusetts, located approximately 10 miles north of Boston (see Figure 1.1), began drawing water from the Aberjona watershed through wells labeled G and H in 1964 and 1967, respectively (Figure 1.2). A high incidence of childhood leukemia in areas served by the wells led to careful analysis of the water, and ultimately their closure in 1979. Two sites within the Aberjona watershed have since been placed on the National Priorities List for remediation under CERCLA, also known as the Superfund.

This project is part of the MIT Superfund Basic Research Program (MSBRP) which has been studying the site and related problems since 1987. This project focuses on the development of equipment and methods that will be used to characterize parameters affecting contaminant transport through the watershed deposits.

1.2 ORGANIZATION

This project has been organized into four chapters. Brief descriptions of the chapters are provided in the following paragraphs.

The remainder of Chapter 1 will provide background information related to this research. It will include a physical description and history of the Aberjona watershed, a discussion of the MIT research effort that is focused on the wetland, the scope and objectives of this thesis, and a literature review. The literature review discusses the equipment, methods, models, and results of previous research, and ends with a discussion of the relevance of results obtained in laboratories to in situ conditions.

Chapter 2 discusses the equipment, procedures, analyses and models used in this research program. Topics include modifications to existing equipment, data acquisition systems, detailed experimental procedures, data reduction spreadsheets, and the computer program used to fit transport parameters to the experimental data.

The results are presented and discussed in Chapter 3. The discussion includes descriptions of the materials tested, the testing conditions, problems encountered, measured and calculated results, and results fitted to the data using the computer package, CXTFIT (Parker and van Genuchten, 1984). The results of experiments conducted using sand and the Aberjona wetland deposits are discussed separately.

Finally, Chapter 4 summarizes the outcome of this research program, and provides recommendations for continued work on the project.

1.3 DESCRIPTION AND HISTORY OF THE ABERJONA WATERSHED

The Aberjona watershed is located approximately 10 miles north of Boston, and encompasses the majority of Winchester and Woburn, as well as portions of Burlington, Lexington, Reading, Stoneham, and Wilmington (see Figure 1.1). The Watershed encompasses approximately 25 square miles, and has a population of approximately 50,000 (MSBRP Project Book). This study concentrated on the wetland in the vicinity of the Wells G and H Superfund site. The locations of Wells G and H are indicated in Figure 1.2.

The Surface waters draining the watershed are shown in Figure 1.3, which also indicates Massachusetts Department of Environmental Protection (DEP) sites as well as the two Superfund sites within the watershed. The largest waterways are the Aberjona River, which flows into the Upper Mystic Lake, and its tributary, the Horn Pond Brook.

A representative geologic section in the vicinity of Wells G and H is presented in Figure 1.4. A buried valley is believed to have been cut by a glacial lobe during the last ice age, and subsequently filled with glacial till and outwash, consisting mainly of fine to

coarse sands and gravels. The valley runs along the length of the Aberjona river, which has subsequently cut its own valley in the sediments (McBrearty, 1995).

In the vicinity of Well G and H, the depth of the till and outwash range from zero, near the east and west banks of the valley, to approximately 120 feet beneath the Aberjona river. Above the till and outwash is a layer 0 to 25 feet thick, consisting of sand, silt, clay or peat. A section along the line containing Wells G and H is provided in Figure 1.5 (Myette et al., 1987).

The Aberjona watershed had been host to many industrial operations, including tanneries, and manufacturing outlets of chemicals, glues, and pesticides. The first tannery was established in 1666, and between 1838 and 1988, over 100 tanneries, finishing companies and rendering operations were operated at 67 sites within the Aberjona watershed (Durant, 1991). In addition, sites such as the Industriplex (the second Superfund site in the watershed), which was established by the Chemical Works Company in 1853, began to appear in the Aberjona Valley in the mid to late 1800s. Many of the operations that were not directly producing leather goods used wastes from the leather industries, from which they extracted grease, glue, and gelatins, while others produced chemicals and supplies to be used by the leather industry. The net effect is that most of the industrial waste found in the watershed was of similar composition, and contained substances related to the leather industry such as Chromium, Copper, Lead, Arsenic, and Zinc.

One of the large attractions of the area to industry was the availability of water, both for use in manufacturing and to carry away the wastes. In 1876, the Massachusetts Board of Health estimated that 7% of the inflow to the Upper Mystic Lake was waste discharge from industries. When municipal sewer systems were placed in service, sediments from industrial discharge began clogging them. Thus, ordinances were passed which led to construction of settling lagoons. One series of lagoons (at the Industriplex site) is estimated to have over 1000 tons of Chromium distributed over a 35 acre area

(Durant, 1991). Groundwater leaching through these sites into the Aberjona River has made it a conduit for the transportation of contaminants.

After the closure of Wells G and H, a pump study was conducted to determine their area of influence and zone of contribution. The resulting cone of depression was 3,000 ft long, 1,700 ft wide, and had a maximum draw-down of 2 feet. Additionally, up to 60% of the water pumped from the wells was drawn through the wetland deposits from the Aberjona River (Myette et al., 1987). Thus, contaminants being transported by the river were drawn into the wetland sediments during the operation of Wells G and H, and may have been consumed by the population that were being served by the wells.

Between 1970 and 1986, the rate of childhood leukemia reported in one neighborhood served by the wells was over 4 times the expected rate based on national statistics. A total of 28 leukemia cases were reported for this 16 year period, 16 of which resulted in death (Latowski, 1994). Residents had complained of foul-tasting and discolored drinking water throughout the late 1960's, but it wasn't until chloroform, trichloroethene, and tetrachloroethene were detected at concentrations above federally acceptable levels that the wells were closed.

When the areas surrounding Wells G and H were determined to be widely contaminated with solvents, plasticizers, pesticides and toxic metals, well water was quickly blamed for the high incidence of leukemia. A highly publicized series of lawsuits ended in 1987, however a plausible cause of the childhood leukemia has never been established (MSBRP Project Book).

1.4 MIT SUPERFUND BASIC RESEARCH PROGRAM AND THIS PROJECT

The focus of the MIT Superfund Basic Research Program can be broken into two broad areas; 1) community assessment, and 2) community cleanup. The Community assessment effort can be further broken down into a) projects relating to identifying the

presence of contaminants and studying their movement within the watershed, and b) measurement of chemicals and their mutational spectra in Aberjona residents.

There are twelve projects involved in the study. The titles of each are listed below and are generally self explanatory. Detailed descriptions can be found in the MSBRP project book.

SECTION 1a.

Project 1: Chemical Transport, Transformation and Human Exposure on the Aberjona Watershed.

Project 2: Fate of Semivolatile Organic Compounds Discharged to Surface Drainage Basins from Superfund Sites.

Project 3: New Approaches for the Physical Characterization of Wetland Deposits with Emphasis on Wells G and H Site. (This thesis forms part of Project 3).

Project 4: Geologic and Geophysical Characterization.

Project 5: Hydrodynamic Controls on Metal Remobilization from Sediments of the Mystic Lakes.

Project 6: Characterizing the Groundwater Contamination at a Heterogeneous Field Site: the Aberjona River Watershed.

SECTION 1b

Project 7: Human Cell Culture Studies of Mutagens on the Aberjona Basin.

Project 8: Mutational Spectrum in Human Blood Samples from the Aberjona Communities.

Project 9: Proteins and DNA - New Methods of Adduct Detection.

SECTION 2

Project 10: Human Cell Mutagen Formation During the Thermal Destruction of Hazardous Wastes.

Project 11: Oxidation and Hydrolysis of Hazardous Chemicals in Subcritical and Supercritical Water.

Project 12: Fundamental Study of Thermal Decontamination of Soils.

As indicated, this research is one phase of Project 3. Previous studies included a determination of the hydraulic conductivities of the wetland sediments (discussed in Section 1.6 below) and the development of a piezocone penetrometer that was used to map the subsurface geology in the vicinity of Wells G and H, in order to obtain a better understanding of the probable paths between the chemical sources and public water supplies.

This research effort focused on developing experimental technology to estimate contaminant transport parameters for deposits present in the wetland. It was the first phase in a project that is intended to ultimately yield a model which will (a) relate the hydraulic properties of the peat to vertical effective stress, (b) relate the physical mechanisms of contaminant transport to vertical effective stress, and (c) describe the behavior of a weakly sorbing ion under changing hydraulic conditions.

The motivation for the overall project is to obtain accurate predictions for contaminant flow through the wetland deposits during, and subsequent to, the operation of the wells. As the wells drew water through the deposits, the induced suction pressures would have increased the effective stress in the deposits, thereby leading to consolidation and changes in the subsurface hydraulics of the wetland system. When the wells were shut down, the excess effective stresses would have dissipated as the pore pressures increased to their equilibrium levels. Thus, the deposits would most likely have experienced an elastic rebound, again altering the subsurface hydraulics of the system (Culligan-Hensley, 1994). Thus, in order to be representative of the conditions operating in the field at the time of pumping, studies of the Aberjona deposits must consider linking changes in the soil effective stress to the subsurface flow conditions.

17

1.5 THESIS SCOPE AND OBJECTIVES

The objective of this work was to develop equipment and methods that would allow determination of the hydraulic characteristics of a sample of wetland sediment under varying effective stresses and flow conditions. The parameters being studied for each specimen include hydraulic conductivity, hydraulic porosity, the macroscopic dispersion coefficient for chloride, and the inter-region transport coefficient. These parameters will be discussed in more detail in the following section. This work will provide the basis for an extensive series of experiments aimed at characterizing representative samples of the different layers and types of soils existing at the Wells G and H study area.

The scope of this project was to develop the physical equipment and methods, complete a series of proof tests on sand, and to obtain some preliminary data on the Aberjona deposits based on existing samples which were obtained during earlier projects (from Borings 1, 2, and 3, located as indicated in Figure 1.6). The equipment development included modifying a standard triaxial permeameter to enable continuous measurements of effluent concentrations, and obtaining better control over flow conditions through alterations to the standard MIT volume change device. The work also included the development of software for data acquisition, and the development of circuitry to perform conductivity measurements with multiple probes (conductivity is an indicator of ion concentration).

1.6 LITERATURE REVIEW

1.6.1 Introduction

In order to understand the processes by which contaminant transport occurred in the Aberjona Watershed, a study of the physical and chemical hydrogeology of the wetland deposits was proposed based on laboratory column testing (Culligan-Hensley, 1994). Laboratory column tests are sometimes used to evaluate and model the flow of

water and contaminants through soil specimens. The flow of water through a porous

media is generally described by Darcy's equation, and is a function of the hydraulic

gradient and hydraulic conductivity of the media. Contaminant transport is often

described by the advection-dispersion equation, which assumes that transport is a function

of advective flow, hydrodynamic dispersion (defined by Daniel (1993) to include diffusion

and mechanical dispersion), and retardation. To determine the hydraulic conductivity of a

soil, a known quantity of water is usually passed through a column of soil of known

diameter, under a known hydraulic gradient. The time it takes for a given quantity of

water to flow through the column is measured, and the hydraulic conductivity of the

specimen is calculated using the Darcy equation mentioned above. The parameters used in

the advection-dispersion equation are often obtained by introducing a conservative tracer

at the inlet of a column of soil, and monitoring changes in the concentration of the effluent

with time. The resulting breakthrough curve is then fitted to the transport parameters

using one of a variety of models, such as the CXTFIT code (Parker and van Genuchten,

1984) that was used for this research.

1.6.2 Equipment

1.6.2.1 Flexible Versus Rigid Wall Columns

The column is the portion of the apparatus that contains the soil specimen, and is

one of two general types; rigid wall or flexible wall (shown in Figures 1.7 and 1.8,

respectively). The rigid-wall column generally consists of a metal or plastic cylinder

clamped between two end caps. The cylinder is often a compaction mold, which facilitates

the testing of compacted soils such as those used in a soil-liner system for a landfill. Three

disadvantages of rigid columns are that (i) stresses can not be applied in any other than the

axial direction, (ii) it is difficult to determine whether or not the specimen is saturated

prior to testing, and (iii) there is the potential for side-wall leakage. For example, if a

permeant which causes the specimen to shrink is used in the experiment, there is the

potential for preferential flow paths at the side walls, or through tension cracks: this would result in the measurement of artificially large values of hydraulic conductivity. However, tests in rigid columns are generally easier to set up and are, therefore, generally less costly than flexible wall tests.

Flexible-wall tests are usually performed in triaxial cells similar to those commonly used in soil strength testing. They generally consist of a cylindrical soil specimen enclosed in a latex, butyl, or neoprene rubber membrane, which is, in turn, submerged in a pressurized cell fluid such as distilled water or silicon oil. Control of the confining (cell) pressure allows approximate replication of the in situ state of stress in the soil. If the drainage valves at the top and bottom of the soil column are closed, the degree of saturation in the specimen can be determined by measuring the response of the pore pressure in the specimen to changes in applied cell pressure. Assuming incompressible soil particles and complete saturation, the ratio of the change in pore pressure to the change in cell pressure should be approximately one (Lambe et al., 1969). If the permeant causes the specimen to shrink or swell, the pressurized cell fluid will ensure continued contact between the membrane and soil. Constant applied cell pressures also reduce the extent of tension cracks under shrinking conditions. The flexible membrane facilitates the testing of "undisturbed" specimens, because they can adapt to slightly irregular surfaces which are present even in the most carefully trimmed specimens. Another advantage includes the ability to monitor changes in the porosity of the specimen during testing, by measuring the flow of the cell fluid in response to changes in the applied effective stress.

A disadvantage of the flexible-wall system that the effective stress must be coordinated with the gradient to maintain contact between the membrane and soil. For example, suppose a clay specimen (7.62 cm in length) was to be tested, a back-pressure of 4 ksc was to be applied to ensure saturation, and a gradient of 100 needed to be introduced in order to complete the test within a reasonable period of time. At the influent end of the specimen, the gradient would require a pressure of 4.76 ksc. To prevent

"ballooning" of the membrane, the minimum cell pressure would also have to be 4.76 ksc. Therefore, the down-gradient end of the specimen (where the pressure would be 4 ksc) must be exposed to a minimum effective stress of 0.76 ksc. In order to reduce the applied effective stress, the gradient must also be reduced, which may require impractical test durations for some low-permeability soils (Daniel et al., 1985).

Thus, there is not a single best column type. The choice as to whether a fixed or flexible wall column should be used depends on the soil type and the desired test conditions.

1.6.2.2 FLOW CONTROL SYSTEMS

There are two types of flow-control systems commonly used in column testing; gradient control, and flow rate control. Gradient control usually consists of a constant or falling head system in which the flow is measured. With a flow rate system, the volumetric discharge is controlled by a constant-rate pump, and the gradient is measured, usually with pressure transducers.

Gradient controlled systems (see Figures 1.9 and 1.10 for diagrams of constant and variable head systems, respectively) have the advantage that they are simple, and therefore inexpensive to set up. They are satisfactory when the hydraulic conductivity of the soil allows measurable flow rates at relatively low gradients. However, with low permeability soils, high gradients must be applied in order to obtain measurable flow within reasonable time periods. In addition to the problems mentioned above, high gradients (which are not common in natural ground water) can cause consolidation of the soil specimen due to seepage forces, and thus change the hydraulic conductivity of the soil. High gradients can also cause migration of particles within a specimen, which could further change the flow characteristics of the specimen. On the other hand, very low gradients applied to specimens of low hydraulic conductivity may require extended testing periods (on the order of months to years). Within that time frame, bacterial growth and fabric changes

21

due to changes in the pore solution chemistry can also alter the flow properties of the specimen (Olsen et al., 1985).

The flow rate system (see diagram in Figure 1.11) eliminates many of the problems associated with gradient driven systems. Assuming saturation of the system, steady flow, even at low gradients, is established quickly. Olsen et al. (1985) report times required for equilibrium ranging from less than a minute for sand, to approximately 200 minutes for a silty clay specimen. Since the flow rate is controlled, the head, and therefore the hydraulic conductivity, can be measured as soon as steady flow is established. Thus, with shorter times to steady state, lower gradients can be used, better simulating in situ conditions. Furthermore, lower gradients permit lower effective stresses in flexible wall systems.

1.6.2.3 Measurement of Breakthrough Curves

Chemical transport parameters are determined using columns similar to those described above. Measurements of hydraulic porosities, hydrodynamic dispersion coefficients, inter-region transfer coefficients, and retardation factors (discussed below, together with the computer model) are usually accomplished by fitting theoretical curves of concentration, as a function of time and distance along a column, to measured values obtained in a column test (Shackelford, 1994). If the distance, x, along the column is equal to the column length, L, the curves are known as break-through curves. Although it is possible to measure concentrations within the soil column (x < L), this approach is often more complicated than measuring the concentration of the effluent, and therefore not commonly done. This section will first discuss some of the experimental methods used to obtain breakthrough curves, and then one of the models used to fit theoretical curves to the experimental data.

There are two different concentrations commonly measured, namely, flux averaged and volume averaged. The flux averaged concentration is the mass passing through a given area over some time interval. The volume averaged is the average concentration in

the pore water of a specified volume of the specimen at a specific point in time. The effluent breakthrough curve, which is being considered here, is, by definition, a flux averaged concentration, being measured at $x = L$. Breakthrough curves can be measured either for an injected pulse of solute, or for a continuous injection. For an injected pulse analysis, a finite amount of a tracer solution is introduced at the influent end of the specimen, and flushed through with distilled water. An injected pulse yields a "bell shaped" breakthrough curve of concentration vs. time. In a continuous injection experiment, the tracer is continuously injected at the influent end of the specimen, and the resulting curve is "S shaped." Figure 1.12 shows a comparison of the two types of curves. In Figure 1.12, time has been normalized and is expressed as pore volumes of flow. Similarly, the concentration of the tracer has been normalized with respect to the concentration initially injected. The disadvantage of a continuous injection system is that the concentration of the influent must be held constant for the duration of the test, whereas for the pulse-type experiment the concentration of the influent must be held constant only for the duration of the pulse (Shackelford, 1994). A diagram of an experimental apparatus used for the pulse-type column tracer experiment conducted by Li et al. (1994) is given in Figure 1.13. This happens to be a flow-controlled experiment conducted in a rigid-wall column. Although not shown, one can imagine two beakers connected to the pump by a three-way valve. Water would be pumped through the specimen until steady flow was obtained, the valve would then be redirected to the tracer solution for the duration of the pulse, after which it would be returned to the beaker of water for the remainder of the experiment. Li et al. (1994) collected the effluent and used an auto-fraction collector to specimen the effluent over a time period, δt. The value of the sampling time was taken to be the middle of the sampling period. The concentration of the tracer in each specimen was obtained using an ion analyzer.

An alternative system used by Taylor et al. (1987) is shown in Figure 1.14. They used a constant head system, a rigid-wall column, and a flow-through system to measure

the changes in concentration continuously with time. Although this setup is designed for continuous injection, a second, identical, influent system could be added with a three-way valve at the inlet of the specimen to accommodate a pulse-type test.

In either of the systems described here, the rigid columns could be replaced with flexible-wall columns. Additionally, the electrical conductivity of the effluent could be measured, either continuously with a flow-through device, or using a fraction collector together with a bench-top conductivity probe, and related to the concentration in order to obtain the break-through curve (Head, 1983).

There are two types of probes commonly used to measure the conductivity of a medium in the laboratory; two-pin and four-pin. With a two-pin probe, a known, constant, alternating current is usually forced through the circuit, the voltage across the pins is measured, and the resistance of the solution can be directly calculated (assuming a geometric probe constant of one). Long-term stability problems with this type of probe often occur when the resistances of the probe wires change due to oxidation, loss of platinum black coating, etc.

The four-pin probe was developed to overcome the long term stability issue. A schematic of a four-pin system is provided in Figure 1.15. An alternating current is applied to the system, and the voltage across the inner two pins (V_m), as well as the voltage (V_r) across the reference resistor (with known resistance R), is measured. Since the current, I, is constant around the circuit, the resistance of the solution (R_s) is proportional to $V_m R / V_r$. In this system, there is a constant of proportionality which is based on the probe geometry that can be calibrated for. In theory, problems with stability are eliminated because voltage is a high impedance measurement, thus, small changes in the resistance of the inner two pins do not affect the voltage measurement across them.

Retardation factors are an indicator of the ability of a given soil to adsorb a given solute during transport. Retardation, usually indicated by tailing in a breakthrough curve, is generally defined as the ratio of the advective seepage velocity of a non-sorbing solution

24

to the average velocity of the center of mass of the sorbing chemical species being studied. Instead of using a conservative tracer in the above systems, the chemical species in question is used as the tracer, and an appropriate detection system is used to monitor the changes in concentration with time.

1.6.3 Model

One model used to fit measured to theoretical breakthrough curves is CXTFIT, developed by Parker & van Genuchten (1984). CXTFIT is a computer program, written in FORTRAN, that uses a nonlinear least-squares inversion method to identify several parameters in a number of one-dimensional theoretical transport models. One of the models is a one region model (ORM) based on the advection-dispersion equation, and includes terms to account for linear equilibrium adsorption, zero-order production, and/or first order decay. Another model, which they call a "two-site/two-region non-equilibrium model," (TRM) does not consider production or decay. CXTFIT also contains models for the evaluation of field tracer studies that are beyond the scope of this paper.

The TRM was the primary model used for the purpose of this research, however the ORM was also used to fit a curve to the data for comparison purposes. The TRM is an extension of the ORM, thus the following discussion will be limited to the two-region, two-site model. "Two-site" refers to the different constituents of a soil specimen for which sorption occurs at varying rates, for example the soil minerals and organic matter. At one site, adsorption is assumed to be instantaneous ("type-1" sites), and at the other, adsorption is assumed to be time dependent ("type-2" sites).

"Two-region" refers to mobile and immobile regions of flow. Mobile regions are pore spaces where there is actual flow of fluid, and advective-dispersive transport takes place. In immobile regions, the pore fluids are stagnant, and transport is assumed to be diffusion-limited (Parker and van Genuchten, 1984).

The governing equations for this model as given by Parker and van Genuchten are:

$$(\Theta_m + f\rho k)\frac{\partial c_m}{\partial t} + [\Theta_{im} + (1\text{-}f)\rho k]\frac{\partial c_{im}}{\partial t} = \Theta_m D_m \frac{\partial^2 c_m}{\partial x^2} - q\frac{\partial c_m}{\partial x} \qquad (1a)$$

and

$$[\Theta_{im} + (1\text{-}f)\rho f k]\frac{\partial c_{im}}{\partial t} = \alpha^*(c_m - c_{im}) \qquad (1b)$$

where Θ_m and Θ_{im} are the volumetric water contents (volume of water / total volume of porous medium) in the mobile and immobile regions, respectively (such that $\Theta = \Theta_m + \Theta_{im}$), f is the fraction of sorption sites that equilibrate with the mobile liquid phase, ρ is the bulk density of the porous medium (mass of solids / total volume), k is an empirical solid-liquid partition coefficient, c_m and c_{im} are the resident concentrations in the mobile and immobile regions, respectively, D_m is the hydrodynamic dispersion coefficient for the mobile region, q is the liquid flux density ($= v_s\Theta_m$, where v_s is the seepage (pore) velocity $= q/n$) and α^* is the first order rate constant that governs the rate for solute transfer between the mobile and immobile regions.

When a conservative tracer is used, as was the case for this research, k approaches zero, and Equations 1a and 1b can be simplified to

$$\Theta_m \frac{\partial c_m}{\partial t} + \Theta_{im}\frac{\partial c_{im}}{\partial t} = \Theta_m D_m \frac{\partial^2 c_m}{\partial x^2} - q\frac{\partial c_m}{\partial x} \qquad (2a)$$

and

$$\Theta_{im}\frac{\partial c_{im}}{\partial t} = \alpha^*(c_m - c_{im}). \qquad (2b)$$

In dimensionless form, Equations 2a and 2b become

$$\frac{\partial C_m}{\partial T} + \frac{1-\beta}{\beta} \frac{\partial C_{im}}{\partial T} = \frac{1}{P} \frac{\partial^2 C_m}{\partial X^2} - \frac{\partial C_m}{\partial X} \tag{3a}$$

and

$$\frac{1-\beta}{\beta} \frac{\partial C_{im}}{\partial T} = \omega (C_m - C_{im}) \tag{3b}$$

where C is the normalized concentration (c/c_0) in either the mobile (C_m) or immobile (C_{im}) regions, T is dimensionless time (pore volumes of flow $= v_s t/L$), β is the ratio of mobile to total porosity (Θ_m/Θ), P is the Peclet number ($v_s L/D$), X is the normalized distance (x/L), and ω is the dimensionless mass transfer coefficient ($\alpha^* L/q$) (Li et al.).

In using the two-site/two-region model, the data points for the break-through curve are entered as part of an input file along with a number of program-control parameters, such as the number of observations, and the number of desired iterations. The seepage velocity, dispersion coefficient, retardation coefficient, duration of pulse, ratio of mobile region to total pore space, and a normalized coefficient describing transport between the mobile and immobile regions can all either be fitted to the data, or fixed if their values are known. Variables that are being fitted can be confined between reasonable upper and lower limits, if such limits are also known in advance. Initial estimates of the variables to be fitted are also required in the input file. For this research, the retardation factor was fixed at unity, and the remaining variables were fit.

The output file produced by the program contains a summary of the fixed and fitted variable values, a statistical evaluation of the fitted values, and a table of actual and fitted data which can be plotted for comparison.

Li et al. provided insight as to the behavior of α in their study of the mechanisms controlling mass transfer in locally stratified soils. To understand their conceptual model,

refer to Figure 1.16, which is reproduced from their paper, and applies to stratified soils with constant hydraulic conductivity contrast between the layers. If the velocity difference between the two layers is large (as shown in Figure 1.16.a), the plumes will separate, as shown, and the resulting concentration gradients will cause inter-region diffusion to dominate mass transfer. In this case, Li et al. indicate that the mass transfer coefficient, α, should scale as D_T/h^2, where D_T is the inter-region diffusion coefficient, and h is the thickness of the stratified layers). If, on the other hand, the velocity contrast between the regions is small (as shown in Figure 1.16.b), the plumes will move together, there will not be a large concentration gradient between the regions, and longitudinal dispersion (due to longitudinal interaction) will dominate inter-region mass transfer. Under these conditions Li et al. theorize that α should scale as V^2/D. For the case where the grain Peclet number (seepage velocity * grain size/molecular diffusion coefficient) is less than unity, Li et al. observed that D did not change linearly with velocity, and α scaled as V^2. For the case where the grain Peclet number was greater than unity, D and α were both observed to scale linearly with velocity. Their work also indicated that β depends on soil structure, and should be approximately constant for a given soil.

1.6.4 Previous Studies of Hydraulic Characteristics of Peat

There have been few studies of the hydraulic characteristics of wetland deposits, and thus the migration of water and contaminants in these soils is poorly understood (Hoag and Price, Price and Woo). The hydraulic conductivity of peats will be discussed first, based on studies by Bialon (1994) and Boelter (1964). This will be followed by a discussion of contaminant transport in peats, which is based on studies by Hoag and Price (1995), Loxham and Burghardt (1983), and Price and Woo (1986).

1.6.4.1 Hydraulic Conductivity of Peats

Boelter (1964) performed a number of field and laboratory experiments to determine the hydraulic conductivities of eight different peats from northern Minnesota. He reported that field-measured values were consistently lower than lab-measured values, but did not offer an explanation. He used a rigid-wall system in his laboratory experiments, which, as discussed above, could result in preferential flow paths along the side walls, thus possibly explaining the higher laboratory values. For relatively undecomposed moss found near the soil surface, he reported hydraulic conductivity values in the range of 6×10^{-4} cm/sec to 4×10^{-2} cm/sec. For more dense, highly decomposed materials, he reported values as low as 8×10^{-6} cm/s.

Bialon (1995) completed an extensive study, based primarily on constant rate of strain (CRS) consolidation testing, to characterize the hydraulic conductivities of the materials at the Wells G and H Superfund site. The results of his testing program are summarized in Table 1.1 and 1.2 for Borings 1 and 2, respectively (the locations of these borings are mapped in Figure 1.6). He reported hydraulic conductivities ranging from 3×10^{-4} cm/sec to 2×10^{-6} cm/s. For the sedge materials (which were tested for this thesis), he reported values ranging from 9×10^{-6} to 2×10^{-5} cm/sec.

Bialon also performed a number of analyses aimed at enabling him to predict the insitu hydraulic conductivities of the wetland deposits. Although he reported that C_k, the ratio of the change in void ratio to change in log of hydraulic conductivity, varied as the initial void ratio and organic content, he found no direct relationship between hydraulic conductivity and either void ratio or organic content. The lack of correlation led him to develop and test three different models, all of which attempted to relate void ratio, organic content, and hydraulic conductivity. These models are described in sequence below.

In the first model, Bialon found a void ratio that was common (but corresponded to different hydraulic conductivities for different specimens) to every specimen within a soil strata, and attempted to correlate hydraulic conductivity and organic content at that

void ratio. In the second model, he found a hydraulic conductivity that was common (but corresponded to different void ratios for different specimens) to every specimen within a soil strata, and attempted to correlate void ratio and organic content at that hydraulic conductivity. For the third model, Bialon assumed that some portion of the pore space was not taking part in the flow through the specimens, and attributed the dead space to pore water being physically bound to organics, and thus immobile. He took a common hydraulic conductivity for the specimens within a strata, assumed an effective void ratio of 1.5, and calculated the volume of "bound water" based on the measured void ratios, measured organic contents, and assumed unit weights of both mineral and organic solids. The bound water was expressed as a multiple (X) of the volume of organics, and correlated to organic content. Bialon reported values of X ranging from 1.9 to 2.3 for sedge specimens with organic contents of 56% and 73%, respectively.

Different models were found to better predict the hydraulic conductivities of specimens from different strata, thus none of the three models were selected over the others as having better universal predictive capabilities. Additionally, there was no consistent trend observed with respect to over or under predicting the measured values. The estimated values he obtained were generally within one order of magnitude of the experimental hydraulic conductivities.

1.6.4.2 Transport of Contaminants in Peat

Loxham (1983) used computer aided image analysis to study sections of peat specimens, which he described to be a "low moor, sedge peat," and concluded that about 15% of the volume of those specimens was taking part in pore fluid movement. Additionally, the specimens had porosities of approximately 85%, hence, approximately 18% of the void space ($\beta \approx 0.18$) was taking part in the flow. Based on these data, he defined an active zone, in which solute migration occurs by advection, dispersion, or molecular diffusion, and an inactive zone, in which transport could only occur by

molecular diffusion. He further assumed that transfer between the two zones occurred only by molecular diffusion across the interface between them. A schematic of his assumed pore-space geometry is reproduced from his paper and presented in Figure 1.17. Using this geometry, and the assumption that adsorption is both linear and reversible in both zones, Loxham presented the following equations for the active and inactive zones, respectively:

$$\frac{\partial C}{\partial t} = \frac{1}{R} \left(-q n_a \frac{\partial C}{\partial z} + D \frac{\partial^2 C}{\partial z^2} + 2 \frac{\bar{D}}{n_a} \frac{\partial C}{\partial x} \Big|_{x=0} \right) \qquad (4a)$$

and

$$\frac{\partial C}{\partial t} = \frac{1}{r} \left(\bar{D} \frac{\partial^2 C}{\partial x^2} \right) \qquad (4b)$$

where R and r are the retardation factors for the active and inactive zones, respectively, C the solute concentration, n_a the active porosity, q the rate of fluid flow divided by the area of the specimen, D the hydrodynamic dispersion coefficient, $\bar{D}$ the in-pore molecular diffusion coefficient, x the distance perpendicular to flow from the zone interface, z the distance in the direction of advective flow, and t the time coordinate.

Loxham ran column tracer experiments to test the model, the results of which are given in Figure 1.18. The best fit occurred with a ratio of active zone to total volume of 0.14, and an in-pore molecular diffusion coefficient of 3.7×10^{-6}. He concludes (as Figure 1.18 indicates) that the model results in a better fit than the advection-dispersion equation without consideration of the structure of peat (i.e. active and inactive zones), which he refers to in the figure as Equation 8.

Price and Woo ran a series of column tracer tests through poorly decomposed mosses and sedges, and used the solution to the one-dimensional advection-dispersion

31

equation, with retardation, to fit a curve to their data. The equation used as a model in their study was:

$$\frac{C}{C_o} = \frac{1}{2}[erfc\,(\frac{x-\bar{v}'t}{2\,(D't)^{-1/2}}) + exp\,(\frac{\bar{v}'t}{D'})\,erfc\,(\frac{x+\bar{v}'t}{2\,(D't)^{-1/2}})] \tag{5}$$

where $\bar{v}' = \bar{v}/R$ with $\bar{v}$ being the linear velocity (seepage velocity, calculated using the active porosity, which was measured from thin sections), R the retardation coefficient, D' = D/R, and *erfc* is the complementary error function.

To determine whether the chloride tracer was sorbing onto the peat, they conducted a series of batch tests in which the chloride solution was mixed with peat specimens. The mixture was allowed to equilibrate for 24 hours, before a chloride analysis was performed on the solution. After the equilibration period, no change in concentration could be detected, thus it was concluded that none of the chloride ions had sorbed to the solid particles.

They ran two tracer tests, one at a fast rate ($\bar{v}$ = 0.043 cm/sec) and one at a slow rate ($\bar{v}$ = 0.0081 cm/sec). They got the best fit using retardation coefficients of 1.6 and 1.5 for the slow and fast tests, respectively. Since there was no sorption, but clear evidence of tailing (or retardation of mass transport), they concluded that the retardation was due to the solute diffusing into and out of the inactive pore spaces of the specimen. With faster flow, there was less time for diffusive flow, hence the lower retardation coefficient. Their results are reproduced as Figure 1.19, and show that better fits are obtained when a retardation factor other than unity is assumed.

Hoag and Price (1995) conducted a field solute transport experiment at a Newfoundland blanket bog, in which they released 200 liters of a 1.4×10^5 mg/l solution of NaCl into the well instrumented wetland area. Although they didn't explicitly describe the subsurface materials, they did report that the primary species covering the surface of

the test area was Sphagnum Hummocks. The solution was released slowly enough (1 liter/min) so that it seeped into the ground rather than running over the surface, yet quickly enough so that they considered it an instantaneous source. The plume was monitored over a 30 day period.

Hoag and Price reported that the average groundwater flow was 2.2 times faster than movement of the front of the plume (thus implying an "effective retardation coefficient" of 2.2). They state that the majority of the flow took place in the upper 0.45 m of the deposits (they call the upper, hydrologically active region the *acrotelm*). Thus the retardation was due both to diffusion into and out of the immobile pore space within the acrotelm, as well as diffusion into and out of the *catotelm*, (lower region where the material is more highly decomposed, the water storage approximately constant, and the average hydraulic conductivity can be 5 orders of magnitude lower than that for the acrotelm). They also measured temporary decreases in concentration during rain events. They hypothesized that mixing due to the rain may have remobilized the solute that had diffused into the immobile zone, thus allowing an increase to the measured pre-rain concentrations. Finally, they noted that evaporation did not have an appreciable effect on the solute concentration, which was attributed to the small flux derived from the unsaturated zone.

1.6.5 The Correlation Between Laboratory Data and In Situ Conditions

The correlation between laboratory and in situ estimates of hydraulic transport parameters is often poor. Olson and Daniel (1981) cite over 60 comparisons of field and laboratory values of hydraulic conductivity. They report ratios of field to laboratory hydraulic conductivities ranging from 0.3 to 46,000, however 90 percent fall in the range from 0.38 to 64.0. Similarly, Taylor et al. (1987) report that "Field measurements of dispersivity have generally produced results that are three to four orders of magnitude greater than laboratory tests." However, Taylor et al. also indicate that with careful

sampling they were able to obtain laboratory values of dispersivity that were within one order of magnitude of the in situ values. The consistent difference between field values and those obtained in the laboratory are generally attributed to scale effects. As Taylor et al. state, it is not possible to obtain a small scale specimen for laboratory testing that is statistically representative of the in situ porous medium. As discussed above, Price and Woo also attribute differences between lab and field-scale experiments to precipitation and evaporation during test periods, and to large scale variabilities in hydraulic conductivities and dispersivities which are characteristic of natural systems.

Range of Various Properties and Test Results for the Wetland Deposits
for Boring 1

Physical Properties and Organic Content

Layer	Depth (cm)	Void Ratio	Moisture Content (%)	Unit Weight (gm/cm^3)	Organic Content (%)
Typha Peat	50-100	6.48-9.65	419-699	1.00-1.10	63-96
Sedge Peat	100-140	13.73	870	.96 ·	83
Red Woody Peat	140-175	11.10-13.00	765-875	0.98-1.04	73-90
Diatomaceous Earth	175-250	1.31-9.51	75-450	1.02-1.48	4-36

Engineering Properties

Layer	Depth (cm)	Hydraulic Conductivity (cm/sec)	Ck	Compressibility Parameters	
				RR	CR
Typha Peat	50-100	5.2E-06 to 2.0E-05	1.04-1.67	0.013-0.029	0.301-0.98
Sedge Peat	100-140	2.0E-05	*****	*****	0.466
Red Woody Peat	140-175	6.0E-06 to 8.5E-05	1.51-1.86	0.027-0.033	0.323-0.649
Diatomaceous Earth	175-250	2.0E-06 to 1.7E-04	0.23-3.38	0.002-0.016	0.224-0.412

Table 1.1: Engineering and Physical Properties of Aberjona Deposits; Boring 1 (Bialon, 1995)

Range of Various Properties and Test Results for the Wetland Deposits
for Boring 2

Physical Properties and Organic Content

Layer	Depth (cm)	Void Ratio	Moisture Content (%)	Unit Weight (gm/cm³)	Organic Content (%)
Live Root Mat	0-30	3.46-6.00	330-475	1.08-1.17	35-53
Typha Peat	30-65	4.67-6.00	300-430	1.03-1.06	51-61
Sedge Peat	65-100	6.48-10.44	481-800	0.97-1.04	56-81
Red Woody Peat	100-140	5.42-9.45	350-645	0.95-1.03	56-81

Engineering Properties

Layer	Depth (cm)	Hydraulic Conductivity (cm/sec)	Ck	Compressibility Parameters	
				RR	CR
Live Root Mat	0-30	6.0E-05 to 1.0E-04	0.51-0.96	0.112	0.275-0.361
Typha Peat	30-65	8.5E-06 to 2.0E-05	0.92-1.29	0.064-0.096	0.313-0.347
Sedge Peat	65-100	8.0E-06 to 8.9E-05	1.33-1.79	*****	0.302-0.391
Red Woody Peat	100-140	8.5E-05 to 3.1E-04	0.87-1.63	0.045-0.086	0.429-0.619

Table 1.2:   Engineering and Physical Properties of Aberjona Deposits; Boring 2 (Bialon, 1995)

36
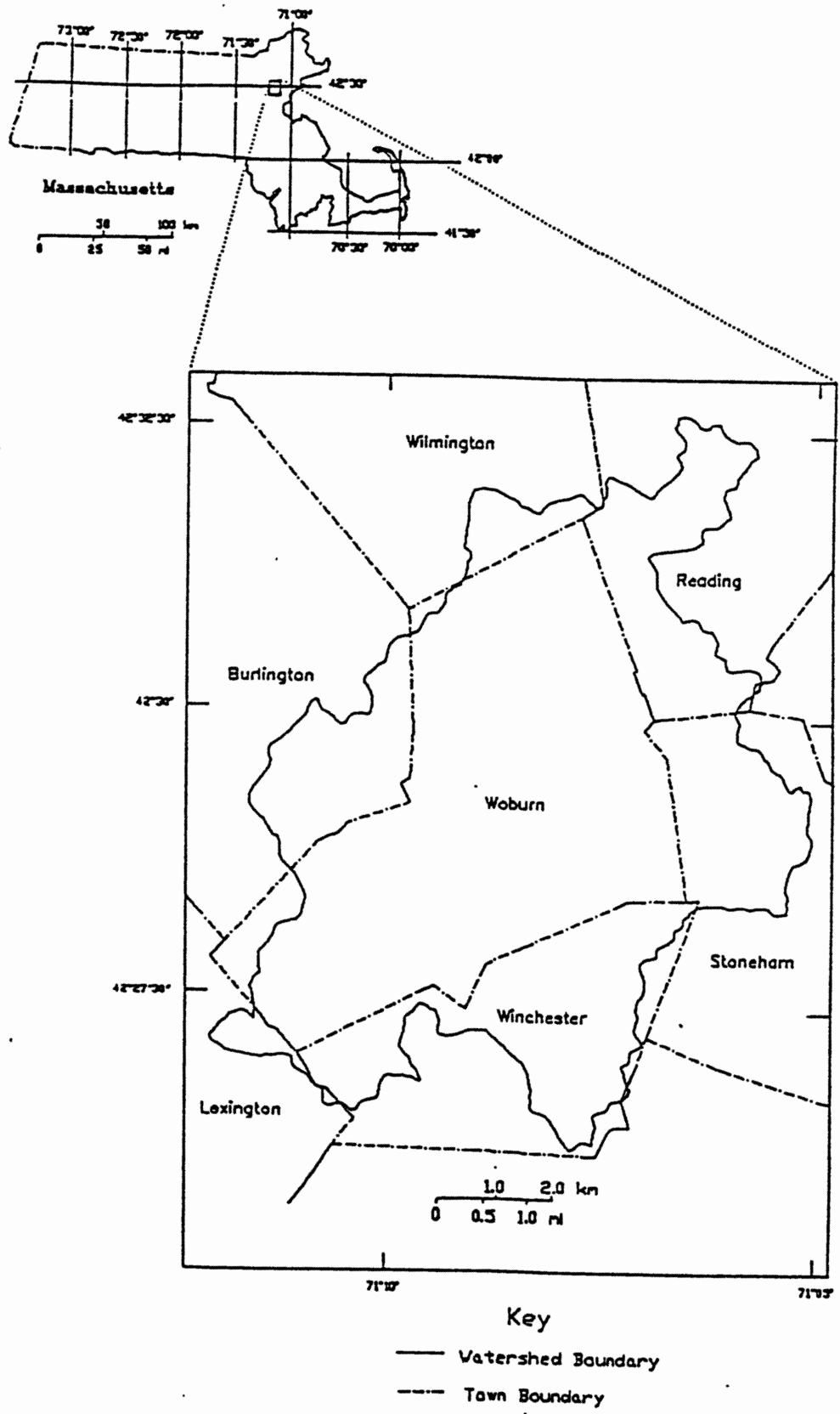
Figure 1.1   Location of the Aberjona Watershed (Durant, 1991)
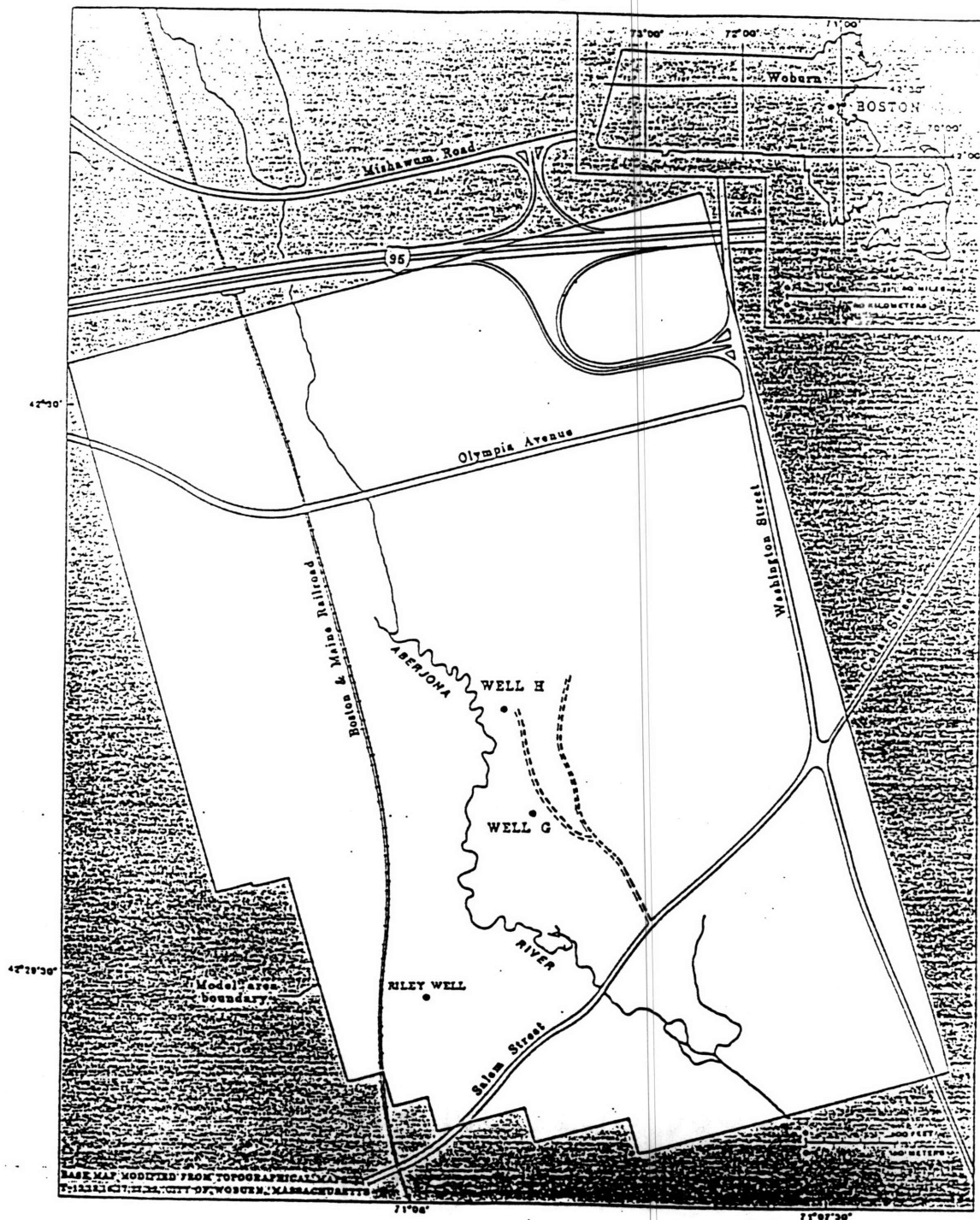
Figure 1.2   Location of Wells G and H (Myette et al., 1987)
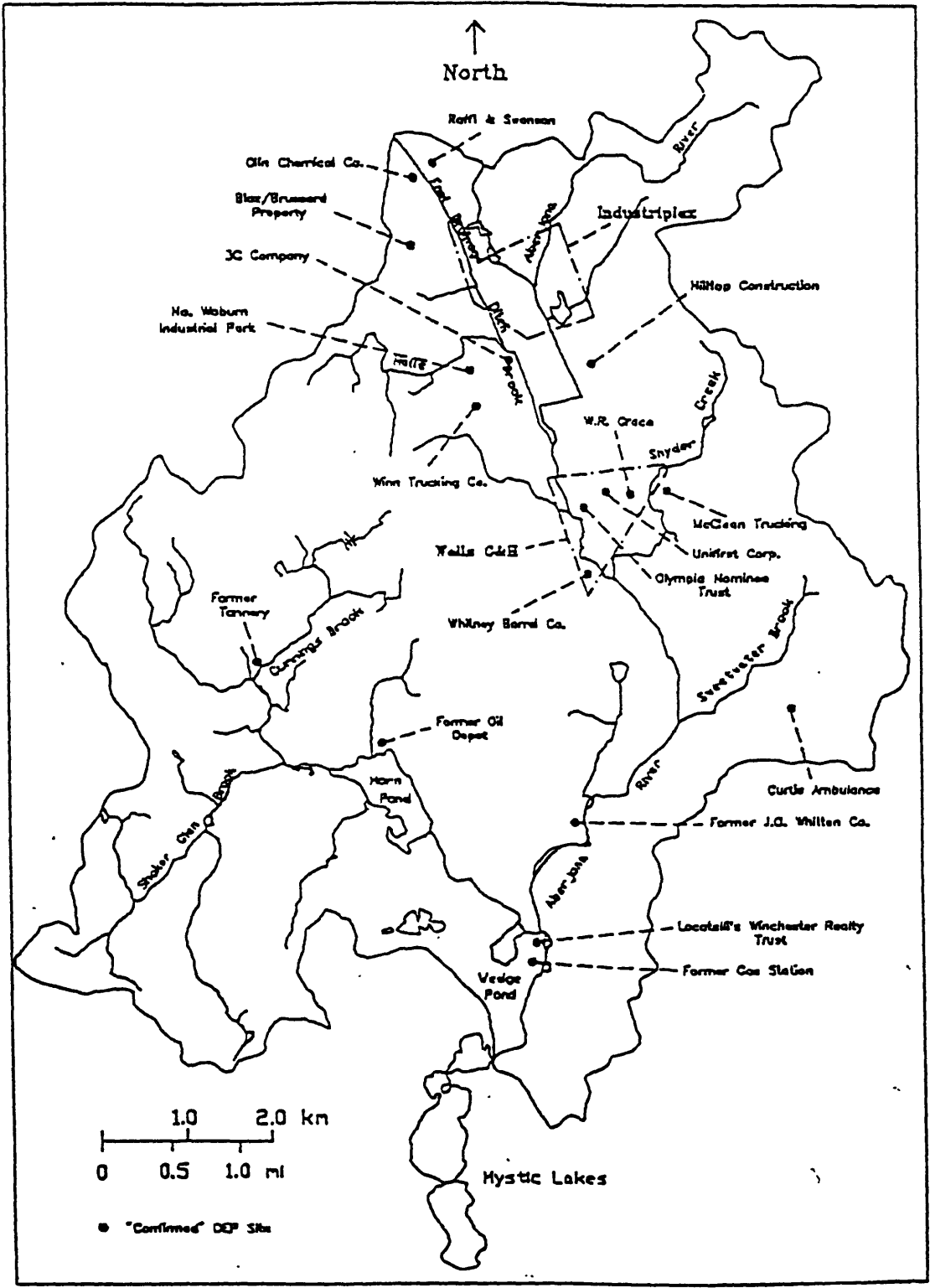
Figure 1.3   Map of Surface Waters in the Aberjona Watershed (Durant, 1991)
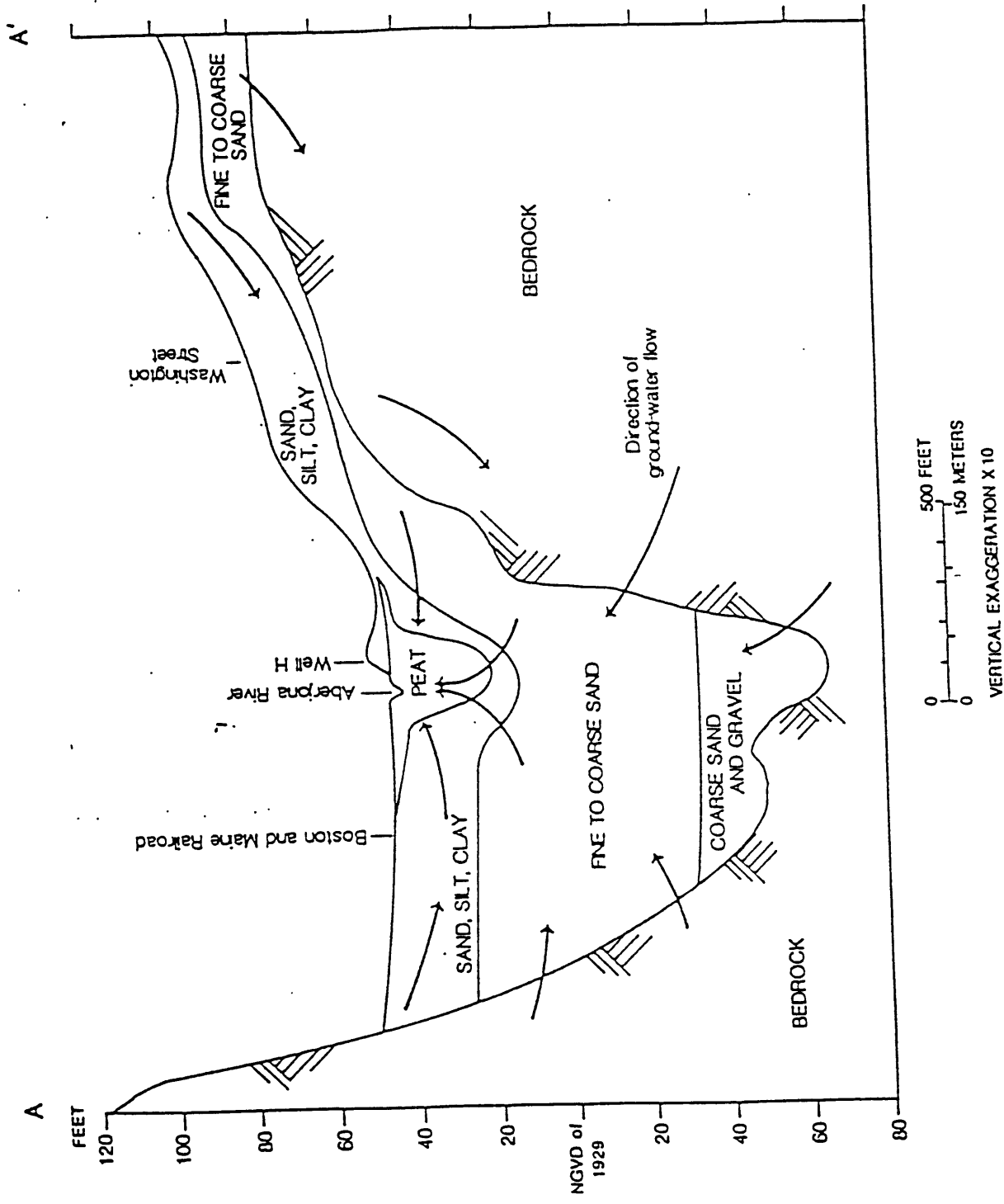
Figure 1.4   Geologic Section at Wells G and H (Myette et al., 1987)

40
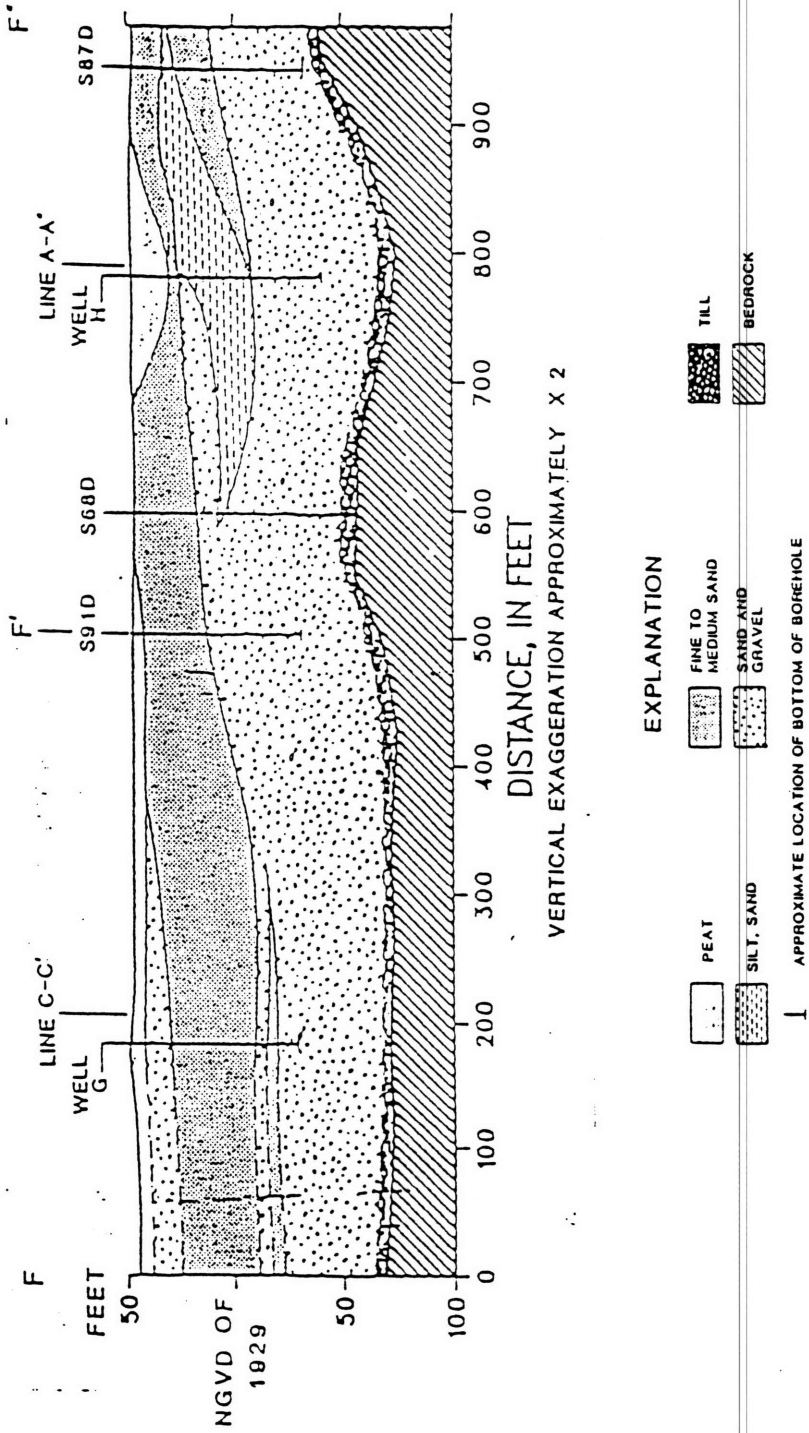
Figure 1.5   Geologic Section Along the Line Containing Wells G and H (Myette et al., 1987)

41
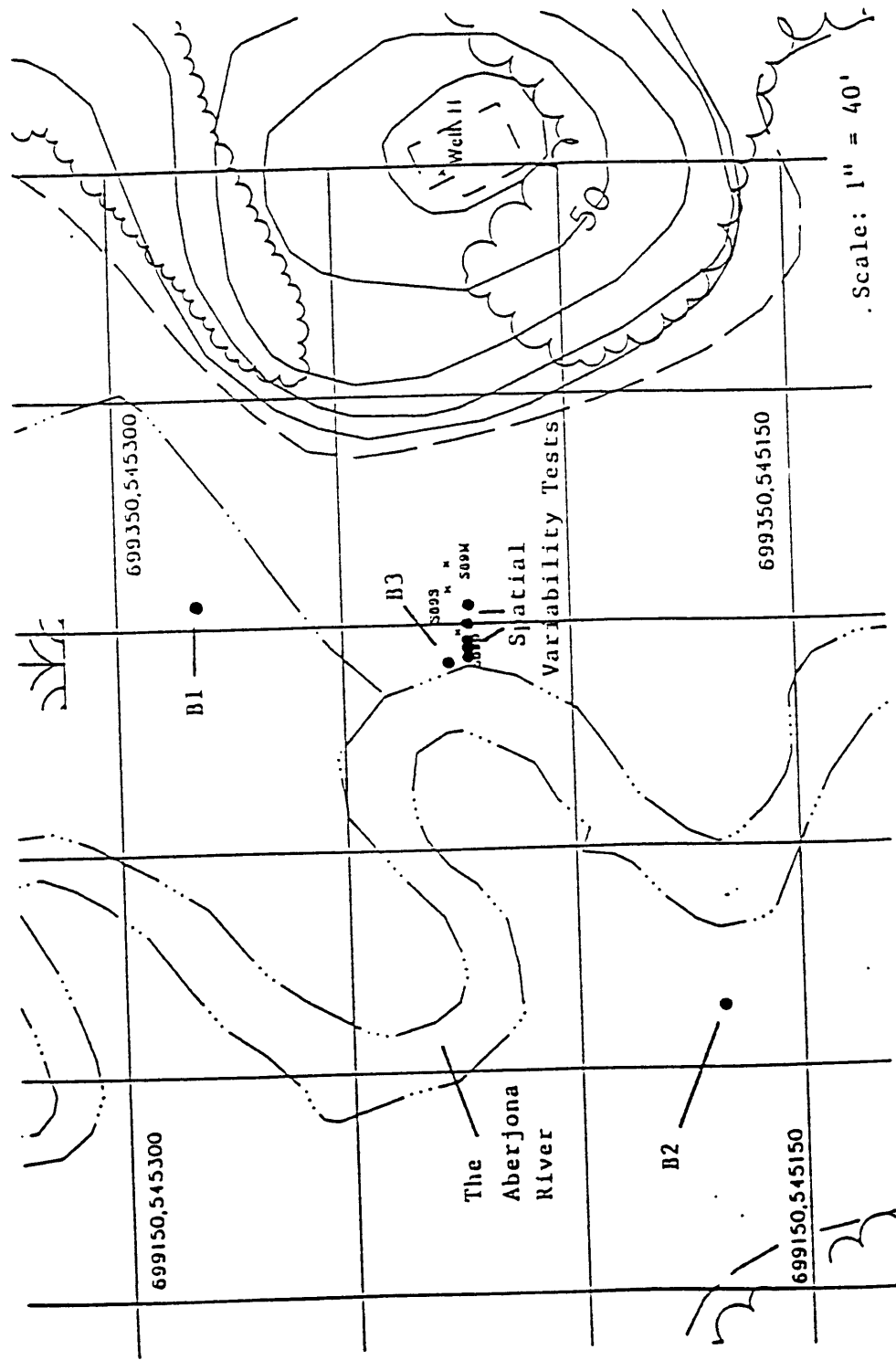
Figure 1.6   Site Map with Locations of Borings 1, 2, and 3 (Bialon, 1995)
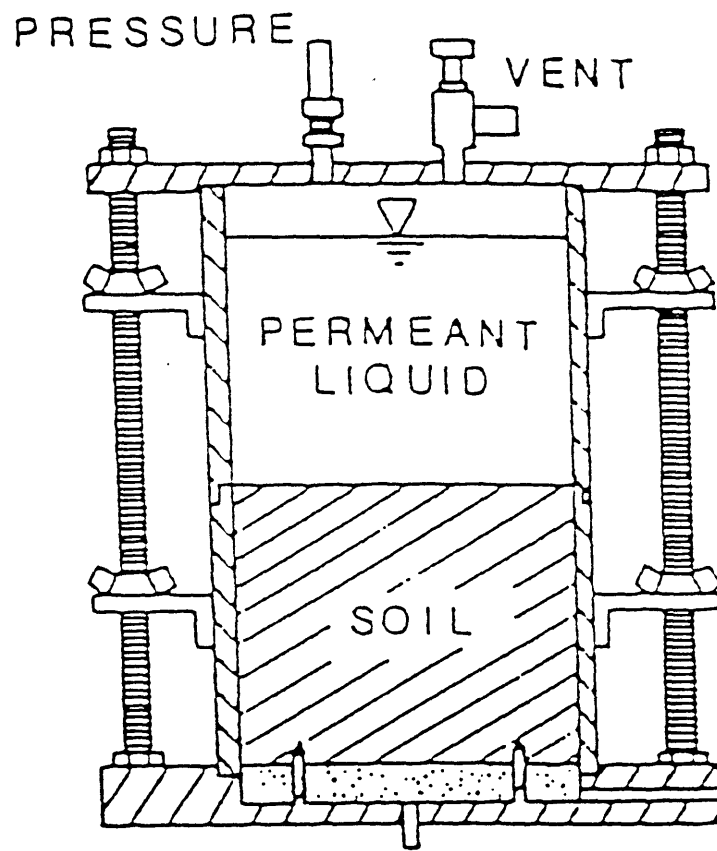
Figure 1.7   Schematic of Rigid Wall Permeameter (Daniel et al., 1985)
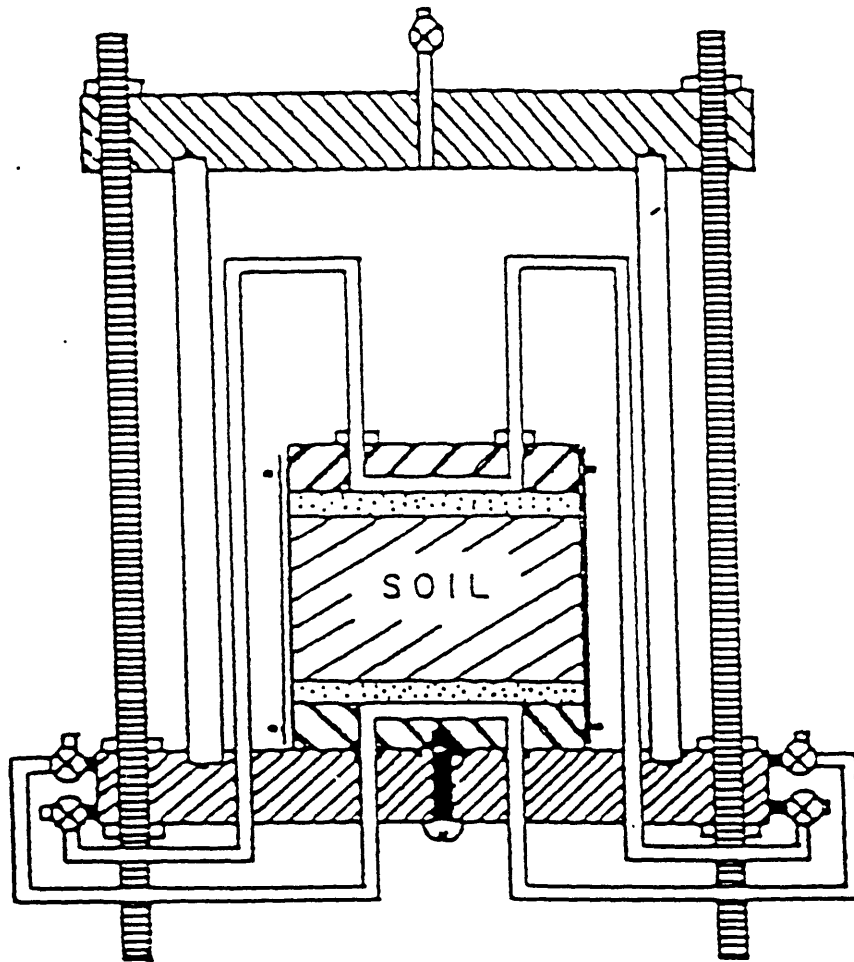
Figure 1.8   Schematic of Flexible Wall Permeameter (Daniel et al., 1985)

44
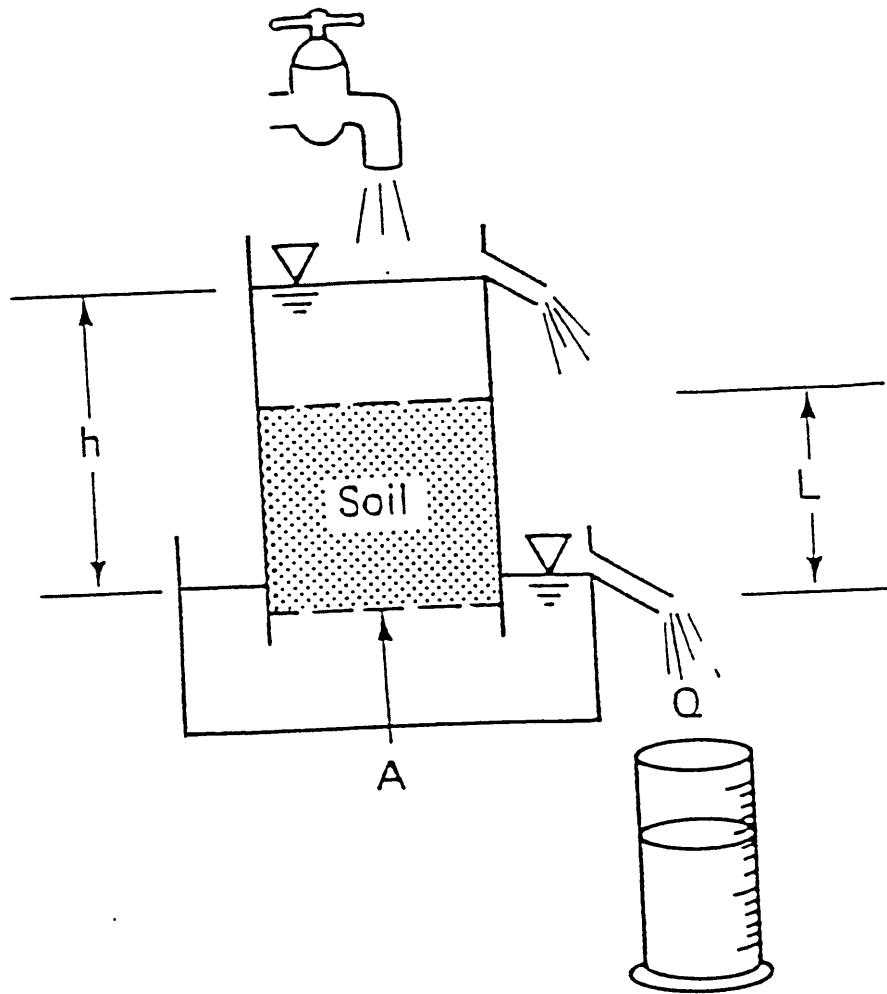
Figure 1.9   Schematic of Constant Head Permeability Test (Holtz et al., 1981)
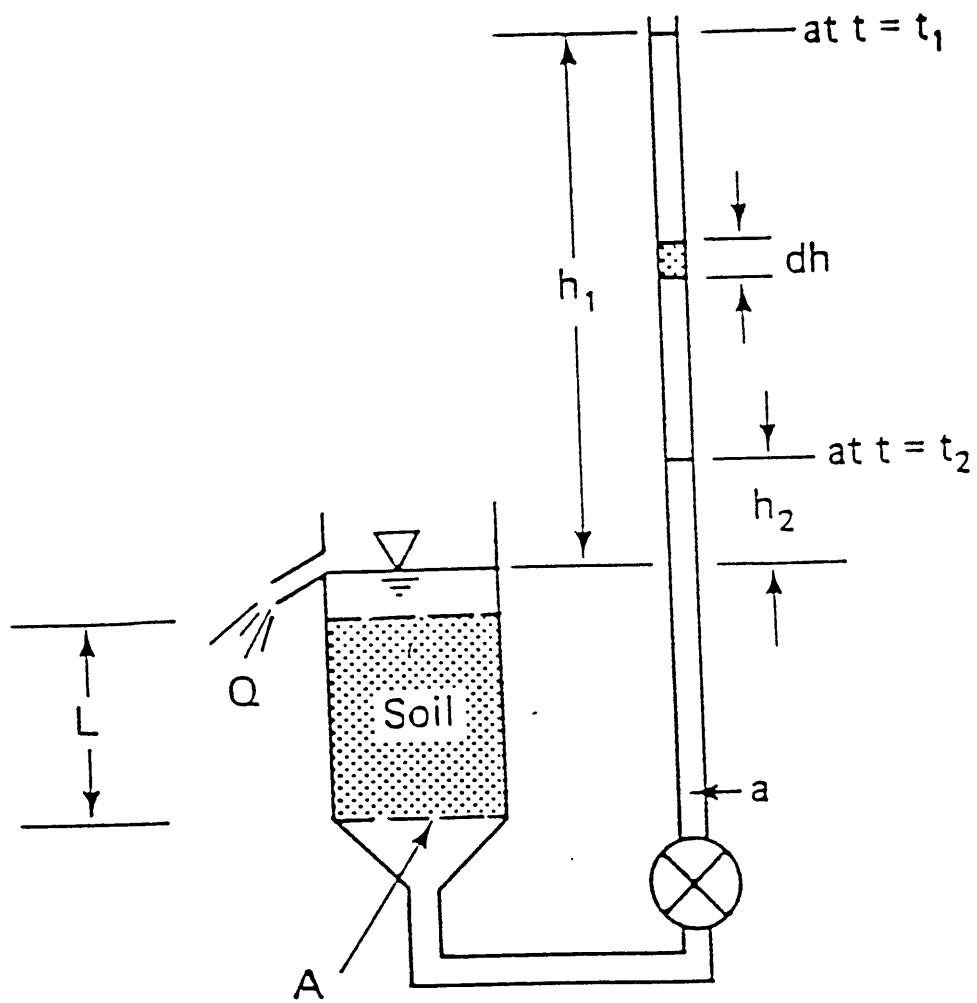
Figure 1.10   Schematic of Falling Head Permeability Test (Holtz et al., 1981)
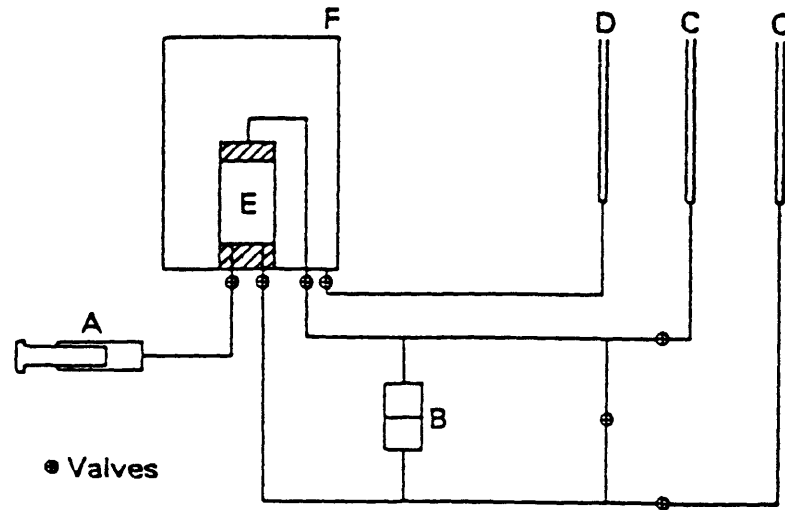
A - FLOW PUMP DRIVEN BY VARIABLE SPEED DRIVE (NOT SHOWN)

B - DIFFERENTIAL PRESSURE TRANSDUCER

C - PERMEANT

D - CELL FLUID

E - SOIL SPECIMEN

F - TRIAXIAL CELL

Figure 1.11   Schematic of Flow-Control Permeability System
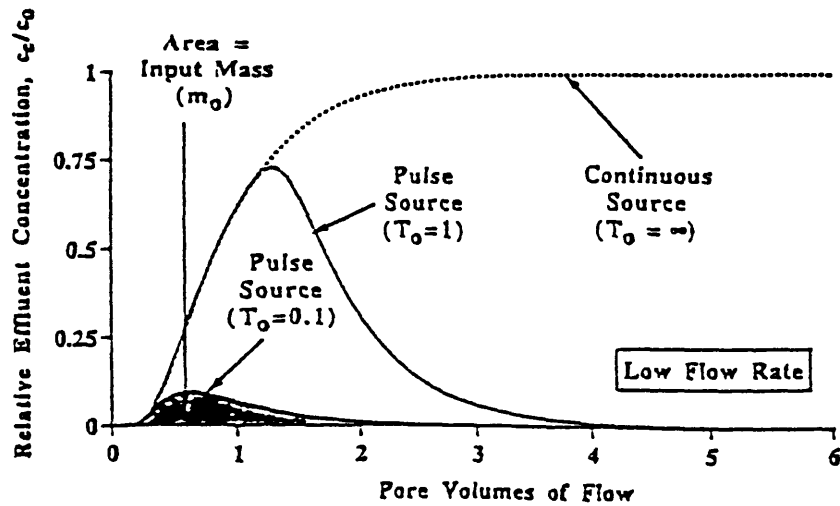
The parameter T_0

represents the volume of injected source solution containing a solute at concentration, c_0, relative to the volume of the void space in the soil. V conducting fluid flow.

Figure 1.12   Sample Break-Through Curves for Pulse and Continuous Source Experiments (Shackelford, 1994)

consolidation weight

peristaltic pump

silt soil

porous
polyethylene
cylinder (PPC)

solute or water

auto-fraction collector
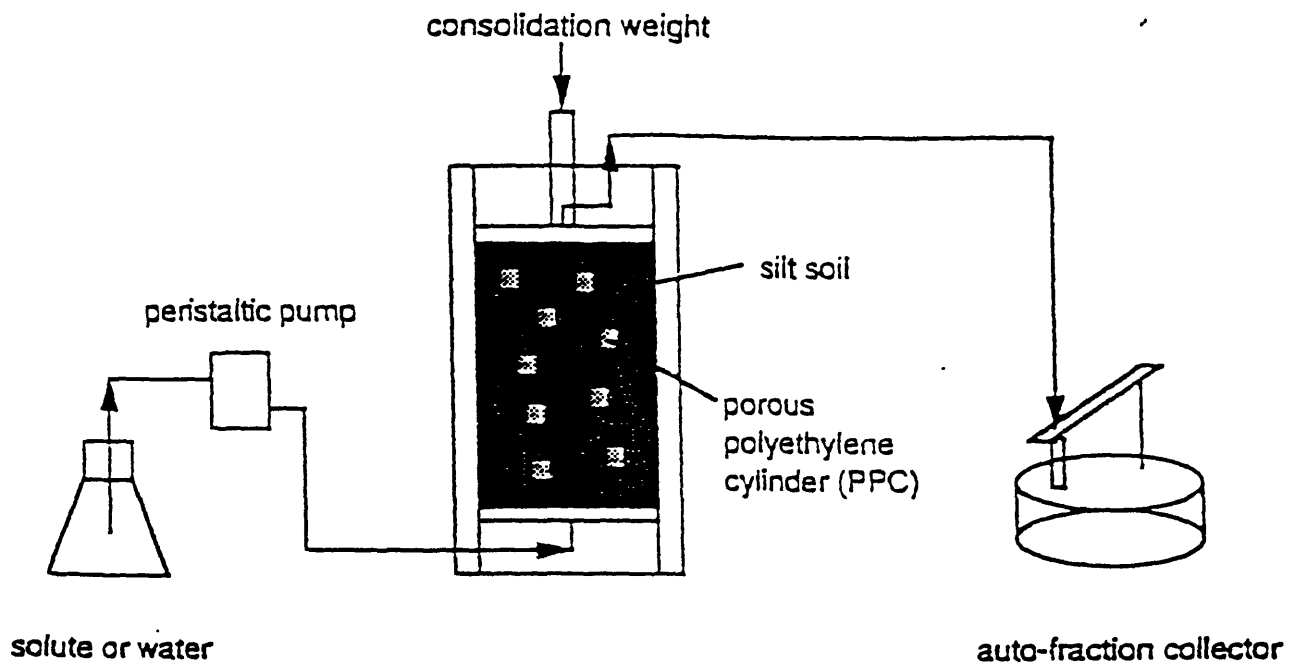
Figure 1.13   Schematic of Column Experiment Apparatus (Li et al., 1994)
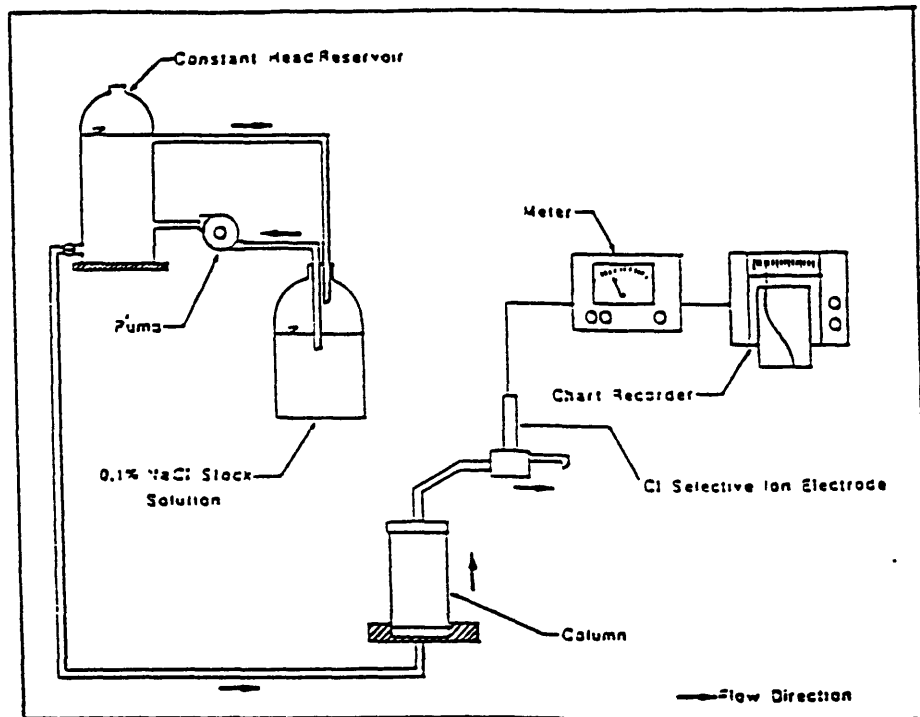
Figure 1.14   Schematic of Column Experiment Apparatus (Taylor et al., 1987)
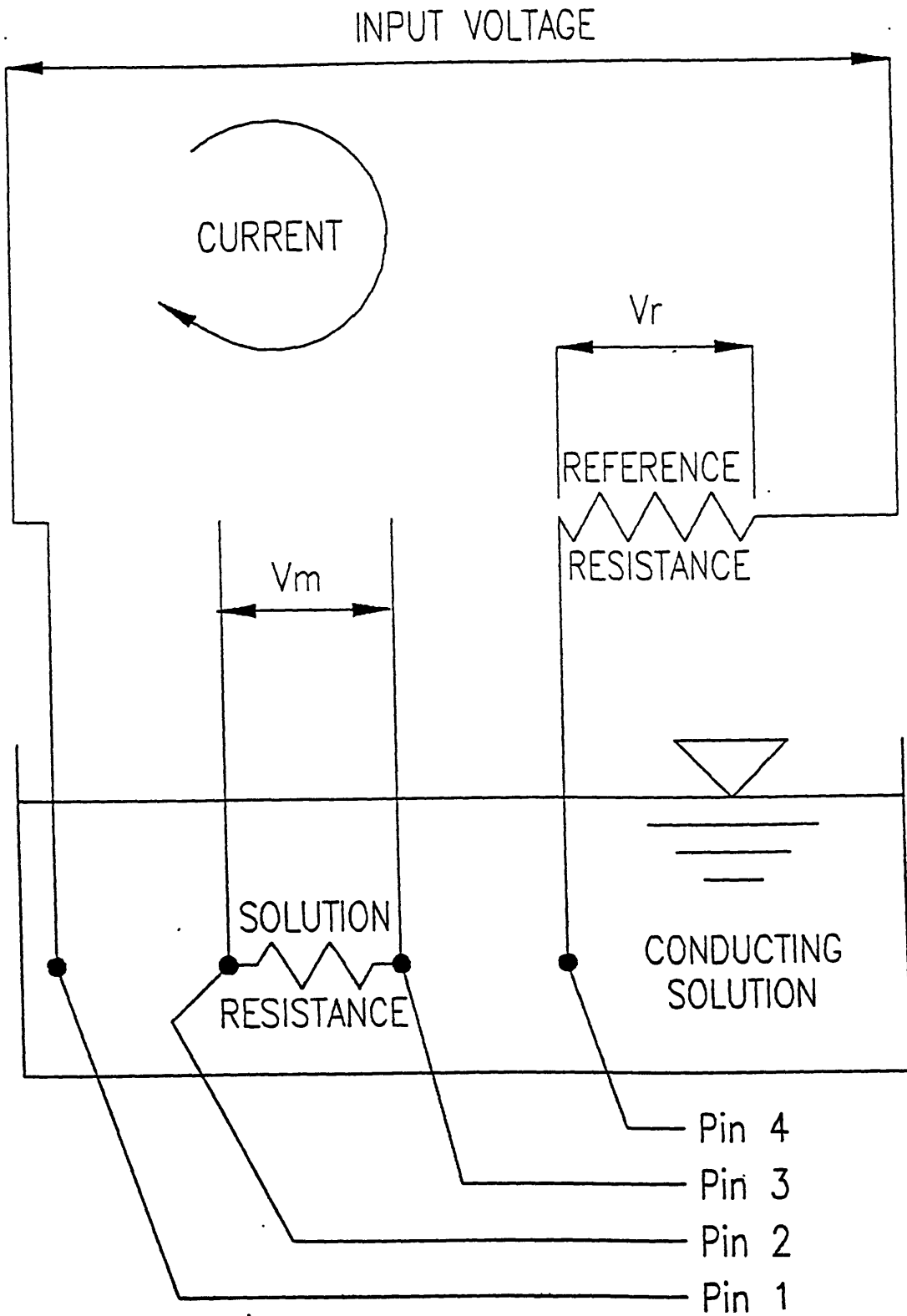
Figure 1.15   Schematic of Four-Pin Electrical Conductivity Probe Operation

Layer 1
V_1, D_{L1}

Layer 2
V_2, D_{L2}

Inter-region Diffusion

Inter-region Diffusion
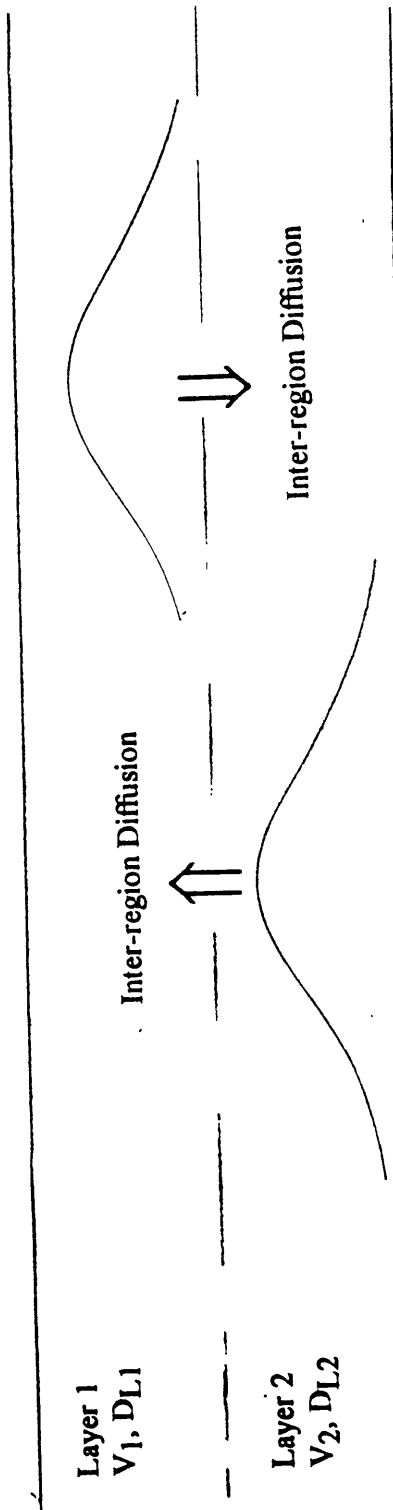
Figure 1.16.a Schematic Soil Model; Layers Have Different Seepage Velocities
(adapted from Li, et al., 1994)

Layer 1
V_1, D_{L1}

Layer 2
V_2, D_{L2}

Mechanical Dispersion
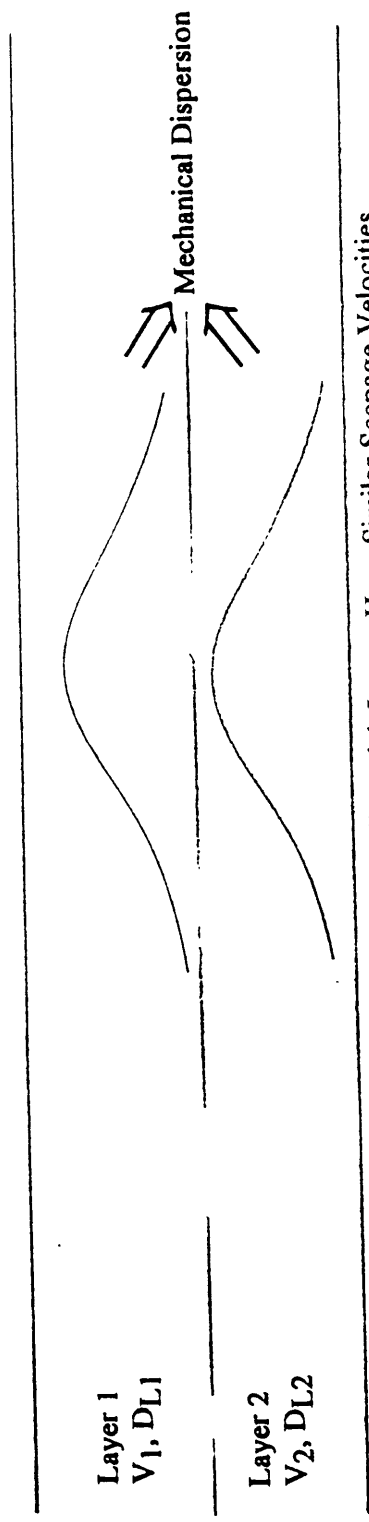
Figure 1.16.b Schematic Soil Model; Layers Have Similar Seepage Velocities
(adapted from Li, et al., 1994)

b) model pore space

a) actual pore space

Flow

Flow

Dead Zone

Adsorption Sites

Active Zone
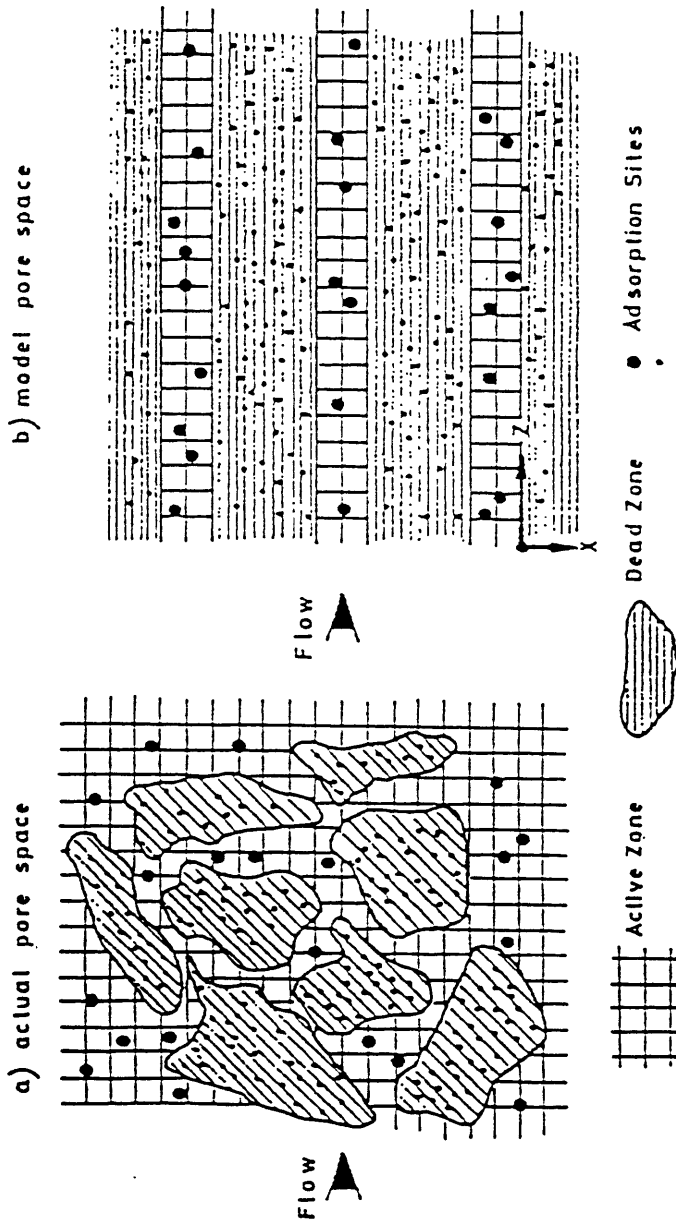
Figure 1.17   Schematic Soil Model (Loxham et al., 1983)

53
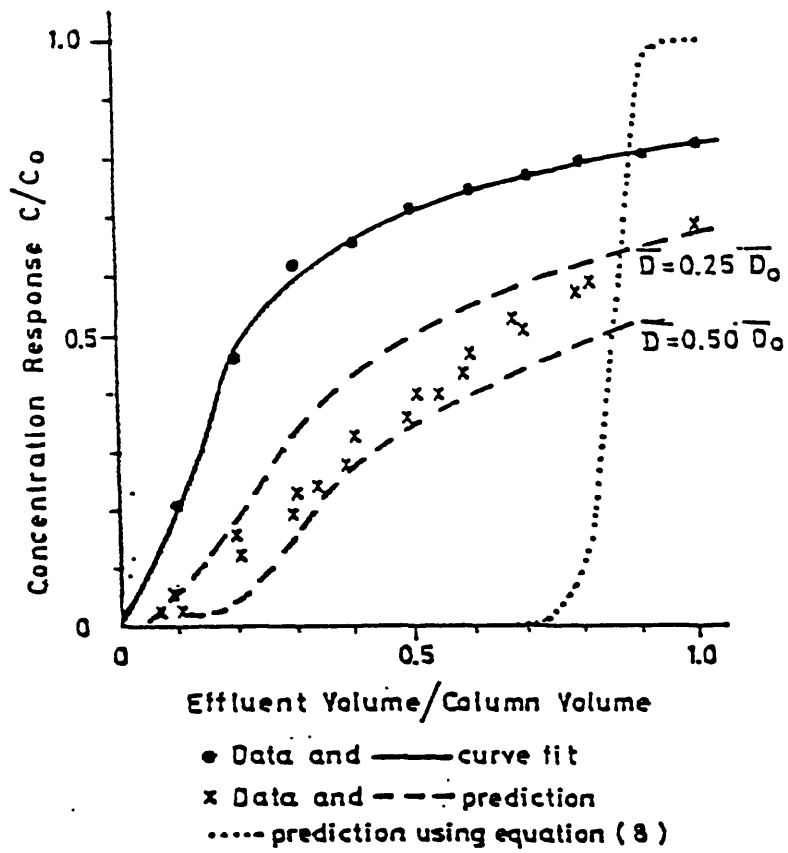
Figure 1.18   Experimental and Model Break-Through Curves (Loxham et al., 1983)

a)

R : 10
D : 05 cm²/s
v̄ : 043 cm/s

R : 15
D : 05 cm²/s
v̄ : 043 cm/s
• Data points

$T \left(\frac{\text{effluent volume}}{\text{column volume}} \right)$

b)

R : 10
D : 02 cm²/s
v̄ : 0081 cm/s

R : 16
D : 02 cm²/s
v̄ : 0081 cm/s
• Data Points

$T \left(\frac{\text{effluent volume}}{\text{column volume}} \right)$
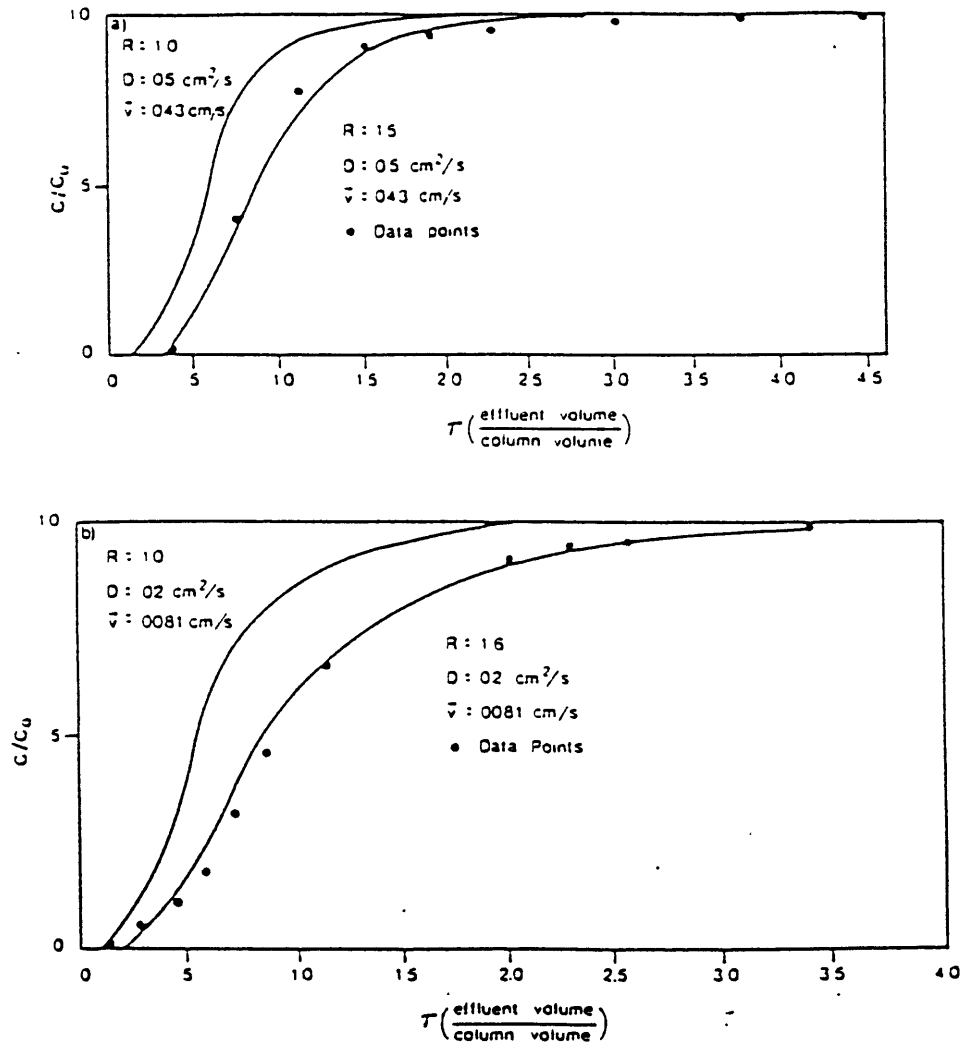
Figure 1.19   Experimental and Model Break-Through Curves (Price and Woo, 1986)

CHAPTER 2

EXPERIMENTAL EQUIPMENT AND PROCEDURES

As discussed in Chapter 1, the objective of this work was to develop the technology required to study the hydraulic characteristics of wetland sediments under varying effective stresses and flow conditions. This required a system that (i) enabled control of effective stresses and flow conditions, (ii) allowed the introduction of a pulse of tracer solution, and (iii) was capable of monitoring changes in the concentration of the effluent with time.

A flexible wall column was selected to allow control of effective stresses, as well as to reduce preferential flow paths along the sides of the specimen. Furthermore, by measuring the flow of fluid into and out of the cell via a double burette system, changes in the volume, and thus the porosity, of the specimen could be monitored.

The usual method of measuring hydraulic conductivity in the laboratory (establishing a known gradient and measuring the flow) was abandoned in favor of a system that controlled the flow (and allowed the gradient to be measured). A flow-controlled system was selected over a gradient-controlled system to provide better flow stability in a shorter period of time. This form of system is especially useful for materials with high hydraulic conductivities, for which steady flow is difficult to establish using gradient controlled systems. The gradient was measured with pressure transducers, to allow calculation of hydraulic conductivity, as was the effective stresses applied to the soil.

Measurement of the electrical conductivity of the effluent was selected as the means to monitor variations in the influent and effluent concentration with time. The effluent conductivity probes were placed in the pedestal to eliminate the need to have wires penetrating the cell. Flow through the samples was thus required to be downward during testing. Two independent conductivity probes were placed in the pedestal to allow redundant monitoring of the effluent concentrations. In addition, a third conductivity

probe was placed in the influent line to provide an indication of the mass entering the specimen, thus enabling a check on the mass balance. Two additional conductivity probes were placed in the effluent drainage line.

The flow system consisted of two influent reservoirs with air-water interfaces connected to the same air-pressure regulator. Equal pressures in the influent lines were designed to maintain a steady flow (and thus gradient and effective stress) while the pulse of tracer solution was being introduced. The system maintained constant pressure and supply of influent at the up-gradient end of the specimen, while the effluent was restrained by a moving piston at the down gradient end, thus forcing a steady flow rate.

The data were recorded using two systems. The influent conductivity, pressures, flow-control piston displacement, and temperature were recorded using the MIT geotechnical laboratory's central data acquisition system (discussed below), while the effluent conductivities were recorded on an IBM PC. An automated conductivity meter was developed to collect data from up to four two-pin conductivity probes at a time. The conductivities were then converted to concentrations, and entered into the CXTFIT model to obtain the fitted hydraulic properties of the specimen.

2.1 TRIAXIAL PERMEAMETER

2.1.1 Triaxial Cell

A standard MIT triaxial cell with a removable pedestal (see Figure 2.1) was selected for this test series to take advantage of existing equipment and parts. The cell manifold and pedestal were modified as discussed in sections 2.1.2 and 2.1.4, respectively. In addition, the fixed top cap was replaced with an independent top cap to facilitate the application of isotropic stresses. The triaxial cell was designed to accommodate a cylindrical specimen 3.56 cm (1.4 in.) in diameter by 8.13 cm (3.2 in.) high. The specimen was confined on the top and bottom by filter fabric, porous stones, and the top cap and pedestal, respectively. The circumference of the specimen was confined by two

prophylactic membranes, which were sealed to the top cap and pedestal using o-rings. Isotropic stresses were applied to the specimen via the cell fluid (distilled water). The cell itself was made of clear acrylic to allow visual inspection of the specimen, which helped in the detection of problems during testing. The acrylic cylinder is clamped between the base and top plate assembly as indicated in Figure 2.1. The valve on the top plate facilitates venting during filling or draining of the cell. The cell was filled through the cell-pressure connection.

The experiments discussed in this paper were performed under isotropic stresses, therefore, the loading piston in the top plate assembly was not utilized. To reduce the probability of leakage, the rolling diaphragm was not cut to allow penetration by the piston. However, the loading piston was left in place to support the diaphragm.

Drainage lines were placed in the center of both the top cap and pedestal. The top cap was connected, via a three-way valve, to two influent reservoirs, one containing distilled water, and the other a salt tracer solution (0.1M NaCl). The pedestal was connected (also via a three-way valve) to the effluent reservoir (flow control device), as well as to the influent reservoir containing distilled water to facilitate back-pressure saturation.

All metal components in contact with the permeant were made of stainless steel to prevent corrosion and reaction. Non-metallic components included the acrylic top cap, the pedestal epoxy, Teflon tubing, Buna-N O-rings, the carborundum porous stones, and filter fabric.

2.1.2 Manifold Control System

Figure 2.2 is a diagram of the manifold control system, which illustrates the functions of the various valves. The pressures of the influent and cell fluid were established at the air-fluid interface of the respective reservoirs. Air pressures were controlled by Fairchild regulators, shown in the wall system of Figure 2.2. To maintain

constant influent pressures during different phases of testing, both of the influent reservoirs were connected to the same air-pressure regulator. The pressure gauges in the wall system provided continuous indication of the cell and pore pressures.

The pressure transducers were made by Data Instruments, Inc. and have a range of 0 to 14 ksc (0-200 psi) with 100 mV full scale output and 5.5 volt input. Their output is stable to ± 0.02 mV, resulting in a stable pressure resolution of $\pm 2.6 \times 10^{-3}$ ksc. To enable detection of small gradients, the zeros of the salt and back-pressure transducers were calculated to produce readings equal to the pressure measured by the pore-pressure transducer under no flow conditions, at elevated back-pressures (approximately 4 ksc).

The double burette, which is connected to the cell fluid, was used to measure the volumetric change during consolidation of the specimen. Assuming complete saturation, and no leakage, the change in the volume of the cell fluid should approximately correspond to the change in the volume of the specimen.

The effective stress was assumed to be the difference between the pressure of the cell fluid, and the average of the pressures at the pedestal and top cap. The minimum effective stress was therefore half of the pressure gradient, as the cell pressure must be at least as great as the pressure at the up-gradient end of the specimen to prevent ballooning of the membranes. The actual equilibrium effective stress was, therefore, not uniform throughout the specimen, rather it varied linearly along the gradient within the specimen.

2.1.3 Flow-Control System

Figure 2.3 illustrates the flow-control system. The pressure at the influent end of the specimen is held steady via the manifold system, while the flow-control device draws pore fluid from the effluent end of the specimen at a constant rate. Steady state flow was assumed when the pore pressure at the pedestal reached a constant value (i.e. when the gradient became constant).

The flow control device is similar to the standard pressure/volume control devices used in the MIT triaxial systems (Figure 2.4), was modified to allow a wider range of flow rates (approximately 10^{-5} cc/s to 10^{-1} cc/s), as well as a larger total volume of flow (approximately 270 cc). The larger range of flow rates was attained with the transmission system described below. The total volumetric flow capacity was improved by increasing the diameter of the piston to 4.128 cm (1.625 in.), and the stroke of the flow control device from the standard 15.24 cm (6 in.), to 20.32 cm (8 in.). The device consists of a stainless steel cylinder, clamped between two stainless steel end caps. The stainless steel piston extends through the bottom end cap into the cylinder, and is sealed to the end cap with O-rings. As the piston is withdrawn, pore fluid is drawn from the specimen into the flow control device.

The piston is driven by an electric DC motor and transmission system, as shown in Figure 2.5. The motor and a matching 180:1 gear reducer can be placed in one of two locations on the transmission to gain additional reductions of 5:1 or 400:1 respectively. In the 5:1 position, a 4-thread worm (Gear A) drives a 20 tooth, 4 thread worm gear (Gear B), which is attached to the ball-screw actuator drive shaft. In the 400:1 position, a single thread worm (Gear C) drives an 80 tooth, single thread worm gear (Gear D), which shares a shaft with a 16-tooth spur gear (Gear E), driving an 80 tooth spur gear (Gear F), which is attached to the actuator drive shaft. The ball screw actuator unit moves the piston 2.54 cm (1 in.) for each 25 revolutions of the drive shaft. The full stroke of the actuator, and therefore the piston, is 20.32 cm (8 inches).

The range of flow rates can be altered by substituting components in the drive system. For example, the flow rate can be reduced by a factor of four by replacing the ball screw actuator with one that produces 2.54 cm (1 in.) of travel per 100 revolutions of the drive shaft. Alternatively the flow rate can be increased by replacing the gear reducer (attached to the DC motor) to achieve reductions of 100:1, 50:1, 25:1, and 12.5:1, rather than 180:1.

The motor has a tachometer which puts out approximately 3.5 volts per thousand rpm (± 10%). The input to the motor is controlled by a manual rheostat, which is adjusted until the motor speed (as indicated by the tachometer) associated with the desired flow rate is attained.

The displacement of the piston is measured by a direct current displacement transducer (DCDT). The DCDT barrel is attached to the flow-control device by an aluminum mounting block, as shown in Figure 2.4. The stem is attached to the plate which connects the ball-screw actuator to the piston. The DCDT output is stable to ± 2 mV, resulting in a stable displacement resolution of ±4.5 x 10^{-3} cm (1.8 x 10^{-3} in.).

2.1.4 Pedestal

A section of the removable pedestal is shown in Figure 2.6. The seating area rests on the base of the triaxial cell, and the narrow gap between the pedestal and the base is sealed with o-rings. The pedestal is held in place by the cell pressure, and has a threaded port in the bottom for the o-ring fitting on the end of the drainage line. The stainless steel component of the pedestal is a continuous machined piece. The transducers (discussed below) were fit into a machined epoxy tube (cast with the same epoxy as that used for the rest of the pedestal to ensure proper adhesion), which held them in place while the remaining epoxy was cast around them. The tube has inside diameter = 0.159 cm (1/16 in.) and serves as the pedestal drainage path. The epoxy was chosen to be machinable, non conducting, resistant to chemicals, and adhesive to stainless steel as well as to components of the transducers (the epoxy manufacturer's data sheets are attached as Appendix A).

There were four transducers cast into the pedestal, three to measure the concentration of the effluent, and one to measure the temperature of the effluent. The three intended to measure the concentration of the effluent included a four-pin conductivity probe (or two independent 2-pin probes), a pH probe, and a probe to

61

measure the oxidation-reduction potential (ORP) of the effluent. Reliable readings were never obtained with the later two due to suspected problems with the reference electrode.

The temperature transducer is an Analog Devices AD 592C (the data sheets are included in Appendix B), which has a linear output of 1 micro amp per degree Kelvin and reads 298.2 μA at 298.2 °K (25 °C). The AD 592C has an operating range of -25°C to 105°C and is positioned to measure the temperature of the fluid in contact with the top surface of the pedestal, thus representing the temperature of the effluent. The output from the transducer is converted from micro-Amps to millivolts with the simple circuit shown in Figure 2.7. The circuit also has a variable resistor to eliminate the calibration offset at 25 °C. The AD 592C is accurate to 0.5 °C, and linear to 0.15 °C when operated between 0 and 70 °C (Analog Devices, 1992). The output signal from the circuit has a resolution of 0.1 mV (0.1 °C), and is stable to ± 0.2 mV (±0.2°C).

The conductivity electrode was made by Microelectrodes, Inc. (Manchester, NH), and consists of four parallel platinum wires (0.0508 cm or 20/1000 in. dia.) spaced 0.159 cm (1/16 in.) on center, and placed horizontally to span the drainage path in the pedestal, as shown in Figure 2.6. The top wire is located 0.635 cm (1/4") below the top surface of the pedestal. The wires are connected to the conductivity meter via banana plugs. The conductivity electrode can either be used as a single four-pin electrode, or as two independent two-pin electrodes. The two-pin mode was used during the evaluation tests discussed in this thesis in order to provide redundant measurements of effluent concentration. The operation of the two-pin conductivity probes, and the associated circuits, will be discussed in the data acquisition section below. Four-pin conductivity was discussed in Section 1.6.2.3.

There are two other conductivity probes, similar to the four-pin probe located in the pedestal, built into the system. The first was placed in the influent line between the top cap valve and cell base plate, and is used to measure the mass of the tracer solution introduced. The second was placed in the effluent line down stream of the manifold

62

system, and provides redundancy to the pedestal measurements. A diagram indicating the locations of all of the conductivity probes is provided in Figure 2.8. Sections of these flow-through probes are shown in Figure 2.9. The probe housings were cast from the same epoxy used for the pedestal, and have Swage-Lock fittings threaded into their ends to facilitate in-line placement. These also can be used as either two-pin or four-pin probes, and, again, the two-pin mode was used for the work presented in this thesis.

The pH electrode consists of a glass bulb protruding into the flow path as shown in Figure 2.10. The oxidation-reduction electrode is a platinum wire spanning the drainage path as shown in Figure 2.6 (identical to one of the conductivity pins). The pH and ORP probes share the same reference, which is located in the effluent line leading from the pedestal. Measurements with these electrodes, and the problems experienced, are discussed in the section on data acquisition systems below. Information sheets from the manufacturer can be found in Appendix B.

2.2 Data Acquisition

Data from the experiments were recorded using two separate systems, as discussed above. Pressure, temperature, piston displacement, pH, ORP, and influent conductivity data were ultimately recorded on the central data acquisition system used in the geotechnical laboratory at MIT. The output signals from the pressure transducers and DCDT, as well as the input voltage to these devices, were recorded directly. Data from the influent conductivity probe, temperature transducer, pH probe, and ORP probe were processed by intermediate circuits and meters, as discussed below, before being recorded on the central data acquisition system. Data from the effluent conductivity probes were obtained from an automated conductivity meter developed at MIT, which is discussed in Section 2.2.2.2.

2.2.1 MIT Geotechnical Central Data Acquisition System

The central data acquisition system is an expanded-channel Hewlet-Packard HP3497A data acquisition unit which works in conjunction with an IBM-compatible 486-66 personal computer. The system was driven by EASYDAT software, written by Dr. John T. Germaine of MIT, and Mr. R.S. Ladd of Woodward-Clyde Consultants (Sheahan, 1991). The system presently has 125 usable channels, of which 12 were used in this project (#60 - #71).

2.2.2 Conductivity Measurement and Data Logging System

2.2.2.1 Conductivity of Influent

The conductivity of the influent was measured with one of the two in-line probes discussed above. Due to a limited number of 2-pin meters, only two of the four pins were used. Thus, there was a single 2-pin measurement of the influent conductivity. The probe was connected to a YSI Model-35 2-pin conductivity meter. The Model 35 adjusts the amplitude of the square-wave current until the time-averaged magnitude of the cell voltage over each half-cycle is equal to a reference voltage. Given that current, together with the voltage, the conductivity of the solution is calculated and displayed. The gain settings, and the associated ranges, resolutions and accuracies are displayed in Table 2.1. The YSI Model 35 displays the conductivity assuming a geometric cell constant of one. If the constant differs from unity, the displayed/recorded value must be manually adjusted accordingly.

There is a recorder output that was connected to the central data acquisition system for data logging. The output range is 0 to 2.0 volts, and is proportional to the display. With the gain set at 20 milliseimens, the recorded data must be multiplied by 10 to obtain units of milliseimens (uncalibrated data). With the central data acquisition system, the output from the meter (set at 20 mS) is stable to ± 0.05 mV, which corresponds to $\pm 1.7 \times 10^{-3}$ milliseimens (calibrated).

2.2.2.2 Conductivity of Effluent

To enable continuous, monitoring of multiple 2-pin probes, an automated multi channel conductivity meter (AMCCM) was constructed at MIT. The AMCCM has two components, a single channel conductivity meter with DC analog output (SCCM), and a computer-controlled digital relay box that allows automated selection of probes and reference resistors. The design of the AMCCM is based on one used by the Cambridge University Engineering Department, U.K., and was modified by Dr. John T. Germaine and Mr. Samir Chauhan, a MIT doctoral student. To understand the operation of the SCCM, refer to Figure 2.11. A constant AC. voltage (AC. minimizes polarization of the ions in solution) is applied to the probe circuit, and the voltage across the 2 pins of the conductivity probe is measured. With a reference resistor (R_r) placed in series with the resistance of the solution (R_s), the ratio of the measured output voltage to the input voltage is equal to the ratio of the (R_s) to $(R_s + R_r)$. The equation can then be solved for the resistance of the solution, the reciprocal of which is its conductivity. The reference resistor can be selected from one of 5 resistors, ranging, in even orders of magnitude, from 100 Ohms to 1 MOhm. The values of the resistors are presented in Table 2.2. The resistor is selected such that the measured V_{out} is as close to 0.5 V_{in} as possible (the best results are obtained when the resistance across the solution matches the reference resistance). The MIT AMCCM gives reliable conductivity readings ranging (in orders of magnitude) from 1 microseimen to 10 milliseimens.

A diagram of the controls and terminals on the SCCM is given in Figure 2.12. A diagram of the circuit is given in Appendix F . In manual operation of the SCCM (with out the relay box), the V_{in} and V_{out} are measured, their ratio is calculated, and a different resistor is selected if necessary. The process is iterated until V_{out}/V_{in} is approximately 0.5, at which time the conductivity is computed. Note that since the circuit holds V_{in} constant, measuring it once at the beginning of each test series should be sufficient.

A diagram of the relay box, which enables monitoring of four probes and automated conductivity data logging, is provided in Figure 2.13. The relay box has its own set of resistors, also controlled by relays. The actual resistances of these resistors were measured and are provided in Table 2.3 The relays are operated by digital signal, and thus require a computer with digital output capabilities to switch them on and off. A program called Conduct.bas was written in Basic to control the relay box, take output readings from the SCCM, calculate the conductivity, and record it to data files.

A listing of Conduct.bas is provided in Appendix D. The program begins by having the user input the number of probes, name of the data input file, maximum number of observations, time increment between readings, and the delay time before it takes the first reading. For each reading, the program sends out a digital signal which activates the appropriate probe, and connects the resistor used for the previous reading (stored in an array). It then takes a reading, calculates the ratio of V_{out} to V_{in}, and changes the resistor if needed, as described above. When the correct resistor has been selected, the program calculates the conductivity and writes it to the data file. The process is repeated for each probe at every reading interval. It takes approximately 6 seconds to select the resistor, allow the probe to stabilize, and take a reading. Thus the minimum theoretical increment for four probes is 24 seconds. However, if resistors must be changed during the course of the experiment (due to significant changes in the effluent concentration), the additional time must be considered in selecting a reading increment. For the test series reported in this thesis, the delay and reading increment were set so that readings coincided with data being recorded on the central data acquisition system.

The digital outputs are sent to the relay box using Strawberry Tree Incorporated's "Analog Connection AO" card. The card has 8 digital I/O lines, as well as 4 analog outputs. The input and output voltages to the probes are obtained and converted to computer-readable digital signals by the Multichannel Analog-To-Digital Conversion

Board developed by Mr. Tom Sheahan at MIT, and described in Appendix B of his doctoral thesis.

2.2.3 pH and Oxidation-Reduction Potential

pH and ORP measurements both require amplifiers with high input impedance to record data in millivolts. "Millivolt Adapters" were obtained from Micro-Electrodes Inc. to produce signals that could be recorded by the central data acquisition system. Stable readings were never obtained by either probe. The instabilities are suspected to have been caused by the configuration of the reference electrode. The reference electrode works by releasing small amounts of the reference solution (3 M KCl saturated with AgCl) into the drainage line, which maintains contact between the Ag/AgCl electrode and the permeant. At back-pressures of 4 ksc, the reverse of the intended flow would take place, thus diluting the reference solution. Possible solutions to this problem are discussed in Chapter 4.

2.3 Experimental Procedures

2.3.1 Test Preparation for Sand Specimen

The following procedure was adopted for the preparation of sand specimens:

(1) The cell manifold tubes were cleaned by filling the salt-solution reservoir with warm diluted Micro-Solution (2 ml per liter water), and connecting the salt line to the various connections on the manifold to force the cleaning solution through the system. Each Probe was then rinsed several times with warm distilled water. After thoroughly rinsing the lines, the water was removed from them using compressed air.

(2) The diameter of sand mold, and thickness of the membrane were measured.

(3) Three O-rings were greased and placed on the O-ring stretcher.

(4) The side of the pedestal was greased, the bottom porous stone (Soiltest #T-300, k ≈ 3 cm/s) positioned, and the thick membrane was sealed to the pedestal with two O-rings. A prophylactic membrane was rolled over the first two O-rings (Figure 2.14), and a third O-ring was positioned between first two (Figure 2.14).

(5) The sand mold was assembled and a vacuum of 5.08 cm Hg (2 in.) was applied to expand the mold.

(6) The height of the mold above the porous stone was measured in three locations.

(7) The initial mass of the container of sand, and the raining device were measured.

(8) The specimen was prepared using the raining method (which is discussed in MIT Course # 1.37, taught by Dr. J.T. Germaine), the top of the sample was leveled with a straight-edge, and the loose sand collected and returned to the container.

(9) The final mass of the sand container and raining device were measured for use in determining the mass of the specimen.

(10) Four O-rings were greased and placed on the O-ring stretcher, which was then set over the top-cap line. The top porous stone and top cap were then positioned, and the thick membrane fixed to the top cap with two O-rings as described for the pedestal.

(11) Vacuum was removed from the mold, and applied to the specimen through the pedestal drainage line.

(12) The mold was removed, and the thin membrane rolled up the specimen, over the two O-rings, and fixed with the third O-ring as described above. If not used, the fourth O-ring was released on the top cap line, so as not to disturb the specimen.

(13) The cell was assembled and partially filled with deaired distilled water.

(14) The cell-pressure transducer zero was measured when the cell fluid reached the mid-point of the specimen, after which the cell was completely filled.

(15) The cell-pressure pot was connected, and a cell pressure of 0.35 ksc was applied.

(16) CO_2 was connected to the pedestal drainage line and allowed to flow up through the specimen for 15 minutes at approximately 0.05 ksc.

(17) The distilled water reservoir was connected to the pedestal drainage line and approximately three pore volumes of deaired distilled water were allowed to flow up through the specimen at a head of approximately 30 cm (1 ft).

(18) The pedestal transducer zero was measured with the phreatic surface (of the water influent reservoir) at the mid-point of the specimen.

(19) The drainage lines were reconnected to the configuration shown in Figure 2.2, and the specimen was back-pressure saturated to 4 ksc, while maintaining the effective stress at or below 0.35 ksc.

(20) The drainage lines were closed, and the B-value (Lambe et al., 1969) was measured with a 0.25 ksc increment.

(21) The zeros of the water and salt solution top-cap transducers were calculated to obtain the same pressure reading as the pedestal transducer under no flow conditions.

2.3.2 Test Preparation for Wetland Deposit Specimen

The following procerdure was adopted for the preparation of wetland deposit specimens:

(1) The cell manifold tubes were cleaned by filling the salt-solution reservoir with warm diluted Micro-Solution (2 ml per liter water), and connecting the salt line to the various connections on the manifold to force the cleaning solution through the system. Each line was then rinsed several times with warm distilled water. After thoroughly rinsing the lines, they were drained and re-saturated with distilled, deaired water at ambient temperature.

(2) The pedestal transducer zero was measured with the phreatic surface at the mid-point of the specimen.

(3) The porous stones and nylon filter fabrics were placed in an ultrasonic bath to saturate them.

(4) The pedestal was greased, the membrane protector positioned, and two prophylactic membranes installed, using the same O-ring configuration as described for the sand specimen.

(5) The membrane protector was installed on the greased top-cap, and four O-rings were placed on the stretcher, which was then set over the pedestal.

(6) The specimen tube was cut to obtain a segment approximately 2.5 cm (1 in.) longer than the desired specimen length, and the specimen location was noted.

(7) The specimen was extruded from the tube, and rough cut to approximately 5 cm (2 in.) diameter using a fabric cutting blade (25.4 cm (10 in.) Eastman Straight Knife #4704).

(8) The specimen was then placed in a two-step triaxial trimming jig and trimmed to a 3.56 cm (1.4 in.) diameter using a fabric cutting blade in the trimming blade-holder.

(9) The specimen was placed in a split cylindrical sleeve, and the ends trimmed, using the fabric cutting blade and guide, to obtain the desired specimen height.

(10) The trimmings from steps 8 and 9 were used to obtain preliminary estimates of the water content of the specimen.

(11) The initial dimensions and mass of the specimen were obtained.

(12) The porous stones and nylon filter fabrics were removed from the ultrasonic bath, and placed in a dish of distilled water. The nylon filter fabric was placed on the bottom stone under water, the stone placed on the pedestal, and the membrane protector folded up.

(13) The specimen was placed on the pedestal, the top nylon filter fabric and stone were installed, the top cap positioned, the top membrane protector folded down, and the membranes rolled up and fixed to the top cap with O-rings as described for the sand preparation. The extra O-ring was released on the base of the pedestal (if not used) and the O-ring stretcher was lowered around the pedestal and left in place.

(14) The cell was assembled and partially filled with deaired distilled water.

(15) The cell-pressure transducer zero was measured when the cell fluid reached the mid-point of the specimen, after which the cell was completely filled.

(16) The cell-pressure pot was connected to the cell, and a pressure of 0.05 ksc applied.

(17) The specimen was back-pressure saturated to 4 ksc, while maintaining an effective stress below 0.05 ksc, at the rate of 0.5 ksc per hour.

(18) The drainage lines were closed, and the B-value was measured with a 0.25 ksc increment.

(19) The zeros of the water and salt solution top-cap transducers were calculated to obtain the same pressure reading as the pedestal transducer under no flow conditions.

2.3.3 Testing Procedures

The following procedure was adopted for testing:

(1) The specimen (sand or wetland deposit) was isotropically consolidated to the desired effective stress while monitoring the corresponding change in the volume using the double burette system.

(2) The porosity of the specimen was estimated using the preliminary water content, and the accumulated volume change due to consolidation (caused both by applied stress increments, and by stress changes due to induced gradients).

(3) The RPM of the flow control device required to obtain the desired seepage velocity was calculated.

(3) The conductivity of a specimen of the salt solution (taken from the influent reservoir) was measured using a pencil-type conductivity probe (with probe constant = 1) and the YSI conductivity meter.

(4) The pore-pressure-transducer valve was set to the effluent line, and the flow-control device SLOWLY moved up until the pressure in the line matched the pore pressure in the specimen. The device was then stopped using the rheostat.

(5) The pore pressure valve was set to the effluent line, and the rheostat was adjusted to attain the desired flow rate.

(6) The Double Burette and pore pressure at the pedestal were monitored until the pore pressure reached a steady value.

(7) The central data acquisition system and conductivity program were set to begin at the same time, and started.

(8) After two readings were taken by the data acquisition systems, the DCDT reading was manually recorded, the air pressure to the salt solution pot was turned on, and the top cap valve was switched to the salt solution for the required pulse duration.

(9) At the end of the pulse interval, the salt was turned off, the DCDT reading was recorded, the air pressure to the salt reservoir was turned off, and the reservoir vented to the atmosphere to release the pressure (minimizing the amount of air forced into solution).

(10) The specimen was flushed with three pore volumes of distilled water, or until the conductivity readings returned to their pre-test values, whichever came last.

(11) Steps two through six were repeated to study the effects of different flow rates and void ratios.

(12) While maintaining the final flow rate, the top-cap valve was switched to the salt solution, and a continuous source experiment was conducted to determine the equilibrium conductivity for each probe corresponding to the solution used for the previous experiment.

(13) Upon completion of the experiment, the air pressure regulators were backed down to their minimum pressures, while maintaining an approximately constant effective stress, and then the drainage lines to the specimen were closed.

(14) The cell fluid was drained, and the cell and top-plate assembly were removed.

(15) The effluent and water influent lines were removed and the corresponding drainage lines opened to prevent water from being drawn from the specimen during removal of the O-rings.

(16) The specimen was removed and sectioned to obtain three water contents.

2.3.4 Data Reduction

At the end of each test, the data were reduced as follows:

(1) The data files were copied from the two data acquisition systems and entered into a Lotus spreadsheet (Figure 2.15.a-i) which performed the following calculations:

a.) Calculated the average effective stress and gradient from the pressure transducer data, V_{in}, the calibration factors, and transducer zeros.

b.) Calculated the average volumetric flow rate using the DCDT data from the flow-control device, V_{in}, the calibration factor, and transducer zero.

c.) Calculated the hydraulic conductivity using Darcy's Law, $Q = kia$, where $Q =$ the average volumetric flow rate, $i =$ the measured hydraulic gradient, $a =$ the cross-sectional area of the specimen, and $k =$ the hydraulic conductivity of the soil.

d.) Converted the temperature data from Kelvin to Celsius.

e.) Adjusted the conductivity values, to reflect the temperature of the solution at the time they were recorded, using the numerical function shown in Figure 2.16.

f.) Converted conductivity values to concentration values using the numerical model shown in Figure 2.17.

g.) Normalized the concentration values from pulse type experiments to the equilibrium concentrations recorded in continuous source experiments, and integrated the areas under the curves.

h.) Normalized the volumetric flow by the pore volume of the specimen.

i.) Averaged the results of Probes 1 and 2 (in pedestal) for use in the CXTFIT input file.

2) The normalized concentration was plotted against the number of pore volumes of flow for each probe (0 pore volumes was the estimated time at which the center of mass of the pulse reached the top of the specimen).

3) The integrated area under the normalized concentration curves were plotted against pore volumes of flow for each probe to check for conservation of mass (effluent probes should have the same integrated area as the influent probe).

4) The data were extracted from main reduction spreadsheet into a new spreadsheet for formatting.

5) The data from the formatting spreadsheet were combined with the CXTFIT input-file command set using the program MS Word.

6) The parameters in the input file were adjusted and the file format was checked using the DOS editor.

7) The normalized concentration data were run in the CXTFIT model, and the fitted data were plotted with the observed data for comparison.

2.3.5 CXTFIT Data Fitting Model: Settings Used for this Research

This section discusses the settings in the input file used to control the model. The theoretical basis for the model was discussed in Section 1.6.3. A sample input file is presented in Figure 2.18. Titles for the various settings have been added in bold typeface for illustrative purposes, but were not part of the actual input files.

Settings:

a.   NC = 1, each experiment was considered individually.

b.   MODE = 4, Model 4, the two site, two region model was used.

c.   NDATA = 1, data from previous experiment were not considered.

d.   NREDU = 1, concentration was normalized, but time was not (to allow fitting of the seepage velocity).

e.   MIT = 30, the maximum number of iterations allowed for the program to converge was arbitrarily set to thirty initially, and adjusted upward when necessary.

74

f.   NOB = the number of data points being fitted. This varied among the experiments. The maximum allowable number of data points was modified from 90 in the original program, to 999 for this work.

g.   NSKIP = 0, executed the program.

h.   NPRINT = 0, suppressed writing of the input file to the output file.

i.   ILIMIT = 1, allowed constrained fitting of the variables between user specified limits. For unconstrained fitting of individual variables, the minimum and maximum values were both set to 0.

j.   NPULSE = 1, only one pulse per experiment.

k.   CI = 0, the initial normalized concentration of the pore fluid.

l.   CO = 1, the normalized concentration of the tracer solution at the inlet.

Variables:

a.   Velocity; The velocity of the interstitial pore water. The initial value for this variable was estimated based on the average flow rate measured during the experiment, and the porosity of the specimen. The velocity was fit to the data, unconstrained.

b.   Dispersion Coefficient; The initial value was set at the theoretical lower limit, the coefficient of molecular diffusion for NaCl. The dispersion coefficient was also fit to the data, unconstrained.

c.   Retardation Factor; NaCl is a theoretically conservative tracer, thus this variable was held constant at one.

d.   Pulse; The duration of the pulse. The initial value of Pulse was estimated as the calculated number of pore volumes of tracer that were introduced to the specimen, based on the average measured flow rate and the timed duration of the pulse. Although the pulse duration was calculated based on experimental data, this

variable was fitted, unconstrained, to ensure that conservation of mass was satisfied by the model.

e.   Beta, the ratio of the mobile region porosity to the total porosity. The initial value was set to 0.5, which assumed that the mobile region is one half of the total porosity. This variable was fit, unconstrained, to the data.

f.   Omega, a normalized coefficient describing the rate of contaminant transport between the mobile and immobile regions. The initial value was set to one, indicating that the transfer rate was assumed to be directly proportional to the ratio of the liquid flux density in the specimen to the specimen length. This variable was also fit, unconstrained to the data.

DISPLAY RANGE	MAX READING	RESOLUTION	15 - 30 °C AMBIENT	Accuracy (% Full Scale) 0 - 15 °C 30 - 45 °C AMBIENT
0 - 20.00 micromho	19.99	0.01 micromho	0.25	0.6
0 - 200.0 micromho	199.9	0.1 micromho	0.25	0.6
0 - 2000 micromho	1999	1 micromho	0.25	0.6
0 - 20.00 millimho	19.99	0.01 millimho	0.25	0.6
0 - 200.0 millimho	199.9	0.1 millimho	0.25	0.6
0 - 2000 millimho	1999	1 millimho	1.00	2.0

Table 2.1: Performance of YSI Model 35 Conductivity Meter (YSI Incorporated)

RESISTOR NUMBER	RESISTANCE
1	100 OHMS
2	1 KILO-OHM
3	10 KILO-OHMS
4	100 KILO-OHMS
5	1 MEGA-OHM

Table 2.2: MIT Conductivity Meter Resistors

RESISTOR NUMBER	MEASURED RESISTANCE
1	100.32 OHMS
2	1.0008 KILO-OHMS
3	10.0047 KILO-OHMS
4	100.04 KILO-OHMS
5	1.00011 MEGA-OHMS

Table 2.3: Measured Resistance of Relay Box Resistors
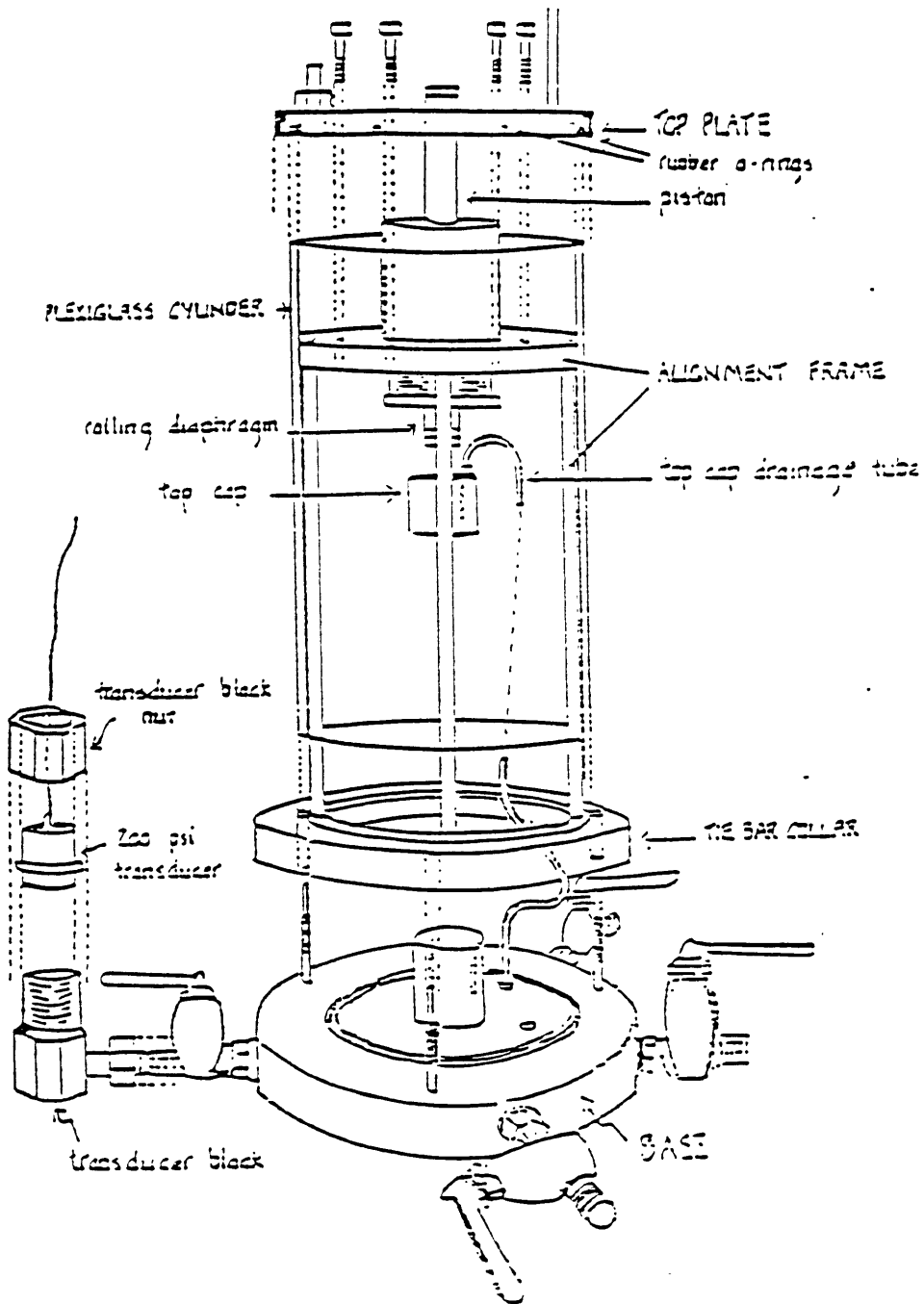
Figure 2.1   Standard MIT Triaxial Cell (from Hadge, 1979)
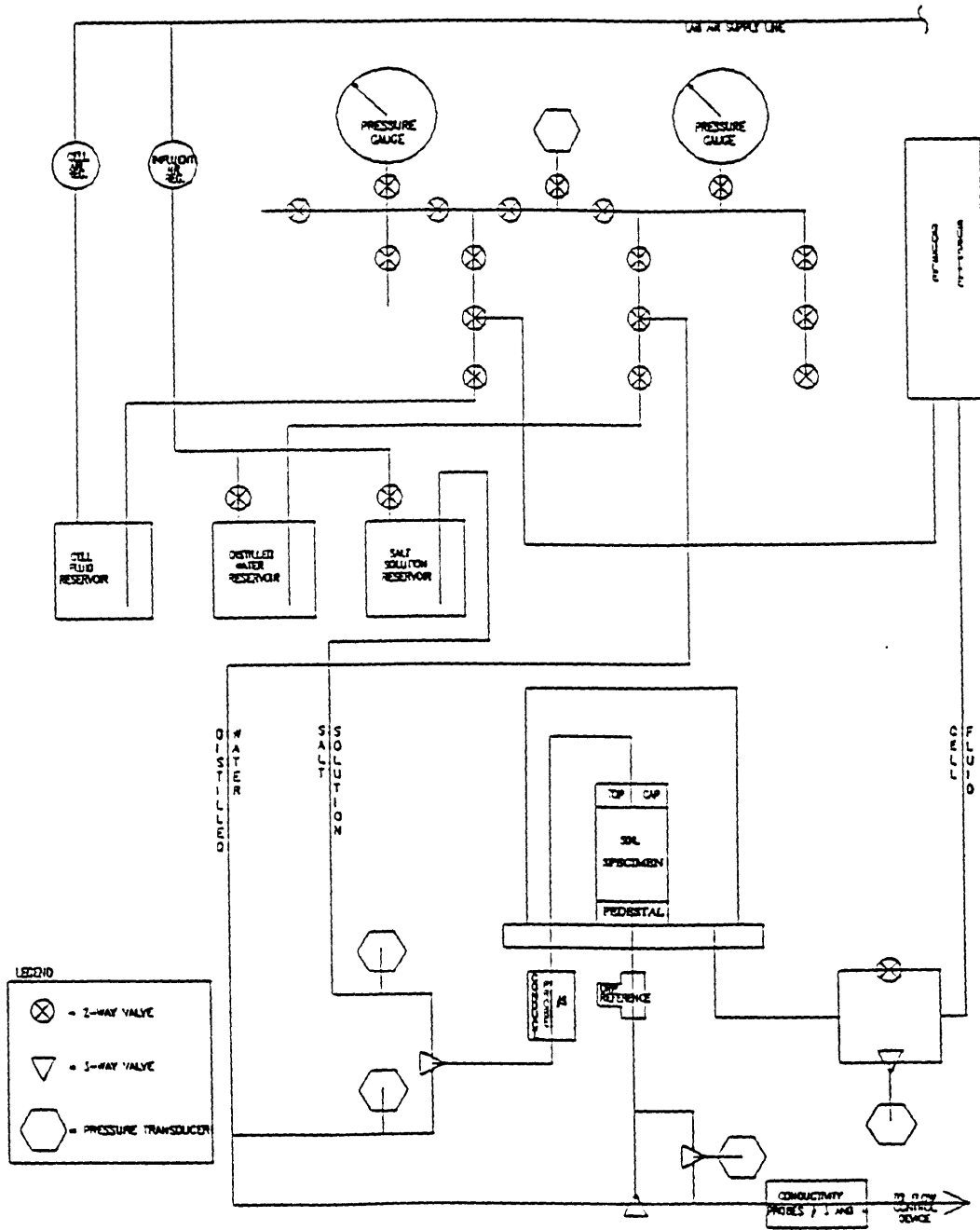
Figure 2.2   Diagram of the Manifold Control System
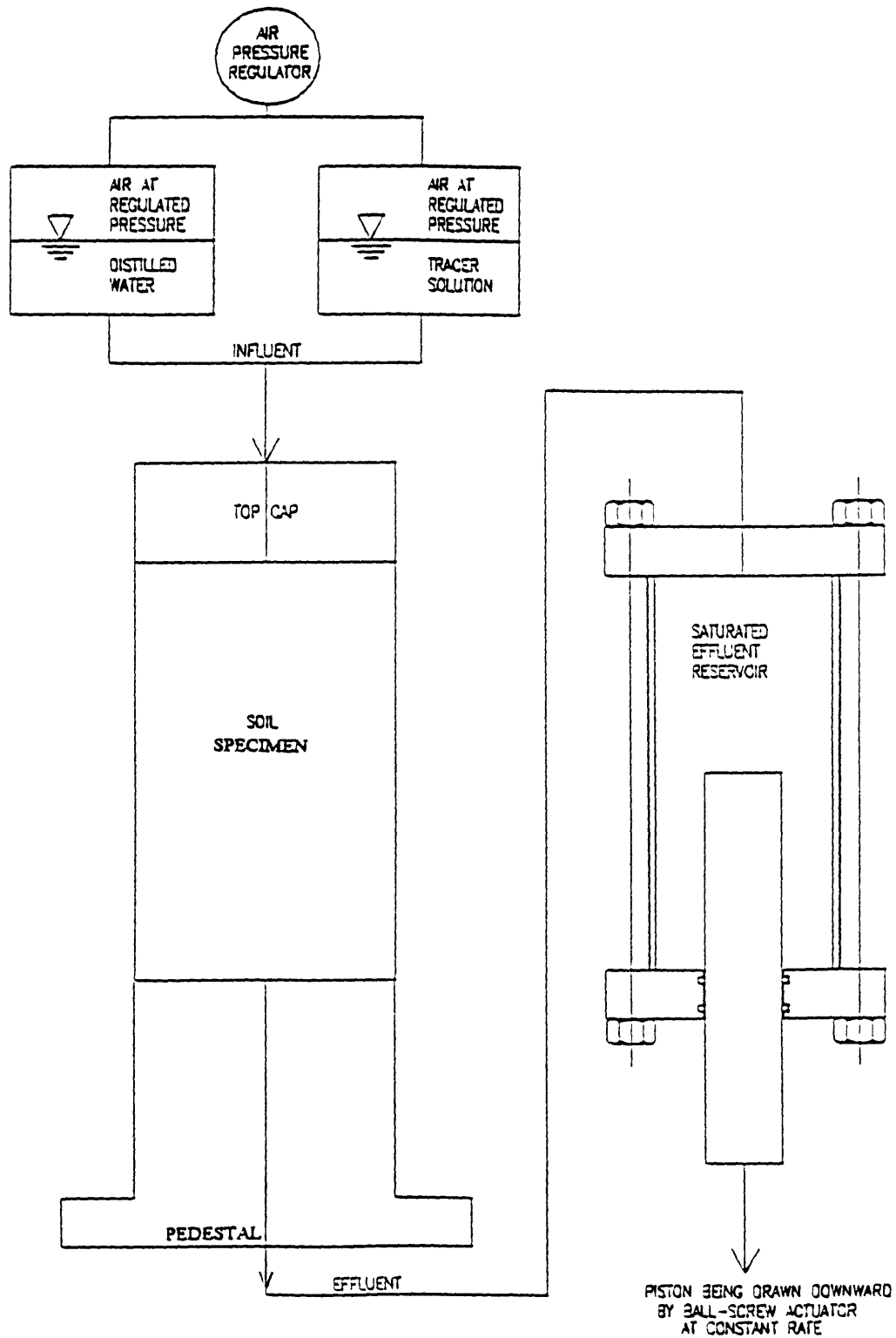
Figure 2.3   Diagram of the Flow Control System
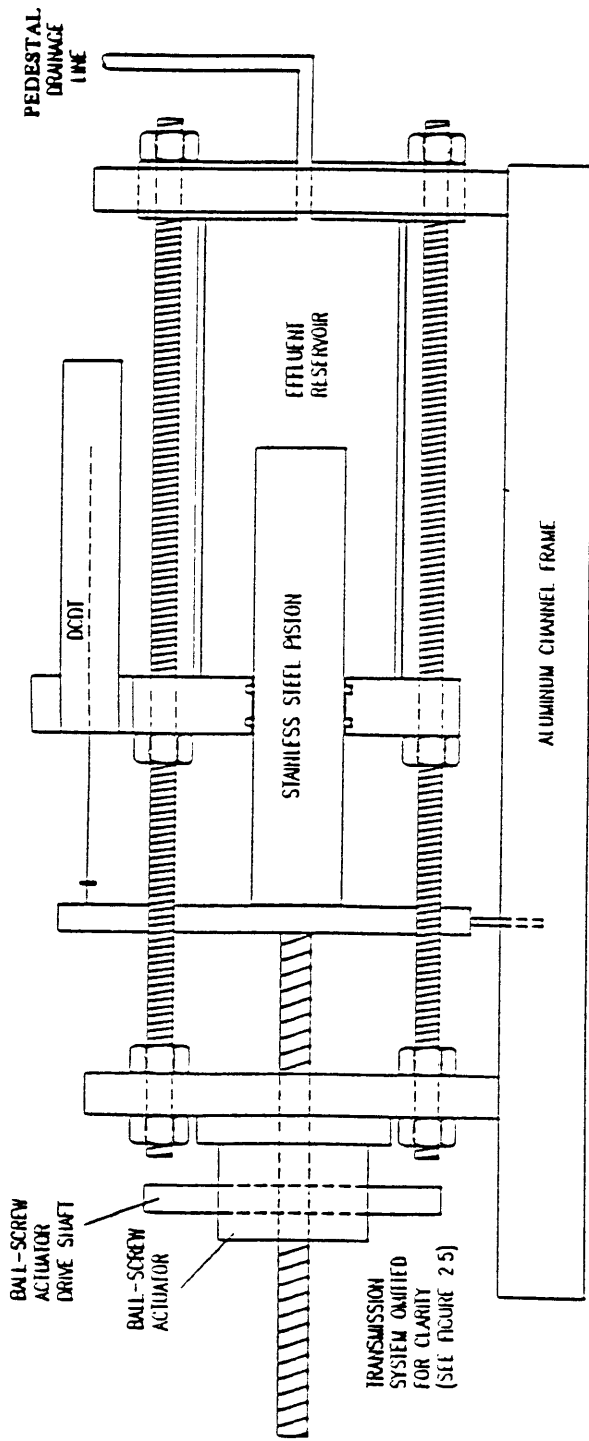
Figure 2.4   Standard MIT volume control device

81

Ball-Screw Actuator Drive Shaft

Gear E
32 pitch, 16 tooth
spur gear

Gear F
32 pitch, 80 tooth
spur gear

32 pitch, 20 tooth
4 thread
worm gear
Gear B

32 pitch
single thread
worm
Gear C

32 pitch, 80 tooth
single thread
worm gear
Gear D

32 pitch
4 thread
worm
Gear A
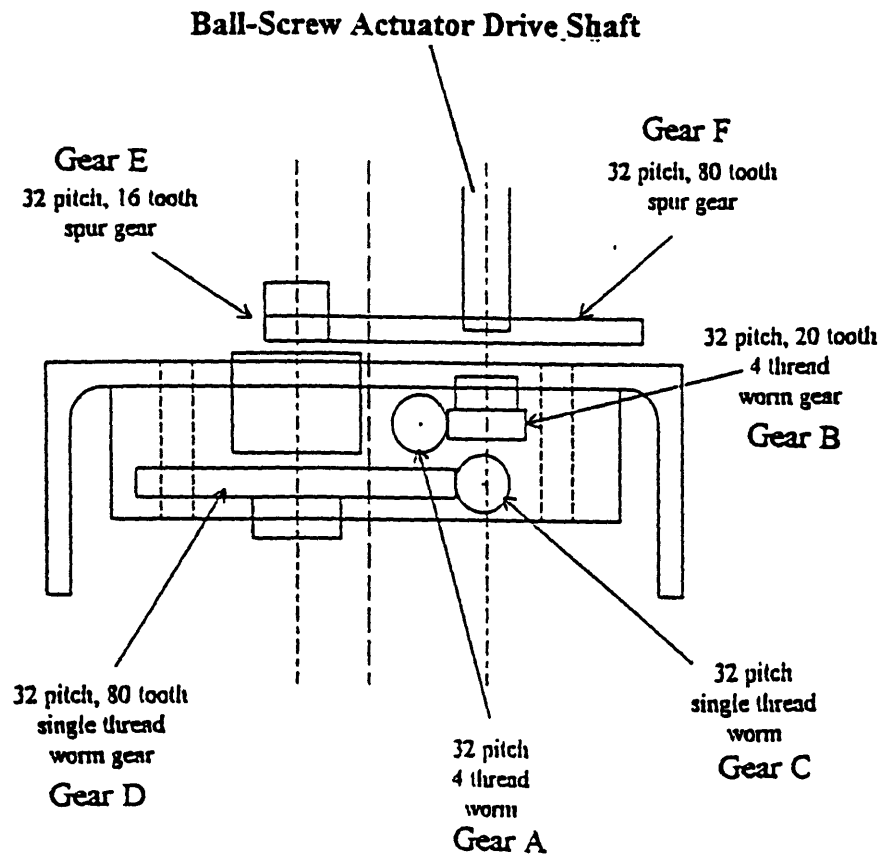
Figure 2.5   Transmission system for Flow-Control Device (Drawn by Steven Rudolf)

TRANSDUCERS FOR:
pH
OXIDATION-REDUCTION POTENTIAL
CONDUCTIVITY
TEMPERATURE

EPOXY

STAINLESSS STEEL

SEATING SURFACE

O-RING GROOVES

DRAINAGE LINE WITH
pH REFERENCE

LINES TO DATA ACQUISITION
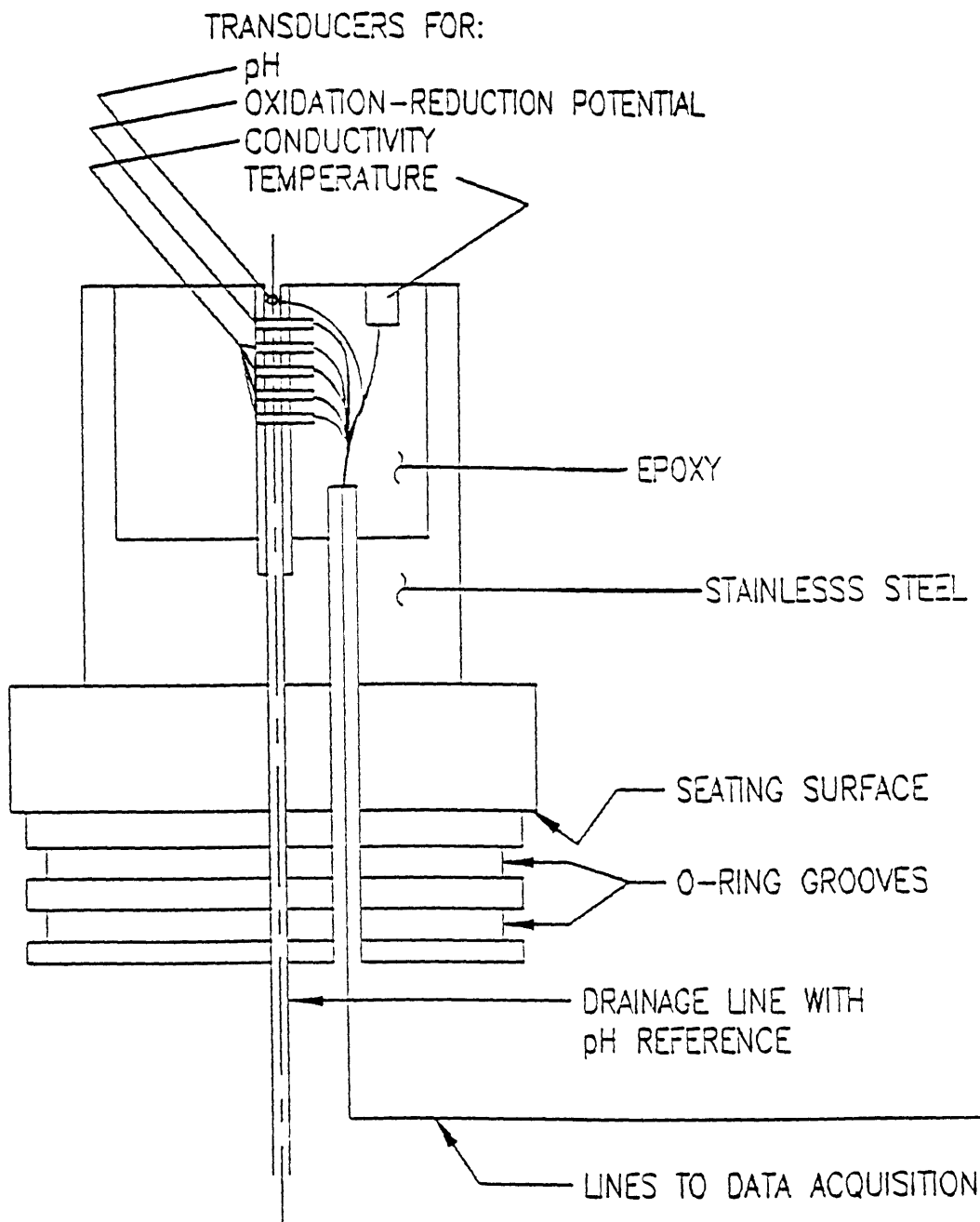
Figure 2.6   Section of Removable Pedestal
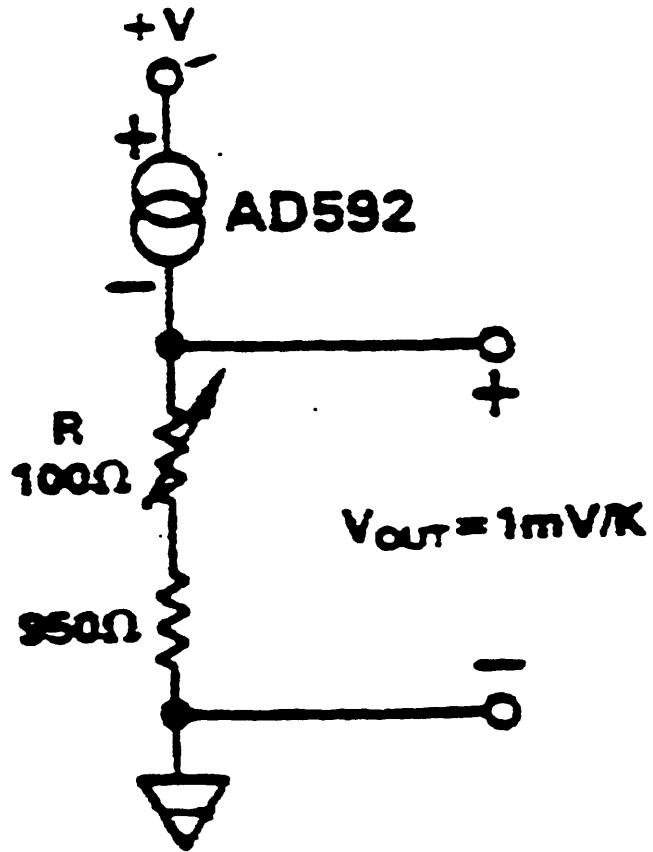
Figure 2.7   Diagram of Temperature Transducer Circuit (Analog Devices)
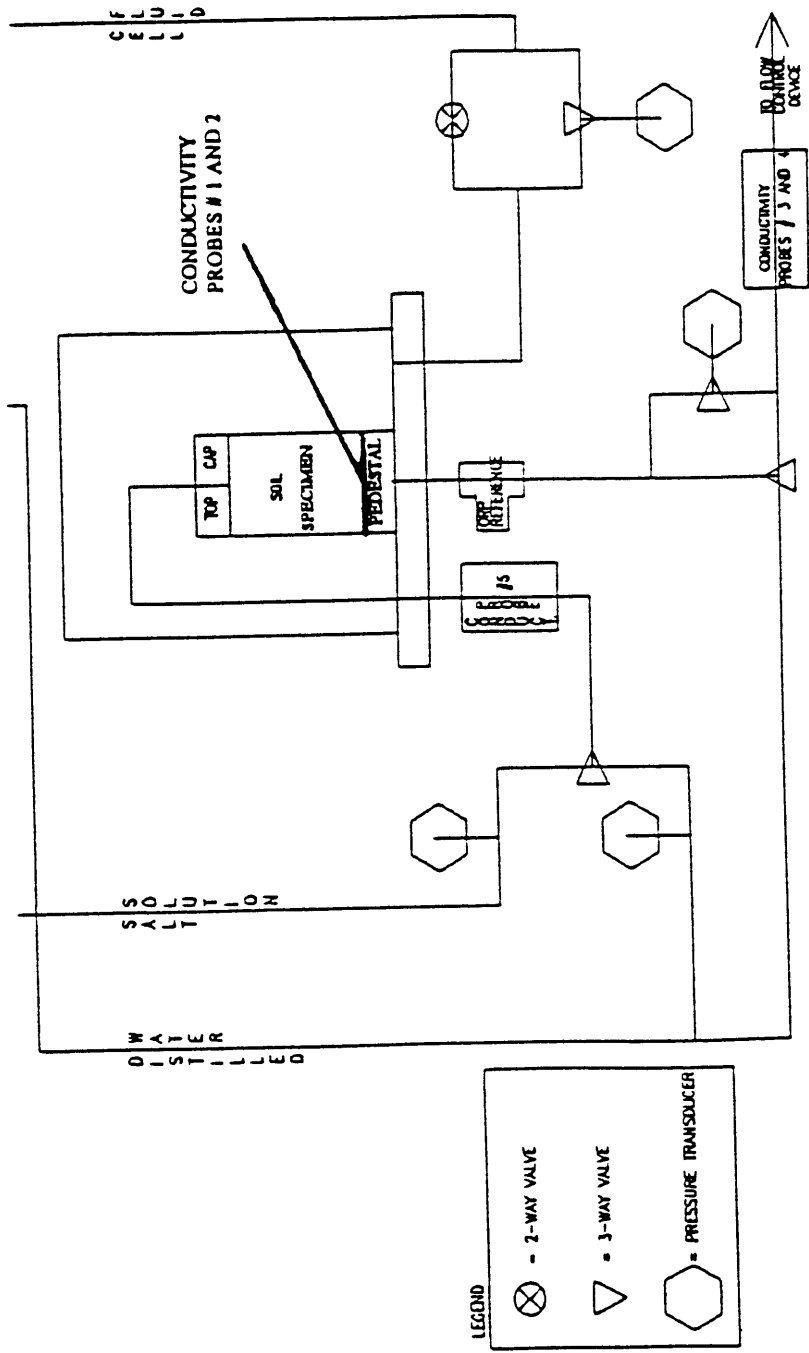
Figure 2.8   Location of Conductivity Probes

SWAGELOCK
FITTING

O-RING

CAST EPOXY

CONDUCTIVITY PINS

TO
CONDUCTIVITY
METER
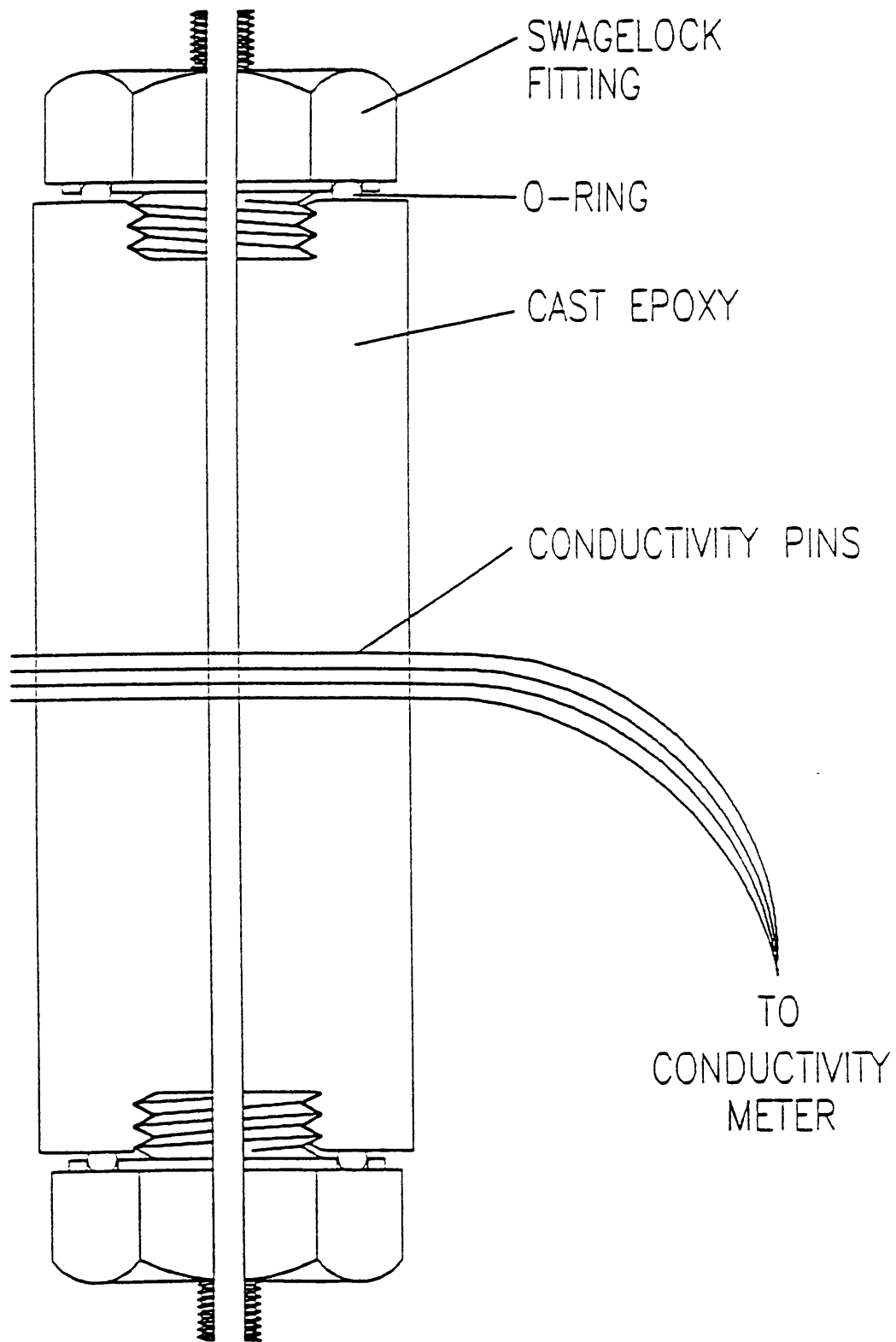
Figure 2.9   Section of In-Line Conductivity Probe

pH PROBE (GLASS TIP)

EFFLUENT DRAINAGE PATH

TEMPERATURE TRANSDUCER

4 CONDUCTIVITY PINS
AND 1 ORP PIN

CAST EPOXY

STAINLESS STEEL
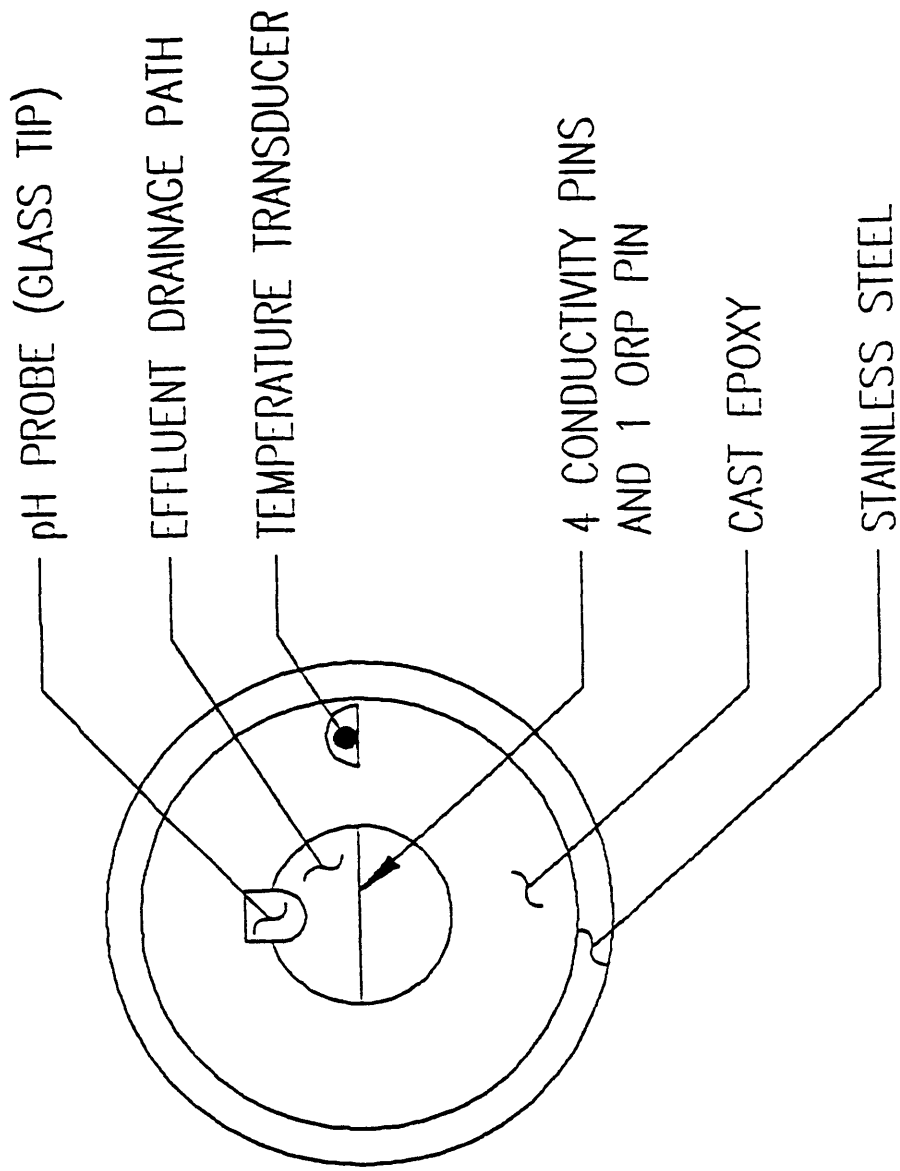
Figure 2.10   Plan View of Drainage Line Through Pedestal

INPUT VOLTAGE

CURRENT

REFERENCE
RESISTANCE

OUTPUT VOLTAGE

CONDUCTING
SOLUTION

SOLUTION
RESISTANCE

PIN #1

PIN #2

$Vin = I * (Rr + Rs)$

$Vout = I * Rs$

$Vout/Vin = Rs/(Rr + Rs)$
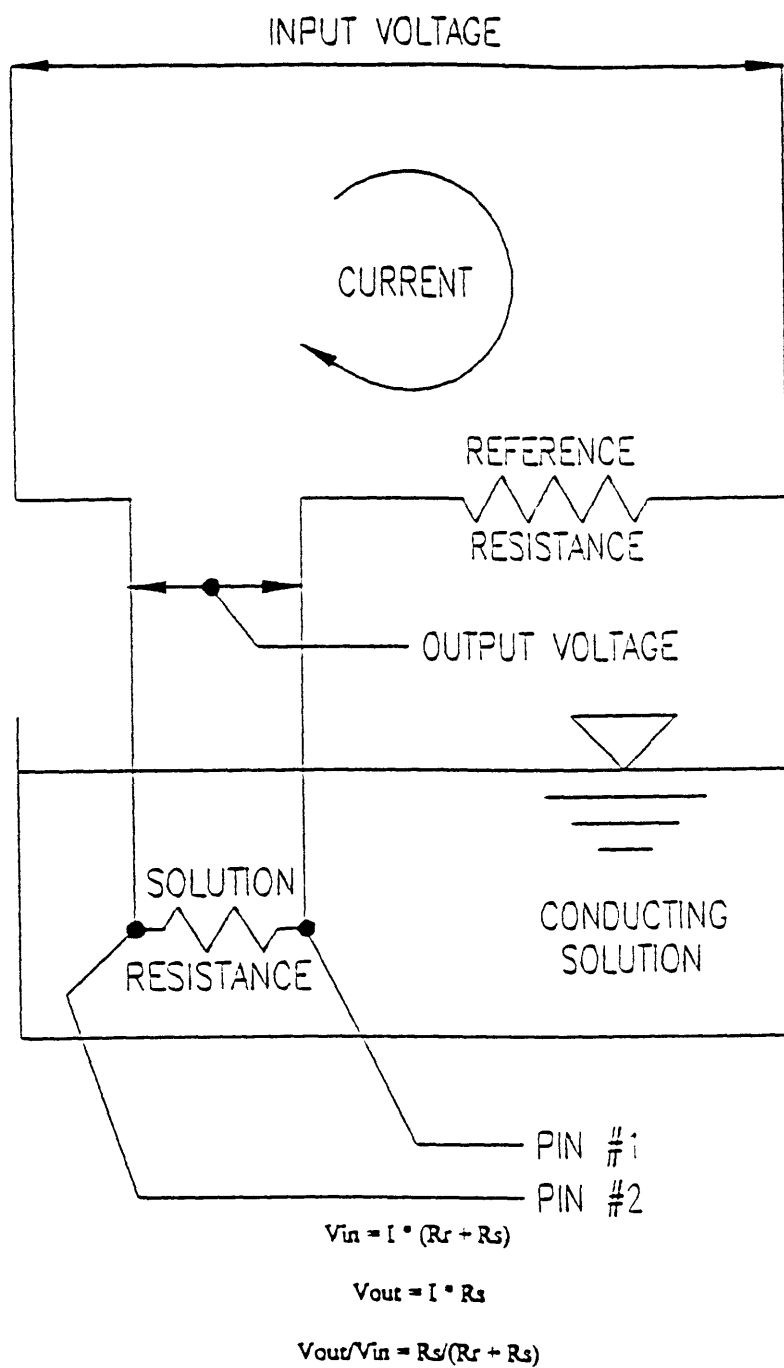
Figure 2.11   Schematic of 2-Pin Probe Operation
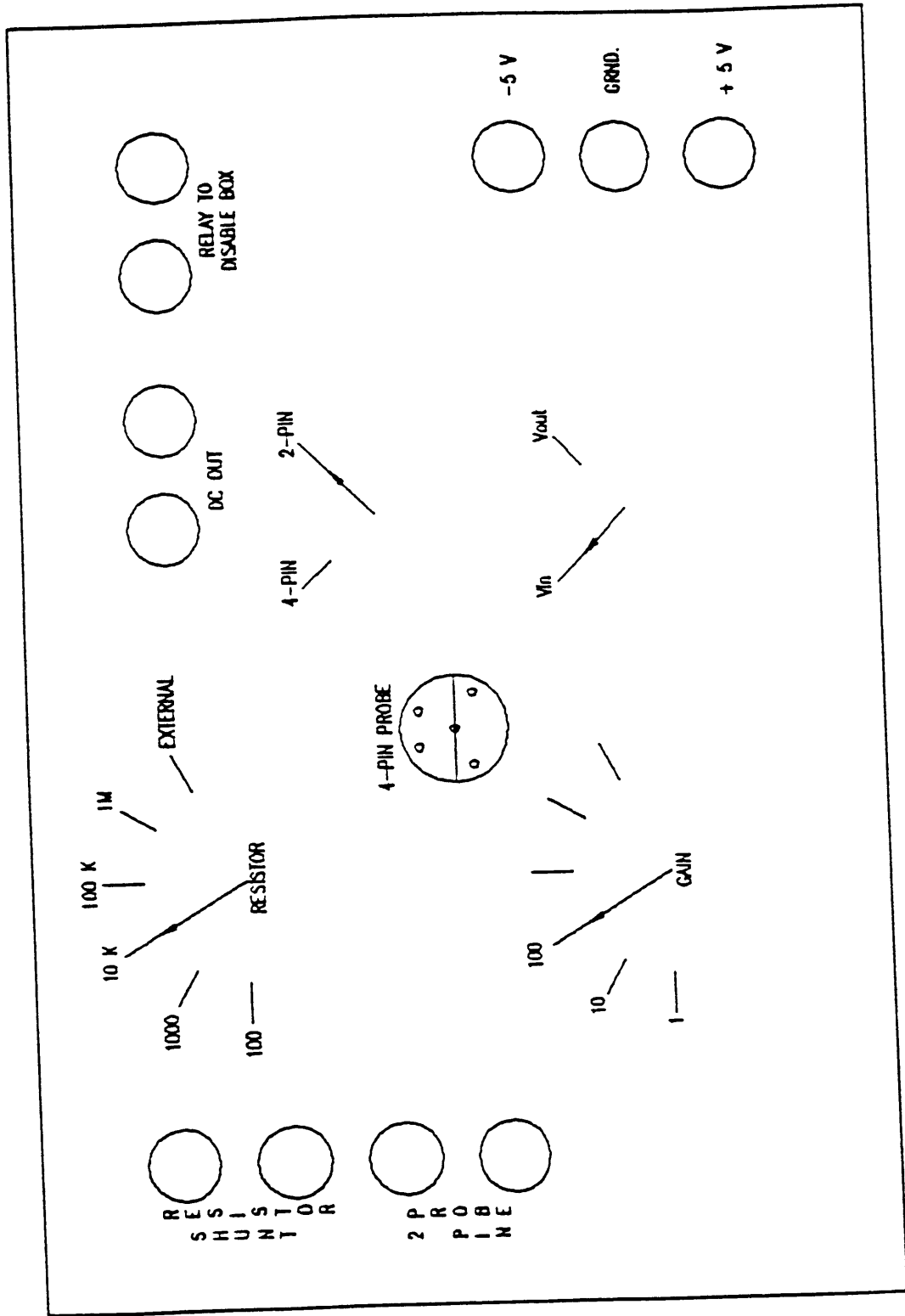
Figure 2.12   Diagram of MIT Single Channel Conductivity Meter (SCCM)
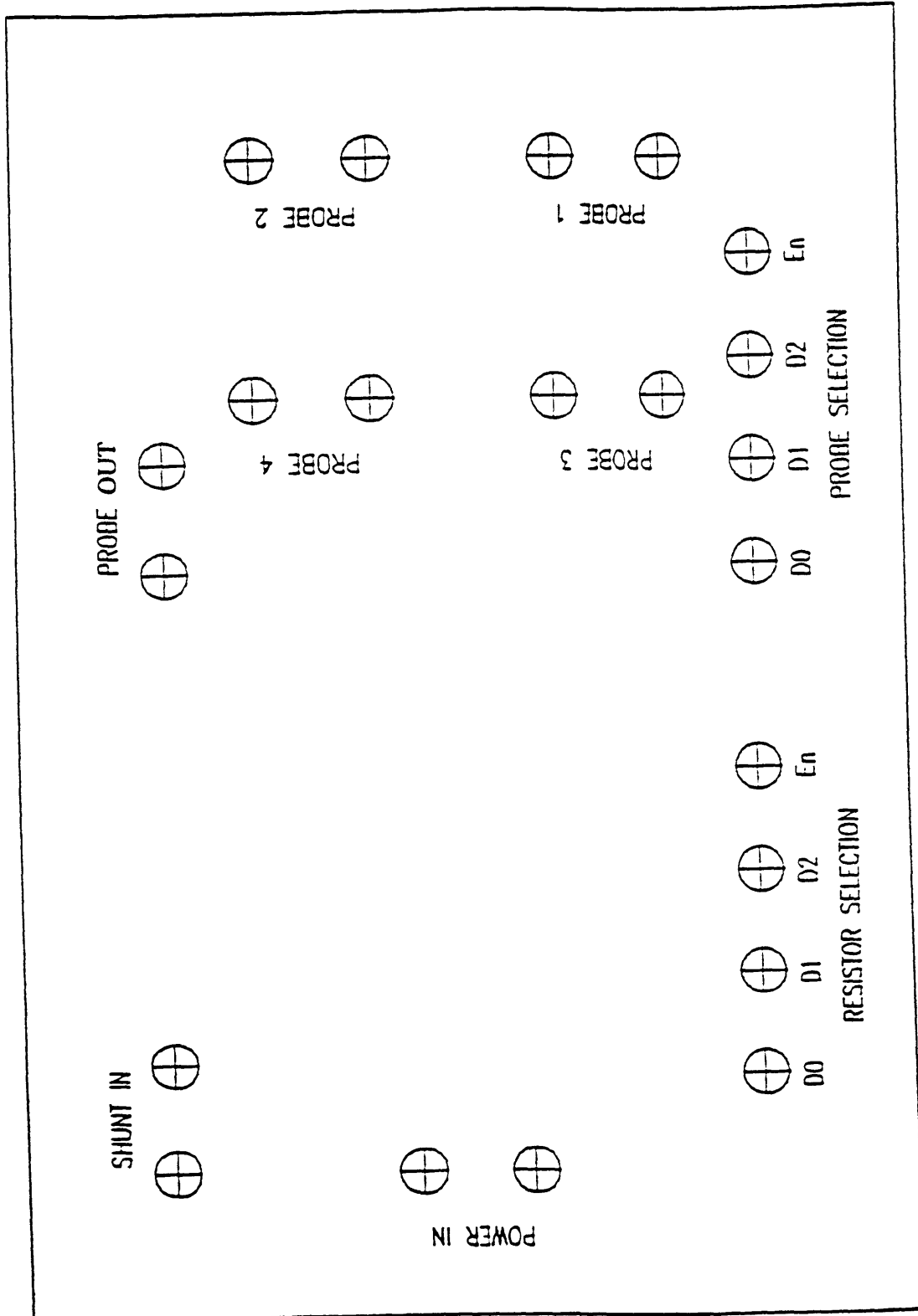
Figure 2.13   Diagram of MIT Relay Box for Conductivity Meter

INNER MEMBRANE

OUTER MEMBRANE

SOIL
SAMPLE

O-RINGS

Pedestal
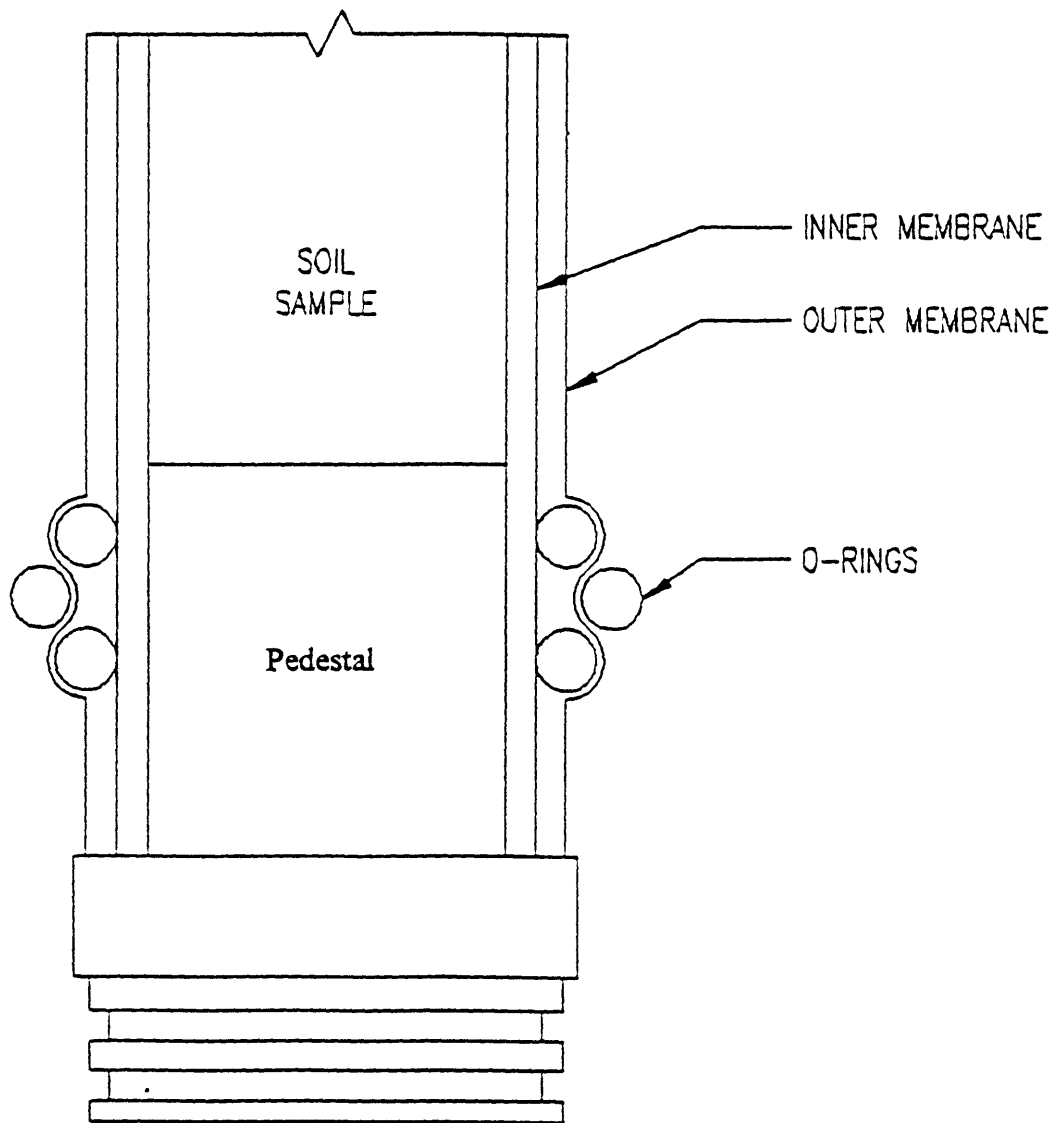
Figure 2.14   Diagram of O-ring Placement

Figure 2.15.a Data Reduction Spreadsheet

perm1123g1.dat

GAIN MULTIPLYER: 10

From Lab PC File

A	probe 1	probe 2	probe 3	probe 4
60	0.0037	0.0035	0.0243	0.0055
159	0.0032	0.0032	0.0238	0.0052
186	0.0032	0.0031	0.0227	0.0049
212	0.003	0.0029	0.0234	0.0047
240	0.003	0.003	0.0231	0.0046
300	0.0029	0.0029	0.0227	0.0042
360	0.0028	0.0028	0.0223	0.0039
420	0.0028	0.0028	0.0222	0.0039
480	0.0028	0.0028	0.0223	0.0039
540	0.0028	0.0028	0.0222	0.0039
600	0.0026	0.0026	0.022	0.0017
660	0.0027	0.0029	0.0218	0.0036
720	0.0237	0.0411	0.0416	0.0443
780	0.3978	0.4668	0.6836	1.0192
840	0.6455	0.6867	1.4197	1.6111
900	0.796	0.7961	1.8527	2.1048

From Central Data Acquisition System

07:41:45 seconds	probe 6 volts	temp. volts	lvdt volts	vln volts	pore pressure volts	cell pressure volts	salt pressure volts	back pressure volts	vln volts
0	-0.00053	0.29285	3.0743	5.4388	0.038855	-0.033632	-0.030318	-0.030118	5.4183
60	-0.0005	0.29284	2.9842	5.4388	0.038842	-0.033630	-0.030319	-0.030116	5.4183
120	-0.00048	0.29283	2.887	5.4388	0.038837	-0.033622	-0.030326	-0.030114	5.4182
180	-0.00046	0.29284	2.8009	5.4388	0.038839	-0.033619	-0.030322	-0.030121	5.4183
240	0.25761	0.29279	2.716	5.4388	0.038795	-0.033618	-0.030282	-0.030169	5.4183
300	0.26451	0.29286	2.629	5.4388	0.038801	-0.033642	-0.030284	-0.030168	5.4183
360	0.26259	0.29279	2.5447	5.4388	0.038799	-0.033621	-0.030286	-0.030177	5.4183
420	0.26572	0.29286	2.4569	5.4388	0.038801	-0.033628	-0.030279	-0.030169	5.4183
480	0.2634	0.29277	2.3776	5.4388	0.038800	-0.033618	-0.030283	-0.030168	5.4183
540	0.26608	0.29286	2.283	5.4388	0.038797	-0.033612	-0.030297	-0.030159	5.4183
600	0.26714	0.29286	2.1997	5.4388	0.038801	-0.033618	-0.030289	-0.030153	5.4183
660	0.26315	0.2928	2.1167	5.4388	0.038801	-0.033630	-0.030280	-0.030161	5.4183
720	0.26211	0.29283	2.0314	5.4388	0.038797	-0.033620	-0.030282	-0.030149	5.4183
780	0.26042	0.29282	1.9468	5.4388	0.038803	-0.033610	-0.030282	-0.030151	5.4183
840	0.00489	0.29282	1.859	5.4389	0.038838	-0.033614	-0.030303	-0.030117	5.4183
900	0.00083	0.29281	1.7737	5.4389	0.038843	-0.033623	-0.030305	-0.030109	5.4183

I14 = Gain multiplier needed to convert from Volts to Conductivity

	R	S	T	U	V		Y	Z	AA	AB	AC
1	PRESSURE TRANSDUCERS						salt start	tube vol	pore vol		T18/T25 =
2	ZERO	-1.53	8.3	0.19	0.12		(sec)	(cm^3)	34.96 CM^3		0.860536
3	ZEROVin	5.418	5.418	5.418	5.418		180	1.29			
4	C.F.	-701.462	-700.4918	-701.181	-702.795		FLOW VOLUME (ML)	FLOW RATE (ML/S)	PORE VOLUMES (ml)		TEMP deg C
6		CELL P KSC	PORE P KSC	BACK P KSC	SALT P KSC						
7							time to top of sample		205.7	sec	23.1
8		4.171	3.914	3.917	3.936		0.00		0.000		23.1
9		4.170	3.915	3.917	3.938		3.08	0.051	-0.210		23.1
10		4.170	3.915	3.917	3.936		6.12	0.051	-0.123		23.1
11		4.166	3.858	3.924	3.920		9.36	0.052	-0.037		23.1
12		4.170	3.913	3.924	3.932		12.46	0.052	0.049		23.1
13		4.170	3.913	3.922	3.932		15.60	0.052	0.136		23.1
14		4.170	3.915	3.923	3.933		18.71	0.052	0.222		23.1
15		4.168	3.915	3.922	3.932		21.72	0.052	0.309		23.1
16		4.170	3.912	3.923	3.932		24.78	0.052	0.395		23.1
17		4.169	3.916	3.922	3.932		27.86	0.052	0.482		23.1
18		4.170	3.911	3.924	3.931		30.86	0.051	0.568		23.1
19		4.169	3.915	3.925	3.930		33.63	0.051	0.655		23.1
20		4.169	3.915	3.925	3.930		36.49	0.051	0.741		23.1
21		4.170	3.915	3.921	3.931		39.60	0.051	0.828		23.1
22		4.169	3.913	3.916	3.935		42.18	0.050	0.914		23.2
23		4.169	3.914	3.915	3.935		44.82	0.050	1.000		23.2

$S23 = [(M23/P23) - (S2/(100*S3))]*S4$

T, U, V23 SIMILAR TO S-23

$Y23 = \{[J8/K8 - J23/K23]*CALIBRATION\ FACTOR\ (4.862711)\}*(AREA\ OF\ PISTON\ (2.074\ IN.^2))*16.387\ ml/in^3$

$Z23 = (Y23-Y22)/TIME\ INCREMENT\ (60\ Sec)$

$AA23 = Y23/AA2$

$AC23 = I23*1000-273.15$

Figure 2.15.b Data Reduction Spreadsheet

AF23 = 10[(LOG B23)*AF3 + AF2]

AG23 = AC23*AG2

COLUMNS AH, AI, AJ, AK, SIMILAR TO AG

AL23 = Σ(AG23 through AK23)

AM23 = AF23/[AC3*(1+AL23*(AC23-18))]

AN23 = AN2*AM23[AN5]

COLUMNS AO THROUGH AS SIMILAR TO AN

AT23 = Σ(AN23 through AS23)

AU2 = THE MINIMUM VALUE IN COLUMN AT

AU23 = (AT23 - AU$2)/AT7

AV23 = [(AU23+AU22)/2]*(G9-G8)

AW23 = AW22+AV23

Figure 2.15.c Data Reduction Spreadsheet

94

SEE FIGURE 2.15.c FOR CALCULATIONS

Figure 2.15.d Data Reduction Spreadsheet

SEE FIGURE 2.15.c FOR CALCULATIONS

Figure 2.15.e Data Reduction Spreadsheet

SEE FIGURE 2.15.c FOR CALCULATIONS

Figure 2.15.f Data Reduction Spreadsheet

SEE FIGURE 2.15.c FOR CALCULATIONS

Figure 2.15.g Data Reduction Spreadsheet

	ED	EE	EF	EG	EH	EI	EJ	EK	EL	EM	EN
	pore volumes (0 = when solute reaches sample)	PROBE 1 NORM CONC. % (WT) NACL IN WATER	PROBE 2 NORM CONC. % (WT) NACL IN WATER	PROBE 3 NORM CONC. % (WT) NACL IN WATER	PROBE 4 NORM CONC. % (WT) NACL IN WATER	PROBE 5 NORM CONC. % (WT) NACL IN WATER	area under curve PROBE 1	area under curve PROBE 2	area under curve PROBE 3	area under curve PROBE 4	area under curve PROBE 5
8		7.1E-04	6.7E-04	2.1E-05	9.3E-04	2.7E-05	0.0E+00	0.0E+00	0.0E+00	0.0E+00	0.0E+00
9	-2.1E-01	7.1E-04	6.7E-04	2.1E-05	9.3E-04	2.1E-05	-1.5E-04	-1.4E-04	-4.3E-06	-2.0E-04	-5.0E-06
10	-1.2E-01	8.1E-04	6.7E-04	1.6E-05	9.3E-04	9.6E-06	-8.4E-05	-8.3E-05	-2.8E-06	-1.1E-04	-3.7E-06
11	-3.7E-02	8.1E-04	6.7E-04	1.6E-05	9.3E-04	2.9E-05	-1.4E-05	-2.5E-05	-1.4E-06	-3.4E-05	-2.0E-06
12	4.9E-02	7.1E-04	6.7E-04	1.5E-05	9.3E-04	2.7E-05	5.2E-05	3.3E-05	-7.9E-08	4.6E-05	4.4E-07
13	1.4E-01	8.1E-04	7.7E-04	1.5E-05	9.3E-04	2.1E-05	1.2E-04	9.5E-05	1.3E-06	1.3E-04	2.5E-06
14	2.2E-01	8.1E-04	7.7E-04	1.6E-05	9.3E-04	2.2E-05	1.9E-04	1.6E-04	2.6E-06	2.1E-04	4.4E-06
15	3.1E-01	8.1E-04	6.7E-04	1.0E-05	9.3E-04	1.5E-05	2.6E-04	2.2E-04	3.7E-06	2.9E-04	6.0E-06
16	4.0E-01	8.1E-04	6.7E-04	1.0E-05	9.3E-04	5.5E-06	3.3E-04	2.8E-04	4.6E-06	3.7E-04	6.9E-06
17	4.8E-01	8.1E-04	6.7E-04	0.0E+00	9.3E-04	9.2E-06	4.0E-04	3.4E-04	5.0E-06	4.5E-04	7.5E-06
18	5.7E-01	2.6E-04	3.1E-07	1.5E-05	7.7E-04	0.0E+00	4.5E-04	3.7E-04	5.7E-06	5.2E-04	7.9E-06
19	6.5E-01	1.1E-01	2.0E-01	8.7E-02	2.3E-01	2.6E-05	5.3E-03	8.8E-03	3.8E-03	1.1E-02	9.0E-06
20	7.4E-01	3.3E-01	3.7E-01	3.3E-01	3.8E-01	1.5E-02	2.5E-02	3.3E-02	2.2E-02	3.7E-02	6.6E-04
21	8.3E-01	4.8E-01	5.3E-01	5.0E-01	5.3E-01	1.5E-01	6.0E-02	7.2E-02	5.8E-02	7.6E-02	7.6E-03
22	9.1E-01	5.8E-01	6.1E-01	6.1E-01	6.3E-01	3.6E-01	1.1E-01	1.2E-01	1.1E-01	1.3E-01	3.0E-02
23	1.0E+00	6.7E-01	7.0E-01	6.9E-01	7.1E-01	5.3E-01	1.6E-01	1.8E-01	1.6E-01	1.8E-01	6.8E-02

SUMMARY COLUMNS USED FOR EXPORTING (e.g. TO SIGMAPLOT)

Figure 2.15.h   Data Reduction Spreadsheet

99

	EP	EQ	ER	ES	ET	EU	EV
1	TEST SUMMARY INFORMATION						
2							
3	DATE:	1-04-96	DATA ACQ	TEST NAME:		104pt1	
4							
5	SAMPLE TYPE	PEAT 1 TEST 1					
6							
7	SAMPLE WT			21.07	g	area (in^2)=	1.51
8	SAMPLE VOLUME			20.72	cc	length (in) =	0.84
9	Gs			1.13			
10	W%			5.73	(FRACTION OF Ms)		
11	PORE VOLUME			17.95	cc		
12	POROSITY			0.87			
13							ksc
14	EFFECTIVE STRESS					avg salt	3.953
15	SALT			0.179	ksc	avg back	3.941
16	BACK P.			0.184	ksc	avg pore	3.805
17	GRADIENT					avg cell	4.057
18	SALT			69.2			
19	BACK P.			64.2			
20							
21	HYDRAULIC CONDUCTIVITY						
22	SALT			1.1E-07	cm/sec		
23	BACK P.			1.2E-07	cm/sec		
24							
25	AVERAGE FLOW			7.4E-05	ml/sec		
26	SPECIFIC DISCHARGE			7.6E-06	cm/sec		
27	AVG PORE WATER VELOCITY			8.7E-06	cm/sec		
28							
29	PORE SOLUTION			0.1 M NaCl			
30	PULSE DURATION			10	min		
31	AREA UNDER INFLUENT CURVE			0.0043			
32	AREA UNDER EFFLUENT CURVE			0.0021			
33	PERCENT RECOVERED			48.8			
34							
35							

ES9 = Calculated from water content, weight of dry solids and total volume

ES10 = Calculated from trimmings, or assumed = 0 for sand

ES11 = ES8-[ES7/(1+ES10)]/ES9

ES15 = EV17-(EV14+EV16)/2

ES16 = EV17-(EV15+EV16)/2

ES18 = ((EV14-EV16)/[((1+AT7)/100) g/cm^3)/(EV8*2 54)])*1000

ES19 = ((EV15-EV16)/[(1 g/cm^3)/(EV8*2 54)])*1000

ES22 = AVERAGE OF COLUMN Z /(SAMPLE AREA (cm^2) * ES18)

ES23 = AVERAGE OF COLUMN Z /(SAMPLE AREA (cm^2) * ES19)

ES25 = AVERAGE COLUMN Z

ES26 = ES25/SAMPLE AREA (cm^2)

ES27 = ES25/[SAMPLE AREA (cm^2) * ES12]

ES31 = TOTAL INTEGRATED AREA FROM PROBE 5

ES32 = AVERAGE TOTAL INTEGRATED AREA, PROBES 1 - 4

ES33 = (ES32/ES33)*100

Figure 2.15.i   Data Reduction Spreadsheet

$$\frac{\sigma(T)}{\sigma(18)} = 1 + b(T - 18)$$

$$b = \sum_{N=0}^{4} a_N \, T^N$$

$$a_0 = 2.1179818 \times 10^{-2}$$

$$a_1 = 7.8601061 \times 10^{-5}$$

$$a_2 = 1.5439826 \times 10^{-7}$$

$$a_3 = -6.2634979 \times 10^{-9}$$

$$a_4 = 2.2794885 \times 10^{-11}$$

Figure 2.16   Numerical Function to Adjust Conductivity Values for Temperature (Head, 1983)

$$C = \sum_{N=0}^{5} a_N \, \sigma(25)^{N/2}$$

$$a_0 = 0.01498478$$
$$a_1 = -0.01458078$$
$$a_2 = 0.05185288$$
$$a_3 = 0.00206994$$
$$a_4 = -0.00010365$$
$$a_5 = 0.00006269$$

Figure 2.17   Numerical Function to Fit Conductivity Data to Concentration Values (Head, 1983)

```
NC
 1 MODE      NDATA      NREDU      MIT       MOB      NSKIP    NPRINT
   4          1          1         30        141        0        0


   V.....     D.....     R.....    PULSE.    BETA..    OMEGA.
   0.0104  0.0000002      1.0      600.0      1.0       2.5
ILIMIT
   1    0      1          0         0         1         1
         0.0        0.0       0.0       0.0       1.0       0.0
         0.0        0.0       0.0       0.0       1.0       2.508
   CI          CO        MPULSE
   0.00000     1.0         1
OBSERVED    DIST FROM
CONCENTRAT.  SOURCE      TIME
2.037E-05    6.6548        0
1.986E-05    6.6548       60
2.026E-05    6.6548      120
1.972E-05    6.6548      180
1.968E-05    6.6548      240
1.973E-05    6.6548      300
1.968E-05    6.6548      360
1.544E-05    6.6548      420
1.862E-05    6.6548      480
0.01064816   6.6548      540
0.28506897   6.6548      600
0.47934739   6.6548      660
0.59474321   6.6548      720
0.69255612   6.6548      780
0.76447797   6.6548      840
0.81539897   6.6548      900
0.85430321   6.6548      960
0.88015735   6.6548     1020
0.8958871    6.6548     1080
0.87699915   6.6548     1140
0.70693946   6.6548     1200
0.50128577   6.6548     1260
0.36185506   6.6548     1320
0.25835399   6.6548     1380
0.17720681   6.6548     1440
0.1265945    6.6548     1500
0.04020803   6.6548     1560
0.02484564   6.6548     1620
0.01440385   6.6548     1680
0.00853661   6.6548     1740
0.00535836   6.6548     1800
0.00089611   6.6548     1860
0.0004684    6.6548     1920
0.00022858   6.6548     1980
0.00012586   6.6548     2040
0.00006098   6.6548     2100
0.00002849   6.6548     2160
```

Figure 2.18   Sample CXTFIT Input File

CHAPTER 3

EXPERIMENTAL RESULTS

3.1 TESTING PROGRAM

This testing program was conducted primarily to evaluate the equipment and procedures discussed in Chapter 2. Throughout the testing process, modifications were made to overcome problems as they were discovered. Section 3.3, below, will discuss these problems, and their effects on the respective experiments. A series of experiments was conducted on sand to provide a preliminary evaluation of the equipment, followed by a series of experiments on wetland deposits obtained from the Wells G and H Superfund site. The experiments are summarized in Table 3.1, and discussed individually in Section 3.1.2. This chapter presents and discusses the results of the experiments that were conducted during this research program.

3.1.1 Materials Tested

3.1.1.1 Sand

The sand used for these experiments was the Type 90P silica sand obtained commercially by Mr. Sangkaran Ratnam for use in his centrifuge experiments (MIT, 1996). Tests to determine the grain size distribution, specific gravity, maximum and minimum void ratios, and hydraulic conductivity were completed by Mr. Ratnam. The grain size distribution presented in Figure 3.1 (Ratnam, 1995), indicates that the sand is relatively uniform with $D_{50} \approx 0.17$ mm. The sand has a specific gravity of 2.66, and void ratios $e_{min} = 0.73$, and $e_{max} = 0.97$. At relative densities between 54.2 % and 79.2 %, Mr. Ratnam obtained hydraulic conductivities between 7×10^{-3} and 1×10^{-2} cm/sec, respectively (the average being 8×10^{-3} cm/sec).

3.1.1.2 Wetland Deposits

The specimens used in this experiment were obtained by Mr. Jason Bialon (MIT, 1995) from the Wells G and H Superfund site. Specimen Peat 1 was obtained 20.3 cm (8 in.) from the bottom of a tube from which the label has fallen off, believed to be from boring #3, while Peat 2 was obtained 21.6 cm (8.5 in.) from the top of tube #3 from boring #1. The locations of the borings were indicated in Figure 1.6. The two specimens (Peat 1 and Peat 2) were very similar in composition, and matched the characteristics given by Bialon (1995) in his description of the Sedge Layer at the Aberjona site. The material was highly decomposed, very dark brown in color, and contained small fragments of wood as well as some greenish, stringy sedge leaves. This identification fits Bialon's boring profile, which is reproduced in Figure 3.2. The specimen location for Peat 2 is approximately 137 cm below the ground surface, which is near the bottom of the sedge layer in that profile.

3.1.2 Testing Conditions

Each experiment consisted of a 10 minute pulse of 0.1 M NaCl, followed by approximately three pore volumes of flushing. After the final pulse-type test was completed on a given specimen, a continuous-source experiment was conducted to determine the equilibrium conductivity readings for each probe. The plots from the continuous-source experiments, and the selected equilibrium values, are provided in Appendix D. The equilibrium readings were then used to normalize the data from the pulse-type experiments.

Sand 1 was subject to two pulse-type experiments. Both were conducted under similar conditions; with effective stresses of approximately 0.25 ksc, and with pore-fluid velocities of approximately 0.01 cm/sec. These two experiments were intended to yield similar results.

Sand 2 was subject to three pulse-type experiments, all at approximately 0.25 ksc effective stress. Each sequential experiment was conducted at an increased pore-fluid velocity to study velocity effects on hydraulic parameters. Test 1 was conducted at 0.001 cm/sec, Test 2 at 0.003 cm/sec, and Test 3 at 0.007 cm/sec.

Peat 1 was subject to two pulse type experiments, at differing pore fluid velocities and effective stresses. Test 1 was conducted at an effective stress of approximately 0.18 ksc, and a pore fluid velocity of approximately 9×10^{-6} cm/sec. Increasing the pore fluid velocity to approximately 5×10^{-5} cm/sec for the second experiment caused the effective stress to increase to approximately 1.5 ksc (due to the increased gradient). Thus, effective stresses and hydraulic gradients were not independently controlled.

Peat 2 was also subject to two pulse-type experiments. The pore fluid velocity for the first test was 1×10^{-5} cm/s, while the effective stress was approximately 0.13 ksc. During the second test, the pore fluid velocity was approximately 4×10^{-5}, and the resulting effective stress was approximately 0.7 ksc.

3.2 Testing Problems

The experiment names used to report the results are based sequentially on tests from which useful breakthrough data were recorded. The first three sand experiments did not provide reliable data due to fluctuating conductivity probe constants using the first pedestal. Additionally, the first peat experiment failed when the specimen consolidated such that it became practically impermeable and the fluid effluent line cavitated. Finally, the second and fourth peat experiments were destroyed by rolling diaphragm failures. Thus, Sand 1 and Sand 2 were actually the fourth and fifth sand specimens. Similarly, Peat 1 and Peat 2 were actually the third and fifth specimens, respectively. Although some of the data in the reported experiments were beset by equipment problems, there were enough remaining data to provide breakthrough curves, and thus fitted results. The problems encountered are described in more detail below.

3.2.1 Pedestal 1

The first generation pedestal was similar to the pedestal described in Chapter 2, except that it had only one conductivity probe which consisted of two platinum opposing wires (see Figure 3.3). The first, and most serious problem with this pedestal, was the failure of the casting epoxy to bond with the probes. This allowed solutions to flow along the wires and corrode the solder joints, thus altering the resistance in the wires, and therefore the conductivity readings. The epoxy also became "spongy" in some areas for unknown reasons. In addition to conductivity instabilities caused by corroded wires, it was also discovered that the platinum black coating rubbed off when touched. Thus, cleaning procedures, which included blotting of the probes, resulted in removal of the platinum black, thus further altering the probe constant. There were three sand specimens tested with this pedestal. However, due to inconsistencies in conductivity readings, reliable data were not obtained, and the results were not processed.

3.2.2 Pressure Transducers

Problems were encountered in measuring small pressure gradients across the specimens. For the two sand specimens described in this thesis, the zeros of each transducer were set such that the transducers were synchronized to produce equal readings with a phreatic surface at the mid-height of the specimen . The tests, however, were conducted at back pressures of 4 ksc, thus slight variations in linearity or calibration factors caused errors in excess of the sensitivity of the transducers to the small gradients. Therefore, the hydraulic conductivities of the two reported sand specimens could not be reliably determined from the test data. Nonetheless, the values were included in Table 3.2, to illustrate the extent of the problem. For the two peat specimens, the resolution problem was corrected by taking the phreatic zero of the pore pressure transducer at the mid-height of the specimen, and using no-flow readings at 4 ksc back pressure to calculate zeros for the salt and back pressure transducers. Thus, the transducers were synchronized

106

to produce equal readings for the three transducers under no-flow conditions at elevated back pressures. This seemed to alleviate the problem, as the gradients and resulting hydraulic conductivities, based on the separate transducer readings, were consistent for the peat specimens. The gradients for the peat specimens were much larger than for the sand, however, and were thus easier to measure. This is discussed further in Chapter 4.

3.2.3 Compressibility of Wetland Deposits

The first peat specimen was trimmed to the dimensions of a standard triaxial specimen (8.13 cm, or 3.2 in., tall). At a seepage velocity of 10^{-5} cm/sec, the gradient across the specimen increased the effective stress, causing the specimen to consolidate, and its porosity to be reduced, which, in turn, decreased the hydraulic conductivity, resulting in a higher gradient for the same flow, which increased the effective stress etc., etc. The first peat specimen continued to consolidate until the soil became practically impermeable, and the effluent cavitated under the suction pressure of the flow-control device. Thus, no reliable data were obtained from the first peat specimen. To reduce the effects of the high compressibility, the specimen height was reduced from 8 cm to 2 cm. This decreased the necessary pressure difference for any given flow by a factor of four, and reduced the consolidation drainage height by the same factor, thus enabling reasonably steady flows over the duration of the testing period. An alternative solution, based on pushing the fluid through the specimen, rather than pulling it, will be discussed in Chapter 4.

3.2.4 Rolling Diaphragms

Neither the author, nor the person who instructed the author on how to replace rolling diaphragms, was aware that there is a proper orientation that must be respected to prevent failure of the rubberized diaphragm coating. Two diaphragms failed during the test series on wetland deposits before the author learned that orientation of the diaphragm

is critical. The second and fourth peat specimens were destroyed before complete data sets could be recorded as a result.

3.2.5 Double Burette

During testing of the third peat specimen (Peat 1), it was discovered that the double burette had a significant leak from the flow-direction valve. Thus, changes in the porosity of the specimen during consolidation remain unknown, and the porosity reported in Table 3.2 for Test 1 is the pre-consolidation value based on the initial water content of the specimen.

3.3 Measured and Calculated Results

The data reported in this section include the water content, specific gravity, porosity, effective stress, flow rate, gradient, and hydraulic conductivity for each specimen. It should be noted that in all cases the effective stress, gradient, and hydraulic conductivity are reported as the average of the two values obtained separately using the influent pressure transducers in the salt solution and back pressure lines. Finally, conservation of mass will be discussed for experiments on each material at the end of the appropriate section.

3.3.1 Experiments on Sand

Table 3.2 presents the measured and calculated results of experiments using sand specimens. The specific gravity of the sand was reported by Ratnam (1996), as discussed above, to be 2.66. The initial water contents of all sand specimens were assumed to be zero. Also, as discussed in Section 3.2.2, transducer problems prevented meaningful calculations of the gradient and thus the hydraulic conductivity for the sand specimens, however, the values are reported to illustrate the magnitude of the problem.

Conservation of mass was measured by taking the difference between the average area under the normalized concentration vs. time curves for Probes 1-4 (effluent) and the area under the corresponding curve for probe 5 (influent). The locations of the conductivity probes were shown in Figure 2.8. Probe 5 was moved from the effluent line to the influent line after completion of the experiments on Sand 1, thus there are no data available for that specimen. For Sand 2, the percentages recovered were 81%, 88%, and 96% for Tests 1, 2, and 3, respectively. A possible explanation for the trend is that at higher flow rates, less time is available for the solute to diffuse into dead spaces within the system. Alternatively, if the same mass of solute was lost in the system during each experiment, higher recovery percentages would be observed in experiments conducted at higher flow rates, because a greater mass of solute would be introduced into the system (for constant pulse durations). To investigate this possibility, the normalized concentrations from the experiments on Sand 2 were converted to absolute mass and integrated over the duration of the respective experiments. The masses "lost" during Sand 2 Test 1, Test 2, and Test 3 were 0.027 g, 0.049 g, and 0.048 g, respectively. The corresponding input masses were 0.144 g, 0.419 g, and 1.177 g, respectively. Thus, the later explanation seems plausible, however additional experiments would have to be performed in order to produce enough data to confirm this phenomenon. Plots of integrated area vs. time for the three experiments are provided in Figures 3.4 through 3.6. The curves on each plot are labeled by probe numbers. The integrated mass values seem to be relatively consistent between the various probes.

3.3.2 Experiments on Wetland Deposits

Table 3.3 presents the measured and calculated results of tests using peat specimens. The target seepage velocities for the first and second experiments on each specimen were 1×10^{-5} cm/sec and 4×10^{-5} cm/s, respectively.

The initial moisture content was determined according to ASTM D 4959. The magnitude of the changes in specimen volume were not available for Peat 1 Test 1, as discussed above, therefore, the reported moisture content and porosity were estimated based on the initial moisture content, a virgin compression index of 3.23 (reported by Bialon, 1995, for sedge materials), and the effective stress measured after steady state flow was observed. The reported values for the second tests of both Peat 1 and Peat 2 are based on the final water content of the specimens. For Peat 2 Test 1, the reported water content is based on the initial value, and adjusted for measured volumetric changes, assuming 100% saturation ("B" values of 0.99, as reported in Table 3.3, indicate that this is a valid assumption).

Bialon (1995) reported that there was too much heterogeneity within the sediment to warrant pycnometer testing for specific gravity. Therefore, the specific gravities of the wetland solids were estimated based on the specimen weight, specimen volume, and measured moisture content, assuming 100% saturation. The values 1.13 for Peat 1, and 1.32 for Peat 2 are in reasonable agreement with the specific gravity of 1.30, which Bialon reported as average for the sedge peat layer in the Aberjona watershed.

The porosities were calculated from the moisture contents discussed above and initial specimen volumes. The initial porosity for Peat 2 was 0.88, which corresponded to an initial moisture content of 548%. The initial values for Peat 1, listed in Table 3.4, were 0.87 and 573%, respectively. These values fall within the range of undisturbed moisture contents (480% to 870%) reported by Bialon.

As discussed above, the hydraulic conductivities changed with the flow rate due to consolidation. For Peat 1, at an estimated initial porosity of 0.81 (as discussed above) the hydraulic conductivity was 1.2×10^{-7} cm/sec, at an average effective stress of 0.18 ksc. For Peat 2, at a porosity of 0.82 the hydraulic conductivity was 2.6×10^{-7} cm/sec with an average effective stress of 0.14 ksc. The corresponding void ratios are 4.3 , and 4.6, respectively. Bialon reported a hydraulic conductivity of 8×10^{-6} cm/sec for sedge at a

void ratio of 6.48. Thus, at reduced void ratios these hydraulic conductivities do not appear to be unreasonable. The hydraulic conductivities were 2.8×10^{-8} cm/sec at a porosity of 0.77 and 5.8×10^{-8} cm/sec at a porosity of 0.80, for Peat 1 Test 2 and Peat 2 Test 2, respectively. Thus Peat 1 exhibited approximately half of the hydraulic conductivity of Peat 2.

There is a clear trend of decreasing hydraulic conductivity with decreasing total porosity, however, the rate of change ($C_k = \Delta e / \Delta \log k$) is not consistent between the two specimens. The data, as reported in Table 3.3, are plotted in Figure 3.7. The C_k values are 1.5 for Peat 1, and 0.84 for Peat 2, based on these data. Bialon reported C_k values ranging from 1.33 to 1.79 for sedge peat. Thus, the value for Peat 1 (based on the estimated porosity for Test 1) falls within his range, while the value for Peat 2 falls below it. If a regression is run through the data from both peat specimens (using the estimated porosity value for Peat 1 Test 1), a value of $C_k = 1.2$ is obtained with an R^2 of 0.97. With only four data points, however, these C_k values would be heavily biased by any non-representative results.

The conservation of mass for the peat deposits was determined as described for the sand specimens. The plots of integrated mass versus reduced time (pore volumes of flow) for the experiments using peat are provided in Figures 3.8 through 3.11. The percentages recovered were 49%, 59%, 81%, and 53% for Peat 1 Tests 1 and 2, and for Peat 2 Tests 1 and 2, respectively. As the figures indicate, there was a lot of variation between the various probes, however, with the exception of Peat 2 Test 1, Probes 1 and 2 (located in the pedestal, which were used with the fitting model) produced similar values, and indicated higher percentages of recovered mass than probes 3 and 4 (which are located in the effluent line) indicated. The percentages recovered, as reported above, are based on the average of the four effluent probes, and are clearly biased by Probes 3 and 4, which are consistently below the other values. Computer problems encountered during the initial portion of the first experiment on Peat 1 caused the test to be restarted, resulting in

approximately one additional week of flow prior to testing (the flow was not stopped in order to maintain steady state flow). Thus some of the ions initially present in the specimen were flushed out prior to testing. This was not the case for Peat 2, which may be the reason for what appears to be an abnormally high recovery percentage.

The experimental breakthrough curves (the average of the curves for probes 1 and 2) for each test (sand and peat) are plotted with the fitted curves and presented in Figures 3.12 through 3.20. As discussed in Chapter 2, each conductivity value is corrected for temperature, and then converted to concentration with the numerical functions shown in Figures 2.16 and 2.17, respectively. As expected, the peat specimens did not exhibit ideal chemical transport. More specifically, the breakthrough curves for peat had significant tailing relative to the breakthrough curves for sand. Such tailing is characteristic of soils with immobile regions, as discussed in Chapter 1.

3.4 Fitted Results

The two site, two region model (TRM), which is part of the CXTFIT code discussed in Chapter 1 (Parker and van Genuchten, 1984), was used to fit hydraulic parameters to the experimental breakthrough curves. As discussed above, the average of the concentrations based on the data from Probes 1 and 2 (which are located immediately below the bottom porous stone) were used with the fitting model. The seepage velocity, dispersion coefficient, pulse duration, ratio of mobile porosity to total porosity, and the first-order rate constant that governs chemical transport between the mobile and immobile regions were all fitted to the experimental data. The time data were not normalized in order that the seepage velocity could be fit, which allowed a better overall fit by the model. NaCl is considered to be a conservative tracer, which theoretically will not adsorb to the solid particles, thus the retardation factor was fixed constant at unity. The pulse duration was allowed to be fit so that conservation of mass would be satisfied by the model. The results are discussed below. Print-outs of the first page of the CXTFIT input

files, and relevant pages of the output files for each experiment are included in Appendix E. Additionally, a one region model (ORM), based on the advection-dispersion equation, was fit to the data for comparison with the TRM. The ORM used for this thesis is included in the CXTFIT code as Model 2, and contains variables to account for production and decay. For the ORM analysis, the seepage velocity, dispersion coefficient, and pulse duration were allowed to vary, and the retardation factor was fixed at unity, as for the TRM. The production and decay coefficients, which can be fit to the data as well, were held constant at zero because NaCl is a relatively conservative tracer, and no sources or sinks within the specimen would be expected over the duration of the experiments discussed in this thesis.

3.4.1 Experiments on Sand

The fitted breakthrough curves for experiments on the sand specimens are plotted with the experimental breakthrough curves in Figures 3.12 through 3.16. The corresponding fitted hydraulic parameters are presented in Table 3.4. In general the fits for both the TRM (Table 3.4.a) and ORM (Table 3.4.b) were relatively good. For the ORM, R^2 ranged from 0.963 to 0.995, while for the TRM, R^2 ranged from 0.996 to 0.999. Thus the TRM provided a slightly better fit to the data from experiments using sand specimens. The close fit obtained from the ORM, however, would support an assumption of equilibrium transport for these relatively uniform specimens, as discussed by Li et al. (1994). The remainder of this section will focus on the parameters obtained using the TRM.

The seepage velocities and pulse durations for Sand 1 closely matched the calculated/measured values. For Sand 2, however the fitted seepage velocities were slightly greater than the calculated values, and the pulse durations were shorter than the observed durations. Higher seepage velocities are consistent with β values less than unity, as there is less cross sectional area available for flow. Decreased pulse durations are

consistent with less than 100% recovery of mass, which was the case for this series of experiments.

The fraction of pore space taking part in the flow (β, the mobile porosity divided by the total porosity) was relatively constant for the sand specimens, at approximately 0.74. The range was 0.72 to 0.77. As Figure 3.21 indicates, there did not appear to be a correlation between β and the seepage velocity, which suggests that β is a parameter characterizing the soil/system's structure. Although dead-end pore spaces are not expected in a specimen of uniform sand, a value less than one was expected as the tracer is initially introduced at a point in the center of the top porous stone, and could not reasonably be expected to be uniformly distributed across the top of the specimen at time t = 0. Thus, the outer area near the top of the specimen might account for a large part of the immobile pore space.

Omega, a dimensionless first order mass transfer coefficient, varied between 1.8 and 3.1 for the sand specimens, with all but one value close to 2.0. The dimensional mass transport coefficient ($\alpha = \omega q/L$) was expected to vary as the velocity for specimens with grain Peclet numbers greater than 1, and for specimens in which there is a low velocity contrast between the mobile and immobile regions, as discussed in Chapter 1. For these experiments, the grain Peclet numbers all exceeded one (Table 3.5), ranging from 1.7 to 12.1, and α did seem to vary linearly with velocity (see Figure 3.21). The best fit regression line had a slope of 0.24, and R^2 of 0.91.

The dispersion coefficient for the sand specimens ranged from 2.1 x 10^{-4} cm^2/sec to 1.3 x 10^{-6} cm^2/sec. These values seem reasonable when compared with the empirical correlation for granular aquifers (Daniel, 1993), which suggests that the mechanical dispersion coefficient can be approximated by multiplying the median grain size by the seepage velocity (1.9 x 10^{-4} cm^2/sec for Sand 1). Both extreme values occurred for Sand 1. There did not appear to be any trend linking D with the seepage velocity values (see Figure 3.21).

For the case where there is a low velocity contrast between the mobile and immobile regions, Li et al. (1994) suggested that α should scale as V_s^2/D, indicating that the mass transfer process is predominantly affected by local flow variations. For these experiments, D was expected to be velocity dependent (scale as V_s, implying that α should also scale as V_s, which, as discussed above, it appears to), since the grain Peclet number was greater than one. Since D was not observed to scale as V_s, α was plotted against the dispersion coefficient (assumed to approximate D_T) to investigate the effects of inter-region diffusion (which would be expected to dominate for the case of significant velocity contrast). No relationship was observed between D and α (Figure 3.22), therefore, α was plotted against V_s^2 in an attempt to confirm the influence of local flow variations on the mass transfer process. The curve in Figure 3.23, however, does not indicate a linear correlation, which, again, could be due to the influence of outlying data points.

Additionally, Bear (1972) presented evidence that for grain Peclet numbers greater than one, there should be a linear relationship between the hydrodynamic dispersion coefficients (normalized by the coefficient of molecular diffusion) and the common log of the grain Peclet numbers. Figure 3.24 indicates that this is not the case for these experiments, however, as discussed above, with these few data points, trends could easily be obscured by out-lying values.

3.4.2 Experiments on Wetland Deposits

The fitted breakthrough curves for the wetland deposits are plotted with the experimental breakthrough curves in Figures 3.18 through 3.21. The fitted parameters are presented in Table 3.5.a and 3.5.b for the TRM and ORM, respectively. In general the fits were not as good as those for sand. As the Figures and R^2 values indicate, the TRM provided a better fit to the experimental data than the fit obtained from the ORM. This indicates, as expected, that non-equilibrium transport is taking place in the wetland

deposits. For the TRM, the fitted curves all had R^2 values greater than 0.96, while for the ORM, R^2 ranged from 0.91 to 0.94. Thus, the following discussion is based on the fitted parameters obtained using the TRM.

The fitted seepage velocities were greater than the calculated values (based on total porosity), which is consistent with the assumption that there are immobile regions within the pore spaces of the specimens. Also, the fitted pulse durations were shorter than the measured values, which is consistent with the percentages of recovered mass being less than 100%, as discussed above. The exception was Peat 2 Test 1, in which some leaching of ions, initially present in the material, appears to have occurred, thus leading to a higher fitted pulse duration then the measured value.

The fraction of pore space taking part in the flow varied from 0.09 for Peat 1 Test 1, to 0.42 for Peat 2 Test 1. The values for Peat 1 Test 2 and Peat 2 Test 2 were 0.37 and 0.31, respectively. Figure 3.25 indicates that there is no consistent trend between β and seepage velocity, which, as for the sand, suggests that β is a parameter characterizing the soil/system's structure. Additionally, β for Peat 1 Test 1 (0.09) is enough of a deviation from the other values that it could be an anomaly.

As discussed in Chapter 1, although Bialon could find no correlation between total void ratio and log of hydraulic conductivity, there was expected to be a correlation between effective void ratio and hydraulic conductivity. As Figure 3.26 indicates, no correlation was exhibited by the data of this research. In fact, the reverse of the logical relationship between void ratio and hydraulic conductivity was indicated by the data from Peat 1, which provides further evidence that the results of Peat 1 Test 1 may be anomalous. In Figure 3.27 an average value of β (= 0.37) was assumed for Peat 1 Test 1, and the effective void ratio was re-plotted against hydraulic conductivity. With the assumed value of β, there did appear to be a trend of increasing hydraulic conductivity with increasing void ratio, however the trend was not observed to be consistent between

Peat 1 and Peat 2. A regression through all of the data in Figure 3.27 resulted in an effective C_k of 0.15, with $R^2 = 0.6$.

Omega, varied between 9.4 for Peat 1 Test 1 and 2.1 for Peat 1 Test 2. For Peat 2, the values for Tests 1 and 2 were 5.4 and 3.6, respectively. As discussed in Chapter 1, for the case of low velocity contrasts, α (Table 3.7), the dimensional form of ω, was expected to vary as v_s^2/D. Calculated values of the grain Peclet number (based on a median grain size of 0.025 mm) were less than unity (Table 3.7), thus, α was expected to vary as v_s^2. No such trend was observed for these experiments (see Figure 3.28), however, again, a non-representative data point would significantly bias the results. Additionally, Figure 3.26 indicates that there is no trend between α and v_s, which would be expected for grain Peclet numbers greater than one.

To investigate the possibility of significant velocity contrasts, α was plotted against the transverse diffusion coefficient, D_T, (assumed to be approximated by the fitted dispersion coefficient). As Figure 3.29 indicates, no trend between α and D_T was observed, thus, significant velocity contrasts were not confirmed.

The dispersion coefficient for the peat specimens ranged from 1.0×10^{-5} cm^2/sec to 8.7×10^{-6} cm^2/sec. These values are similar in magnitude to the coefficient of molecular diffusion for NaCl, which does not seem unreasonable, given the low seepage velocities of these experiments. There did not appear to be any trend linking D to seepage velocity values (see Figure 3.26), which is consistent with the grain Peclet numbers being less than unity for the case of low velocity contrast. Additionally, as discussed above, there did not appear to be any correlation between α and D. Thus, based on these data, the transport mechanisms could not be characterized for these wetland deposit specimens.

EXPERIMENT:	Seepage Velocity (cm/sec)	Effective Stress (ksc)	Pulse Duration (sec)
Sand 1 Test 1	0.011	0.25	600
Sand 1 Test 2	0.011	0.25	600
Sand 2 Test 1	0.001	0.23	600
Sand 2 Test 2	0.003	0.23	600
Sand 2 Test 3	0.007	0.24	600
Peat 1 Test 1	9E-06	0.18	600
Peat 1 Test 2	5E-05	1.47	600
Peat 2 Test 1	1E-05	0.14	600
Peat 2 Test 2	4E-05	0.69	600

Table 3.1: Summary of Experimental Conditions

EXPERIMENT:	WATER CONTENT (%)	SPECIFIC GRAVITY	POROSITY	EFFECTIVE STRESS (ksc)	"B" Value	SEEPAGE VELOCITY (cm/sec)	GRADIENT	HYD. CONDUCT. (cm/sec)
Sand 1 Test 1	0	2.66	0.46	0.25	0.95	0.011	2.02	3.9E-03
Sand 1 Test 2	0	2.66	0.46	0.25		0.011	1.07	9.5E-03
Sand 2 Test 1	0	2.66	0.42	0.23	0.96	0.001	-0.17	N/A
Sand 2 Test 2	0	2.66	0.42	0.23		0.003	0.21	1.1E-02
Sand 2 Test 3	0	2.66	0.42	0.24		0.007	1.68	8.1E-03

Table 3.2 Measured and Calculated Results of Tests Using Sand

EXPERIMENT:	WATER CONTENT (%)	SPECIFIC GRAVITY	POROSITY	EFFECTIVE STRESS (ksc)	"B" Value	SEEPAGE VELOCITY (cm/sec)	GRADIENT	HYD. CONDUCT. (cm/sec)
Peat 1 Initial Conditions	573	1.13	0.87	0.05	0.99			
Peat 1 Test 1	*359	1.13	*0.81	0.18		8.7E-06	66.80	1.2E-07
Peat 1 Test 2	285	1.13	0.77	1.47		4.8E-05	1283.00	2.9E-08
Peat 2 Initial Conditions	548	1.32	0.88	0.05	0.99			
Peat 2 Test 1	346	1.32	0.82	0.14		1.1E-05	34.73	2.6E-07
Peat 2 Test 2	322	1.32	0.8	0.69		3.8E-05	531.64	5.8E-08

* Estimated based on a virgin compression index of 3.23 for sedge peat (Bialon, 1995).

Table 3.3 Measured and Calculated Results of Tests Using Wetland Deposits

EXPERIMENT:	SEEPAGE VELOCITY (cm/sec)	DISP. COEF. (cm^2/sec)	PULSE DURATION (sec)	BETA	OMEGA	R SQUARE
Sand 1 Test 1	1.1E-02	2.1E-04	600	0.72	1.8E+00	0.998
Sand 1 Test 2	1.1E-02	1.3E-06	604	0.72	1.8E+00	0.999
Sand 2 Test 1	1.5E-03	3.2E-05	467	0.77	2.1E+00	0.999
Sand 2 Test 2	4.0E-03	7.0E-05	530	0.73	3.1E+00	0.997
Sand 2 Test 3	9.7E-03	1.0E-05	585	0.75	2.0E+00	0.996

Table 3.4.a: Fitted Results of Tests on Sand; TRM

EXPERIMENT:	SEEPAGE VELOCITY (cm/sec)	DISP. COEF. (cm^2/sec)	PULSE DURATION (sec)	R SQUARE
Sand 1 Test 1	1.1E-02	3.1E-03	591	0.994
Sand 1 Test 2	1.1E-02	2.8E-03	633	0.995
Sand 2 Test 1	1.6E-03	2.2E-04	450	0.963
Sand 2 Test 2	4.1E-03	6.4E-04	523	0.993
Sand 2 Test 3	9.9E-03	1.9E-03	576	0.991

Table 3.4.b: Fitted Results of Tests on Sand; ORM

EXPERIMENT:	SEEPAGE VELOCITY (cm/sec)	DISP. COEF. (cm^2/sec)	PULSE DURATION (sec)	BETA	OMEGA	R SQUARE
Peat 1 Test 1	2.7E-05	1.0E-05	398	0.09	9.4E+00	0.993
Peat 1 Test 2	7.9E-05	2.3E-05	482	0.37	2.1E+00	0.970
Peat 2 Test 1	2.4E-05	8.7E-06	786	0.42	5.4E+00	0.960
Peat 2 Test 2	7.7E-05	4.6E-06	486	0.31	3.6E+00	0.984

Table 3.5.a   Fitted Results of Tests on Peat; TRM

EXPERIMENT:	SEEPAGE VELOCITY (cm/sec)	DISP. COEF. (cm^2/sec)	PULSE DURATION (sec)	R SQUARE
Peat 1 Test 1	2.0E-05	2.0E-05	411	0.911
Peat 1 Test 2	4.2E-05	1.0E-04	560	0.929
Peat 2 Test 1	2.0E-05	1.6E-05	827	0.929
Peat 2 Test 2	6.8E-05	3.8E-05	502	0.943

Table 3.5.b   Fitted Results of Tests on Peat; ORM

EXPERIMENT:	COLUMN LENGTH (cm)	EFFECT. VOID RATIO	alpha (1/sec)	COLUMN PECLET NUMBER	GRAIN PECLET NUMBER	D/Dmd
Sand 1 Test 1	6.655	0.50	2.8E-03	339	11.9	1.4E+01
Sand 1 Test 2	6.655	0.50	3.0E-03	55556	12.1	8.6E-02
Sand 2 Test 1	6.655	0.48	4.6E-04	305	1.7	2.2E+00
Sand 2 Test 2	6.655	0.44	1.9E-03	378	4.5	4.7E+00
Sand 2 Test 3	6.655	0.46	3.0E-03	6207	11.0	6.9E-01

Table 3.6: Column Length, e_{eff}, α, Column and Grain Peclet Numbers, and D/D$_{md}$ for Sand

EXPERIMENT:	COLUMN LENGTH (cm)	EFFECT. VOID RATIO	alpha (1/sec)	COLUMN PECLET NUMBER	GRAIN PECLET NUMBER	D/Dmd
Peat 1 Test 1	2.125	0.085	1.2E-04	5.6	0.005	2.7E+07
Peat 1 Test 2	2.125	0.398	7.8E-05	7.5	0.013	3.2E+07
Peat 2 Test 1	2.208	0.525	5.9E-05	6.2	0.004	5.2E+07
Peat 2 Test 2	2.208	0.330	1.3E-04	36.8	0.013	3.2E+07

Table 3.7: Column Length, e_{eff}, α, Column and Grain Peclet Numbers, and D/D$_{md}$ for Wetland Deposits

EQUATIONS

EFFECTIVE VOID RATIO = ne / 1-ne   where ne = BETA *n

alpha = omega *seepage velocity / column length

Pc = seepage velocity * column length / dispersion coef.

Pg = seepage velocity * grainsize / fitted coefficient of molecular diffusion
        where grain size = 0.017 cm for sand and 0.0025 cm for wetland deposits
           (0.0025 cm was measured from SEM figures in Bialon, (1995))
           Dmd = 1.5 x 10^-5 sq cm/sec for NaCl
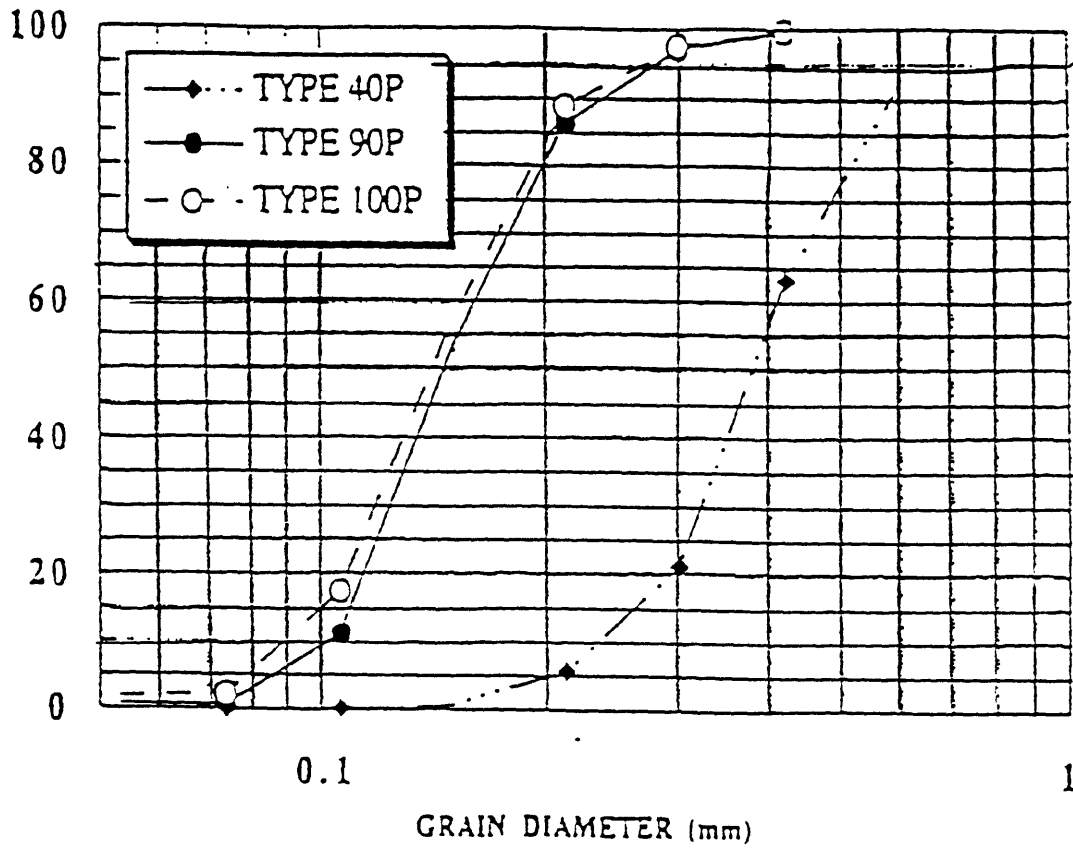
Figure 3.1 Grain Size Distribution for Sand Samples (Ratnam, 1996)

Boring 1

Depth (cm)	
0	
20	Live Root Mat
40	
60	Typha Peat
80	
100	
120	Sedge Peat
140	
160	Red Woody Peat Layer
180	White Sand Layer
200	Diatomaceous Earth
220	
240	
260	

Boring 2

Depth (cm)	
0	
20	Live Root Mat
40	Typha Peat Layer
60	
80	Sedge Peat Layer
100	
120	Red Woody Peat Layer
140	
160	White Sand Layer
180	
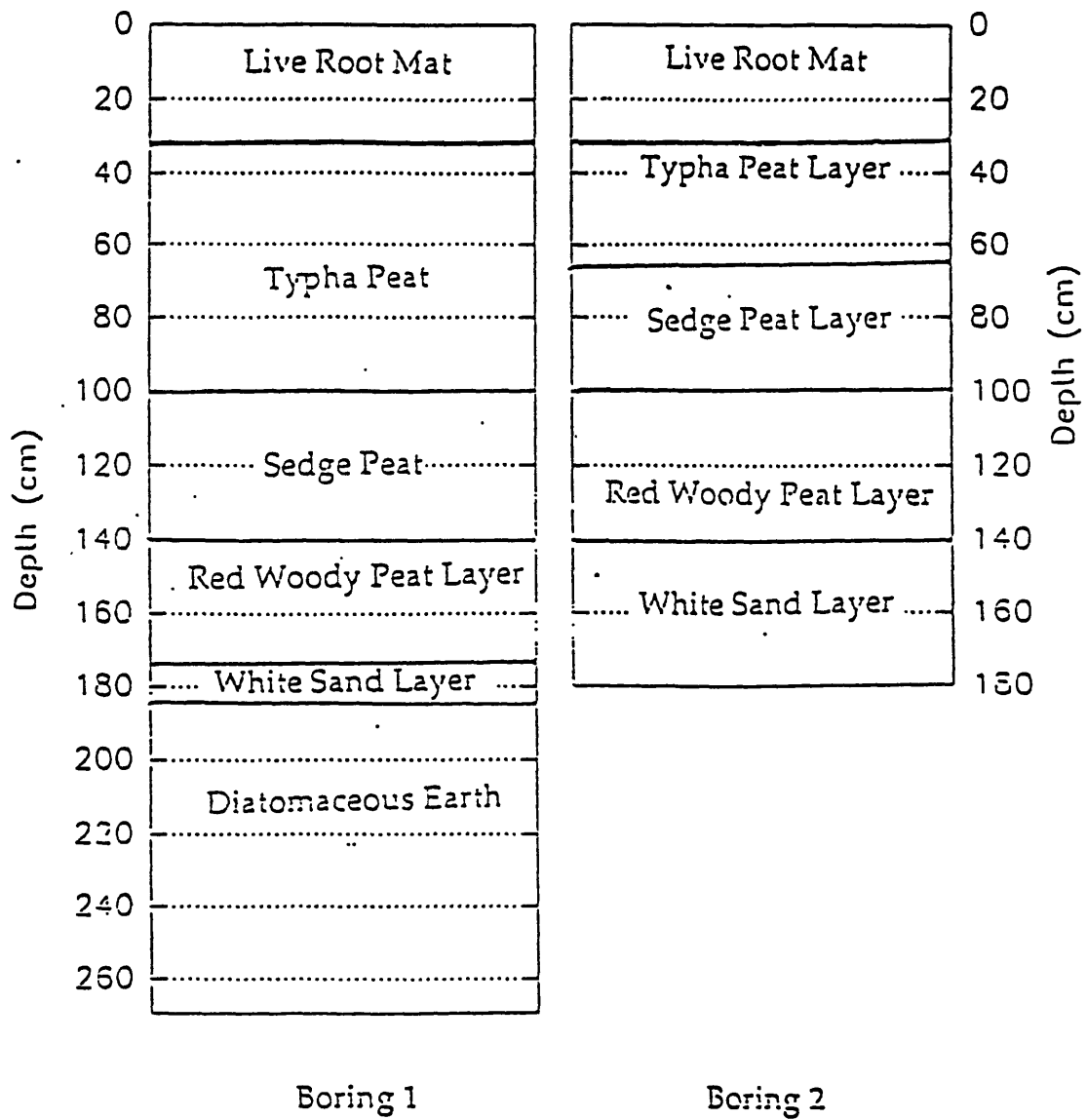
Figure 3.2   Boring Profiles (Bialon, 1995)

123
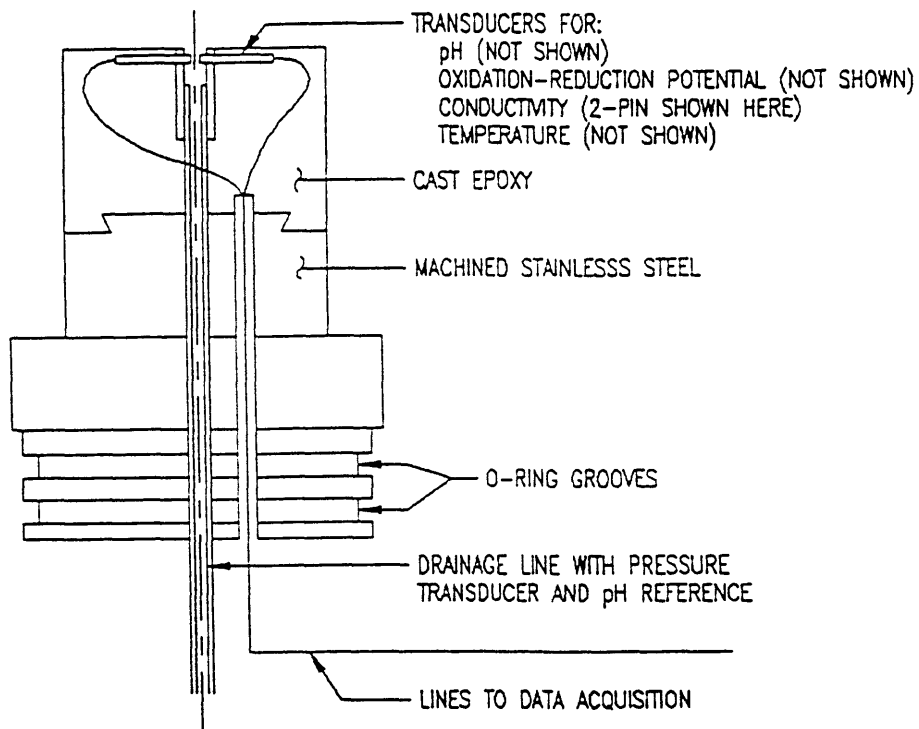
Figure 3.3   First Generation Removable Pedestal

INTEGRATED AREA VS PORE VOLUMES
SAND 2 TEST 1   11-22-95
10 min PULSE, 0.1 M NaCl, SEEPAGE VEL. = 0.001 cm/sec

Legend:
- Probe 1
- Probe 2
- Probe 3
- Probe 4
- Probe 5

Y-axis: INTEGRATED AREA (0.000, 0.025, 0.050, 0.075, 0.100)

X-axis: PORE VOLUMES OF FLOW (0, 1, 2, 3, 4)
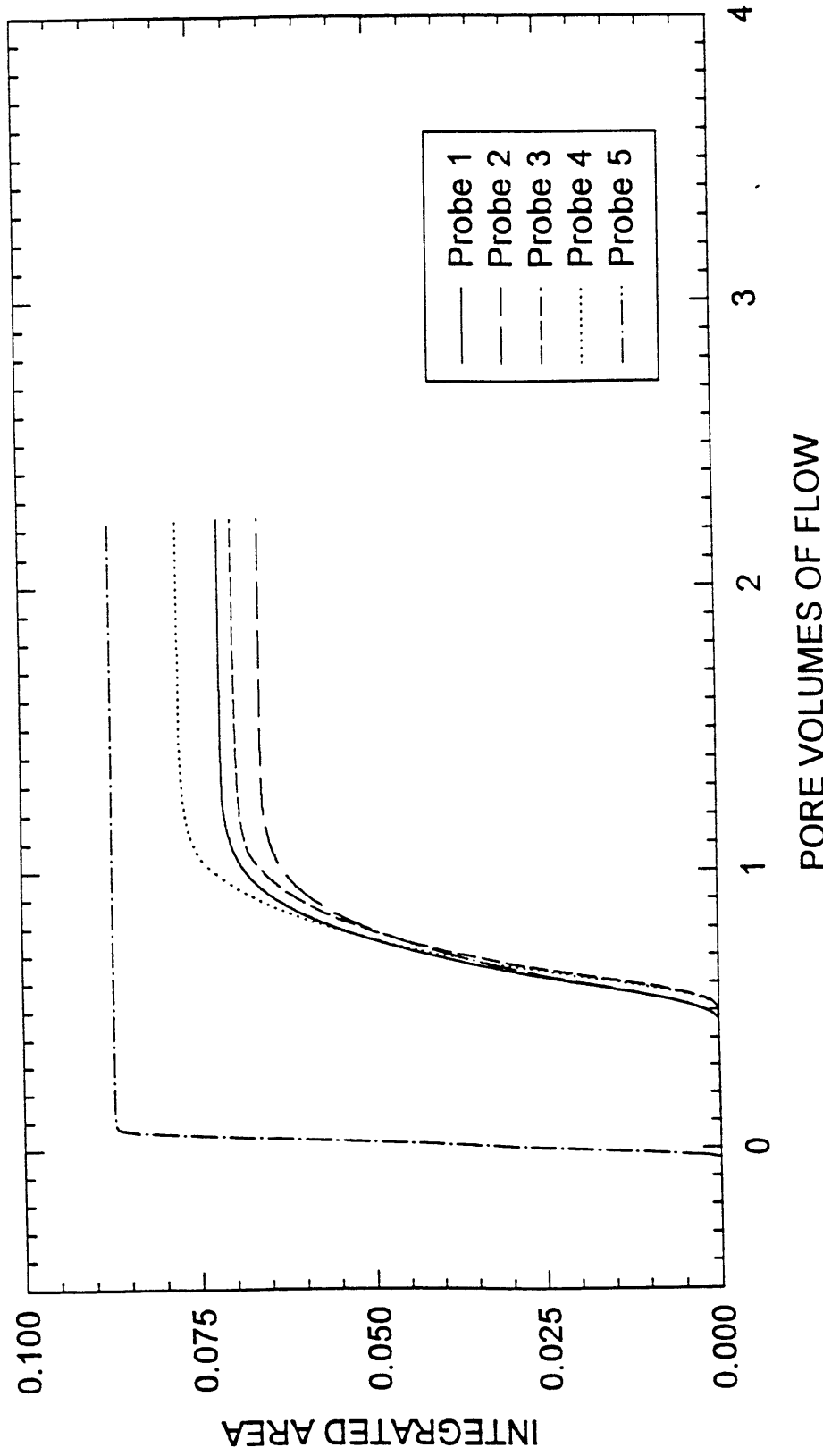
Figure 3.4   Integrated Mass Curves for Influent and Effluent Probes, Sand 2 Test 1

INTEGRATED AREA VS PORE VOLUMES
SAND 2 TEST 2   11-22-95
10 min PULSE, 0.1 M NaCl, SEEPAGE VEL. = 0.003 cm/sec
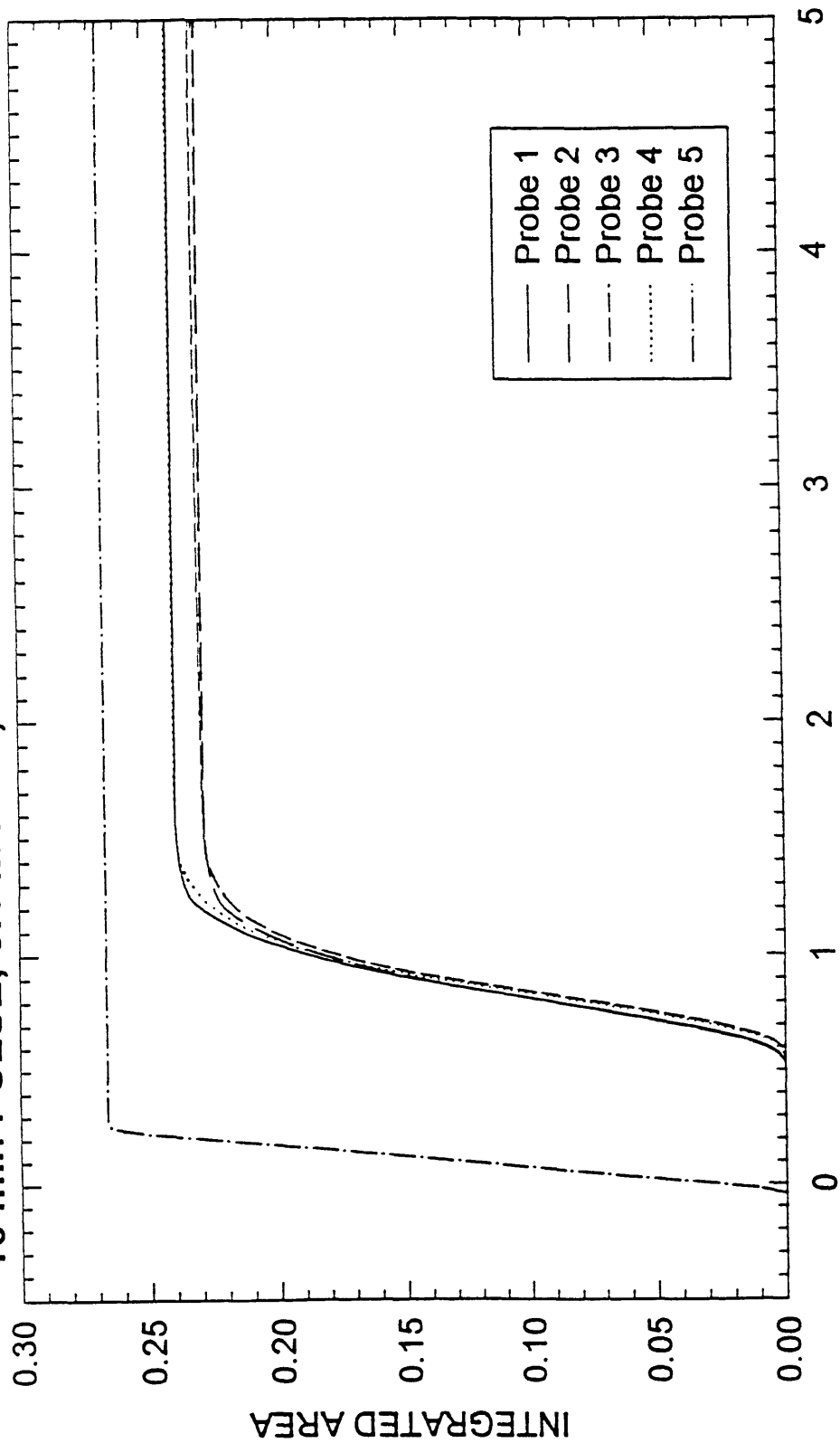
Figure 3.5   Integrated Mass Curves for Influent and Effluent Probes, Sand 2 Test 2

INTEGRATED AREA VS PORE VOLUMES
SAND 2 TEST 3   11-23-95
10 min PULSE, 0.1 M NaCl, SEEPAGE VEL. = 0.007 cm/sec

Probe 1
Probe 2
Probe 3
Probe 4
Probe 5
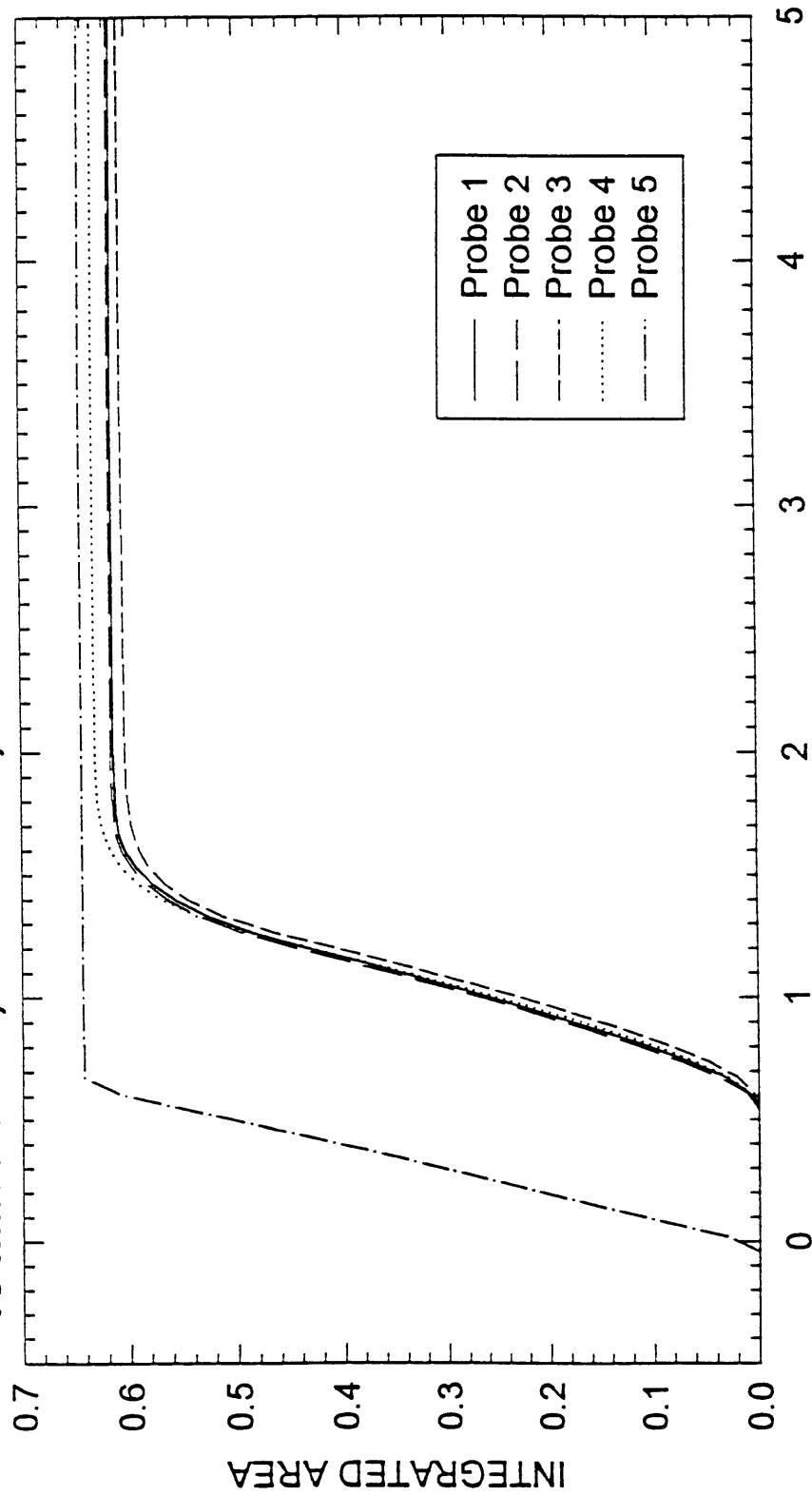
INTEGRATED AREA

PORE VOLUMES OF FLOW

Figure 3.6   Integrated Mass Curves for Influent and Effluent Probes, Sand 2 Test 3

127

e VS LOG HYDRAULIC CONDUCTIVITY
ABERJONA WETLAND DEPOSITS
PEAT 1 AND PEAT 2

PEAT 1, C_k = 1.5
PEAT 2, C_k = 0.84

HYDRAULIC CONDUCTIVITY (cm/sec)
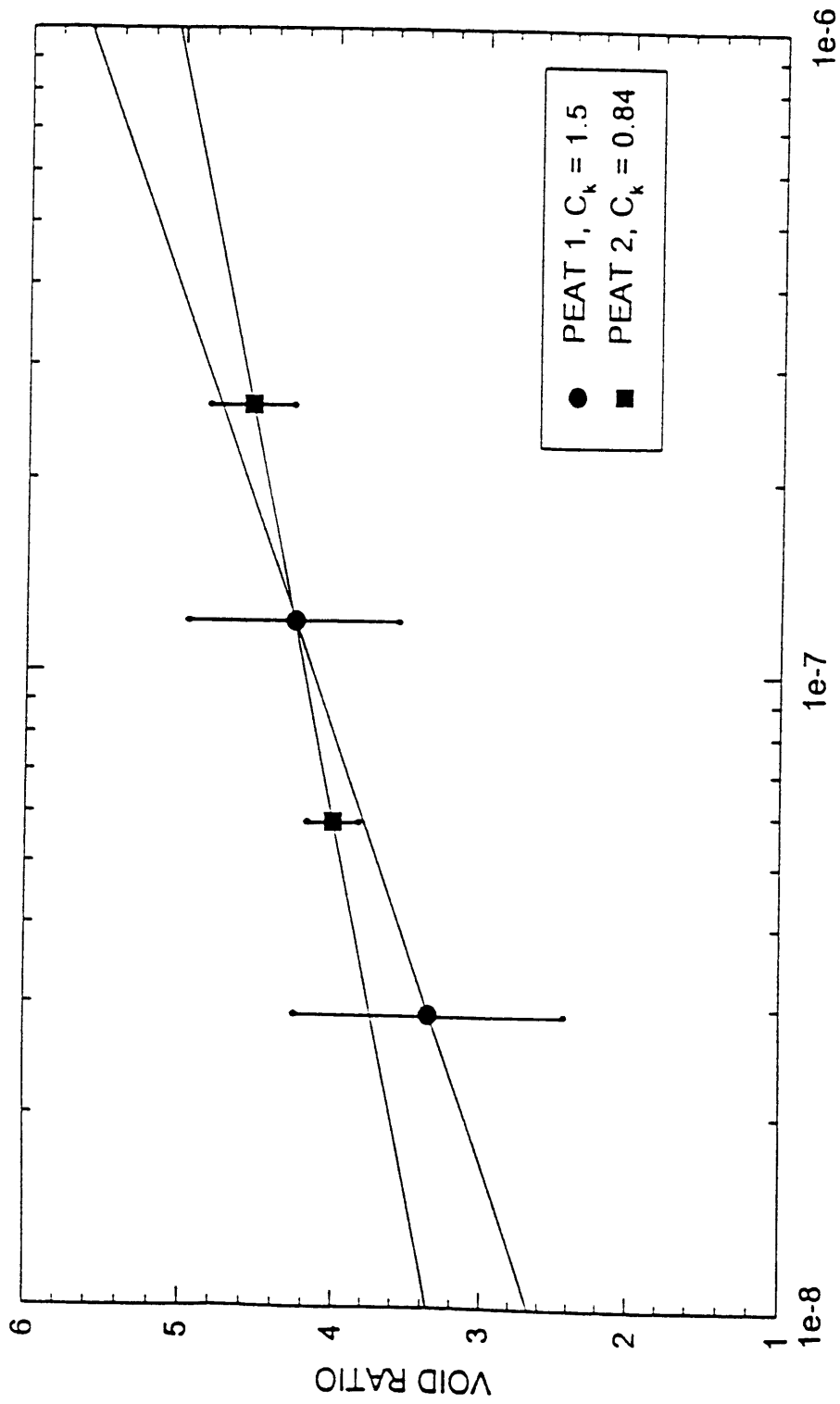
VOID RATIO

Figure 3.7   Plot of Void Ratio vs. log of Hydraulic Conductivity, Peat 1 and Peat 2

128

INTEGRATED AREA VS PORE VOLUMES
PEAT 1 TEST 1 1-04-96
10 min PULSE, 0.1 M NaCl, SEEPAGE VEL. = 9×10^{-6} cm/sec
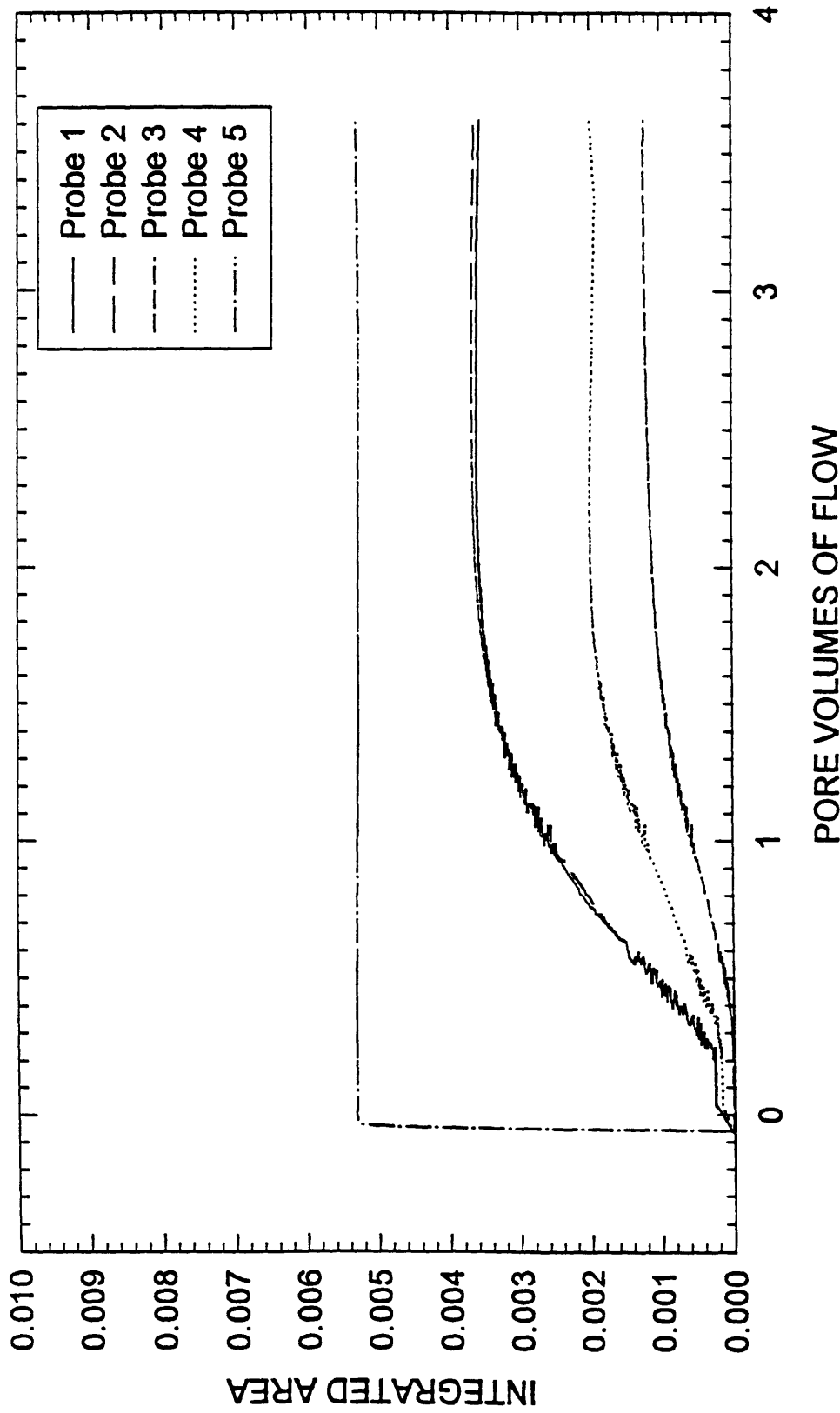
Figure 3.8   Integrated Mass Curves for Influent and Effluent Probes, Peat 1 Test 1
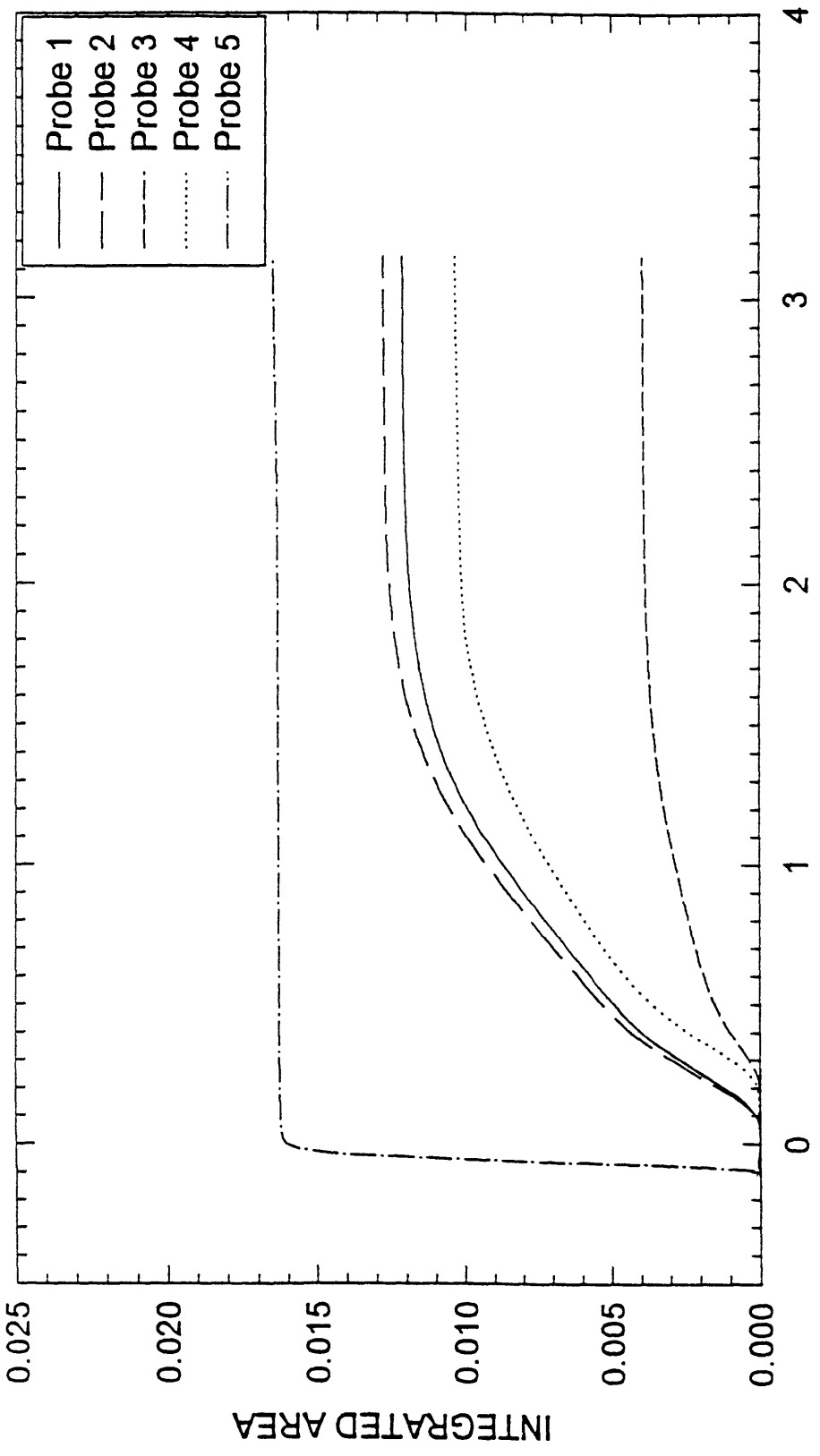
Figure 3.9   Integrated Mass Curves for Influent and Effluent Probes, Peat 1 Test 2

130

INTEGRATED AREA VS PORE VOLUMES
PEAT 2 TEST 1, 1-29-96
10 min PULSE, 0.1 M NaCl, SEEPAGE VEL. = 1X10^{-5} cm/sec
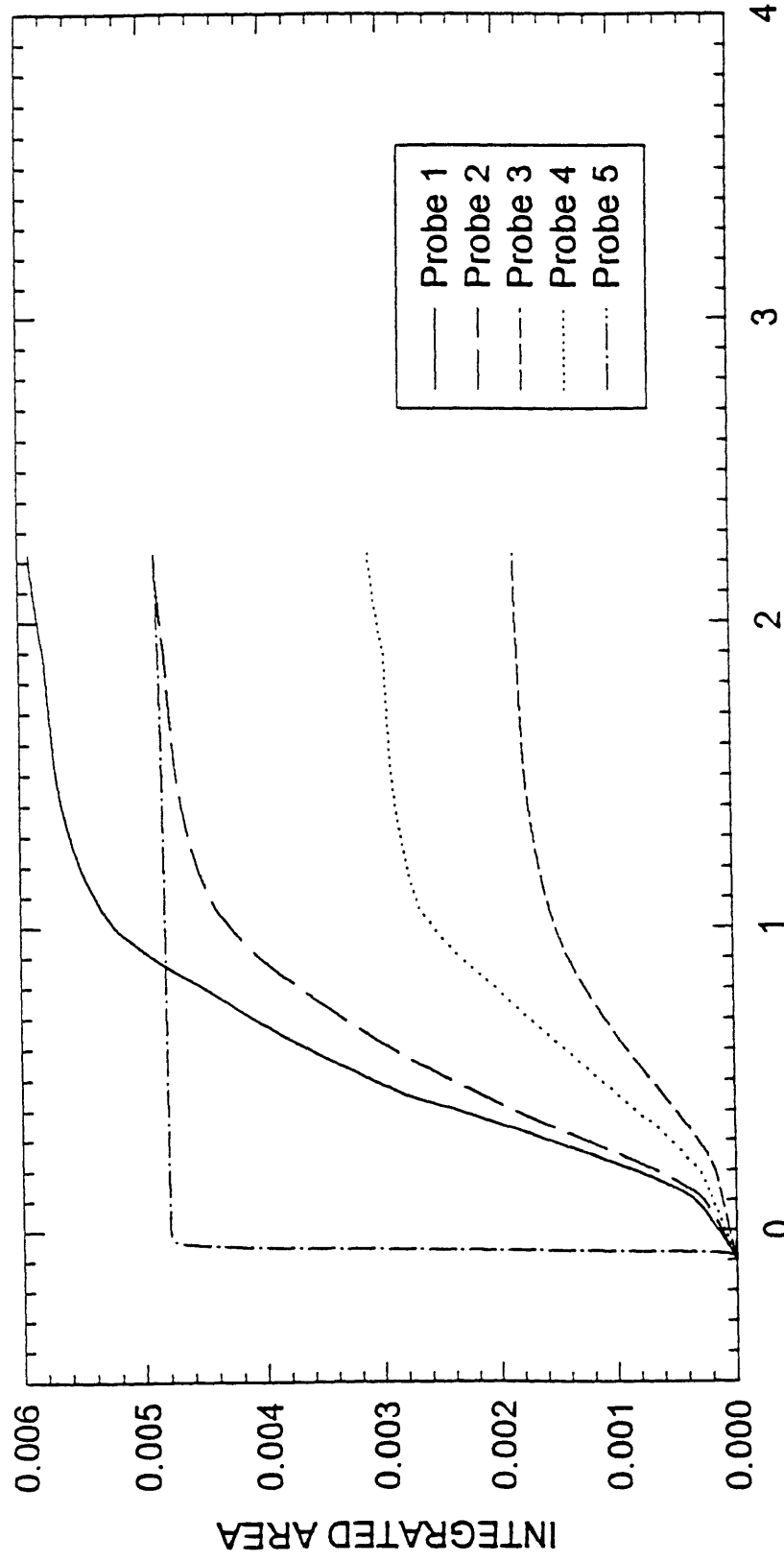
Figure 3.10   Integrated Mass Curves for Influent and Effluent Probes, Peat 2 Test 1

131

INTEGRATED AREA VS PORE VOLUMES
PEAT 2 TEST 2, 2-04-96
10 min PULSE, 0.1 M NaCl, SEEPAGE VEL. = 4X10^{-5} cm/sec

Probe 1
Probe 2
Probe 3
Probe 4
Probe 5

INTEGRATED AREA

PORE VOLUMES OF FLOW

Figure 3.11   Integrated Mass Curves for Influent and Effluent Probes, Peat 2 Test 2
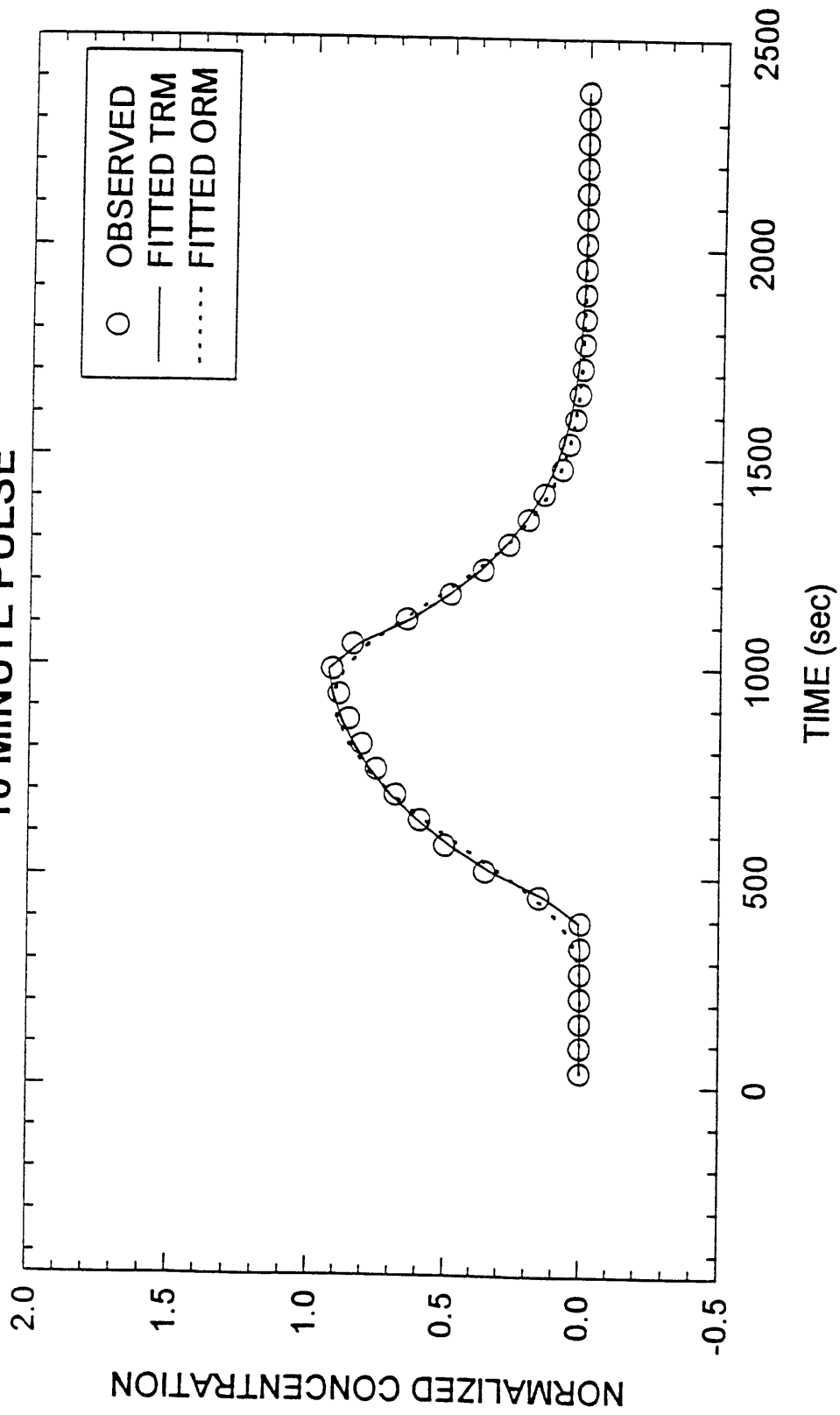
Figure 3.12   Plot of Observed and Fitted Breakthrough Curves Sand 1 Test 1
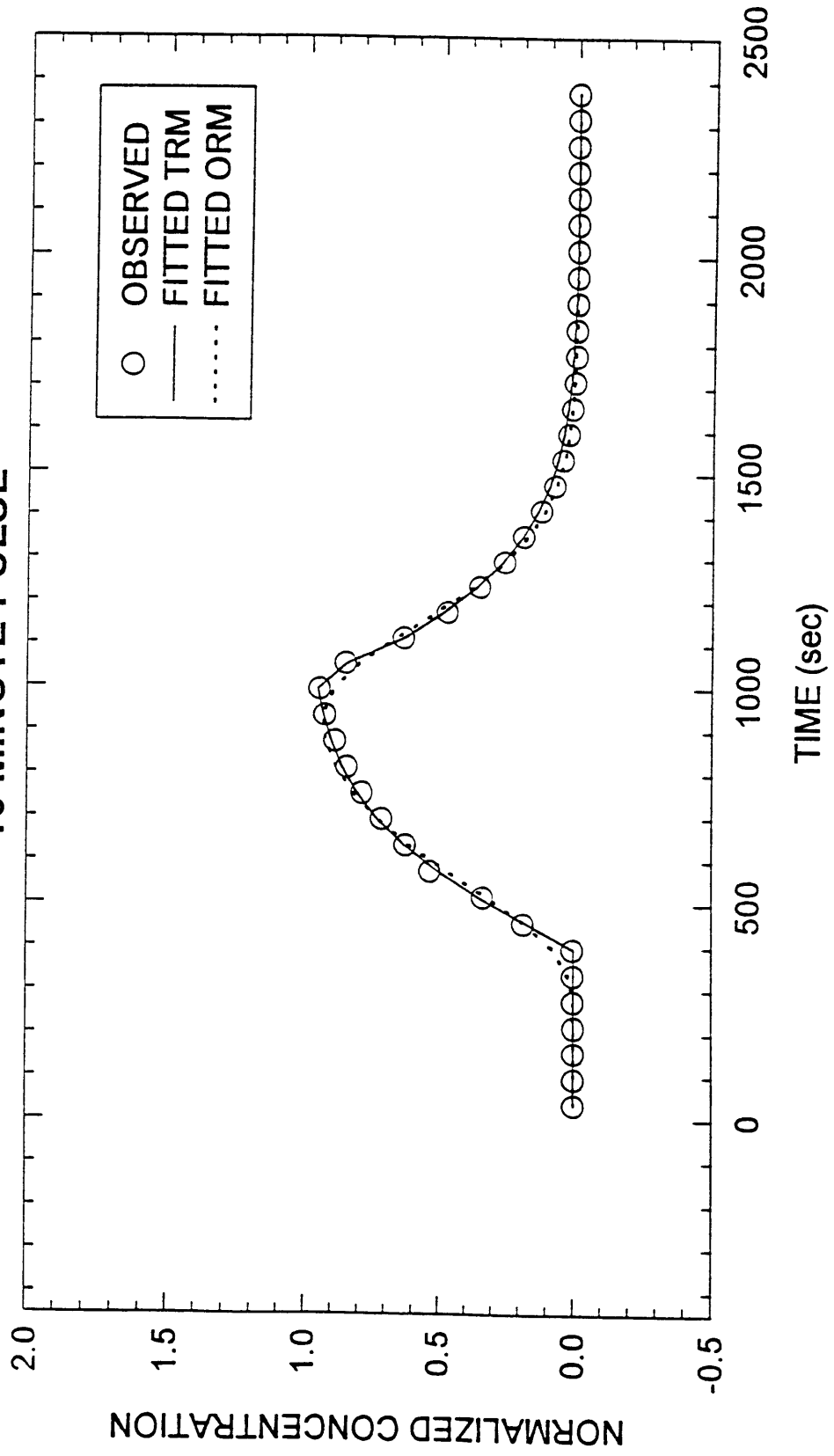
Figure 3.13   Plot of Observed and Fitted Breakthrough Curves Sand 1 Test 2

134

Figure 3.14   Plot of Observed and Fitted Breakthrough Curves Sand 2 Test 1

135
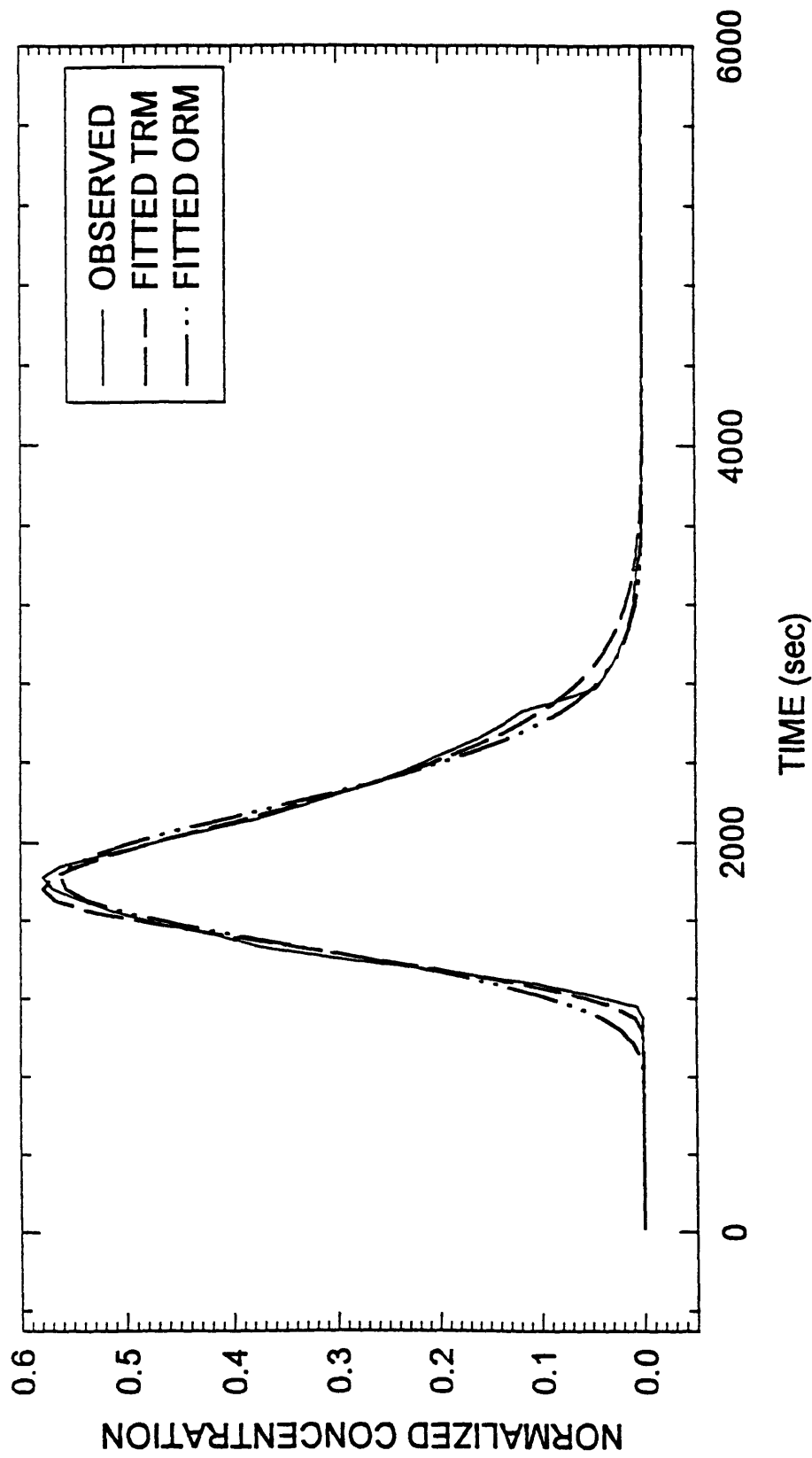
Figure 3.15   Plot of Observed and Fitted Breakthrough Curves Sand 2 Test 2
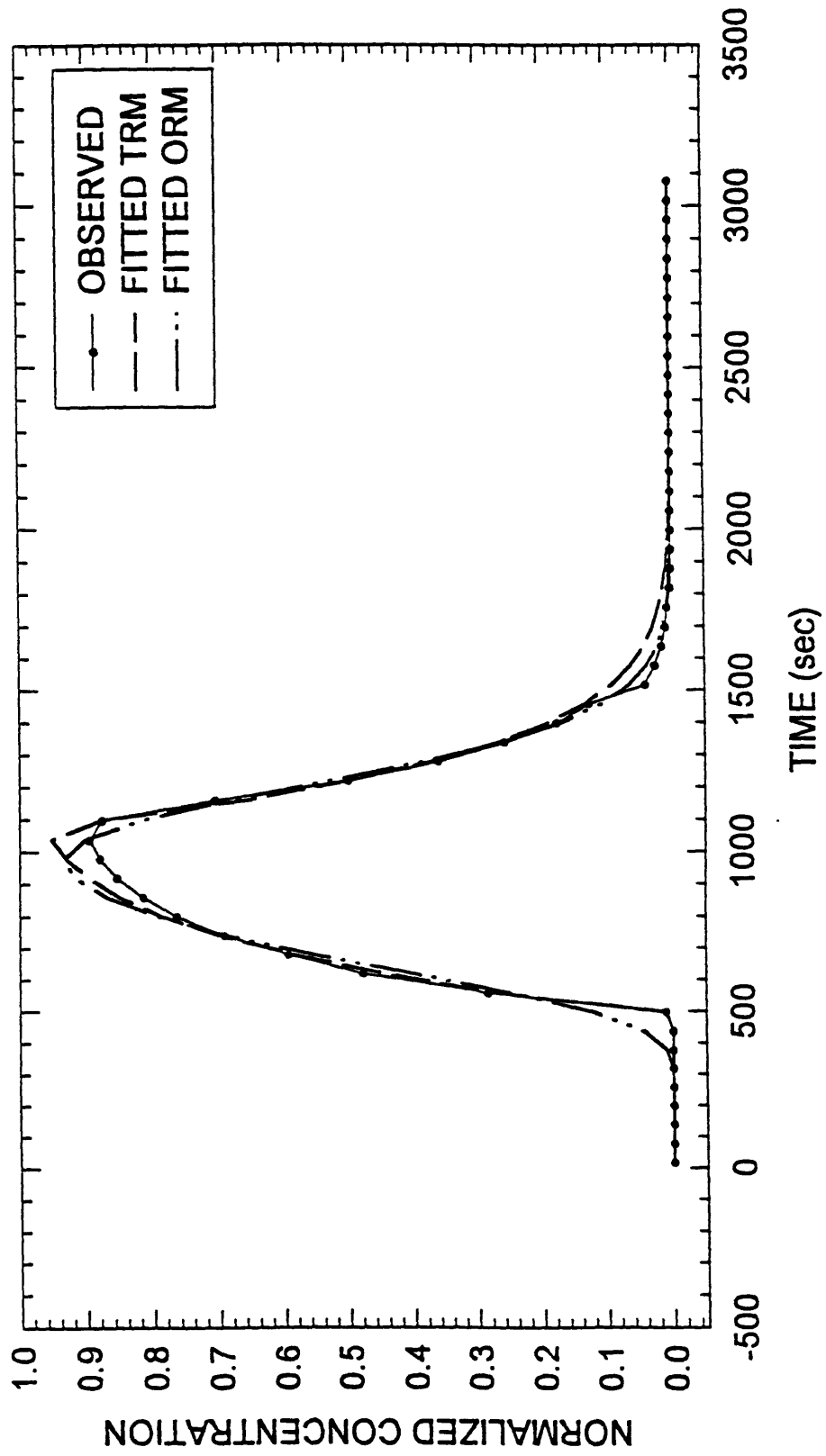
Figure 3.16   Plot of Observed and Fitted Breakthrough Curves Sand 2 Test 3

137

Figure 3.17. Plot of Observed and Fitted Breakthrough Curves Peat 1 Test 1

Figure 3.18   Plot of Observed and Fitted Breakthrough Curves Peat 1 Test 2

NORMALIZED CONCENTRATION VS TIME
0.10 M NaCl
PEAT 2 TEST 1, 1-29-96
10 MINUTE PULSE
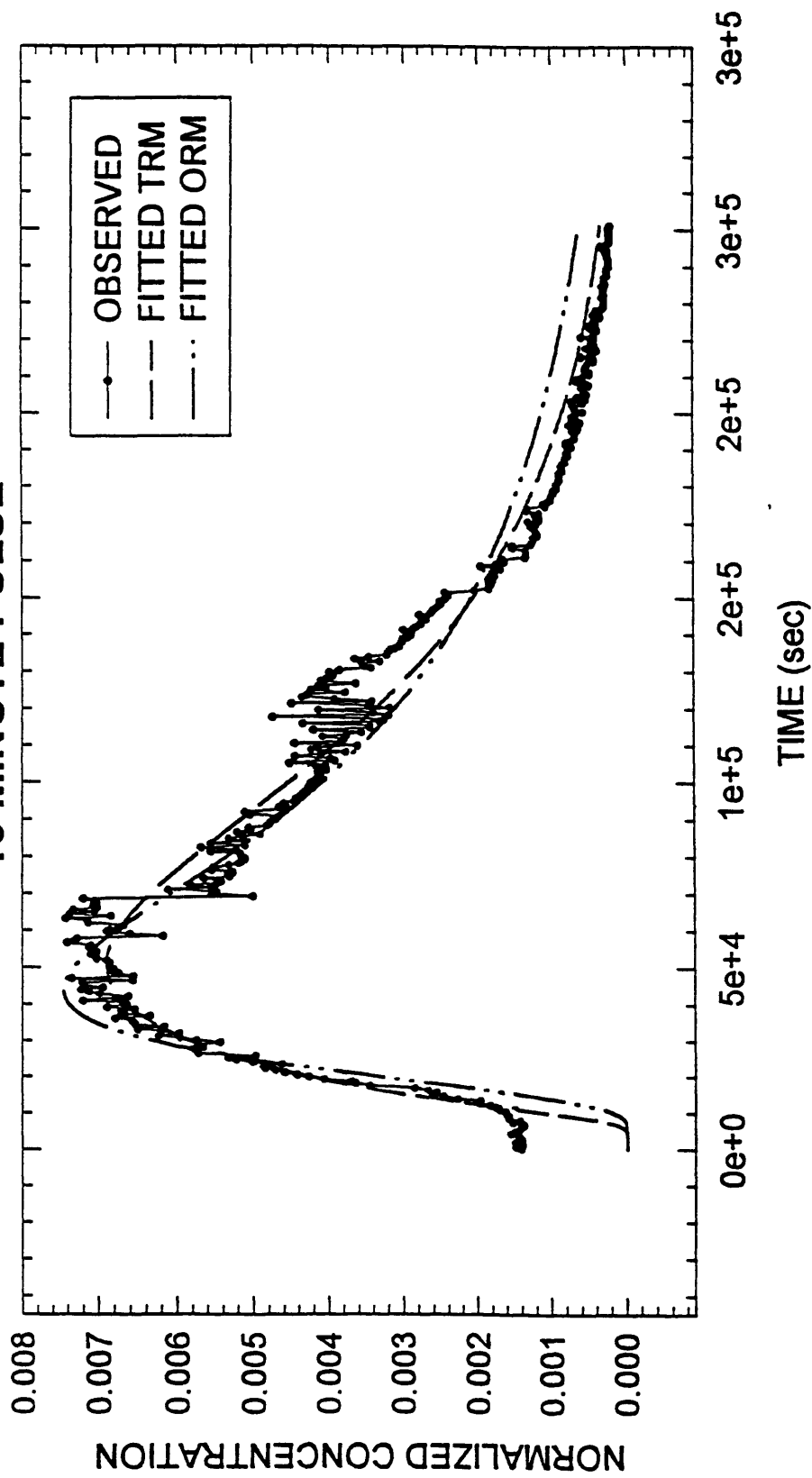
Figure 3.19   Plot of Observed and Fitted Breakthrough Curves Peat 2 Test 1

Figure 3.20   Plot of Observed and Fitted Breakthrough Curves Peat 2 Test 2

Figure 3.21   Plots of α, D, and β vs. Seepage Velocity for Sand

Figure 3.22   Plot of α vs. D_T for Sand Specimens

alpha vs. Seepage Velocity^2
Sand 1 and Sand 2
Fitted Parameters
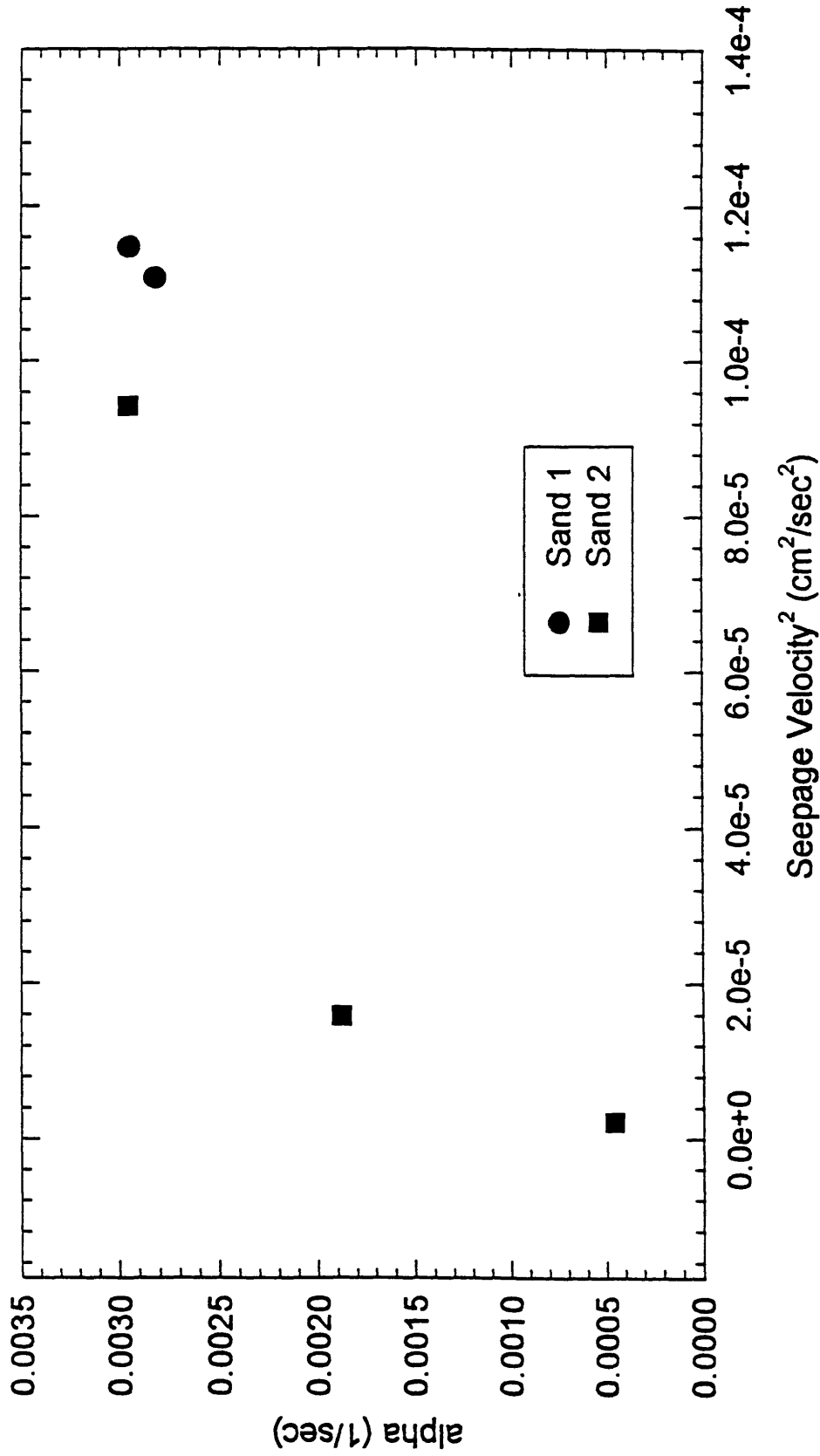
Figure 3.23   Plot of α vs. v_s^2 for Sand Experiments

D / Dmd vs Grain Peclet Number
Tests Using Sand Specimens

Sand 1 ●
Sand 2 ◆

D / D_{md}

Grain Peclet Number $(V_s d / D_{md})$
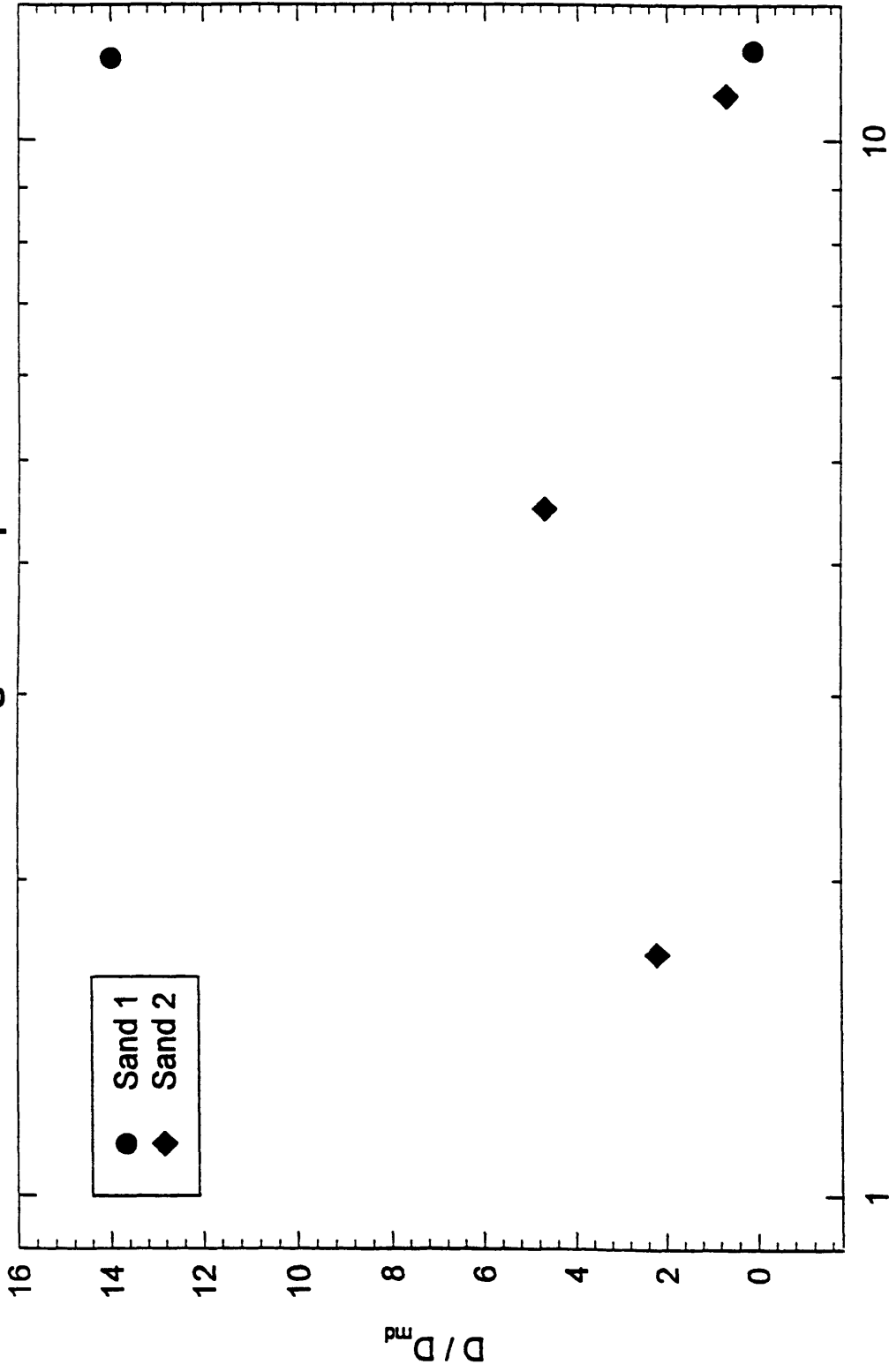
Figure 3.24   Plot of D / D_{md} vs. Grain Peclet Number for Sand Experiments

145
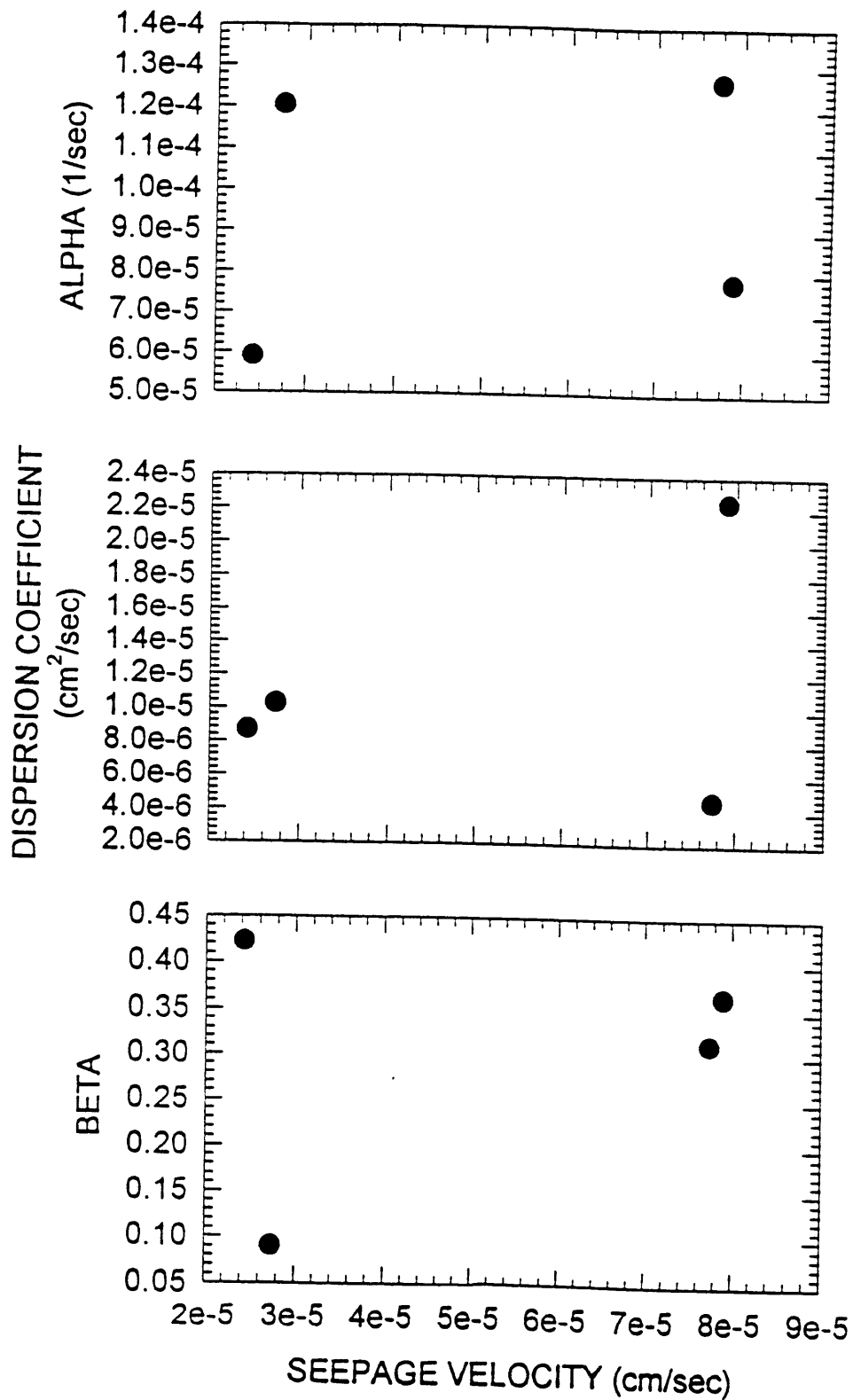
Figure 3.25   Plots of α, D, and β vs. Seepage Velocity for Peat

Effective Void Ratio vs. Hydraulic Conductivity
Peat 1 and Peat 2
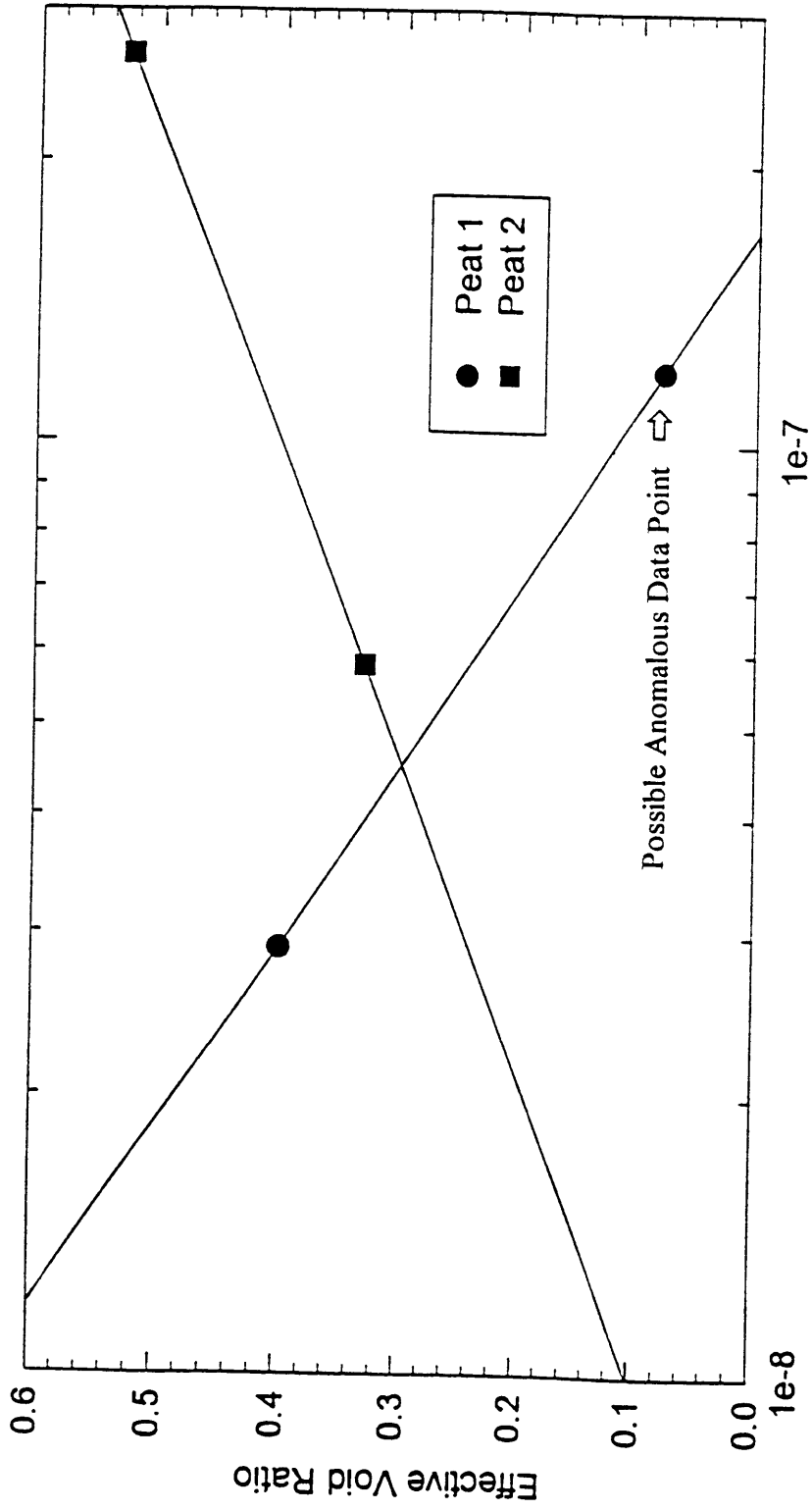
Figure 3.26   Plot of Effective Void Ratio vs. Hydraulic Conductivity, Peat 1 and Peat 2

147

Effective Void Ratio vs. Hydraulic Conductivity
Peat 1 and Peat 2
With Assumed β = .37 for Peat 1 Test 1
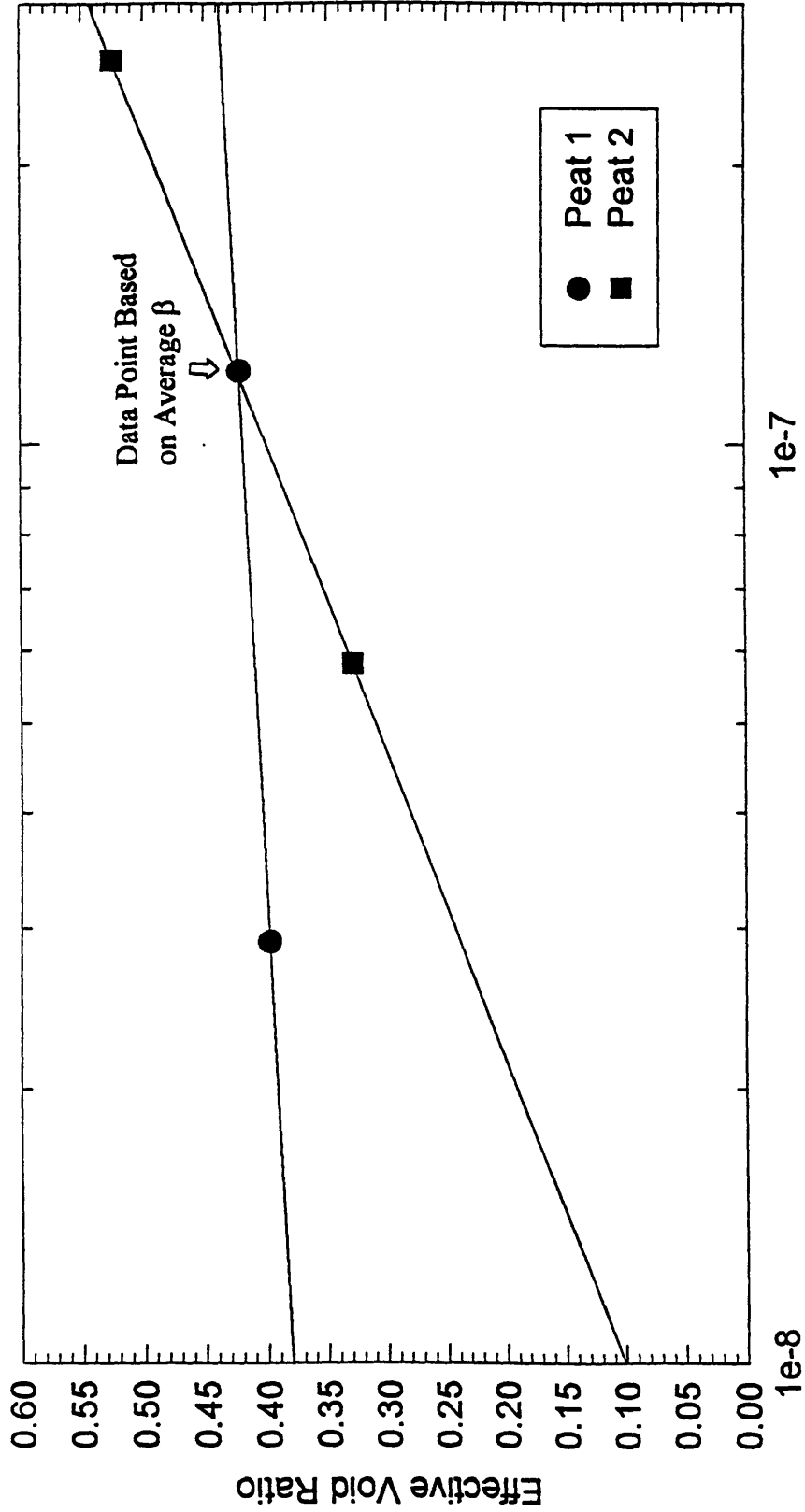
Figure 3.27   Plot of Effective Void Ratio vs. Hydraulic Conductivity,
Peat 1 and Peat 2 With β = 0.37 Assumed for Peat 1 Test 1

alpha vs. Seepage Velocity^2
Peat 1 and Peat 2
Fitted Parameters

Possible Anomalous Data Point

Peat 1
Peat 2

alpha (1/sec)
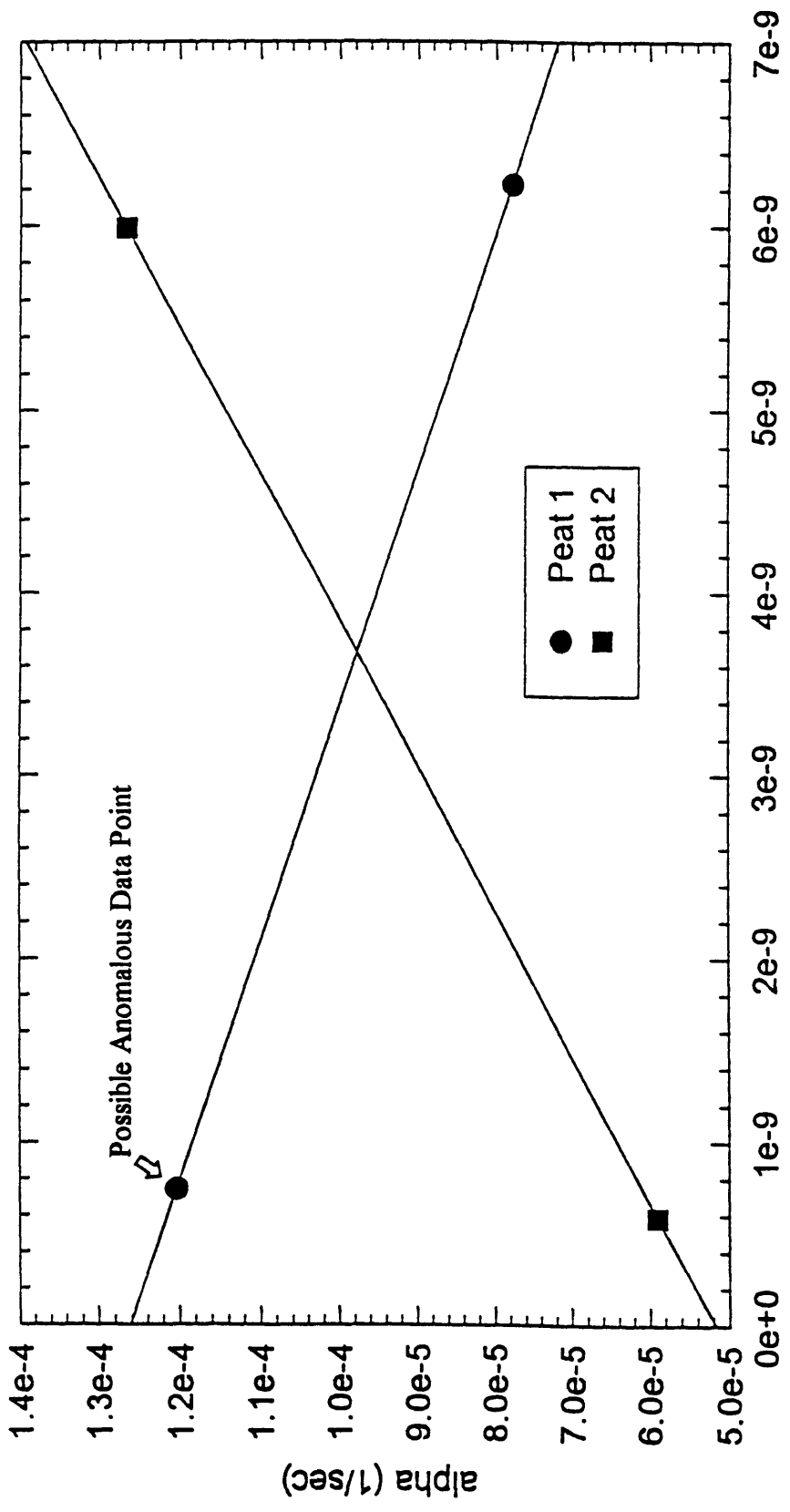
Seepage Velocity^2 (cm^2/sec^2)

Figure 3.28   Plot of α vs. v_s^2 for Peat Experiments

α vs. Transverse Dispersivity D_T

(Where D_T is approximated by the fitted Dispersion Coefficient) For Wetland Deposit Specimens

Possible Anomalous Data Point

Peat 1
Peat 2
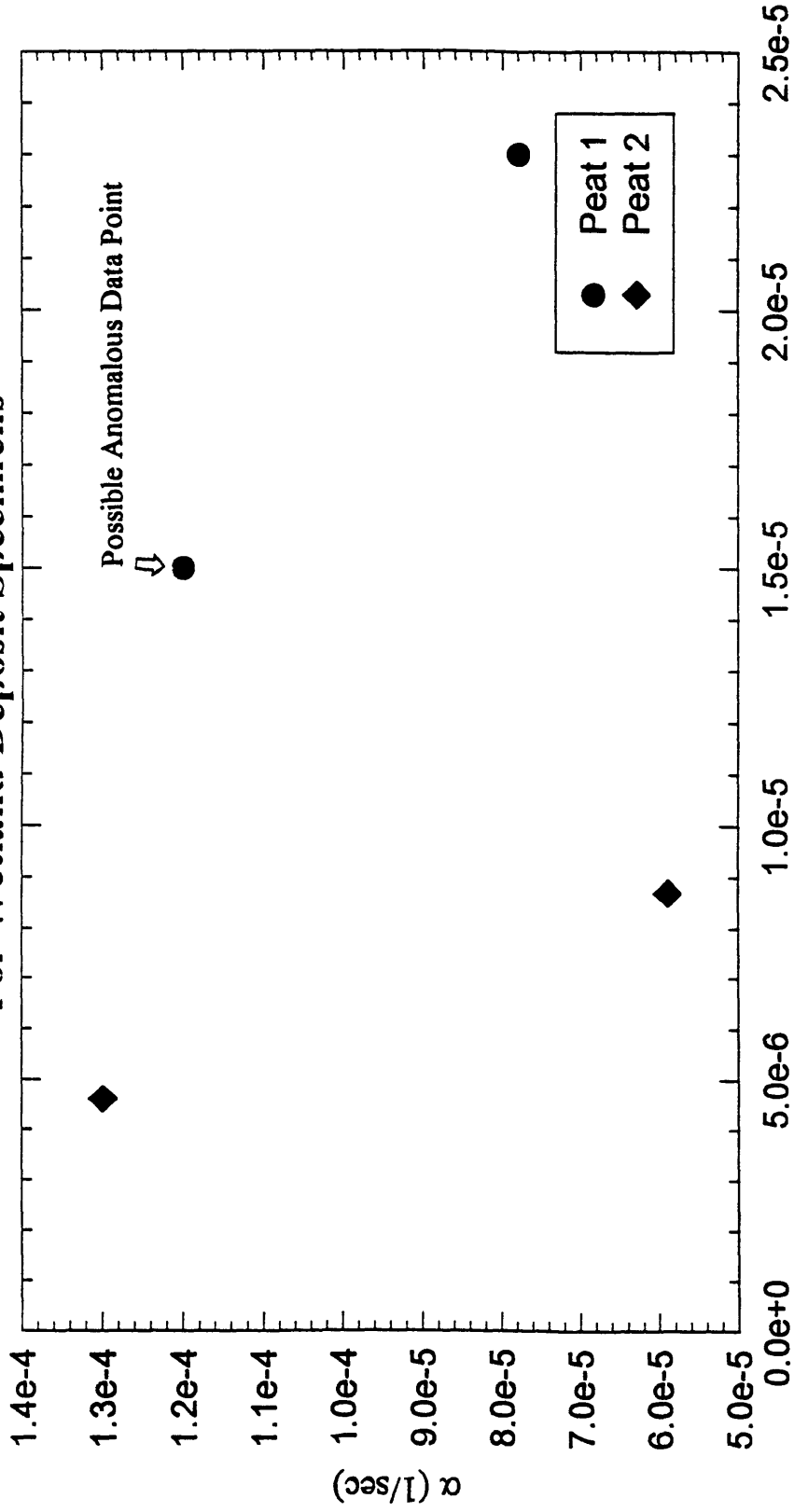
Transverse Dispersivity (D_T, cm^2/sec)

α (1/sec)

Figure 3.29   Plot of α vs. D_T for Peat Experiments

CHAPTER 4

SUMMARY AND RECOMMENDATIONS

4.1 Summary of Objectives

The Aberjona watershed had been an industrial center since the 1600's, consisting primarily of leather producing operations. With time, wastes from industrial processes made their way into the Aberjona River, and were subsequently drawn through the wetland deposits during pumping of municipal water wells labeled G and H. The Wells G and H site is now a federal Superfund site, and is being studied by a number of research groups at MIT. Initial research at MIT (Bialon, 1995) did not indicate the classical trend linking changes in hydraulic conductivity with changes in void ratio, which led to the hypothesis that the hydraulic conductivity was changing with the effective porosity. The objective of this research was to develop the equipment and procedures necessary to determine the hydraulic characteristics that govern contaminant transport through the Aberjona wetland deposits. More specifically, the goal was to be able to measure the hydraulic conductivity and obtain breakthrough curves from pulses of conservative tracers, while controlling the flow rate and effective stress acting on the specimen. The break-through curves (concentration vs. time data) could then be analyzed with a curve fitting package to obtain estimates of the hydrodynamic dispersion coefficient, effective porosity, and the mass transfer coefficient that governs the transport of contaminants between the mobile and immobile regions.

The scope of this research was to develop the equipment and methods required to make these measurements, and then to perform a preliminary set of experiments to evaluate the system. Two series of experiments were performed, one using a uniform silica sand, and the other using wetland deposits (sedge peat) obtained from the Wells G and H site,.

4.2 Summary of Equipment, Procedures, and Model

A flexible wall column was selected to allow control of effective stresses, as well as to reduce preferential flow paths along the sides of the specimen. Furthermore, by monitoring the flow of fluid into and out of the cell via a double burette system, changes in the volume, and thus the porosity, of the sample could be monitored.

The usual method of measuring hydraulic conductivity in the laboratory (establishing a known gradient and measuring the flow) was abandoned in favor of a system in which the flow was controlled, and the gradient was measured. A flow-controlled system was selected over a gradient-controlled system to provide better flow stability in a shorter period of time. The gradient was measured with pressure transducers, as was the effective stresses applied to the specimens.

. The flow system consisted of two influent reservoirs with air-water interfaces connected to the same air-pressure regulator. Equal pressures in the influent lines were designed to maintain a steady flow (and thus gradient and effective stress) while the pulse of tracer solution was being introduced. The system maintained constant pressure and supply of influent at the up-gradient end of the specimen, while the effluent was restrained by a moving piston at the down gradient end, thus forcing a steady flow rate.

Measurement of the electrical conductivity of the effluent was selected as the means to monitor variations in the concentration with time (i.e. to obtain breakthrough curves). Additionally, there were probes placed in both the influent and effluent lines to enable a conservation of mass analysis.

The data were recorded using two systems. The conductivity of the influent, pressures, volumetric flow, and temperature were recorded using the MIT geotechnical laboratory's central data acquisition system, while the conductivity of the effluent was recorded on a IBM PC. An automated multi-channel conductivity meter was developed to monitor up to four two-pin conductivity probes simultaneously. The conductivities were

then converted to concentrations, and entered into the CXTFIT code (Parker and van Genuchten, 1984) to obtain the fitted hydraulic properties of the sample.

4.3 Summary of Results

As discussed above, experiments were conducted on two different materials, a silica sand, and a sedge-type peat obtained from the Wells G and H Superfund site. Each experiment consisted of a 10 minute pulse of 0.1 M NaCl, followed by approximately three pore volumes of flushing. After the final pulse-type test was completed on a given specimen, a continuous-source experiment was conducted to determine the equilibrium conductivity reading from each probe. The results were separated into two sections; i) measured and calculated results, which included phase relations (moisture content, specific gravity, porosity and "B" value), testing conditions (seepage velocity, gradient, effective stress), hydraulic conductivity, and conservation of mass, and (ii) fitted results, which include the seepage velocities, hydrodynamic dispersion coefficients, pulse durations, β (the fraction of pore volume through which advective transport occurs), and ω (the dimensionless first order mass transfer coefficient, which describes transport between mobile and immobile regions). Sections i and ii were further separated by the type of material being tested (i.e. sand and wetland deposits).

4.3.1 Measured and Calculated Results

4.3.1.1 Experiments on Sand

The specific gravity of the sand was reported by Ratnam (1996), to be 2.66. The initial water contents of all sand specimens were assumed to be zero. Transducer problems prevented meaningful calculations of the gradient and thus the hydraulic conductivity for the sand specimens.

For Sand 2, the percentages of mass recovered ranged from 81%, to 96%. A possible explanation for the trend is that the same mass of solute was lost in the system

during each experiment, thus, for constant pulse durations, higher recoveries would be observed in experiments conducted at higher flow rates. Probe 5 was moved from the effluent line to the influent line after completion of the experiments on Sand 1, thus there are no data available on the conservation of mass for experiments using that specimen.

4.3.1.2 Experiments on Wetland Deposits

The initial moisture contents were 573% and 548% for Peat 1 and Peat 2, respectively. The corresponding specific gravities were estimated to be 1.13 and 1.32, and the initial porosities were 0.87 and 0.88, for Peat 1 and Peat 2, respectively.

For Peat 1 Test 1, at an estimated total porosity of 0.81 ($e = 4.3$), the hydraulic conductivity was 1.2×10^{-7} cm/sec. For Peat 2 Test 1, at a total porosity of 0.82 ($e = 4.6$), the hydraulic conductivity was 2.6×10^{-7} cm/sec. For the second experiments, the hydraulic conductivities were 2.8×10^{-8} cm/sec at a total porosity of 0.77 ($e = 3.3$), and 5.8×10^{-8} cm/sec at a total porosity of 0.80 ($e = 4$), for Peat 1 and Peat 2, respectively. Thus Peat 1 exhibited approximately half of the hydraulic conductivity of Peat 2.

A trend of decreasing hydraulic conductivity (k) with decreasing total porosity was observed, however, the rate of change was not consistent between the two specimens. The C_k ($\Delta e / \Delta \log k$) values were 1.5 for Peat 1, and 0.84 for Peat 2, respectively. If a regression is run through the data from both peat specimens, a value of $C_k = 1.2$ is obtained. With only four data points, however, these C_k values would be heavily biased by any non-representative results.

The conservation of mass analyses for the peat deposits indicated that the percentages recovered were 49%, 59%, 81%, and 53% for Peat 1 Tests 1 and 2, and for Peat 2 Tests 1 and 2, respectively. Peat 1 was subjected to approximately one additional week of flow prior to testing (relative to Peat 2), thus some of ions initially present in the specimen were flushed out prior to testing. This was not the case for Peat 2, which may

154

be the reason for what appears to be an abnormally high recovery percentage observed for Peat 2 Test 1.

4.3.2 Fitted Results

The two site, two region model (TRM, Model 4 of Parker and van Genuchten's CXTFIT code) was used to fit hydraulic parameters to the experimental breakthrough curves. Additionally, a one region model (ORM, Model 2 of Parker and van Genuchten's CXTFIT code), based on the advection-dispersion equation, was fit to the data for comparison with the TRM. In all cases, the TRM resulted in a better fit.

4.3.2.1 Experiments on Sand

In general the fits for both the TRM and ORM were relatively good. For the ORM, R^2 ranged from 0.963 to 0.995, while for the TRM, R^2 ranged from 0.996 to 0.999. The close fit obtained from the ORM would support an assumption of equilibrium transport for these relatively uniform specimens. The fitted parameters discussed below were obtained using the TRM.

The fitted seepage velocities and pulse durations for Sand 1 closely matched the calculated/measured values. For Sand 2, however, the fitted seepage velocities were slightly greater than the calculated values, and the pulse durations were shorter than the observed durations. β, the fraction of pore volume participating in advective flow, was relatively constant for the sand specimens at approximately 0.74. There did not appear to be a correlation between β and the seepage velocity, which confirms that β is a parameter characterizing the soil/system's structure. ω, the dimensionless mass transfer coefficient, varied between 1.8 and 3.1. The grain Peclet numbers exceeded one in all experiments, ranging from 1.7 to 12.1, thus α (the dimensional mass transfer coefficient, $= \omega q/L$) was expected to vary linearly as the velocity, which it did to some degree. The best fit regression line had $R^2 = 0.91$.

The dispersion coefficient for the sand specimens ranged from 2.1×10^{-4} cm^2/sec to 1.3×10^{-6} cm^2/sec. There did not appear to be any relationship between D and the seepage velocity. For these experiments, D was expected to vary approximately linearly with V_s, since the grain Peclet number was greater than one. However, no such correlation was observed, suggesting that inter region diffusion might have been dominating the mass transfer process, rather than local flow variations (additionally, there was no observed correlation between α and V_s^2). This process was not confirmed either, however, as no linear correlation was observed between α and D_T. The failure to observe the expected trends was attributed an insufficient number of data points.

4.3.2.2 Experiments on Wetland Deposits

In general the fitted curves were not as good a match with the experimental data for the wetland deposits as they were for the sand specimens. Additionally, the breakthrough curves for peat had significant tailing relative to the breakthrough curves for sand. Such tailing is characteristic of soils with immobile regions, and is thus indicative of non-ideal chemical transport. The TRM provided consistently better fits to the experimental data than the fits obtained from the ORM, which further indicated that non-equilibrium transport was taking place in the wetland deposits. The following discussion is based on the fitted parameters obtained using the TRM.

The fitted seepage velocities were greater than the calculated values (based on total porosity), which is consistent with immobile regions within the pore spaces of the specimens. Also, the fitted pulse durations were shorter than the measured values, which is consistent with the percentages of recovered mass being less than 100%. The exception was Peat 2 Test 1, in which some leaching of ions initially present in the material appears to have occurred, thus leading to a higher fitted pulse duration then the measured value.

β varied from 0.09, to 0.42, and no consistent trend between β and seepage velocity, was observed, however 0.09 (β for Peat 1 Test 1) is enough of a deviation from

the other values (0.31 and 0.37) that it could be an anomaly. There was expected to be a correlation between effective void ratio and log of hydraulic conductivity, however no correlation was exhibited by the data of this research. This lack of correlation was also attributed to outlying values among few data points.

Omega, varied between 9.4 and 2.1 for the wetland deposits. Calculated values of the grain Peclet number were less than unity for the experiments using peat specimens, thus, α was expected to vary as v_s^2 for the case of low velocity contrasts between the two regions. No trend was observed between α and v_s^2, nor between α and v_s for these experiments, which suggests that there were significant velocity contrasts between the mobile and immobile regions. However, if significant velocity contrasts existed, α should have scaled as D_T, which was not exhibited by these data. Again, a non-representative data point would have significantly biased the results.

The fitted hydrodynamic dispersion coefficients for the peat specimens ranged from 1.0×10^{-5} cm^2/sec to 8.7×10^{-6} cm^2/sec. There did not appear to be any trend linking D with seepage velocity values, which is consistent with the grain Peclet numbers being less than unity.

4.4 Recommendations for Continued Research

The following recommendations are made with respect to future research involving this equipment:

1) The flow control device could be placed at the influent end of the specimen rather than at the effluent end. With this configuration, increases in the gradient will reduce the effective stress rather than increase it, thus eliminating flow induced consolidation and reducing the time to steady flow. It is recommended that the flow control device be attached to a three way valve that will allow it to a) force distilled water into the

sample at a steady rate, or, b) force distilled water into a bag within the tracer reservoir, which will send the tracer through the sample at a steady rate.

2) A differential pressure transducer would eliminate the problems associated with measuring small gradients at elevated back pressures. To avoid diffusion of solutes into and out of the transducer (which could affect results) it would have to measure the differential pressure between the line above the three-way valve to direct flow from the flow control device (discussed above) and the effluent below the last conductivity probe.

3) To improve the pH and Eh stability, a pressurized reference electrode could replace the current reference. With the current electrode, the pressure in the effluent line is greater than that in the reference barrel, which forces the effluent into the barrel (the opposite of the intended flow direction), thus diluting reference solution. For back pressures of 4 ksc, the pressure in the reference barrel should be greater than 4 ksc.

4) The stability of the pH and Eh transducers might also be improved if the other transducers are turned off while the pH and Eh readings are recorded. This would eliminate the possibility of the alternating current from the conductivity transducers interfering with the recorded values. To facilitate this, it is suggested that all of the conductivity probes, the temperature probe, and the pH and Eh probes be recorded using the Sheahan (MIT, 1991) card and the conductivity control program. This will eliminate the need for coordinating reading times between the geotechnical central data acquisition system and the conductivity data acquisition system.

5) A DCDT with a 21 cm (8 in.) linear range would eliminate the need to set the barrel at the top of the linear range before each experiment

6) As previously stated, the primary focus of this thesis was the development of equipment and procedures. There were not enough data to enable conformation of the presence or absence of expected trends, from which the hydraulic behavior of the Wells G and H sediments could be characterized. It is therefore recommended that this research effort be continued as originally outlined in the proposal by Professor Culligan-Hensley (1994).

REFERENCES

1. Analog Devices, <u>Special Linear Reference Manual</u>, Analog Devices, Inc., 1992.

2. Bear, Jocob, <u>Dynamics of Fluids in Porous Media</u>, American Elsivier Publishing Company, Inc., 1972

3. Bialon, J.L., <u>Characterization of the Physical and Engineering Properties of the Aberjona Wetland Sediment</u>. Sc.M. Thesis, Massachusetts Institute of Technology, Cambridge, MA. 1995.

4. Boelter, D.H., <u>Hydraulic Conductivity of Peats</u>, Soil Science, Vol. 100, No. 4, October, 1965.

5. Culligan-Hensley, P.J., <u>Physical Characterization of Parameters Effecting Subsurface Contaminant Transport in the Aberjona Watershed, with Emphasis on Wells G and H Site.</u> Research Proposal, MIT, 1994.

6. Daniel, D.E., <u>Geotechnical Practice for Waste Disposal</u>. Chapman & Hall, 1993.

7. Daniel, D.E., Anderson, D.C., and Boynton, S.S., <u>Fixed-Wall Versus Flexible-Wall Permeameters</u>, Hydraulic Barriers in Soil and Rock, ASTM STP 874, Philidelphia, 1985, pages 107-126.

8. de Lima, V., and Olimpio, J.C., <u>Hydrogeology and Simulation of Groundwater Flow at Superfund Site Wells G and H, Woburn, Massachusetts</u>, U.S. Geological Survey, Water-Resources Investigations Report 89-4059, 1989.

9. Durant, J.L., <u>Industrial History, Mutagenicity, and Hydrologic Transport of Pollutants in the Aberjona Watershed</u>. Sc.M. Thesis, Massachusetts Institute of Technology, Cambridge, MA. 1991.

10. Head, M.J., <u>The use of Miniature Four-Electrode Conductivity Probes for High Resolution Measurement of Turbulent Density or Temperature Variations in Salt-Stratified Water Flows</u>. PhD thesis, University of California, San Diego. 1983.

11. Hoag, R.S., and Price, J.S., <u>A field-Scale, Natural Gradient Solute Transport Experiment in Peat at a Newfoundland Blanket Bog</u>, Journal of Hydrology No. 172, 1995.

12. Holtz, R.D., and Kovacs, W.D., <u>An Introduction to Geotechnoical Engineering</u>, Prentice-Hall, Inc., 1981

13. Lambe, T.W. and Whitman, R.V., <u>Soil Mechanics</u>, John Wiley & Sons, 1969.

REFERENCES (Continued)

14. Latowski, G.P., A Case Study: Woburn Massachusetts, Research and Training Institute, Inc., presented at the Internatioal Symposium on Women, Politics, and Environmental Action, Mosow, Russia, June 1994

15. Li, L., Barry, D.A., Culligan Hensley, P.J., Bajracharya, K., Mass transfer in soils with local stratification of hydraulic conductivity. Water Resources Research, Vol. 30, No. 11, pages 2891-2900, November 1994.

16. Loxham, M., and Burghardt, W., Peat as a Barrier to the Spread of Micro-Contaminants to the Groundwater, Proceedings of the International Symposium on Peat Utilization, Bemidji State University, 1983.

17. McBrearty, D, Fracture Flow as Influenced by Geologic Features in the Aberjona Valley, Massachusetts. Sc.M. Thesis, Massachusetts Institute of Technology, Cambridge, MA. 1995.

18. MIT Superfund Basic Reasearch Program, Project Book

19. Myette, C.F., Olimpio, J.C., and Johnson, D.G., Area of Influence and Zone of Contribution to Superfund-Site Wells G and H, Woburn, Massachusetts. U.S. Geological Survey, Water-Resources Investigations Report 87-4100, Boston, MA, 1987

20. Olsen, H.W., Nichols, R.W., and Rice, T.L., Low gradient permeability measurements in a triaxial system, Geotechnique 35, No. 2, pages 145-157.

21. Olson, R.E., and Daniel, D.E., Measurement of the Hydraulic Conductivity of Fine-Grained Soils, Permeability and Groundwater Contaminant Transport, ASTM STP 746, pages 18-64, 1981.

22. Parker, J.C., and van Genuchten, M.Th., Determining Transport Parameters from Laboratory and Field Tracer Experiments, Virginia Agricultural Experiment Station, Bulletin 84-3, 1984.

23. Price, J.S., and Woo, M., Wetlands as Waste Repositories?: Solute transport in Peat, Proceedings of the National Student Conference on Northern Studies, Ottawa, Ontario, 1986.

24. Ratnam, S., Geotechnical Centrifuge Modeling of the Behavior of Light Nonaqueous Phase Liquids (LNAPLs) in Sand Samples Under Hydraulic Flushing, Sc.M. Thesis, Massachusetts Institute of Technology, Cambridge, MA. 1996.

REFERENCES (Continued)

25. Shackelford, C.D., Critical Concepts for Column Testing, Journal of Geotechnical Engineering, Vol. 120, No. 10, October 1994, pages 1804 - 1828.

26. Sheahan, T.C., An Experimental Study of the Time-Dependent Undrained Shear Behavior of Resedimented Clay Using Automated Stress Path Triaxial Equipment, Sc.D. Thesis, Massachusetts Institute of Technology, Cambridge, MA. 1991.

27. Taylor, S.R., Moltyaner, G.L., Howard, K.W.F., and Killey, R.W.D., A Comparison fo Field and Laboratory Methods for Determining Contaminant Flow Parameters, Groundwater, Vol. 25, No. 3, 1987, pages 321 - 330.

APPENDIX A: EPOXY DATA SHEETS

STYCAST® 2651 MM Epoxy Encapsulant

KEY FEATURES:

• General purpose
• Excellent machinability
• Low viscosity
• A variety of hardeners possible
• Dispensable

PRODUCT DESCRIPTION:

STYCAST 2651 MM is a filled, low viscosity, general purpose, epoxy encapsulant which can be cured with a variety of hardeners. It contains a soft filler that makes it a natural for automatic meter/mix dispensing equipment.

When cured, STYCAST 2651 MM has excellent machinability along with a good balance of physical, thermal and electrical properties.

INSTRUCTIONS FOR USE:

General:

Thoroughly read the information concerning health and safety contained in this bulletin before using. Observe all precautionary statements that appear on the product label and/or contained in individual Material Safety Data Sheets (MSDS).

To ensure the long term performance of the potted or encapsulated electrical/electronic assembly, complete cleaning of components and substrates should be performed to remove contamination such as dust, moisture, salt,

and oils which can cause electrical failure, poor adhesion or corrosion in an embedded part.

Mixing:

Some filler settling is common during shipping or storage. For this reason, it is recommended that each component be thoroughly mixed in its shipping container prior to use. Power mixing is preferred to ensure a homogeneous product.

Accurately weigh resin and selected hardener into a clean container in the recommended ratio. Weighing apparatus having an accuracy in proportion to the amounts being weighed should

always be used.

Blend components by hand, using a kneading motion for 2-3 minutes. Scrape the bottom and sides of the mixing container frequently to produce a uniform mixture. If possible, power mix for an additional 2-3 minutes. Avoid high mixing speeds which could entrap excessive amounts of air or cause overheating of the mixture resulting in reduced working life.

Deairing:

To ensure a void-free embedment, vacuum deairing should be used to remove any entrapped air introduced during the mixing operation.

TYPICAL HANDLING PROPERTIES

Property	Value	Test Method
Color	Black	Visual
Viscosity, cps @ 25°C, Brookfield RVT Spindle #5 @ 5 rpm	35,000	ASTM D2393
Specific Gravity, @ 25°C	1.61	ASTM D1875
Shelf Life, months @ 25°C	12	

CHOICE OF HARDENER*

Product	Type of Cure	Product Description
Catalyst 9	Room	General purpose epoxy hardener. Imparts good chemical resistance and physical strength to cured castings.
Catalyst 11	Heat	General purpose epoxy hardener with long working life. Yields castings with excellent chemical resistance. Good physical and electrical properties at elevated temperatures.
Catalyst 23 LV	Room	Low color, low viscosity epoxy hardener. Long pot life. Imparts excellent thermal shock and impact resistance to cured castings. Excellent adhesion to glass.

* For more information concerning these epoxy curing agents, please refer to Grace Specialty Polymers Curing Agent Selector Guide.

TYPICAL MIXED PROPERTIES				
Resin	2651 MM	2651 MM	2651 MM	Test Method
Catalyst	9	11	23 LV	
Mix Ratio, by weight	100:6-7	100:8	100.15	
Mix Ratio by volume	100:12	100:13	100:25	
Viscosity, cps @ 25°C, Brookfield RVT	14,000	13,000		ASTM D2393
Specific Gravity @ 25°C	1.58	1.59	1.52	ASTM D1875
Working Life (100 g @ 25°C)	45 min	> 4 hr	60 min	ERF15-70

Vacuum deair mixture at 1-5 mm mercury. The foam will rise several times the liquid height and then subside. Continue vacuum deairing until most of the bubbling has ceased. This usually requires 3-10 minutes.

To facilitate deairing in difficult-to-deair materials, add 1-3 drops of an air release agent, such as Antifoam 88, into 100 grams of mixture. Gentle warming will also help, but working life will be shortened.

Application:

Pour mixture into cavity or mold. Gentle warming of the mold or assembly reduces the viscosity improving the flow of material into unit having intricate shapes or tightly packed coils or components. Further vacuum deairing in the mold may be required for critical applications.

Cure using any one of the recommended schedules. For optimum performance, the initial cure schedule should be followed with a post cure. In general, a post cure of 4-16 hours at the highest expected use temperature is recommended. Alternate cure schedules may also be possible. Contact your Grace Specialty Polymers Technical Representative for further information.

STORAGE & HANDLING:

For best results, store resins and hardeners in original, unopened containers. Storage in cool, clean and dry areas is recommended. Usable shelf life may

TYPICAL CURE SCHEDULE			
Resin	2651 MM	2651 MM	2651 MM
Catalyst	9	11	23 LV
@ 25°C	16-24 hr		24 hr
@ 45°C	4-6 hr		4-6 hr
@ 65°C	1-2 hr		2-4 hr
@ 80°C		8-16 hr	
@ 100°C		2-4 hr	
@ 120°C		30-60 min	

vary depending on method of application and storage temperature.

Certain resins and hardeners are prone to crystallization. If crystallization does occur, warm the contents of the shipping container to 50-65°C until all crystals have dissolved. Be sure the shipping container is loosely covered during the warming stage to prevent any pressure build-up. Allow contents to cool to room temperature before continuing.

ATTENTION SPECIFICATION WRITERS:

The technical information contained herein outlines the typical properties of this material and should not be used in the preparation of specifications as it is intended for reference only.

For assistance in preparing specifications, please contact our Specifications Coordinator for specific recommendations.

SAFETY/HYGIENE:

This product like most epoxy compounds possesses the ability to cause skin and eye irritation upon contact. Certain individuals

may also develop an allergic reaction after exposure (skin contact, inhalation of vapors, etc.) which may manifest itself in a number of ways including skin rashes and an itching sensation. Handling this product at elevated temperatures may also generate vapors irritating to the respiratory system.

Good industrial hygiene and safety practices should be followed when handling this product. Proper eye protection and appropriate chemical resistant clothing should be worn to minimize direct contact. Consult the Material Safety Data Sheet (MSDS) for detailed recommendations on the use of engineering controls and personal protective equipment.

This information is only a brief summary of the available safety and health data. Thoroughly review the MSDS for more complete information before using this product.

TYPICAL CURED PROPERTIES				
Resin	2651 MM	2651 MM	2651 MM	Test Method
Catalyst	9	11	23 LV	
PHYSICAL PROPERTIES				
Hardness, Shore @25°C	98D	89D	86D	ASTM D2240
Flexural Strength, psi	10,700	12,000	15,000	ASTM D790
Compressive Strength, psi	21,500	15,000	12,000	ASTM D695
Tensile Strength, psi	5,600	7,000	8,000	ASTM D638
Linear Shrinkage, in/in	0.001	0.002		ASTM D2566
Water Absorption, % (24 hr)	0.2	0.1	0.2	ASTM D570
Machinability	Excellent	Excellent	Excellent	
THERMAL PROPERTIES				
Coefficient of Thermal Expansion /°C	57.5x10⁻⁶	40x10⁻⁶	51.5x10⁻⁶	ASTM E831
Thermal Conductivity (BTU)(in)/(hr)(ft²)(°F) (cal)(cm)/(sec)(cm²)(°C)	4.2 0.0015	4.2 0.0015	4.2 0.0015	ASTM F433
Temperature Range of Use, °C	-40 to +130	-55 to +155	-55 to +105	
Outgassing⁽¹⁾ % TML % CVCM	0.38 0.00			ASTM E595
ELECTRICAL PROPERTIES				
Dielectric Strength, volts/mil	450	450	450	ASTM D149
Dielectric Constant, 60 Hz 1 KHz 1 MHz	4.42	4.6 4.4 3.7	4.8	ASTM D150
Dissipation Factor, 60 Hz 1 KHz 1 MHz	0.04	0.02 0.01 0.02	0.06	ASTM D150
Volume Resistivity, ohm-cm @ 25°C @ 150°C	5x10¹⁵	4x10¹⁴ 7x10¹²	5x10¹⁵	ASTM D257

⁽¹⁾per NASA Reference Publication 1124. Samples tested were cured for 7 days @ 25°C.

Gallon w/out
cct 9
$56
2651 mm Block

508 - 664-9355

Machinable
Bond to Stainless, wire coatings
Non conducting (electrical)
Non Corrosive
Fungus Resistant (Non nutrient)

APPENDIX B: TRANSDUCER DATA SHEETS

ANALOG DEVICES

Low Cost, Precision IC Temperature Transducer

AD592*

FEATURES
High Precalibrated Accuracy: 0.5°C max @ 25°C
Excellent Linearity: 0.15°C max (0 to +70°C)
Wide Operating Temperature Range: −25°C to +105°C
Single Supply Operation: +4V to +30V
Excellent Repeatability and Stability
High Level Output: 1µA/K
Two Terminal Monolithic IC: Temperature In/Current Out
Minimal Self-Heating Errors

CONNECTION DIAGRAM

PIN 3   PIN 2   PIN 1
(−)   (NC)   (+)
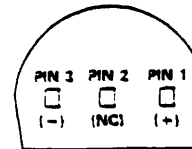
*PIN 2 CAN BE EITHER ATTACHED OR UNCONNECTED

BOTTOM VIEW

PRODUCT DESCRIPTION

The AD592 is a two terminal monolithic integrated circuit temperature transducer that provides an output current proportional to absolute temperature. For a wide range of supply voltages the transducer acts as a high impedance temperature dependent current source of 1µA/K. Improved design and laser wafer trimming of the IC's thin film resistors allows the AD592 to achieve absolute accuracy levels and nonlinearity errors previously unattainable at a comparable price.

The AD592 can be employed in applications between −25°C and +105°C where conventional temperature sensors (i.e., thermistor, RTD, thermocouple, diode) are currently being used. The inherent low cost of a monolithic integrated circuit in a plastic package, combined with a low total parts count in any given application, make the AD592 the most cost effective temperature transducer currently available. Expensive linearization circuitry, precision voltage references, bridge components, resistance measuring circuitry and cold junction compensation are not required with the AD592.

Typical application areas include; appliance temperature sensing, automotive temperature measurement and control, HVAC (heating/ventilating/air conditioning) system monitoring, industrial temperature control, thermocouple cold junction compensation, board-level electronics temperature diagnostics, temperature readout options in instrumentation, and temperature correction circuitry for precision electronics. Particularly useful in remote sensing applications, the AD592 is immune to voltage drops and voltage noise over long lines due to its high impedance current output. AD592s can easily be multiplexed; the signal current can be switched by a CMOS multiplexer or the supply voltage can be enabled with a tri-state logic gate.

The AD592 is available in three performance grades; the AD592AN, AD592BN and AD592CN. All devices are packaged in a plastic TO-92 case rated from −45°C to +125°C. Performance is specified from −25°C to +105°C. AD592 chips are also available, contact the factory for details.

PRODUCT HIGHLIGHTS

1. With a single supply (4V to 30V) the AD592 offers 0.5°C temperature measurement accuracy.

2. A wide operating temperature range (−25°C to +105°C) and highly linear output make the AD592 an ideal substitute for older, more limited sensor technologies (i.e., thermistors, RTDs, diodes, thermocouples).

3. The AD592 is electrically rugged; supply irregularities and variations or reverse voltages up to 20V will not damage the device.

4. Because the AD592 is a temperature dependent current source, it is immune to voltage noise pickup and IR drops in the signal leads when used remotely.

5. The high output impedance of the AD592 provides greater than 0.5°C/V rejection of supply voltage drift and ripple.

6. Laser wafer trimming and temperature testing insures that AD592 units are easily interchangeable.

7. Initial system accuracy will not degrade significantly over time. The AD592 has proven long term performance and repeatability advantages inherent in integrated circuit design and construction.

REV. A

AD592—SPECIFICATIONS (typical @ +25°C, V_S = +5V unless otherwise noted)

Model	AD592AN Min	Typ	Max	AD592BN Min	Typ	Max	AD592CN Min	Typ	Max	Units
ACCURACY										
Calibration Error @25°C[1]		1.5	2.5		0.7	1.0		0.3	0.5	°C
T_A = 0 to +70°C										
Error over Temperature		1.8	3.0		0.8	1.5		0.4	0.8	°C
Nonlinearity[2]		0.15	0.35		0.1	0.25		0.05	0.15	°C
T_A = −25 to +105°C										
Error over Temperature[3]		2.0	3.5		0.9	2.0		0.5	1.0	°C
Nonlinearity[2]		0.25	0.5		0.2	0.4		0.1	0.35	°C
OUTPUT CHARACTERISTICS										
Nominal Current Output @25°C (298.2K)		298.2			298.2			298.2		μA
Temperature Coefficient		1			1			1		μA/°C
Repeatability[4]			0.1			0.1			0.1	°C
Long Term Stability[5]			0.1			0.1			0.1	°C/month
ABSOLUTE MAXIMUM RATINGS										
Operating Temperature	−25		+105	−25		+105	−25		+105	°C
Package Temperature[6]	−45		+125	−45		+125	−45		+125	°C
Forward Voltage (+ to −)			44			44			44	V
Reverse Voltage (− to +)			20			20			20	V
Lead Temperature (Soldering 10 sec)			300			300			300	°C
POWER SUPPLY										
Operating Voltage Range	4		30	4		30	4		30	V
Power Supply Rejection										
+4V<V_S<+5V			0.5			0.5			0.5	°C/V
+5V<V_S<+15V			0.2			0.2			0.2	°C/V
+15V<V_S<+30V			0.1			0.1			0.1	°C/V

NOTES
[1] An external calibration trim can be used to zero the error @25°C.
[2] Defined as the maximum deviation from a mathematically best fit line.
[3] Parameter tested on all production units at +105°C only. C grade at −25°C also.
[4] Maximum deviation between +25°C readings after a temperature cycle between −45°C and +125°C. Errors of this type are noncumulative.
[5] Operation @125°C, error over time is noncumulative.

[6] Although performance is not specified beyond the operating temperature range, temperature excursions within the package temperature range will not damage the device.
Specifications subject to change without notice.
Specifications shown in boldface are tested on all production units at final electrical test. Results from these tests are used to calculate outgoing quality levels. All min and max specifications are guaranteed, although only those shown in boldface are tested on all production units.

METALIZATION DIAGRAM
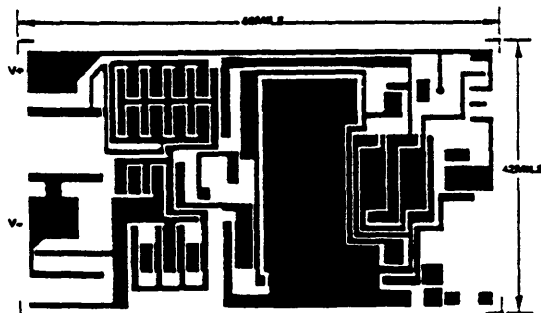
THE AD592 IS AVAILABLE IN LASER-TRIMMED CHIP FORM.
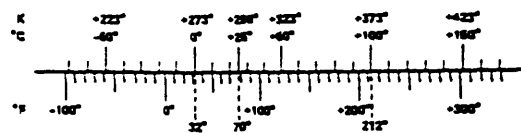
TEMPERATURE SCALE CONVERSION EQUATIONS

$$°C = \frac{5}{9}(°F - 32) \qquad K = °C + 273.15$$

$$°F = \frac{9}{5}°C + 32 \qquad °R = °F + 459.7$$

ORDERING GUIDE

Model	Max Cal Error @ 25°C	Max Error −25°C to +105°C	Max Nonlinearity −25°C to +105°C	Package Option[a]
AD592CN	0.5°C	1.0°C	0.35°C	TO-92
AD592BN	1.0°C	2.0°C	0.4°C	TO-92
AD592AN	2.5°C	3.5°C	0.5°C	TO-92

For outline information see Package Information section.

169

Typical @ V_s = +5V
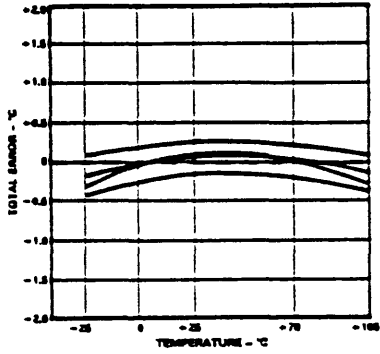
AD592CN Accuracy Over Temperature
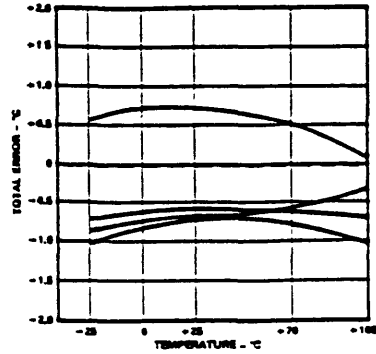
AD592BN Accuracy Over Temperature
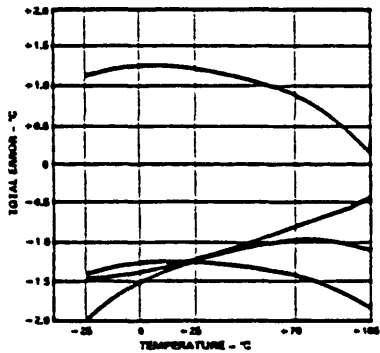
AD592AN Accuracy Over Temperature
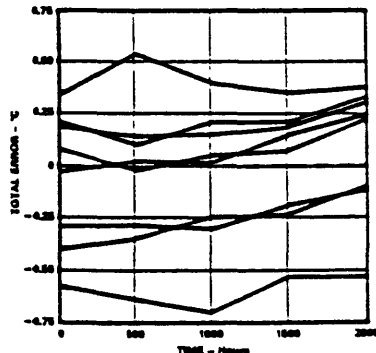
Long-Term Stability @ 85°C and 85% Relative Humidity
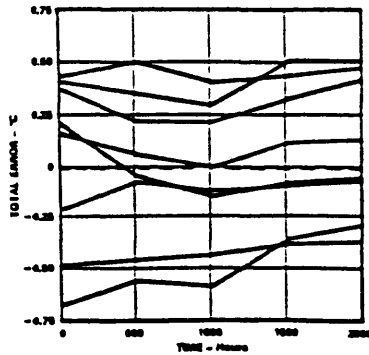
Long-Term Stability @ 125°C

AD592

THEORY OF OPERATION

The AD592 uses a fundamental property of silicon transistors to realize its temperature proportional output. If two identical transistors are operated at a constant ratio of collector current densities, r, then the difference in base-emitter voltages will be (kT/q)(ln r). Since both k, Boltzman's constant and q, the charge of an electron are constant, the resulting voltage is directly Proportional To Absolute Temperature (PTAT). In the AD592 this difference voltage is converted to a PTAT current by low temperature coefficient thin film resistors. This PTAT current is then used to force the total output current to be proportional to degrees Kelvin. The result is a current source with an output equal to a scale factor times the temperature (K) of the sensor. A typical V-I plot of the circuit at +25°C and the temperature extremes is shown in Figure 1.
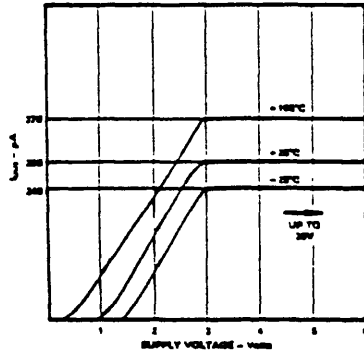
Figure 1. V-I Characteristics

Factory trimming of the scale factor to 1μA/K is accomplished at the wafer level by adjusting the AD592's temperature reading so it corresponds to the actual temperature. During laser trimming the IC is at a temperature within a few degrees of 25°C and is powered by a 5V supply. The device is then packaged and automatically temperature tested to specification.

FACTORS AFFECTING AD592 SYSTEM PRECISION

The accuracy limits given on the Specifications page for the AD592 makes it easy to apply in a variety of diverse applications. To calculate a total error budget in a given system it is important to correctly interpret the accuracy specifications, nonlinearity errors, the response of the circuit to supply voltage variations and the effect of the surrounding thermal environment. As with other electronic designs external component selection will have a major effect on accuracy.

CALIBRATION ERROR, ABSOLUTE ACCURACY AND NONLINEARITY SPECIFICATIONS

Three primary limits of error are given for the AD592 such that the correct grade for any given application can easily be chosen for the overall level of accuracy required. They are the calibration accuracy at 25°C, and the error over temperature from 0 to 70°C and -25°C to +105°C. These specifications correspond to the actual error the user would see if the current output of a AD592 were converted to a voltage with a precision resistor. Note that the maximum error at room temperature, over the commercial IC temperature range, or an extended range including the boiling point of water, can be directly read from the Specifications Table. All three error limits are a combination of initial error,

scale factor variation and nonlinearity deviation from the ideal 1μA/K output. Figure 2 graphically depicts the guaranteed limits of accuracy for an AD592CN.
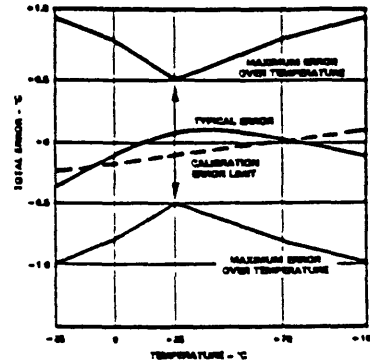
Figure 2. Error Specifications (AD592CN)

The AD592 has a highly linear output in comparison to older technology sensors (i.e., thermistors, RTDs and thermocouples), thus a nonlinearity error specification is separated from the absolute accuracy given over temperature. As a maximum deviation from a best-fit straight line this specification represents the only error which cannot be trimmed out. Figure 3 is a plot of typical AD592CN nonlinearity over the full rated temperature range.
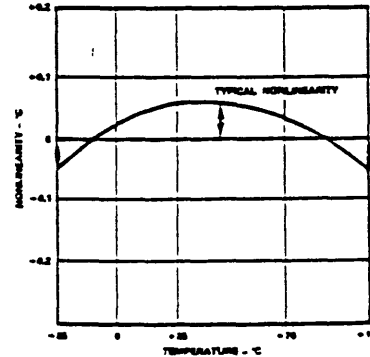
Figure 3. Nonlinearity Error (AD592CN)

TRIMMING FOR HIGHER ACCURACY

Calibration error at 25°C can be removed with a single temperature trim. Figure 4 shows how to adjust the AD592's scale factor in the basic voltage output circuit.
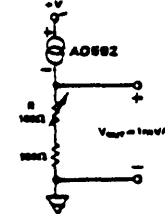
Figure 4. Basic Voltage Output (Single Temperature Trim)

REV. A

171

To trim the circuit the temperature must be measured by a reference sensor and the value of R should be adjusted so the output (V_{OUT}) corresponds to 1mV/K. Note that the trim procedure should be implemented as close as possible to the temperature highest accuracy is desired for. In most applications if a single temperature trim is desired it can be implemented where the AD592 current-to-output voltage conversion takes place (e.g., output resistor, offset to an op amp). Figure 5 illustrates the effect on total error when using this technique.
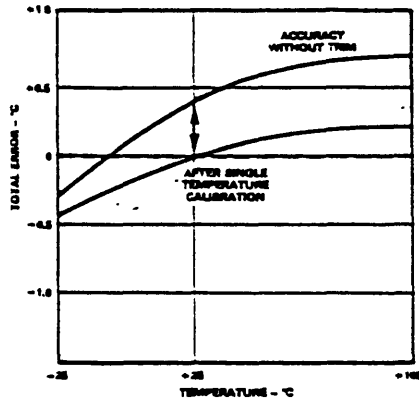
Figure 5. Effect of Scale Factor Trim on Accuracy

If greater accuracy is desired, initial calibration and scale factor errors can be removed by using the AD592 in the circuit of Figure 6.
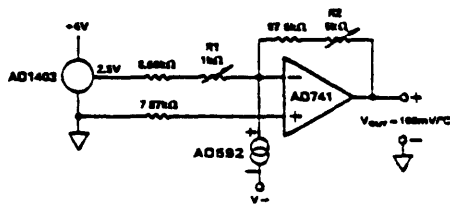
Figure 6. Two Temperature Trim Circuit

With the transducer at 0°C adjustment of R1 for a 0V output nulls the initial calibration error and shifts the output from K to °C. Tweaking the gain of the circuit at an elevated temperature by adjusting R2 trims out scale factor error. The only error remaining over the temperature range being trimmed for is nonlinearity. A typical plot of two trim accuracy is given in Figure 7.

SUPPLY VOLTAGE AND THERMAL ENVIRONMENT EFFECTS

The power supply rejection characteristics of the AD592 minimizes errors due to voltage irregularity, ripple and noise. If a supply is used other than 5V (used in factory trimming), the power supply error can be removed with a single temperature trim. The PTAT nature of the AD592 will remain unchanged. The general insen-
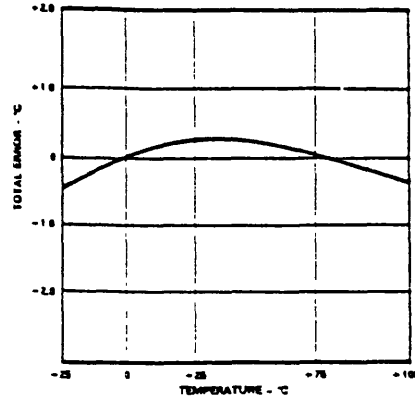
Figure 7. Typical Two Trim Accuracy

sitivity of the output allows the use of lower cost unregulated supplies and means that a series resistance of several hundred ohms (e.g., CMOS multiplexer, meter coil resistance) will not degrade the overall performance.

The thermal environment in which the AD592 is used determines two performance traits: the effect of self-heating on accuracy and the response time of the sensor to rapid changes in temperature. In the first case, a rise in the IC junction temperature above the ambient temperature is a function of two variables; the power consumption level of the circuit and the thermal resistance between the chip and the ambient environment (θ_{JA}). Self-heating error in °C can be derived by multiplying the power dissipation by θ_{JA}. Because errors of this type can vary widely for surroundings with different heat sinking capacities it is necessary to specify θ_{JA} under several conditions. Table I shows how the magnitude of self-heating error varies relative to the environment. In typical free air applications at 25°C with a 5V supply the magnitude of the error is 0.2°C or less. A common clip-on heat sink will reduce the error by 25% or more in critical high temperature, large supply voltage situations.

Medium	θ_{JA} (°C/watt)	τ (sec)*
Still Air		
Without Heat Sink	175	60
With Heat Sink	130	55
Moving Air		
Without Heat Sink	60	12
With Heat Sink	40	10
Fluorinert Liquid	35	5
Aluminum Block**	30	2.4

*τ is an average of five time constants (99.3% of final value). In cases where the thermal response is not a simple exponential function, the actual thermal response may be better than indicated.
**With thermal grease.

Table I. Thermal Characteristics

Response of the AD592 output to abrupt changes in ambient temperature can be modeled by a single time constant τ exponential function. Figure 8 shows typical response time plots for several media of interest.
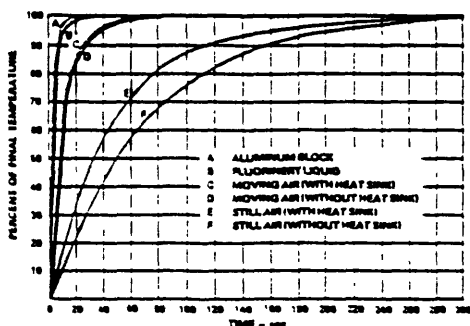
Figure 8. Thermal Response Curves

The time constant, τ, is dependent on θ_{JA} and the thermal capacities of the chip and the package. Table I lists the effective τ (time to reach 63.2% of the final value) for several different media. Copper printed circuit board connections were neglected in the analysis, however, they will sink or conduct heat directly through the AD592's solder dipped Kovar leads. When faster response is required a thermally conductive grease or glue between the AD592 and the surface temperature being measured should be used. In free air applications a clip-on heat sink will decrease output stabilization time by 10–20%.

MOUNTING CONSIDERATIONS

If the AD592 is thermally attached and properly protected, it can be used in any temperature measuring situation where the maximum range of temperatures encountered is between −25°C and +105°C. Because plastic IC packaging technology is employed, excessive mechanical stress must be safeguarded against when fastening the device with a clamp or screw-on heat tab. Thermally conductive epoxy or glue is recommended under typical mounting conditions. In wet or corrosive environments any electrically isolated metal or ceramic well can be used to shield the AD592. Condensation at cold temperatures can cause leakage current related errors and should be avoided by sealing the device in nonconductive epoxy paint or dips.

APPLICATIONS

Connecting several AD592 devices in parallel adds the currents through them and produces a reading proportional to the average temperature. Series AD592s will indicate the lowest temperature
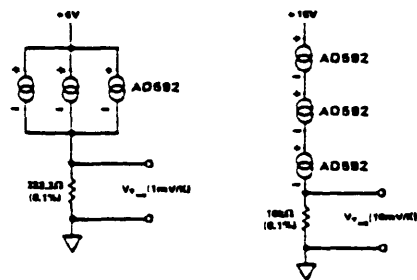
Figure 9. Average and Minimum Temperature Connections

because the coldest device limits the series current flowing through the sensors. Both of these circuits are depicted in Figure 9.

The circuit of Figure 10 demonstrates a method in which a voltage output can be derived in a differential temperature measurement.
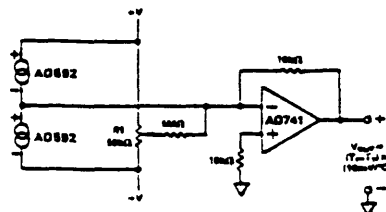
Figure 10. Differential Measurements

R1 can be used to trim out the inherent offset between the two devices. By increasing the gain resistor (10kΩ) temperature measurements can be made with higher resolution. If the magnitude of V+ and V− is not the same, the difference in power consumption between the two devices can cause a differential self-heating error.

Cold junction compensation (CJC) used in thermocouple signal conditioning can be implemented using an AD592 in the circuit configuration of Figure 11. Expensive simulated ice baths or hard to trim, inaccurate bridge circuits are no longer required.
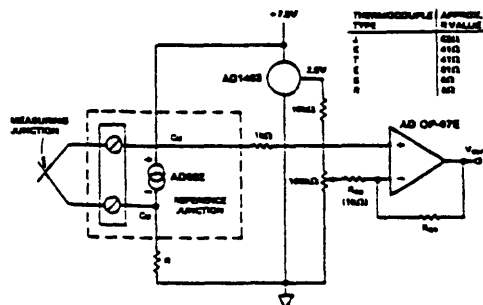
Figure 11. Thermocouple Cold Junction Compensation

The circuit shown can be optimized for any ambient temperature range or thermocouple type by simply selecting the correct value for the scaling resistor – R. The AD592 output (1μA/K) times R should approximate the line best fit to the thermocouple curve (slope in V/°C) over the most likely ambient temperature range. Additionally, the output sensitivity can be chosen by selecting the resistors R_{G1} and R_{G2} for the desired noninverting gain. The offset adjustment shown simply references the AD592 to °C. Note that the TC's of the reference and the resistors are the primary contributors to error. Temperature rejection of 40 to 1 can be easily achieved using the above technique.

Although the AD592 offers a noise immune current output, it is not compatible with process control/industrial automation current loop standards. Figure 12 is an example of a temperature to 4–20mA transmitter for use with 40V, 1kΩ systems.

In this circuit the 1μA/K output of the AD592 is amplified to 1mA/°C and offset so that 4mA is equivalent to 17°C and 20mA is equivalent to 33°C. Rt is trimmed for proper reading at an
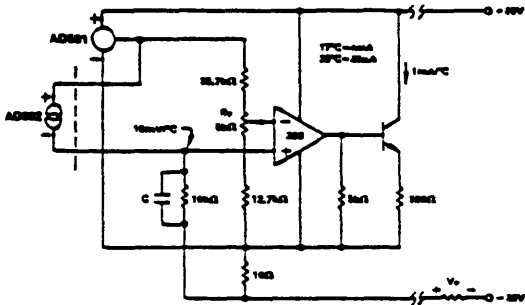
Figure 12. Temperature to 4-20mA Current Transmitter

intermediate reference temperature. With a suitable choice of resistors, any temperature range within the operating limits of the AD592 may be chosen.

Reading temperature with an AD592 in a microprocessor based system can be implemented with the circuit shown in Figure 13.
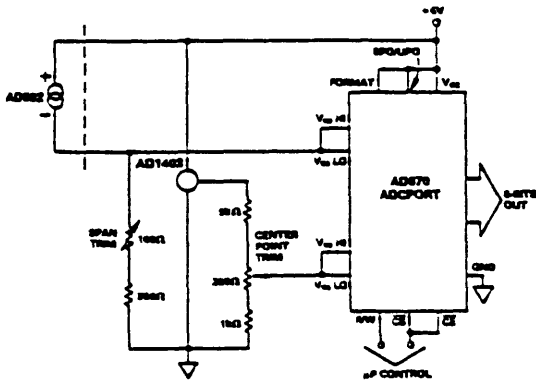
Figure 13. Temperature to Digital Output

By using a differential input A/D converter and choosing the current to voltage conversion resistor correctly any range of temperatures (up to the 130°C span the AD592 is rated for) centered at any point can be measured using a minimal number of components. In this configuration the system will resolve up to 1°C.

A variable temperature controlling thermostat can easily be built using the AD592 in the circuit of Figure 14.

R_{HIGH} and R_{LOW} determine the limits of temperature controlled by the potentiometer R_{SET}. The circuit shown operates over the full temperature range (-25°C to +105°C) the AD592 is rated for. The reference maintains a constant set point voltage and insures that approximately 7V appears across the sensor. If it is necessary to guardband for extraneous noise hysteresis can be added by tying a resistor from the output to the ungrounded end of R_{LOW}.
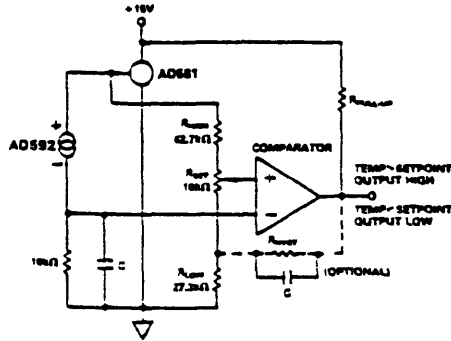
Figure 14. Variable Temperature Thermostat

Multiple remote temperatures can be measured using several AD592s with a CMOS multiplexer or a series of 5V logic gates because of the device's current-mode output and supply-voltage compliance range. The on-resistance of a FET switch or output impedance of a gate will not effect the accuracy, as long as 4V is maintained across the transducer. MUXs and logic driving circuits should be chosen to minimize leakage current related errors. Figure 15 illustrates a locally controlled MUX switching the signal current from several remote AD592s. CMOS or TTL gates can also be used to switch the AD592 supply voltages, with the multiplexed signal being transmitted over a single twisted pair to the load.
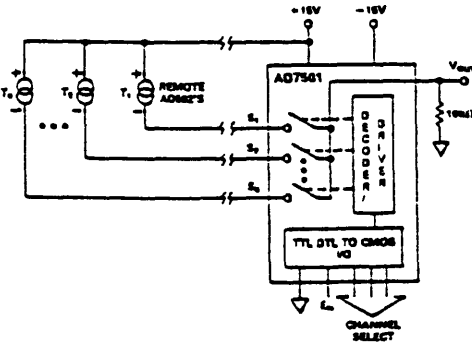
Figure 15. Remote Temperature Multiplexing

To minimize the number of MUXs required when a large number of AD592s are being used, the circuit can be configured in a matrix. That is, a decoder can be used to switch the supply voltage to a column of AD592s while a MUX is used to control which row of sensors are being measured. The maximum number of AD592s which can be used is the product of the number of channels of the decoder and MUX.

174

AD592

An example circuit controlling 80 AD592s is shown in Figure 16. A 7-bit digital word is all that is required to select one of the sensors. The enable input of the multiplexer turns all the sensors off for minimum dissipation while idling.
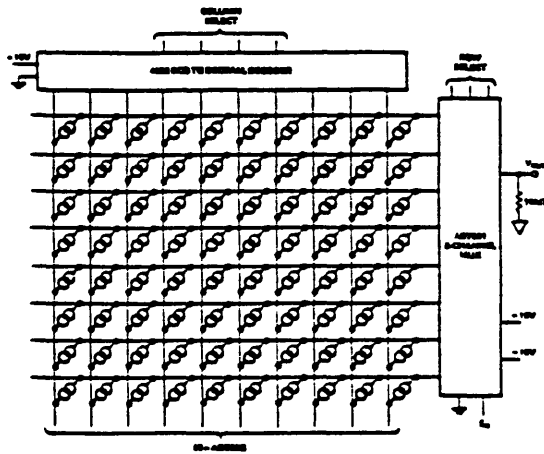
Figure 16. Matrix Multiplexer

To convert the AD592 output to °C or °F a single inexpensive reference and op amp can be used as shown in Figure 17. Although this circuit is similar to the two temperature trim circuit shown in Figure 6, two important differences exist. First, the gain resistor is fixed alleviating the need for an elevated temperature trim. Acceptable accuracy can be achieved by choosing an inexpensive resistor with the correct tolerance. Second, the AD592 calibration error can be trimmed out at a known convenient temperature (i.e., room temperature) with a single pot adjustment. This step is independent of the gain selection.
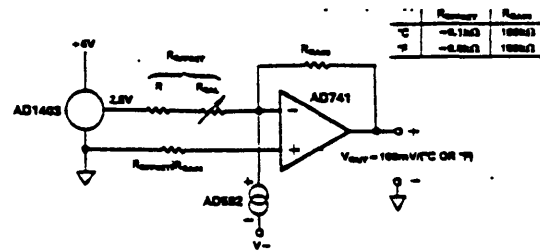
Figure 17. Celsius or Fahrenheit Thermometer

MI-900 Series
Conductivity Electrodes
Operating Instructions

Use of the Electrode

The electrode is ready to use. Some of the smaller diameter probes are shipped to you in a protective glass tube. If so, carefully unwind the green tape and remove the probe from the protective glass tube.

Calibration

Any cell that has been stored dry should be soaked in distilled or deionized water for 24 hours prior to use to assure complete wetting of the cell.

Each conductivity cell manufactured is calibrated to obtain, as close as possible, a cell constant (K) of 1.0/cm using the 0.01 N KCl solution method as determined by Jones and Bradshaw in 1937. However, to obtain more accurate results, you should calibrate the cell and calculate a new cell constant using conductivity standards that more closely resemble the anticipated range of your samples as well as the size of your samples.

You may use the standard solution and the following table to check the accuracy of the cell's constant or to determine an unknown constant. The formula is $K = (k1)(k2)(1/R)$ where

K = cell constant in c g s metric units (km)
$1/R$ = measured conductance in micromhos
$k1$ = conductivity in absolute micromhos/km from table below
$k2$ = conductivity in absolute micromhos/km of the distilled water used in making the solution

Note: $1/R$, $k1$, and $k2$ must either be determined at the same temperature or corrected to the same temperature to make the equation valid.

Temperature (T) vs. Conductivity(k1), 0.01 N KCl

T	Cond (k1)	T	Cond (k1)
15	1141.5	23	1353.6
16	1167.5	24	1380.8
17	1193.6	25	1408.1
18	1219.9	26	1435.6
19	1246.4	27	1463.2
20	1273.0	28	1490.9
21	1299.7	29	1518.7
22	1326.6	30	1546.7

T = Degrees Celsius
k1 = Absolute Micromhos/km

Handling, Cleaning, and Storing of the Electrode

Handling: When handling the conductivity cell, be careful not to allow any sharp objects to enter the area of the electrodes of the cell. Damage to the platinum black coating can result. This coating is extremely important to cell operation especially in solutions of high conductivity. Always rinse the cell between standards and samples. Remove any excess solution from the cell using a piece of absorbent towel to prevent carry over contamination.

Cleaning: A clean cell is the most important requirement for accurate and reproducible results. The cell can be cleaned using any one of the foaming acid type cleaners such as Dow Chemical "Bathroom Cleaner." When a stronger cleaning solution is required, a solution of equal parts of isopropyl alcohol and 10 N HCl can be used.

Caution: Cells should not be cleaned in aqua regia or in any solution known to etch platinum.

Dip the cell into the cleaning solution and agitate it for 2-3 minutes. Rinse the cell thoroughly with distilled water (several times). Inspect the platinum black coating for flaking or bare spots (replatinization may be required).

Storing: Always clean the electrode before storing.

Long term (over 2 weeks): return the electrode to its original container. It can be stored dry or in deionized water. Electrodes stored in water will require less frequent replatinization than those stored dry. Any probe that has been stored dry should be soaked in distilled or deionized water for 24 hours before use to assure complete wetting of the cell.

Short term: the electrode can be left in distilled or deionized water.

Troubleshooting

A. Readings Are Zero In All Standards:

1. Inspect the electrode for visible cracks or breaks in the wire. If any exist, the electrode cannot be repaired and must be replaced.

2. Check connectors for good contact into meter or for broken connections to the plugs. Repair as required.

B. Excessive Drift or Sluggish Response:

1. Inspect platinum black coating on the two electrodes in the cell. If flaking off or if bare metal is exposed, replatinization of the cell is required.

2. Check for possible carry over of previous solutions or standards.

For additional assistance, call our Customer Service Department at (603)668 0692.

Microelectrodes, Inc.

298 Rockingham Rd., Londonderry, NH 03053
U S A
Tel (603)668 0692 Fax (603)668 7926

MI-405 Glass pH Electrode

Operating Instructions

Use of the Electrode

The electrode is ready to use. Carefully unwind the tape and remove the probe from the protective glass tube.

The use of a separate Reference Electrode such as our MI-401 is required

Calibration

The MI-405 is standardized in two (2) pH buffers. Follow the procedure recommended by the manufacturer of your pH meter for calibrating your pH meter with our MI-405.

Optimum Response Time: Optimum response time will be obtained after the probe has been exercised in two (2) buffer solutions. Place a pH 4.01 buffer or equivalent in a 50 ml beaker and a pH 6.86 buffer or equivalent in a 50 ml beaker (other beakers can also be used). Hold the MI-405 and reference electrode together and touch the pH 4.01 buffer allowing 15-20 seconds for equilibration. Rinse the two electrodes with distilled water and then touch the pH 6.86 buffer in the same manner. Do this several times.

Handling, Cleaning, and Storing of the Electrode

Handling: Always handle the electrode with the same care you would use with other glass electrodes.

Cleaning: When using the electrodes in solutions containing protein, the MI-405 and the reference electrode should be rinsed with an enzyme cleaning solution such as our A-50 Cleaning Agent or a chromic/sulfuric acid

glass cleaning solution after each use for a couple of minutes to remove the protein from the glass and the reference junction. This will prolong the useful life of the electrodes.

Storing: Always clean the electrodes before storing.

Long term (over 2 weeks): return the electrode to its original container and prepare it in the same condition in which you received it. Usually this means simply moistening the sponge located in the bottom of the protective glass tube with distilled water.

Short term: the electrode can be left in an acid pH buffer solution, e.g. pH 4.01.

Troubleshooting

A. Little or No Response

Inspect the electrode for visible cracks (usually occurring around the tip of the electrode) using a jeweler's loupe or a stereo microscope. If any exist, the electrode cannot be rejuvenated and must be replaced. The slightest crack in or around the membrane will cause the electrode to read about the same in all solutions.

B. Response Pegs Off Scale

1. Visually inspect the pH electrode for a broken bulb. Check connections for broken wires or connections. Are both electrodes in the same standard or buffer?

2. Blocked or clogged liquid junction (reference) - soak the tip of the reference electrode in warm (50°C) distilled water for 5 to 10 minutes. If still clogged, then soak overnight in distilled water.

C. Sluggish Response

If the electrode becomes sluggish in responding to changes in pH, the response time can be improved using the following procedure. First, clean the electrode as described earlier. Second, soak the electrode in 0.1 HCl (or

for 5 minutes followed by soaking in 0.1 N NaOH for 5 minutes. After doing this several times, rinse the electrode thoroughly with distilled water. The electrode can then be calibrated in the usual manner.

MI-800-XXX Micro ORP (Redox) Series Electrodes

Operating Instructions

Use of the Electrode

A. Combination Electrodes

All of the MI-800-XXX Series combination electrodes are ready to use. Carefully unwind the green tape and remove the probe from the protective glass tube. The white sleeve which covers the fill hole should be moved down the glass barrel to ventilate the reference chamber and re-placed after use.

A separate reference electrode is not required.

B. Single Electrodes

All of the MI-800-XXX Series single electrodes are ready to use. Carefully unwind the green tape and remove the probe from the protective glass tube (if appropriate).

A separate reference electrode is required.

Calibration

Since ORP is a characteristic measure of redox equilibrium, it should not require standardization or calibration. However, it is desirable to check the electrode for proper operation and electrode poisoning. Solutions of known potential can be made by saturating pH buffers with quinhydrone using the following procedure:

1. Place 20 ml of pH 4 buffer into one beaker and 20 ml of pH 7 buffer into a second beaker. Saturate each buffer with quinhydrone. Quinhydrone is not readily soluble in the buffers so a few crystals stirred into the buffer is sufficient. The resultant solution will be amber colored. Saturated quinhydrone buffers need to be made up fresh each time you want to check the electrode.

2. Place the tip of the MI-800-XXX Series ORP Electrode (with an appropriate reference electrode such as our MI-401/MI-402 if it is not a combination electrode) into the first beaker containing the quinhydrone/buffer solution. Record the millivolt reading and the temperature of the solution.

3. Rinse the electrode with distilled water and place it into the second beaker. Record the millivolt reading and the temperature of the solution.

4. The measured potentials will generally be within 10 mv of the theoretical values listed below

Reference type	Ag/AgCl			Calomel		
Temp (Celsius)	20	25	30	20	25	30
pH4	+268	+263	+258	+233	+218	+213
pH7	+92	+86	+79	+47	+41	+31

ORP of Quinhydrone Solutions, mv ±20

Handling, Cleaning, and Storing of Electrode

Handling: (for combination electrodes) When necessary, the outer reference chamber of the electrode can be refilled using the 3 M KCl dispensing bottle provided with the probe. This may be a slow process, but introducing syringe needles or plastic tubes into the fill hole generally results in breaking the inner glass capillary rendering the probe inoperative.

Care must be taken that the delicate inner glass capillary is not cracked when refilling. Do not apply pressure against the inner glass capillary tube.

Cleaning: Cleaning of the electrode can be accomplished by immersing the tip of the electrode into a chromic/sulfuric acid glass cleaning solution or nitric and for a couple of minutes to remove the contaminants. Rinsing the electrode thoroughly after cleaning is required

Storing: Always clean the electrode before storing

Long term (over 2 weeks) return the electrode to its original container and prepare it in the same condition in which you received it. For combination type electrodes this means simply moistening the sponge located in the bottom of the protective glass tube with distilled water.

Short term: the electrode can be left in a 0.1 M KCl solution

Troubleshooting

A. Little or No Response: (Combination)

Inspect the electrode for visible cracks (usually occurring around the tip of the electrode) If any exist, the electrode cannot be rejuvenated and must be replaced The slightest crack in or around the tip will cause the electrode to read about the same in all solutions

B. Response Pegs Off Scale: (Combination)

1. Visually inspect the electrode for broken or dissolving internal elements or for inadequate volume of filling solution Filling solution level should be above the internal elements

2. Blocked or clogged liquid junction - soak the tip of the electrode in warm (30°C) distilled water for 5 to 10 min utes If still clogged, then soak overnight in distilled water

Microelectrodes, Inc.

298 Rockingham Rd, Londonderry, N H 03053
U S A
Tel (603)668 0692 Fax (603)668 7926

178

MI-402 Micro-Reference Electrode with Flexible Barrel

Operating Instructions

Contents and Specifications

This Reference Electrode Kit contains the following:

- MI-402 Electrode (assembled)
- Bottle of electrolyte
- Replaceable barrel
- Filling Tube
- Set of Instructions

Specifications:

Internal Element	Ag AgCl
Electrolyte	3 M KCl
Junction	Ceramic frit
Electrode Length	9.5 cm
Dia. of Ref Barrel	1.9 mm
Mat'l of Barrel	PVC tubing
Electrode Cap	2 parts
Cap Diameter	0.64 cm
Lead Length	2 meter
Depth of Immersion	Surface contact

Use of the Electrode

The MI-402 Micro-Reference Electrode can be used with any pH, ion selective, or redox electrode. The electrode is composed of an internal silver silver chloride electrode with an internal filling solution of 3 M KCl saturated with AgCl.

Before the electrode can be placed into operation, the PVC reference barrel must be filled with the internal reference solution supplied.

Filling the Reference Barrel

Filling of the reference barrel is accomplished in the following manner:

1. The PVC barrel is removed from the electrode cap by grasping each end of the cap and pulling them apart.

2. The internal reference solution is added to the PVC barrel using the polyethylene tubing (filling fiber) provided. A 26 ga or 27 ga syringe needle will fit inside the tubing.

3. After filling the PVC barrel with the reference electrolyte, the silver wire is inserted into the PVC barrel and the electrode cap is re-assembled.

Cleaning and Storing of the Electrode

Cleaning: When using the electrode in solutions containing protein, the electrode should be soaked in an enzyme cleaning solution such as our A-50 Cleaning Solution or a chromic/sulfuric acid glass cleaning solution after each use for 10-15 seconds to remove the protein from the reference barrel and the reference junction. This will prolong the useful life of the electrode.

Storing: Always clean the electrode before storing.

Long-term (over 4 weeks): remove the PVC barrel containing the electrolyte and store the entire PVC barrel in a stoppered test tube filled with reference electrolyte. Rinse the silver wire and electrode cap to remove the salt solution and dry using an absorbent towel. Store the electrode in its original box or any closed container to keep dust off of the electrode.

Short-term: place the tip of the electrode into a test tube or beaker containing reference electrolyte.

Some of the MI-402 have a screw type cap. If the cap does not pull apart easily try unscrewing the cap.

Can Ter 4 Fill w/ AgCl

Troubleshooting

A. Little or No Response:

Inspect the indicating electrode for visible cracks. If any exist, the indicating electrode is defective and must be replaced. The slightest crack in or around the tip of the indicating electrode will cause the electrode to read about the same in all solutions.

B. Response Pegs Off Scale:

1. Visually inspect the reference electrode for broken or dissolving internal Ag-AgCl wire or for inadequate volume of reference electrolyte. Reference electrolyte level should be above the Ag-AgCl element.

2. Blocked or clogged liquid junction - Clean electrode tip then soak the tip of the electrode in warm (not hot) distilled water for 5 to 10 minutes. If still clogged, then soak overnight in distilled water or replace reference barrel with extra barrel supplied.

MI-402A Replacement Barrels are available.

For additional assistance, call our customer service department at (603)668 0692.

Insert filling tube into nipple of electrolyte bottle. Push until tube locks into place. Insert tube into reference barrel and squeeze bottle.

Fill reference barrel within one ha nch from top.

Microelectrodes, Inc.

APPENDIX C: CONDUCT.BAS LISTING

```
1 REM *****************CONDUCT4.BAS***LAST EDITED 1-4-96 *****************
2 REM PROGRAM TO CONTROL CONDUCTIVITY BOX BUILT BY SAMIR
3 REM WRITTEN BY BRAD RAMSAY, 1995 (SOME CODE FROM S.TREE AND OTHERS @ MIT)
4 REM USES SECOND STRAWBERRY TREE CARD FOR DIGITAL OUTPUTS (ASSUMES 2nd CARD)
5 REM USES THE SHEAHAN DATA ACQ CARD
10 REM
14 REM Don't change the name AM1 used for calls, it's an external procedure.
17 REM ***************************************************************************
20 CLS:LOCATE 10,10
30 REM
34 REM ********** MAIN PROGRAM *****************************************
35 REM
40 GOSUB 40000              :REM SET UP SHEAHAN CARD
67 GOSUB 53000              :REM INITIALIZE RESISTOR ARRAYS
70 GOSUB 41000              :REM GET THE INPUT VOLTAGE
80 GOSUB 10000              :REM INPUT TEST SET UP INFORMATION
90 OPEN DATAFILE$ FOR OUTPUT AS #1  :REM OPEN DATA FILE (ERASES OLD DATA)
93 PRINT#1, "TIME   PROBE 1   PROBE 2   PROBE 3   PROBE 4"
94 NOB = 0                  :REM INITIALIZE CURRENT OBSERVATION NUMBER
95 LASTTIME=0
96 PTIME = 0
97 TIME$="00:00:00"
100 START!=TIMER            :REM INITIALIZE TIMER
110 WHILE TIMER<START!+DELAY%  :REM WAIT FOR THE SPECIFIED DELAY TIME
120     A$ = INKEY$             :REM CHECK FOR "QUIT" DURING DELAY
130     IF INKEY$ ="Q" THEN GOTO 210
140 WEND
150 WHILE NOB<MAXNOB%                   :REM CHECK OBSERVATION NUMBER
155     GOSUB 1000                      :REM CHECK TIMER FOR 24 HRS
160     WHILE (TIMER+PTIME) < (START! + NOB*TINC%) :REM WAIT FOR READING INCREME
NT
165        GOSUB 1000                   :REM CHECK TIMER FOR 24 HRS
170        A$ = INKEY$                  :REM CHECK FOR USER QUIT
180        IF A$ = "Q" THEN GOTO 210
190     WEND
195 GOSUB 20000             :REM CALCULATE CONDUCTIVITIES & WRITE TO FILE
200 WEND
210 CLOSE #1               :REM CLOSE DATA FILE
220 OUT 6932,0             :REM TURN OFF ALL PROBES AND RESISTORS
250 END
300 REM ********************END OF MAIN PROGRAM*************************
1000 REM
1001 REM ***SUBROUTINE TO CHECK TIMER
1002 REM
1010 IF (TIMER < LASTTIME) THEN (PTIME=PTIME+86400!)
1020 LASTTIME = TIMER
1030 RETURN
10000 REM
10001 REM ***SUBROUTINE TO ENTER TEST INFORMATION*************************
10002 REM
10010 CLS
10020 LOCATE 10,10
10030 INPUT "ENTER THE NUMBER OF PROBES";NUMPROBES%
10040 CLS:LOCATE 10,10
10050 INPUT "ENTER THE NAME OF THE DATA FILE";DATAFILE$
10060 CLS:LOCATE 10,10
10070 INPUT "ENTER THE MAXIMUM NUMBER OF OBSERVATIONS";MAXNOB%
10080 CLS:LOCATE 10,10
10090 INPUT "ENTER THE TIME INCREMENT IN SECONDS";TINC%
10100 CLS:LOCATE 10,10
```

```
10110 PRINT "ENTER THE DELAY, IN SECONDS, BETWEEN THE TIME YOU ACCEPT"
10120 LOCATE 11,10:INPUT "YOUR CHOICES, AND THE BEGINNING OF THE TEST";DELAY%
10140 CLS
10150 LOCATE 5,10:PRINT "NUMBER OF PROBES = ";NUMPROBES%
10160 LOCATE 7,10:PRINT "OUTPUT FILE NAME = ";DATAFILE$
10170 LOCATE 9,10:PRINT "MAX # OF OBSERVATIONS = ";MAXNOB%
10180 LOCATE 11,10:PRINT "TIME INCREMENT = ";TINC%;" SECONDS"
10190 LOCATE 13,10:PRINT "DELAY TIME = ";DELAY%;" SECONDS"
10200 LOCATE 16,10:INPUT "ENTER Y TO ACCEPT";Q$
10210 IF Q$ = "Y" THEN GOTO 10220 ELSE GOTO 10010 :REM TO CHECK INPUT
10220 CLS:LOCATE 8,10
10230 PRINT "PRESS Q TO END TEST"
10231 LOCATE 10,9: PRINT "probe 1 = "
10232 LOCATE 12,9: PRINT "probe 2 = "
10233 LOCATE 14,9: PRINT "probe 3 = "
10234 LOCATE 16,9: PRINT "probe 4 = "
10240 RETURN
20000 REM
20001 REM ***SUBROUTINE TO TAKE READINGS*****************************************
20002 REM
20004 ETIME=(TIMER+PTIME)-START!          :REM TO INITIALIZE TEST TIMER
20005 ETIME = INT(ETIME)         :REM TRUNCATE TO AN INTEGER VALUE
20010 FOR X = 1 TO NUMPROBES%
20040    RESIST% = RARRAY(X)        :REM GET CURRENT RESISTOR FOR PROBE X
20050    OUT 6912+4,((256-(16*X))+(16-RESIST%)):REM TURN ON RESISTOR & PROBE
20051 GOSUB 1000
20052 PAUSE = (TIMER+PTIME)
20053 WHILE (TIMER+PTIME) < (PAUSE + 6)
20054    GOSUB 1000
20055 WEND
20060    GOSUB 42000               :REM TAKE READING
20070    IF (VOUT/VIN)>(5/6) AND RESIST%<5 THEN RESIST%=RESIST% + 1
20080    IF (VOUT/VIN)<(1/6) AND RESIST%>1 THEN RESIST%=RESIST% - 1
20090    IF RESIST% = RARRAY(X) THEN GOTO 20120
20100    RARRAY(X) = RESIST%
20110    GOTO 20050
20120    CONDUCTIVITY = (1/(OHMARRAY(RESIST%)/(VIN/VOUT-1)))*1000:REM mS
20130    PROBENUM(X)=CONDUCTIVITY :REM STORE VALUE UNTIL ALL PROBES ARE READ
20140 NEXT X
20150 PRINT#1, USING "###.####"; ETIME, PROBENUM(1), PROBENUM(2), PROBENUM(3), P
ROBENUM(4)
20155 LOCATE 10,20:PRINT USING "###.####";PROBENUM(1)
20156 LOCATE 12,20:PRINT USING "###.####";PROBENUM(2)
20157 LOCATE 14,20:PRINT USING "###.####";PROBENUM(3)
20158 LOCATE 16,20:PRINT USING "###.####";PROBENUM(4)
20159 LOCATE 18,10:PRINT "nob = ";NOB," etime = ";ETIME
20160 NOB = NOB + 1
20170 OUT 6932, 0                 :REM TURN OFF PROBES
21000 RETURN
40000 REM
40001 REM ***SUBROUTINE TO SET UP THE SHEAHAN CARD ***************************
40002 REM
40010 AD1170=768                 :REM SETS THE ADDRESS OF THE SHEAHAN CARD
40015 MUX!=776                   :REM SETS THE ADDRESS OF THE MULTIPLEXOR
40030 INTTIME = 21               :REM SETS THE INTIGRATION TIME
40040 INTBIT = 13                :REM SETS THE BIT RESOLUTION TO 20
40045 GRDCHANNEL = 15
40070 OUT AD1170+1, INTBIT       :REM LOAD DATA FORMAT IN 2ND BIT SLOT
40090 OUT AD1170,48              :REM LOCK-IN RESOLUTION FORMAT
40100 WAIT AD1170, 1, 1          :REM WAIT FOR ABOVE TASK TO FINISH
```

```
40110 OUT AD1170,69              :REM SET CALIBRATION TIME TO 167 MS
40120 WAIT AD1170, 1, 1          :REM WAIT FOR ABOVE TASK TO FINISH
40150 RETURN
41000 REM
41001 REM ***SUBROUTINE TO READ THE INPUT VOLTAGE*****************************
41002 REM
41010 CLS
41020 LOCATE 10,10
41030 INPUT "SWITCH TO INPUT VOLTAGE AND PRESS ENTER TO CONTINUE";Q$
41040 GOSUB 43000                :REM TAKE READING
41050 VIN=VOLT                   :REM "VOLT" IS RETURNED FROM SUBROUTINE
41060 CLS:LOCATE 10,10
41070 INPUT "SWITCH TO OUTPUT VOLTAGE AND PRESS ENTER TO CONTINUE";Q$
41080 RETURN
42000 REM
42001 REM *** SUBROUTINE TO GET OUTPUT VOLTAGE
42002 REM
42010 GOSUB 43000                :REM TAKE READING
42020 VOUT=VOLT                  :REM "VOLT" IS RETURNED FROM SUBROUTINE
42030 RETURN
43000 REM
43001 REM ***SUBROUTINE TO TAKE READING ************************************
43002 REM
43010 OUT MUX!,0                 :REM SETS THE MULTIPLEXOR TO CHANNEL 1
43020 OUT AD1170,INTTIME         :REM STARTS CONVERSION USING CNV COMMAND
43030 WAIT AD1170, 1, 1          :REM WAIT FOR ABOVE TASK TO FINISH
43035 OUT MUX!,GNDCHANNEL
43040 LOBYTE= INP(AD1170+1)      :REM READ THE LOWEST 8 BITS
43050 MIDBYTE=INP(AD1170+2)      :REM READ THE MIDDLE 8 BITS
43060 HIBYTE =INP(AD1170+3)      :REM READ THE HIGHEST 8 BITS
43070 COUNT=LOBYTE+MIDBYTE*256+HIBYTE*65536! :REM COMPUTE BIT COUNT
43080 VOLT=(COUNT*10/2^(INTBIT+7)-5)  :REM CONVERT TO VOLTS
43090 OUT AD1170,192:WAIT AD1170,1,1      :REM DO 1 BACKGROUND CALIBRATION
43100 RETURN
53000 REM ***SUBROUTINE TO INITIALIZE ARRAYS*******************************
53001 REM
53010 DIM RARRAY(4)              :REM AN ARRAY TO STORE THE CURRENT RESISTOR #
53020 FOR X = 1 TO 4
53030    RARRAY(X)=1
53040 NEXT X
53050 DIM OHMARRAY(5)            :REM TO STORE MEASURED VALUES OF RESISTORS
53060 OHMARRAY(1) = 100.32
53070 OHMARRAY(2) = 1000.8
53080 OHMARRAY(3) = 10004.7
53090 OHMARRAY(4) = 100040!
53100 OHMARRAY(5) = 1000110#
53110 DIM PROBENUM(4)            :REM AN ARRAY TO STORE CONDUCTIVITY VALUES
53120 FOR X = 1 TO 4             :REM WHILE COMPUTER READS OTHER PROBES
53130    PROBENUM(X)=0
53140 NEXT X
53999 RETURN
```

APPENDIX D: CONTINUOUS INPUT CURVES AND ASSOCIATED EQUILIBRIUM READINGS

CONCENTRATION VS PORE VOLUMES
SAND 1 TEST 3 10-26-95
CONTINUOUS SOURCE, 0.1 M NaCl, SEEPAGE VEL. = 0.011 cm/sec

PROBE 1 = 0.5668
PROBE 2 = 0.5883
PROBE 4 = 0.5557
PROBE 3 = 0.5617
PROBE 5 = 0.6072

PORE VOLUMES OF FLOW
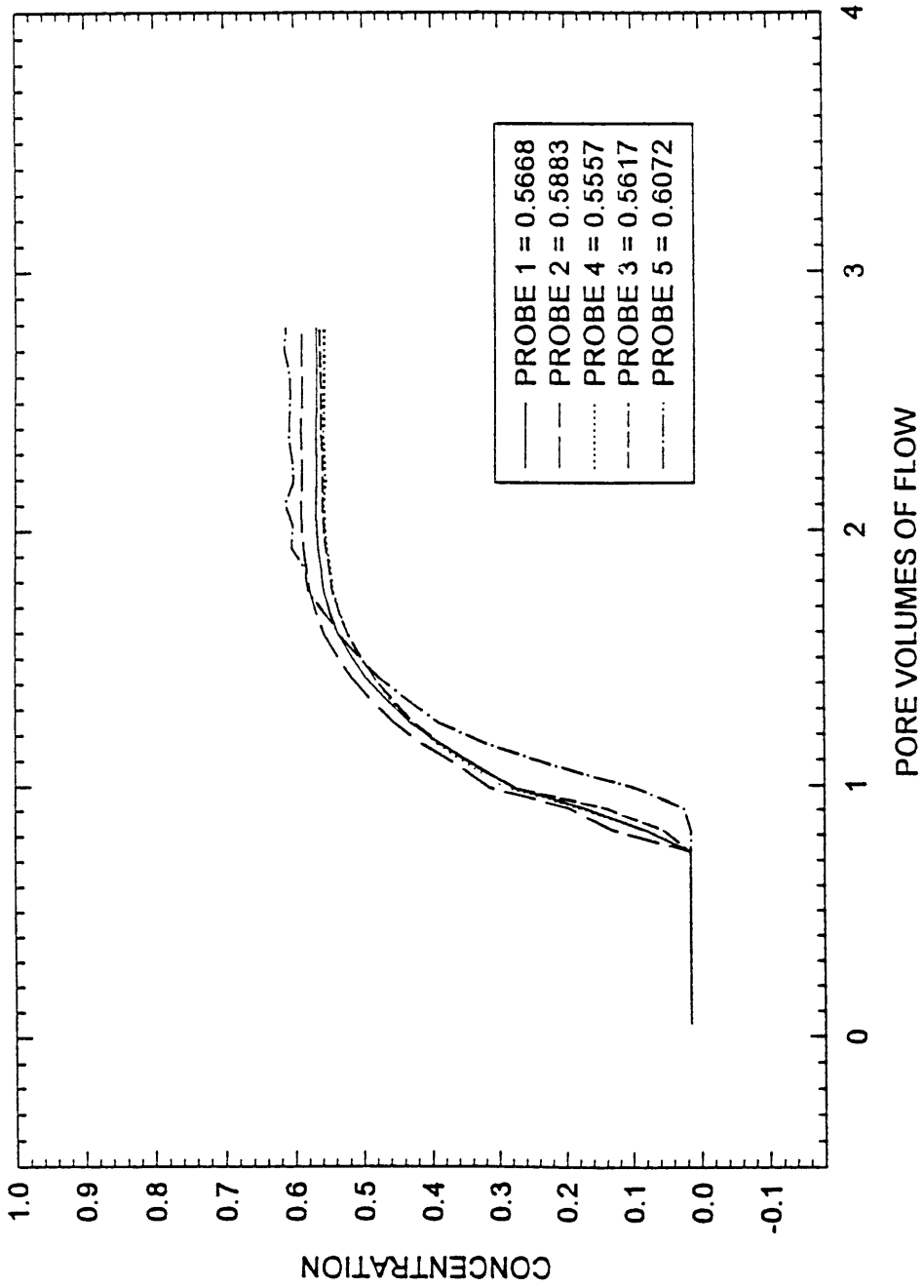
CONCENTRATION

CONCENTRATION VS TIME
SAND 2 TEST 4, 11-23-95
CONTINUOUS SOURCE, 0.1 M NaCl, SEEPAGE VELOCITY = 0.007 cm/sec

PROBE 1 = 0.7223
PROBE 2 = 0.7565
PROBE 3 = 0.9280
PROBE 4 = 0.8472
PROBE 5 = 0.6551

CONCENTRATION (%)

TIME (sec)
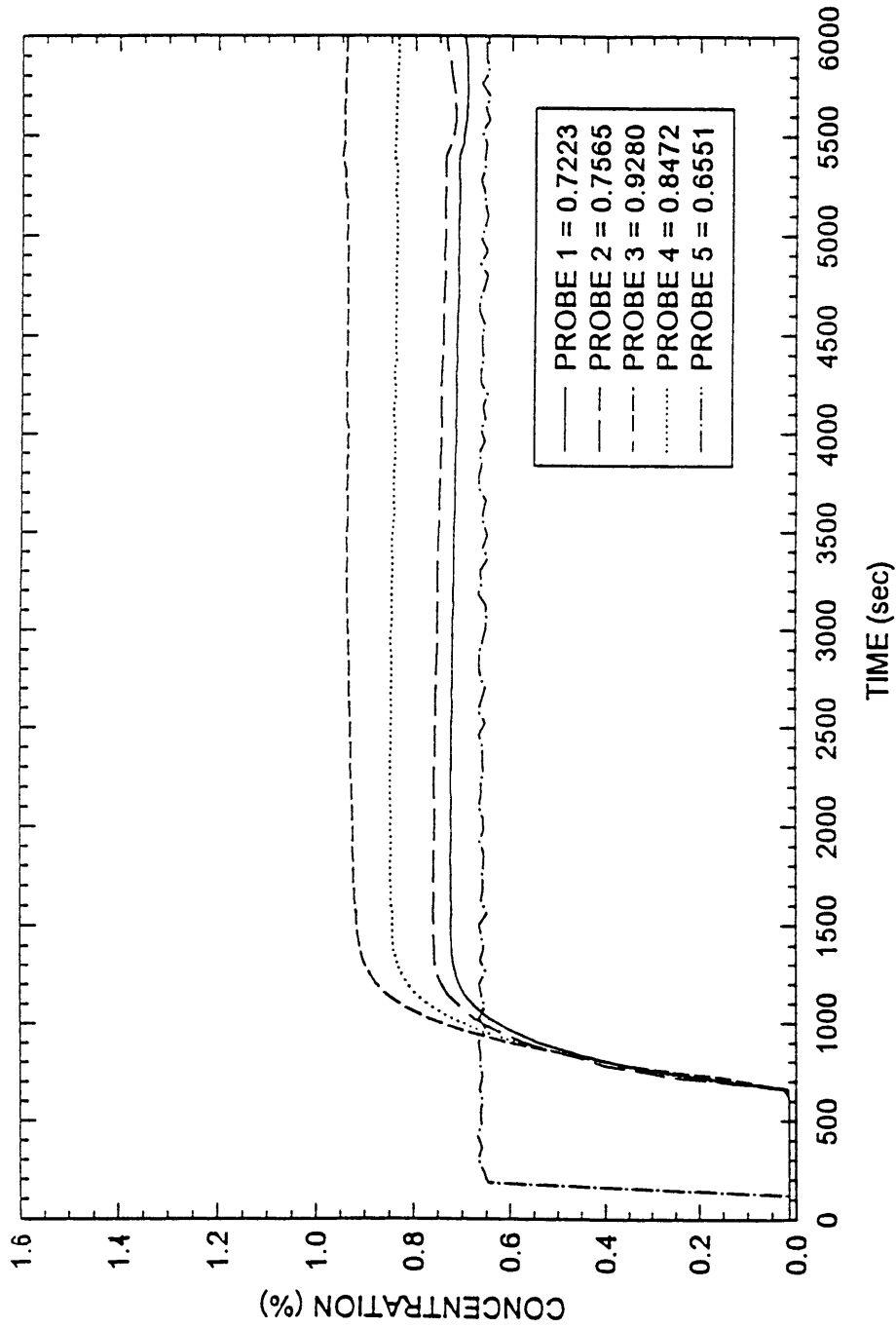
CONCENTRATION VS PORE VOLUMES
PEAT 1 TEST 3 1-11-96
CONTINUOUS SOURCE, 0.1 M NaCl, SEEPAGE VEL. = 2.8 X 10^{-5} cm/sec

PROBE 1 = 0.4811
PROBE 2 = 0.4810
PROBE 4 = 0.7151
PROBE 3 = 1.06
PROBE 5 = 0.537

PORE VOLUMES OF FLOW
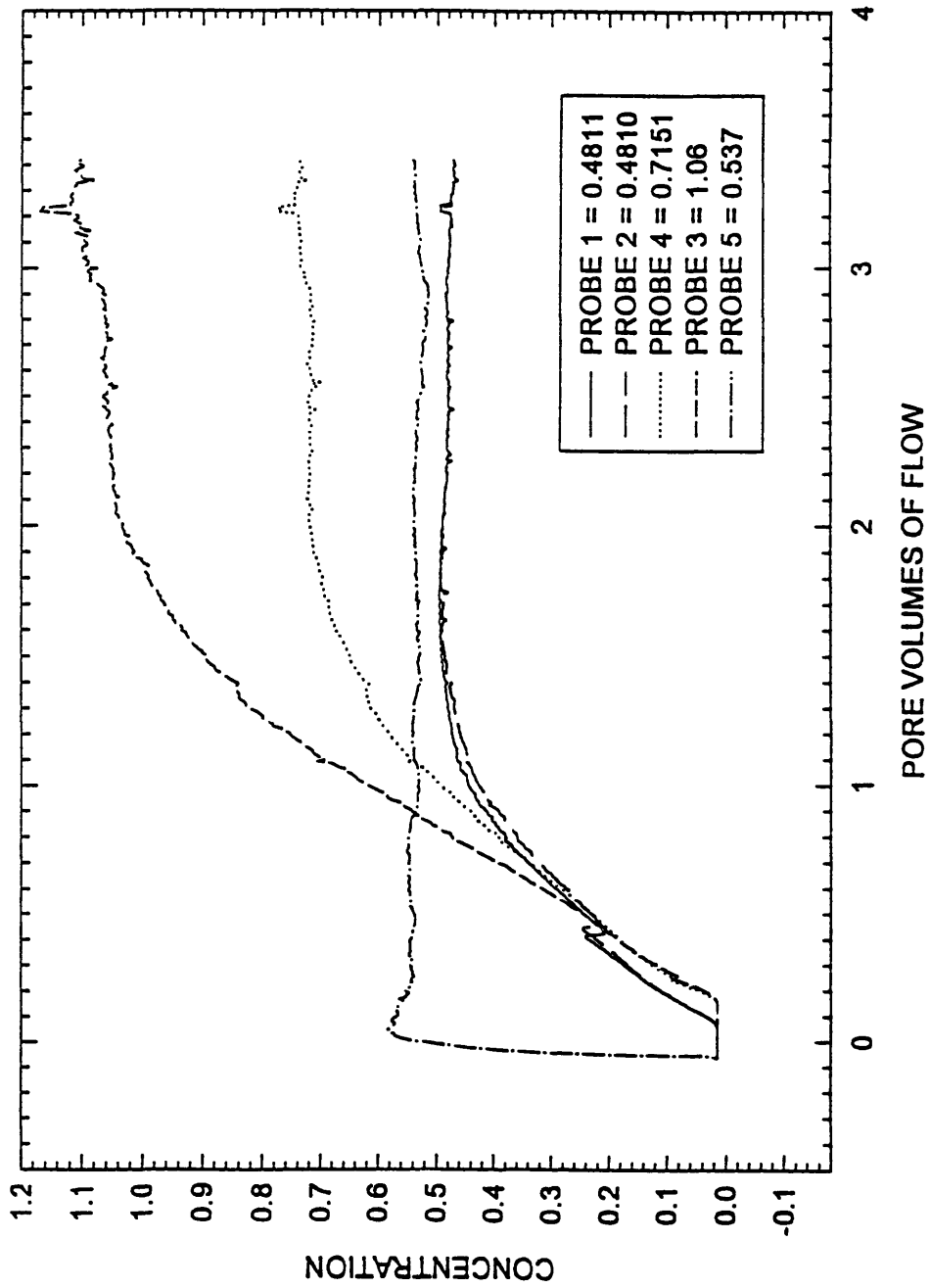
CONCENTRATION

CONCENTRATION VS PORE VOLUMES
PEAT 2 TEST 3 2-05-96
CONTINUOUS SOURCE, 0.1 M NaCl, SEEPAGE VEL. = 4.4 X 10^{-5} cm/sec

PROBE 1 = 0.3203
PROBE 2 = 0.4116
PROBE 4 = 0.7082
PROBE 3 = 1.033
PROBE 5 = 0.4723

PORE VOLUMES OF FLOW

CONCENTRATION
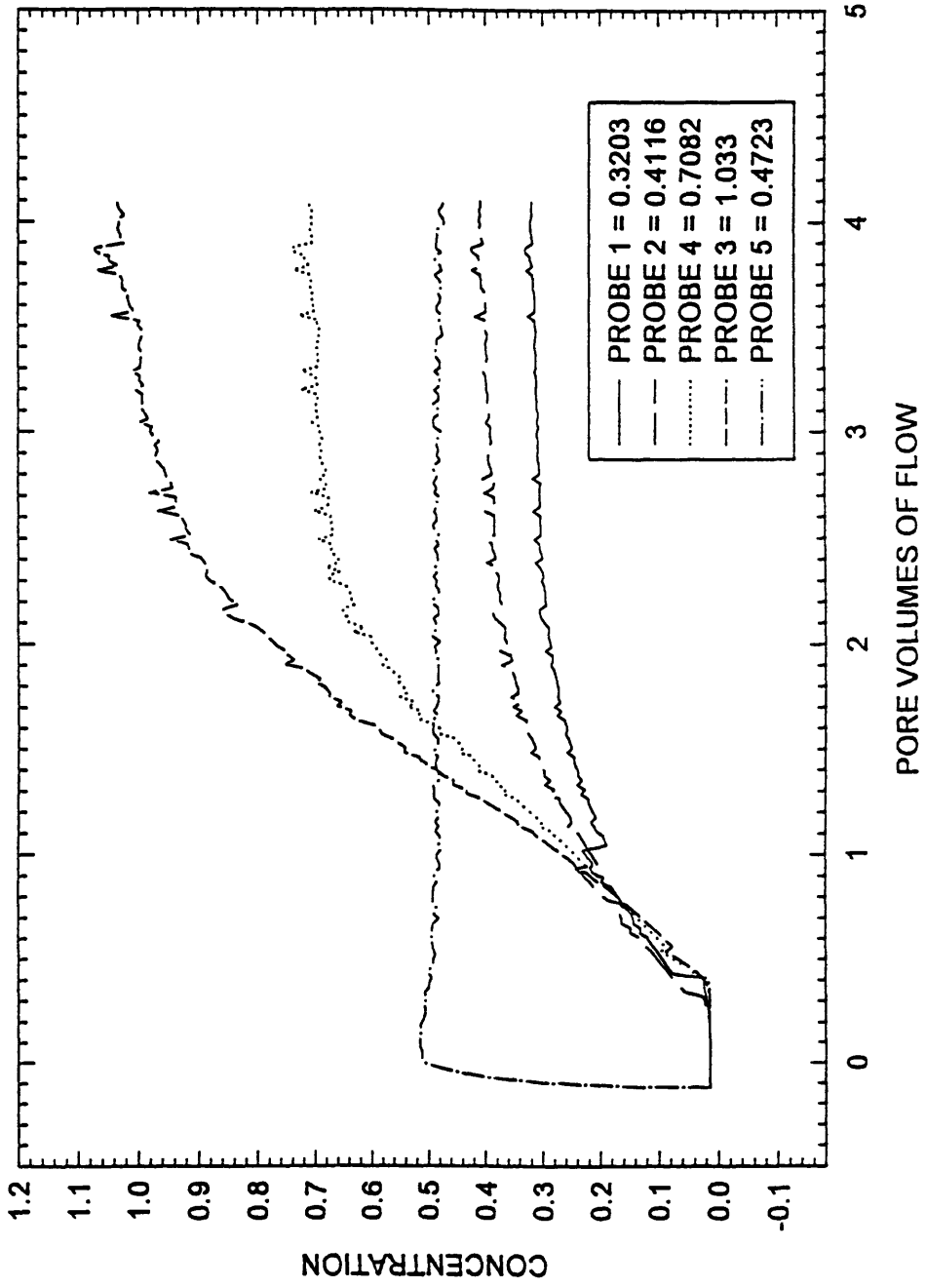
APPENDIX E: INFORMATIONAL PAGES OF CXTFIT INPUT AND OUTPUTFILES

1

| | 4 | 1 | 1 | 50 | 40 | 0 | 0 |

V.....	D.....	R.....	PULSE.	BETA..	OMEGA.
0.011	0.0000002	1.0	600.0	0.3	1.0

| 1 | 1 | 1 | 0 | 1 | 1 | 1 |

| 0.0 | 0.0 | 0.0 | 0.0 | 0.0 | 0.0 |
| 0.0 | 0.0 | 0.0 | 0.0 | 0.0 | 0.0 |

0.00000	1.0	1
0.00069	6.65480	34
0.00079	6.65480	94
0.00079	6.65480	154
0.00074	6.65480	214
0.00074	6.65480	274
0.00074	6.65480	334
0.00013	6.65480	394
0.15376	6.65480	454
0.35300	6.65480	514
0.50294	6.65480	574
0.59702	6.65480	634
0.63510	6.65480	694
0.75436	6.65480	754
0.80801	6.65480	814
0.85797	6.65480	874
0.89427	6.65480	934
0.91865	6.65480	994
0.84389	6.65480	1054
0.64836	6.65480	1114
0.48908	6.65480	1174
0.36707	6.65480	1234
0.27413	6.65480	1294
0.20271	6.65480	1354
0.14485	6.65480	1414
0.08197	6.65480	1474
0.05595	6.65480	1534
0.03318	6.65480	1594
0.01821	6.65480	1654
0.00941	6.65480	1714
0.00317	6.65480	1774
0.00137	6.65480	1834
0.00044	6.65480	1894
0.00008	6.65480	1954
0.00000	6.65480	2014
0.00000	6.65480	2074
0.00003	6.65480	2134
0.00005	6.65480	2194
0.00007	6.65480	2254
0.00027	6.65480	2314
0.00051	6.65480	2374

S1T1.DAT

```
***********************************************************************
*
*          ONE-DIMENSIONAL CONVECTION-DISPERSION EQ. SOLUTION
*          NON-LINEAR LEAST-SQUARES ANALYSIS
*
*          DETERMINISTIC TWO-SITE/TWO-REGION NONEQUILIBRIUM MODEL FOR
*          PULSE-TYPE INJECTION WITH NO PRODUCTION OR DECAY
*          SOLUTION FOR FLUX CONCENTRATIONS
*          REDUCED CONCENTRATION DATA
*
*
*
*
***********************************************************************
```

INITIAL VALUES OF COEFFICIENTS
================================
NAME	INITIAL VALUE
V.........	.0110
D.........	.0000
R.........	1.0000
PULSE.....	600.0000
BETA......	.3000
OMEGA.....	1.0000
CI........	.0000
CO........	1.0000

ITERATION	SSQ	V.....	D.....	PULSE.	BETA..
0	3.093490	.01100	.00000	600.00000	.30000
1	3.093471	.01100	.00000	599.99995	.30000
2	3.093469	.01100	.00000	599.99995	.30000
3	3.093468	.01100	.00000	599.99995	.30000
4	3.093467	.01100	.00000	599.99995	.30000
5	3.093467	.01100	.00000	599.99995	.30000
6	3.093467	.01100	.00000	599.99995	.30000
7	3.093467	.01100	.00000	599.99995	.30000
8	3.093467	.01100	.00000	599.99995	.30000
9	1.369952	.01470	.00005	692.45775	.88382
10	1.152426	.01379	.00011	690.30994	.85316
11	.080150	.01079	.00048	647.39814	.71820
12	.012683	.01061	.00035	601.08125	.74472
13	.009343	.01053	.00021	599.67016	.71555
14	.009307	.01052	.00021	599.62216	.71598
15	.009307	.01052	.00021	599.61464	.71596
16	.009307	.01052	:00021	599.61488	.71595

CORRELATION MATRIX
==================
	1	2	3	4	5
1	1.0000				
2	.1391	1.0000			
3	.4330	.0885	1.0000		
4	.0392	.8367	.0592	1.0000	

<div align="center">S1T1.OUT</div>

```
     5       .1225      -.6954       -.1846       -.9164      1.0000
```

RSQUARE FOR REGRESSION = .99774614

NON-LINEAR LEAST SQUARES ANALYSIS, FINAL RESULTS
==

```
                                                          95% CONFIDENCE LIM
VARIABLE     NAME        VALUE       S.E.COEFF.   T-VALUE    LOWER        UP
    1        V.....    .105236E-01   .571851E-04   184.03   .104075E-01  .106
    2        D.....    .206703E-03   .126371E-03     1.64  -.498594E-04  .463
    3        PULSE.    .599615E+03   .397215E+01   150.95   .591551E+03  .607
    4        BETA..    .715955E+00   .167350E-01    42.78   .681979E+00  .749
    5        OMEGA.    .178429E+01   .206361E+00     8.65   .136533E+01  .220
```

```
-----------------------ORDERED BY COMPUTER INPUT-----------------------
                                        CONCENTRATION            RESI-
NO    DISTANCE          TIME         OBS          FITTED         DUAL
 1   6.6548000    34.0000000      .0006900      .0000000      .0006900
 2   6.6548000    94.0000000      .0007900      .0000000      .0007900
 3   6.6548000   154.0000000      .0007900      .0000000      .0007900
 4   6.6548000   214.0000000      .0007400      .0000000      .0007400
 5   6.6548000   274.0000000      .0007400      .0000000      .0007400
 6   6.6548000   334.0000000      .0007400      .0000112      .0007288
 7   6.6548000   394.0000000      .0001300      .0093032     -.0091732
 8   6.6548000   454.0000000      .1537600      .1360413      .0177187
 9   6.6548000   514.0000000      .3530000      .3366147      .0163853
10   6.6548000   574.0000000      .5029400      .4867403      .0161997
11   6.6548000   634.0000000      .5970200      .6080029     -.0109829
12   6.6548000   694.0000000      .6851000      .7056971     -.0205971
13   6.6548000   754.0000000      .7543600      .7822756     -.0279156
14   6.6548000   814.0000000      .8080100      .8409651     -.0329551
15   6.6548000   874.0000000      .8579700      .8851211     -.0271511
16   6.6548000   934.0000000      .8942700      .9178192     -.0235492
17   6.6548000   994.0000000      .9186500      .9321805     -.0135305
18   6.6548000   **********      .8438900      .8216477      .0222423
19   6.6548000   **********      .6483600      .6336627      .0146973
20   6.6548000   **********      .4890800      .4925472     -.0034672
21   6.6548000   **********      .3670700      .3776044     -.0105344
22   6.6548000   **********      .2741800      .2843565     -.0101765
23   6.6548000   **********      .2027100      .2108867     -.0081767
24   6.6548000   **********      .1448500      .1543572     -.0095072
25   6.6548000   **********      .0819700      .1116935     -.0297235
26   6.6548000   **********      .0559500      .0800089     -.0240589
27   6.6548000   **********      .0331800      .0567985     -.0236185
28   6.6548000   **********      .0182100      .0399964     -.0217864
29   6.6548000   **********      .0094100      .0279591     -.0185491
30   6.6548000   **********      .0031700      .0194145     -.0162445
31   6.6548000   **********      .0013700      .0133991     -.0120291
32   6.6548000   **********      .0004400      .0091956     -.0087556
33   6.6548000   **********      .0000800      .0062780     -.0061980
34   6.6548000   **********      .0000000      .0042655     -.0042655
35   6.6548000   **********      .0000000      .0028851     -.0028851
36   6.6548000   **********      .0000300      .0019432     -.0019132
37   6.6548000   **********      .0000500      .0013037     -.0012537
38   6.6548000   **********      .0000700      .0008714     -.0008014
39   6.6548000   **********      .0002700      .0005804     -.0003104
```

<div align="center">S1T1.OUT</div>

```
1
      4              1              1              50             40              0              0

      V.....    D.....      R.....      PULSE.    BETA..      OMEGA.
       0.011  0.0000002         1.0       600.0       0.5         1.0
      1    1              1           0           1           1              1
          0.0         0.0         0.0         0.0         0.0         0.0
          0.0         0.0         0.0         0.0         0.0         0.0
     0.00000         1.0           1
     0.00000     6.65480          35
     0.00001     6.65480          95
     0.00002     6.65480         155
     0.00004     6.65480         215
     0.00051     6.65480         275
     0.00057     6.65480         335
     0.00336     6.65480         395
     0.13623     6.65480         455
     0.33642     6.65480         515
     0.53426     6.65480         575
     0.62691     6.65480         635
     0.71560     6.65480         695
     0.78897     6.65480         755
     0.84433     6.65480         815
     0.89001     6.65480         875
     0.92811     6.65480         935
     0.94726     6.65480         995
     0.85195     6.65480        1055
     0.63787     6.65480        1115
     0.47502     6.65480        1175
     0.35360     6.65480        1235
     0.25996     6.65480        1295
     0.18926     6.65480        1355
     0.12518     6.65480        1415
     0.07582     6.65480        1475
     0.04854     6.65480        1535
     0.02723     6.65480        1595
     0.01354     6.65480        1655
     0.00630     6.65480        1715
     0.00165     6.65480        1775
     0.00045     6.65480        1835
     0.00007     6.65480        1895
     0.00000     6.65480        1955
     0.00003     6.65480        2015
     0.00006     6.65480        2075
     0.00027     6.65480        2135
     0.00054     6.65480        2195
     0.00054     6.65480        2255
     0.00057     6.65480        2315
     0.00061     6.65480        2375
```

S1T2.DAT

```
**************************************************************************
*
*          ONE-DIMENSIONAL CONVECTION-DISPERSION EQ. SOLUTION
*          NON-LINEAR LEAST-SQUARES ANALYSIS
*
*          DETERMINISTIC TWO-SITE/TWO-REGION NONEQUILIBRIUM MODEL FOR
*          PULSE-TYPE INJECTION WITH NO PRODUCTION OR DECAY
*          SOLUTION FOR FLUX CONCENTRATIONS
*          REDUCED CONCENTRATION DATA
*
*
*
*
**************************************************************************
```

INITIAL VALUES OF COEFFICIENTS
================================

NAME	INITIAL VALUE
V.........	.0110
D.........	.0000
R.........	1.0000
PULSE.....	600.0000
BETA......	.5000
OMEGA.....	1.0000
CI........	.0000
CO........	1.0000

ITERATION	SSQ	V.....	D.....	PULSE.	BETA..
0	1.668690	.01100	.00000	600.00000	.50000
1	1.668668	.01100	.00000	599.99996	.50000
2	1.668663	.01100	.00000	599.99995	.50000
3	1.668660	.01100	.00000	599.99994	.50000
4	1.668659	.01100	.00000	599.99994	.50000
5	1.668659	.01100	.00000	599.99994	.50000
6	1.668659	.01100	.00000	599.99994	.50000
7	1.668659	.01100	.00000	599.99994	.50000
8	1.668659	.01100	.00000	599.99994	.50000
9	.199970	.01142	.00091	587.60640	.94500
10	.094856	.01139	.00098	589.34355	.91064
11	.054336	.01089	.00100	601.04789	.84477
12	.026099	.01106	.00070	598.39490	.82271
13	.009867	.01086	.00075	602.75124	.77791
14	.007109	.01078	.00004	601.62301	.70076
15	.006038	.01079	.00009	604.36803	.71000
16	.005970	.01078	.00007	604.47693	.71183
17	.005916	.01078	.00005	604.55637	.71182
18	.005854	.01078	.00003	604.70617	.71194
19	.005824	.01077	.00003	604.89122	.71215
20	.005803	.01077	.00003	605.02881	.71233
21	.005741	.01076	.00001	605.22640	.71424
22	.005558	.01075	.00001	605.47545	.71570
23	.005463	.01075	.00001	605.47675	.71728
24	.005336	.01074	.00001	605.50894	.71837
25	.005247	.01074	.00000	605.26871	.71946
26	.005170	.01073	.00000	605.21179	.72016

S1T2.OUT

```
        27          .005098          .01072          .00000       604.97080       .72142
        28          .005035          .01072          .00000       604.74098       .72160
        29          .005008          .01072          .00000       604.67508       .72180
        30          .004946          .01071          .00000       604.42263       .72275
        31          .004932          .01071          .00000       604.12295       .72268
        32          .004922          .01071          .00000       604.14291       .72269
        33          .004921          .01071          .00000       604.14639       .72268
        34          .004921          .01071          .00000       604.14638       .72268
```

CORRELATION MATRIX
========================

```
            1           2           3           4           5
    1    1.0000
    2     .8847     1.0000
    3    -.6281     -.8743     1.0000
    4    -.8824     -.9986      .8591     1.0000
    5     .9021      .9883     -.8348     -.9913     1.0000
```

RSQUARE FOR REGRESSION = .99888151

NON-LINEAR LEAST SQUARES ANALYSIS, FINAL RESULTS
===

					95% CONFIDENCE LIM	
VARIABLE	NAME	VALUE	S.E.COEFF.	T-VALUE	LOWER	UP
1	V.....	.107107E-01	.904457E-04	118.42	.105271E-01	.108
2	D.....	.128298E-05	.367508E-04	.03	-.733296E-04	.758
3	PULSE.	.604146E+03	.298708E+01	202.25	.598082E+03	.610
4	BETA..	.722681E+00	.313031E-01	23.09	.659128E+00	.786
5	OMEGA.	.183345E+01	.383257E+00	4.78	.105535E+01	.261

```
-----------------------ORDERED BY COMPUTER INPUT-----------------------
                                          CONCENTRATION           RESI-
NO    DISTANCE        TIME            OBS          FITTED          DUAL
 1   6.6548000    35.0000000      .0000000      .0000000       .0000000
 2   6.6548000    95.0000000      .0000100      .0000000       .0000100
 3   6.6548000   155.0000000      .0000200      .0000000       .0000200
 4   6.6548000   215.0000000      .0000400      .0000000       .0000400
 5   6.6548000   275.0000000      .0005100      .0000000       .0005100
 6   6.6548000   335.0000000      .0005700      .0000000       .0005700
 7   6.6548000   395.0000000      .0033600      .0000000       .0033600
 8   6.6548000   455.0000000      .1862300      .1756383       .0105917
 9   6.6548000   515.0000000      .3364200      .3558817      -.0194617
10   6.6548000   575.0000000      .5342600      .5092623       .0249977
11   6.6548000   635.0000000      .6269100      .6346511      -.0077411
12   6.6548000   695.0000000      .7156000      .7331421      -.0175421
13   6.6548000   755.0000000      .7889700      .8081983      -.0192283
14   6.6548000   815.0000000      .8443800      .8640409      -.0196609
15   6.6548000   875.0000000      .8900100      .9047820      -.0147720
16   6.6548000   935.0000000      .9281100      .9340213      -.0059113
17   6.6548000   995.0000000      .9472600      .9547137      -.0074537
18   6.6548000   ***********      .8519500      .8469217       .0050283
19   6.6548000   ***********      .6378700      .6348804       .0029896
20   6.6548000   ***********      .4750200      .4864894      -.0114694
21   6.6548000   ***********      .3536000      .3638185      -.0102185
```

S1T2.OUT

1

	4	1	1	50	250	0	0

V.....	D.....	R.....	PULSE.	BETA..	OMEGA.
0.0010	0.0000002	1.0	600.0	0.5	1.0
1 1	1	0	1	1	1
0.0	0.0	0.0	0.0	0.0	0.0
0.0	0.0	0.0	0.0	0.0	0.0
0.00000	1.0	1			
0.00045	6.6548	51			
0.00042	6.6548	111			
0.00041	6.6548	171			
0.00040	6.6548	231			
0.00039	6.6548	291			
0.00038	6.6548	351			
0.00038	6.6548	411			
0.00037	6.6548	471			
0.00036	6.6548	531			
0.00036	6.6548	591			
0.00035	6.6548	651			
0.00035	6.6548	711			
0.00034	6.6548	771			
0.00034	6.6548	831			
0.00034	6.6548	891			
0.00034	6.6548	951			
0.00033	6.6548	1011			
0.00033	6.6548	1071			
0.00033	6.6548	1131			
0.00033	6.6548	1191			
0.00033	6.6548	1251			
0.00034	6.6548	1311			
0.00034	6.6548	1371			
0.00033	6.6548	1431			
0.00033	6.6548	1491			
0.00033	6.6548	1551			
0.00033	6.6548	1611			
0.00033	6.6548	1671			
0.00033	6.6548	1731			
0.00033	6.6548	1791			
0.00033	6.6548	1851			
0.00033	6.6548	1911			
0.00033	6.6548	1971			
0.00033	6.6548	2031			
0.00033	6.6548	2091			
0.00033	6.6548	2151			
0.00033	6.6548	2211			
0.00033	6.6548	2271			
0.00033	6.6548	2331			
0.00033	6.6548	2391			
0.00033	6.6548	2451			
0.00033	6.6548	2511			
0.00033	6.6548	2571			
0.00033	6.6548	2631			
0.00033	6.6548	2691			
0.00033	6.6548	2751			
0.00034	6.6548	2811			
0.00043	6.6548	2871			
0.00096	6.6548	2931			
0.00289	6.6548	2991			

S2T1.DAT

```
*******************************************************************************
*
*         ONE-DIMENSIONAL CONVECTION-DISPERSION EQ. SOLUTION
*         NON-LINEAR LEAST-SQUARES ANALYSIS
*
*         DETERMINISTIC TWO-SITE/TWO-REGION NONEQUILIBRIUM MODEL FOR
*         PULSE-TYPE INJECTION WITH NO PRODUCTION OR DECAY
*         SOLUTION FOR FLUX CONCENTRATIONS
*         REDUCED CONCENTRATION DATA
*
*
*
*
*******************************************************************************
```

INITIAL VALUES OF COEFFICIENTS
================================

NAME	INITIAL VALUE
V.........	.0010
D........	.0000
R........	1.0000
PULSE.....	600.0000
BETA......	.5000
OMEGA.....	1.0000
CI........	.0000
CO........	1.0000

ITERATION	SSQ	V.....	D.....	PULSE.	BETA..
0	.861382	.00100	.00000	600.00000	.50000
1	.357896	.00100	.00000	609.94018	.50125
2	.286733	.00101	.00000	624.78707	.50522
3	.262395	.00102	.00000	634.47311	.51397
4	.231171	.00104	.00000	635.62701	.52663
5	.161826	.00115	.00001	585.49912	.59780
6	.097513	.00138	.00001	486.26222	.72950
7	.029561	.00149	.00001	452.75759	.77836
8	.002151	.00148	.00002	464.20744	.76500
9	.000579	.00148	.00003	466.95380	.76812
10	.000545	.00148	.00003	466.75128	.76806
11	.000545	.00148	.00003	466.84239	.76825
12	.000545	.00148	.00003	466.84278	.76825

CORRELATION MATRIX
==================

	1	2	3	4	5
1	1.0000				
2	-.1813	1.0000			
3	-.4654	.3255	1.0000		
4	.1172	.7673	-.0510	1.0000	
5	.4269	-.7828	-.3105	-.7937	1.0000

RSQUARE FOR REGRESSION = .99939804

S2T1.OUT

NON-LINEAR LEAST SQUARES ANALYSIS, FINAL RESULTS

VARIABLE	NAME	VALUE	S.E.COEFF.	T-VALUE	95% CONFIDENCE LIM LOWER	UP
1	V.....	.148266E-02	.107629E-05	1377.57	.148054E-02	.148
2	D.....	.323763E-04	.680527E-06	47.58	.310358E-04	.337
3	PULSE.	.466843E+03	.879616E+00	530.73	.465110E+03	.468
4	BETA..	.768251E+00	.100631E-02	763.44	.766269E+00	.770
5	OMEGA.	.206239E+01	.223424E-01	92.31	.201838E+01	.210

```
------------------------ORDERED BY COMPUTER INPUT---------------------
                                    CONCENTRATION            RESI-
NO    DISTANCE         TIME         OBS        FITTED         DUAL
 1    6.6548000    51.0000000    .0004500    .0000000     .0004500
 2    6.6548000   111.0000000    .0004200    .0000000     .0004200
 3    6.6548000   171.0000000    .0004100    .0000000     .0004100
 4    6.6548000   231.0000000    .0004000    .0000000     .0004000
 5    6.6548000   291.0000000    .0003900    .0000000     .0003900
 6    6.6548000   351.0000000    .0003800    .0000000     .0003800
 7    6.6548000   411.0000000    .0003800    .0000000     .0003800
 8    6.6548000   471.0000000    .0003700    .0000000     .0003700
 9    6.6548000   531.0000000    .0003600    .0000000     .0003600
10    6.6548000   591.0000000    .0003600    .0000000     .0003600
11    6.6548000   651.0000000    .0003500    .0000000     .0003500
12    6.6548000   711.0000000    .0003500    .0000000     .0003500
13    6.6548000   771.0000000    .0003400    .0000000     .0003400
14    6.6548000   831.0000000    .0003400    .0000000     .0003400
15    6.6548000   891.0000000    .0003400    .0000000     .0003400
16    6.6548000   951.0000000    .0003400    .0000000     .0003400
17    6.6548000   **********     .0003300    .0000000     .0003300
18    6.6548000   **********     .0003300    .0000000     .0003300
19    6.6548000   **********     .0003300    .0000000     .0003300
20    6.6548000   **********     .0003300    .0000000     .0003300
21    6.6548000   **********     .0003300    .0000000     .0003300
22    6.6548000   **********     .0003400    .0000000     .0003400
23    6.6548000   **********     .0003400    .0000000     .0003400
24    6.6548000   **********     .0003300    .0000000     .0003300
25    6.6548000   **********     .0003300    .0000000     .0003300
26    6.6548000   **********     .0003300    .0000000     .0003300
27    6.6548000   **********     .0003300    .0000000     .0003300
28    6.6548000   **********     .0003300    .0000000     .0003300
29    6.6548000   **********     .0003300    .0000000     .0003300
30    6.6548000   **********     .0003300    .0000000     .0003300
31    6.6548000   **********     .0003300    .0000000     .0003300
32    6.6548000   **********     .0003300    .0000000     .0003300
33    6.6548000   **********     .0003300    .0000000     .0003300
34    6.6548000   **********     .0003300    .0000000     .0003300
35    6.6548000   **********     .0003300    .0000000     .0003300
36    6.6548000   **********     .0003300    .0000000     .0003300
37    6.6548000   **********     .0003300    .0000000     .0003300
38    6.6548000   **********     .0003300    .0000000     .0003300
39    6.6548000   **********     .0003300    .0000002     .0003298
40    6.6548000   **********     .0003300    .0000008     .0003292
41    6.6548000   **********     .0003300    .0000033     .0003267
42    6.6548000   **********     .0003300    .0000119     .0003181
43    6.6548000   **********     .0003300    .0000378     .0002922
```

S2T1.OUT

```
1
      4           1           1          40         207          0           0

      V.....    D.....      R.....     PULSE.    BETA..     OMEGA.
      0.0030 0.0000002       1.0        600.0        0.5        1.0
      1    1          1         0           1          1          1
          0.0        0.0       0.0         0.0        0.0        0.0
          0.0        0.0       0.0         0.0        0.0        0.0
      0.00000       1.0         1
      0.00032    6.6548        18
      0.00032    6.6548        78
      0.00032    6.6548       138
      0.00033    6.6548       198
      0.00033    6.6548       258
      0.00033    6.6548       313
      0.00033    6.6548       373
      0.00033    6.6548       438
      0.00033    6.6548       498
      0.00033    6.6548       558
      0.00033    6.6548       613
      0.00033    6.6548       678
      0.00033    6.6548       738
      0.00034    6.6548       798
      0.00033    6.6548       853
      0.00033    6.6548       913
      0.00034    6.6548       978
      0.00033    6.6548      1038
      0.00043    6.6548      1098
      0.00634    6.6548      1158
      0.05158    6.6548      1218
      0.10672    6.6548      1278
      0.19560    6.6548      1338
      0.29350    6.6548      1398
      0.36912    6.6548      1458
      0.41440    6.6548      1518
      0.46642    6.6548      1578
      0.50789    6.6548      1638
      0.54143    6.6548      1698
      0.56860    6.6548      1758
      0.57390    6.6548      1818
      0.56242    6.6548      1878
      0.51962    6.6548      1938
      0.47371    6.6548      1998
      0.42556    6.6548      2058
      0.37730    6.6548      2118
      0.33825    6.6548      2178
      0.30084    6.6548      2238
      0.26546    6.6548      2298
      0.23605    6.6548      2358
      0.20796    6.6548      2418
      0.17984    6.6548      2478
      0.15588    6.6548      2538
      0.13514    6.6548      2598
      0.11813    6.6548      2658
      0.07979    6.6548      2718
      0.04498    6.6548      2778
      0.03698    6.6548      2838
      0.02967    6.6548      2898
      0.02363    6.6548      2958
```

S2T2.DAT

```
**********************************************************************
*
*          ONE-DIMENSIONAL CONVECTION-DISPERSION EQ. SOLUTION
*          NON-LINEAR LEAST-SQUARES ANALYSIS
*
*          DETERMINISTIC TWO-SITE/TWO-REGION NONEQUILIBRIUM MODEL FOR
*          PULSE-TYPE INJECTION WITH NO PRODUCTION OR DECAY
*          SOLUTION FOR FLUX CONCENTRATIONS
*          REDUCED CONCENTRATION DATA
*
*
*
*
**********************************************************************
```

INITIAL VALUES OF COEFFICIENTS
================================
NAME	INITIAL VALUE
V.........	.0030
D.........	.0000
R.........	1.0000
PULSE.....	600.0000
BETA......	.5000
OMEGA.....	1.0000
CI........	.0000
CO........	1.0000

ITERATION	SSQ	V.....	D.....	PULSE.	BETA..
0	1.571125	.00300	.00000	600.00000	.50000
1	.392983	.00300	.00000	649.50023	.59996
2	.365975	.00311	.00000	654.24607	.60603
3	.291000	.00315	.00001	647.77502	.63271
4	.190834	.00347	.00001	609.68839	.70675
5	.115021	.00381	.00000	590.60356	.76741
6	.046904	.00381	.00004	547.36930	.77545
7	.018159	.00396	.00006	534.04336	.77218
8	.009018	.00397	.00007	531.86851	.74494
9	.008403	.00398	.00006	529.22521	.72839
10	.008373	.00398	.00007	529.14307	.72951
11	.008372	.00398	.00007	529.09101	.72946
12	.008372	.00398	.00007	529.08742	.72945

CORRELATION MATRIX
===================
	1	2	3	4	5
1	1.0000				
2	.0096	1.0000			
3	-.0512	.2753	1.0000		
4	-.1497	.9547	.2791	1.0000	
5	.2960	-.8878	-.3625	-.9751	1.0000

RSQUARE FOR REGRESSION = .99731054

S2T2.OUT

200

NON-LINEAR LEAST SQUARES ANALYSIS, FINAL RESULTS

VARIABLE	NAME	VALUE	S.E.COEFF.	T-VALUE	95% CONFIDENCE LIM	
					LOWER	UP
1	V.....	.398399E-02	.711133E-05	560.23	.396997E-02	.399
2	D.....	.702304E-04	.248050E-04	2.83	.213190E-04	.119
3	PULSE.	.529087E+03	.242619E+01	218.07	.524303E+03	.533
4	BETA..	.729448E+00	.157737E-01	46.24	.698345E+00	.760
5	OMEGA.	.314198E+01	.304084E+00	10.33	.254238E+01	.374

```
------------------------ORDERED BY COMPUTER INPUT------------------------
                                           CONCENTRATION            RESI-
NO    DISTANCE           TIME          OBS          FITTED          DUAL
 1   6.6548000     18.0000000      .0003200      .0000000      .0003200
 2   6.6548000     78.0000000      .0003200      .0000000      .0003200
 3   6.6548000    138.0000000      .0003200      .0000000      .0003200
 4   6.6548000    193.0000000      .0003300      .0000000      .0003300
 5   6.6548000    258.0000000      .0003300      .0000000      .0003300
 6   6.6548000    318.0000000      .0003300      .0000000      .0003300
 7   6.6548000    378.0000000      .0003300      .0000000      .0003300
 8   6.6548000    438.0000000      .0003300      .0000000      .0003300
 9   6.6548000    498.0000000      .0003300      .0000000      .0003300
10   6.6548000    558.0000000      .0003300      .0000000      .0003300
11   6.6548000    618.0000000      .0003300      .0000000      .0003300
12   6.6548000    678.0000000      .0003300      .0000000      .0003300
13   6.6548000    738.0000000      .0003300      .0000000      .0003300
14   6.6548000    798.0000000      .0003400      .0000000      .0003400
15   6.6548000    858.0000000      .0003300      .0000001      .0003299
16   6.6548000    918.0000000      .0003300      .0000063      .0003237
17   6.6548000    978.0000000      .0003400      .0001493      .0001907
18   6.6548000   **********        .0003300      .0015810     -.0012510
19   6.6548000   **********        .0004300      .0084548     -.0080248
20   6.6548000   **********        .0063400      .0290010     -.0226610
21   6.6548000   **********        .0515800      .0686252     -.0170452
22   6.6548000   **********        .1067200      .1250283     -.0183083
23   6.6548000   **********        .1956000      .1915824      .0040176
24   6.6548000   **********        .2935000      .2627779      .0307221
25   6.6548000   **********        .3691200      .3351943      .0339257
26   6.6548000   **********        .4144000      .4066969      .0077031
27   6.6548000   **********        .4664200      .4737245     -.0073045
28   6.6548000   **********        .5078900      .5301817     -.0222917
29   6.6548000   **********        .5414300      .5667094     -.0252794
30   6.6548000   **********        .5686000      .5786748     -.0100748
31   6.6548000   **********        .5789000      .5694191      .0094809
32   6.6548000   **********        .5624200      .5456909      .0167291
33   6.6548000   **********        .5196200      .5127592      .0068608
34   6.6548000   **********        .4737100      .4740434     -.0003334
35   6.6548000   **********        .4255600      .4318160     -.0062560
36   6.6548000   **********        .3773000      .3883641     -.0110641
37   6.6548000   **********        .3382500      .3452893     -.0070393
38   6.6548000   **********        .3008400      .3038465     -.0030065
39   6.6548000   **********        .2654600      .2649083      .0005517
40   6.6548000   **********        .2360500      .2290246      .0070254
41   6.6548000   **********        .2079600      .1964875      .0114725
42   6.6548000   **********        .1798400      .1673903      .0124497
43   6.6548000   **********        .1558800      .1416800      .0142000
```

S2T2.OUT

```
1
    4           1           1          40          52           0           0


    V.....      D.....      R.....     PULSE.     BETA..     OMEGA.
    0.0073  0.0000002      1.0        600.0        0.5        1.0
    1    1          1          0           1           1          1
        0.0         0.0         0.0         0.0         0.0         0.0
        0.0         0.0         0.0         0.0         0.0         0.0
    0.00000       1.0          1
    0.00000     6.6548         18
    0.00000     6.6548         78
    0.00000     6.6548        138
    0.00000     6.6548        198
    0.00000     6.6548        258
    0.00000     6.6548        318
    0.00000     6.6543        373
    0.00000     6.6548        438
    0.01067     6.6548        498
    0.28509     6.6548        558
    0.47937     6.6548        618
    0.59476     6.6543        673
    0.69258     6.6543        738
    0.76450     6.6543        798
    0.81542     6.6548        858
    0.85432     6.6548        918
    0.88013     6.6548        973
    0.89591     6.6548       1038
    0.87702     6.6548       1098
    0.70696     6.6548       1158
    0.50131     6.6548       1218
    0.36188     6.6548       1278
    0.25837     6.6548       1338
    0.17723     6.6548       1398
    0.12661     6.6548       1458
    0.04023     6.6548       1518
    0.02487     6.6548       1578
    0.01442     6.6548       1638
    0.00856     6.6548       1698
    0.00538     6.6548       1758
    0.00092     6.6548       1818
    0.00049     6.6548       1878
    0.00025     6.6548       1938
    0.00015     6.6548       1998
    0.00008     6.6548       2058
    0.00005     6.6548       2118
    0.00003     6.6548       2178
    0.00002     6.6548       2238
    0.00001     6.6548       2298
    0.00000     6.6548       2358
    0.00000     6.6548       2418
    0.00000     6.6548       2478
    0.00000     6.6548       2538
    0.00000     6.6548       2598
    0.00000     6.6548       2658
    0.00000     6.6548       2718
    0.00000     6.6548       2778
    0.00000     6.6548       2838
    0.00000     6.6548       2898
    0.00000     6.6548       2958
```

S2T3.DAT

```
*****************************************************************************
*
*          ONE-DIMENSIONAL CONVECTION-DISPERSION EQ. SOLUTION
*          NON-LINEAR LEAST-SQUARES ANALYSIS
*
*          DETERMINISTIC TWO-SITE/TWO-REGION NONEQUILIBRIUM MODEL FOR
*          PULSE-TYPE INJECTION WITH NO PRODUCTION OR DECAY
*          SOLUTION FOR FLUX CONCENTRATIONS
*          REDUCED CONCENTRATION DATA
*
*
*
*
*****************************************************************************
```

INITIAL VALUES OF COEFFICIENTS
================================

NAME	INITIAL VALUE
V.........	.0073
D.........	.0000
R.........	1.0000
PULSE.....	600.0000
BETA......	.5000
OMEGA.....	1.0000
CI........	.0000
CO........	1.0000

ITERATION	SSQ	V.....	D.....	PULSE.	BETA..
0	1.116645	.00730	.00000	600.00000	.50000
1	1.116634	.00730	.00000	599.99982	.50000
2	1.116634	.00730	.00000	599.99981	.50000
3	1.116634	.00730	.00000	599.99980	.50000
4	1.116634	.00730	.00000	599.99980	.50000
5	1.116634	.00730	.00000	599.99980	.50000
6	1.116634	.00730	.00000	599.99980	.50000
7	.484389	.00997	.00009	483.60416	.82297
8	.074715	.00952	.00026	551.45020	.72579
9	.026214	.00971	.00053	579.27715	.80771
10	.020977	.00968	.00000	582.79928	.74142
11	.019490	.00971	.00001	584.53615	.74281
12	.019192	.00971	.00001	584.72672	.74497
13	.019179	.00971	.00001	584.72330	.74556
14	.019178	.00971	.00001	584.70610	.74566
15	.019178	.00971	.00001	584.70609	.74566
16	.019178	.00971	.00001	584.70485	.74567
17	.019178	.00971	.00001	584.70355	.74567
18	.019178	.00971	.00001	584.70048	.74567
19	.019178	.00971	.00001	584.69961	.74568

CORRELATION MATRIX
====================

	1	2	3	4	5
1	1.0000				

S2T3.OUT

```
 2   -.4613     1.0000
 3    .6955     -.4896     1.0000
 4   -.3042      .4842     -.6567     1.0000
 5    .4053     -.3742      .3700     -.7216     1.0000
```

RSQUARE FOR REGRESSION = .99598611

NON-LINEAR LEAST SQUARES ANALYSIS, FINAL RESULTS
===

VARIABLE	NAME	VALUE	S.E.COEFF.	T-VALUE	95% CONFIDENCE LIM LOWER	UP
1	V.....	.970637E-02	.622361E-04	155.96	.958116E-02	.983
2	D.....	.103853E-04	.164667E-04	.63	-.227433E-04	.435
3	PULSE.	.584700E+03	.545300E+01	107.23	.573729E+03	.595
4	BETA..	.745676E+00	.827903E-02	90.07	.729020E+00	.762
5	OMEGA.	.202258E+01	.145238E+00	13.93	.173039E+01	.231

```
-----------------------ORDERED BY COMPUTER INPUT----------------------
                                       CONCENTRATION          RESI-
NO    DISTANCE          TIME         OBS        FITTED        DUAL
 1   6.6548000    18.0000000     .0000000     .0000000     .0000000
 2   6.6548000    78.0000000     .0000000     .0000000     .0000000
 3   6.6548000   138.0000000     .0000000     .0000000     .0000000
 4   6.6548000   198.0000000     .0000000     .0000000     .0000000
 5   6.6548000   258.0000000     .0000000     .0000000     .0000000
 6   6.6548000   318.0000000     .0000000     .0000000     .0000000
 7   6.6548000   378.0000000     .0000000     .0000000     .0000000
 8   6.6548000   438.0000000     .0000000     .0000000     .0000000
 9   6.6548000   498.0000000     .0106700     .0105251     .0001449
10   6.6548000   558.0000000     .2850900     .2759300     .0091600
11   6.6548000   618.0000000     .4793700     .4444742     .0348958
12   6.6548000   678.0000000     .5947600     .5865008     .0082592
13   6.6548000   738.0000000     .6925800     .6996769    -.0070969
14   6.6548000   798.0000000     .7645000     .7862823    -.0217823
15   6.6548000   858.0000000     .8154200     .8505247    -.0351047
16   6.6548000   918.0000000     .8543200     .8970071    -.0426871
17   6.6548000   978.0000000     .8801800     .9299563    -.0497763
18   6.6548000   **********      .8959100     .9529118    -.0570018
19   6.6548000   **********      .8770200     .8786043    -.0015843
20   6.6548000   **********      .7069600     .6583311     .0486289
21   6.6548000   **********      .5013100     .5030807    -.0017707
22   6.6548000   **********      .3618800     .3731759    -.0112959
23   6.6548000   **********      .2583700     .2702212    -.0118512
24   6.6548000   **********      .1772300     .1917842    -.0145542
25   6.6548000   **********      .1266100     .1338154    -.0072054
26   6.6548000   **********      .0402300     .0920048    -.0517748
27   6.6548000   **********      .0248700     .0624489    -.0375789
28   6.6548000   **********      .0144200     .0419075    -.0274875
29   6.6548000   **********      .0085600     .0278332    -.0192782
30   6.6548000   **********      .0053800     .0183236    -.0129436
31   6.6548000   **********      .0009200     .0119612    -.0110412
32   6.6548000   **********      .0004900     .0077490    -.0072590
33   6.6548000   **********      .0002500     .0049853    -.0047353
34   6.6548000   **********      .0001500     .0031869    -.0030369
35   6.6548000   **********      .0000800     .0020251    -.0019451
36   6.6548000   **********      .0000500     .0012798    -.0012298
```

S2T3.OUT

```
1
    4              1              1             40            602              0              0


    V.....    D.....         R.....     PULSE.       BETA..        OMEGA.
    0.00001 0.0000002          1.0       600.0          0.1           0.5
      1   1              1           0            1            1            1
            0.0           0.0          0.0         0.0          0.0          0.0
            0.0           0.0          0.0         0.0          0.0          0.0
    0.00000           1.0            1
    0.00096      2.125472          443
    0.00098      2.125472         1043
    0.00099      2.125472         1643
    0.00105      2.125472         2243
    0.00114      2.125472         2843
    0.00121      2.125472         3443
    0.00132      2.125472         4043
    0.00141      2.125472         4643
    0.00151      2.125472         5243
    0.00160      2.125472         5843
    0.00170      2.125472         6443
    0.00130      2.125472         7043
    0.00190      2.125472         7643
    0.00197      2.125472         8243
    0.00207      2.125472         8843
    0.00215      2.125472         9443
    0.00223      2.125472        10043
    0.00234      2.125472        10643
    0.00239      2.125472        11243
    0.00245      2.125472        11843
    0.00250      2.125472        12443
    0.00259      2.125472        13043
    0.00262      2.125472        13643
    0.00265      2.125472        14243
    0.00273      2.125472        14843
    0.00276      2.125472        15443
    0.00280      2.125472        16043
    0.00283      2.125472        16643
    0.00286      2.125472        17243
    0.00289      2.125472        17843
    0.00294      2.125472        18443
    0.00300      2.125472        19043
    0.00306      2.125472        19643
    0.00310      2.125472        20243
    0.00313      2.125472        20843
    0.00314      2.125472        21443
    0.00320      2.125472        22043
    0.00320      2.125472        22643
    0.00321      2.125472        23243
    0.00327      2.125472        23843
    0.00327      2.125472        24443
    0.00328      2.125472        25043
    0.00328      2.125472        25643
    0.00331      2.125472        26243
    0.00332      2.125472        26843
    0.00335      2.125472        27443
    0.00337      2.125472        28043
    0.00334      2.125472        28643
    0.00339      2.125472        29243
    0.00339      2.125472        29843
```

P1T1.DAT

```
***********************************************************************
*
*          ONE-DIMENSIONAL CONVECTION-DISPERSION EQ. SOLUTION
*          NON-LINEAR LEAST-SQUARES ANALYSIS
*
*          DETERMINISTIC TWO-SITE/TWO-REGION NONEQUILIBRIUM MODEL FOR
*          PULSE-TYPE INJECTION WITH NO PRODUCTION OR DECAY
*          SOLUTION FOR FLUX CONCENTRATIONS
*          REDUCED CONCENTRATION DATA
*
*
*
*
***********************************************************************
```

INITIAL VALUES OF COEFFICIENTS
==================================

NAME	INITIAL VALUE
V.........	.0000
D.;.......	.0000
R.........	1.0000
PULSE.....	600.0000
BETA......	.1000
OMEGA.....	.5000
CI........	.0000
CO........	1.0000

ITERATION	SSQ	V.....	D.....	PULSE.	BETA..
0	.018915	.00001	.00000	600.00000	.10000
1	.002956	.00001	.00000	602.39932	.10200
2	.000855	.00001	.00000	544.51909	.10455
3	.000546	.00001	.00000	454.42536	.13310
4	.000495	.00001	.00000	453.61548	.13593
5	.000479	.00001	.00000	463.17481	.13766
6	.000462	.00001	.00000	455.20268	.14249
7	.000384	.00001	.00000	465.67279	.16037
8	.000306	.00002	.00000	435.61076	.16200
9	.000180	.00002	.00000	410.53011	.17789
10	.000141	.00002	.00000	428.90340	.19385
11	.000054	.00003	.00000	388.84860	.25452
12	.000032	.00003	.00001	403.31375	.26754
13	.000019	.00003	.00001	384.38248	.26714
14	.000014	.00003	.00001	390.08206	.26357
15	.000013	.00003	.00001	398.60511	.26446
16	.000009	.00003	.00001	394.63220	.17948
17	.000008	.00003	.00001	395.41079	.16278
18	.000008	.00003	.00001	396.15040	.14934
19	.000008	.00003	.00001	396.55192	.13784
20	.000007	.00003	.00001	396.51905	.13007
21	.000007	.00003	.00001	396.75515	.12226
22	.000007	.00003	.00001	397.48225	.12056
23	.000007	.00003	.00001	397.16330	.11185
24	.000007	.00003	.00001	397.65271	.11180
25	.000007	.00003	.00001	397.46772	.10692
26	.000007	.00003	.00001	397.59825	.10224

P1T1.OUT

```
27          .000007        .00003      .00001    397.73658      .09798
28          .000007        .00003      .00001    397.80236      .09414
29          .000007        .00003      .00001    397.77580      .09131
30          .000007        .00003      .00001    397.78417      .09079
31          .000007        .00003      .00001    397.79042      .09061
32          .000007        .00003      .00001    397.79329      .09052
33          .000007        .00003      .00001    397.79397      .09050
```

CORRELATION MATRIX

```
            1           2           3           4           5
  1      1.0000
  2      -.5937      1.0000
  3      -.5921       .2660      1.0000
  4      -.4073       .7490       .1155      1.0000
  5      -.4491       .5892       .0850       .3273      1.0000
```

RSQUARE FOR REGRESSION = .99273472

NON-LINEAR LEAST SQUARES ANALYSIS, FINAL RESULTS

					95% CONFIDENCE LIM	
VARIABLE	NAME	VALUE	S.E.COEFF.	T-VALUE	LOWER	UP
1	V.....	.273074E-04	.118977E-06	229.52	.270737E-04	.275
2	D.....	.102801E-04	.132056E-06	77.85	.100208E-04	.105
3	PULSE.	.397794E+03	.135153E+01	294.33	.395140E+03	.400
4	BETA..	.905015E-01	.329051E-02	27.50	.840390E-01	.969
5	OMEGA.	.937041E+01	.107511E+00	87.16	.915926E+01	.958

```
------------------------ORDERED BY COMPUTER INPUT------------------------
                                    CONCENTRATION             RESI-
NO    DISTANCE         TIME         OBS        FITTED         DUAL
 1   2.1254720   443.0000000    .0009600    .0000000     .0009600
 2   2.1254720   **********     .0009800    .0000473     .0009327
 3   2.1254720   **********     .0009900    .0007772     .0002128
 4   2.1254720   **********     .0010500    .0014913    -.0004413
 5   2.1254720   **********     .0011400    .0017137    -.0005737
 6   2.1254720   **********     .0012100    .0015894    -.0003794
 7   2.1254720   **********     .0013200    .0014802    -.0001602
 8   2.1254720   **********     .0014100    .0014453    -.0000353
 9   2.1254720   **********     .0015100    .0014656     .0000444
10   2.1254720   **********     .0016000    .0014978     .0001022
11   2.1254720   **********     .0017000    .0015863     .0001137
12   2.1254720   **********     .0018000    .0016544     .0001456
13   2.1254720   **********     .0019000    .0017259     .0001741
14   2.1254720   **********     .0019700    .0017993     .0001707
15   2.1254720   **********     .0020700    .0018704     .0001996
16   2.1254720   **********     .0021500    .0019422     .0002078
17   2.1254720   **********     .0022300    .0020129     .0002171
18   2.1254720   **********     .0023400    .0020825     .0002575
19   2.1254720   **********     .0023900    .0021508     .0002392
20   2.1254720   **********     .0024500    .0022178     .0002322
21   2.1254720   **********     .0025000    .0022835     .0002165
22   2.1254720   **********     .0025900    .0023478     .0002422
```

PlT1.OUT

```
1
          4            1            1           40          116           0                    0


          V.....    D.....      R.....      PULSE.      BETA..      OMEGA.
     0.000042  0.0000002       1.0       600.0         0.5         1.0
       1    1            1            0            1            1            1
          0.0          0.0          0.0          0.0          0.0          0.0
          0.0          0.0          0.0          0.0          0.0          0.0
     0.00000       1.0            1
     0.00010   2.125472        560
     0.00002   2.125472       1160
     0.00050   2.125472       1760
     0.00331   2.125472       2360
     0.00570   2.125472       2960
     0.00883   2.125472       3560
     0.01156   2.125472       4160
     0.01556   2.125472       5360
     0.01680   2.125472       5960
     0.01810   2.125472       6560
     0.01805   2.125472       7160
     0.01815   2.125472       7760
     0.01709   2.125472       8960
     0.01687   2.125472       9560
     0.01613   2.125472      10160
     0.01547   2.125472      10760
     0.01430   2.125472      11360
     0.01379   2.125472      11960
     0.01261   2.125472      12560
     0.01237   2.125472      13160
     0.01158   2.125472      13760
     0.01125   2.125472      14360
     0.01071   2.125472      14960
     0.00987   2.125472      16160
     0.00943   2.125472      16760
     0.00972   2.125472      17360
     0.00918   2.125472      17960
     0.00931   2.125472      18560
     0.00898   2.125472      19760
     0.00922   2.125472      20360
     0.00915   2.125472      20960
     0.00895   2.125472      21560
     0.00904   2.125472      22160
     0.00893   2.125472      23360
     0.00906   2.125472      23960
     0.00899   2.125472      24560
     0.00898   2.125472      25160
     0.00894   2.125472      25760
     0.00891   2.125472      26960
     0.00862   2.125472      27560
     0.00877   2.125472      28160
     0.00857   2.125472      28760
     0.00863   2.125472      29360
     0.00840   2.125472      30560
     0.00826   2.125472      31160
     0.00816   2.125472      31760
     0.00810   2.125472      32360
     0.00782   2.125472      32960
     0.00753   2.125472      34160
     0.00747   2.125472      34760
```

P1T2.DAT

```
****************************************************************************
*
*         ONE-DIMENSIONAL CONVECTION-DISPERSION EQ. SOLUTION
*         NON-LINEAR LEAST-SQUARES ANALYSIS
*
*         DETERMINISTIC TWO-SITE/TWO-REGION NONEQUILIBRIUM MODEL FOR
*         PULSE-TYPE INJECTION WITH NO PRODUCTION OR DECAY
*         SOLUTION FOR FLUX CONCENTRATIONS
*         REDUCED CONCENTRATION DATA
*
*
*
*
****************************************************************************
```

INITIAL VALUES OF COEFFICIENTS
=================================
```
   NAME              INITIAL VALUE
V.........           .0000
D.........           .0000
R.........          1.0000
PULSE.....        600.0000
BETA......           .5000
OMEGA.....          1.0000
CI........           .0000
CO........          1.0000
```

ITERATION	SSQ	V.....	D.....	PULSE.	BETA..
0	.013336	.00004	.00000	600.00000	.50000
1	.005322	.00004	.00000	293.28544	.50177
2	.004744	.00004	.00000	289.89074	.50101
3	.004631	.00004	.00000	295.79385	.48916
4	.004312	.00005	.00000	288.33813	.54604
5	.004094	.00005	.00000	312.91577	.50454
6	.003467	.00005	.00001	343.72848	.58412
7	.003190	.00008	.00000	280.73788	.58266
8	.001680	.00008	.00001	353.90121	.26828
9	.000763	.00008	.00001	382.09726	.16761
10	.000290	.00009	.00002	445.70891	.24308
11	.000131	.00008	.00003	475.28672	.38108
12	.000097	.00008	.00003	485.64582	.38928
13	.000091	.00008	.00003	483.16110	.39118
14	.000089	.00008	.00002	482.38381	.37195
15	.000089	.00008	.00002	481.67156	.36697
16	.000089	.00008	.00002	481.77099	.36700
17	.000089	.00008	.00002	482.02324	.36652
18	.000089	.00008	.00002	482.10184	.36648
19	.000089	.00008	.00002	482.40414	.36659
20	.000089	.00008	.00002	482.40456	.36659

CORRELATION MATRIX
====================
```
         1           2           3           4           5
```

P1T2.OUT

```
    1   1.0000
    2   -.3000      1.0000
    3   -.6988       .1829      1.0000
    4    .0152       .5671     -.1458      1.0000
    5    .2963      -.1035     -.0390     -.4764      1.0000
```

RSQUARE FOR REGRESSION = .96982559

NON-LINEAR LEAST SQUARES ANALYSIS, FINAL RESULTS
===

					95% CONFIDENCE LIM	
VARIABLE	NAME	VALUE	S.E.COEFF.	T-VALUE	LOWER	UP
1	V.....	.789205E-04	.183977E-05	42.90	.752747E-04	.825
2	D.....	.225073E-04	.853665E-06	26.37	.208156E-04	.241
3	PULSE.	.482405E+03	.772048E+01	62.48	.467105E+03	.497
4	BETA..	.366589E+00	.724830E-02	50.58	.352225E+00	.380
5	OMEGA.	.209664E+01	.725300E-01	28.91	.195291E+01	.224

```
-----------------------ORDERED BY COMPUTER INPUT----------------------
                                      CONCENTRATION           RESI-
NO    DISTANCE         TIME          OBS        FITTED         DUAL
 1   2.1254720    560.0000000    .0001000     .0000000      .0001000
 2   2.1254720    **********     .0000200     .0000005      .0000195
 3   2.1254720    **********     .0005000     .0000967      .0004033
 4   2.1254720    **********     .0033100     .0011390      .0021710
 5   2.1254720    **********     .0057000     .0040906      .0016094
 6   2.1254720    **********     .0088300     .0082731      .0005569
 7   2.1254720    **********     .0115600     .0123021     -.0007421
 8   2.1254720    **********     .0155600     .0167860     -.0012260
 9   2.1254720    **********     .0168000     .0177292     -.0009292
10   2.1254720    **********     .0181000     .0179616      .0001384
11   2.1254720    **********     .0180500     .0177398      .0003102
12   2.1254720    **********     .0181500     .0172635      .0008865
13   2.1254720    **********     .0170900     .0160460      .0010440
14   2.1254720    **********     .0168700     .0154406      .0014294
15   2.1254720    **********     .0161300     .0148786      .0012514
16   2.1254720    **********     .0154700     .0143694      .0011006
17   2.1254720    **********     .0143000     .0139137      .0003863
18   2.1254720    **********     .0137900     .0135073      .0002827
19   2.1254720    **********     .0126100     .0131442     -.0005342
20   2.1254720    **********     .0123700     .0128176     -.0004476
21   2.1254720    **********     .0115800     .0125213     -.0009413
22   2.1254720    **********     .0112500     .0122493     -.0009993
23   2.1254720    **********     .0107100     .0119968     -.0012868
24   2.1254720    **********     .0098700     .0115348     -.0016648
25   2.1254720    **********     .0094300     .0113192     -.0018892
26   2.1254720    **********     .0097200     .0111110     -.0013910
27   2.1254720    **********     .0091800     .0109084     -.0017284
28   2.1254720    **********     .0093100     .0107102     -.0014002
29   2.1254720    **********     .0089800     .0103235     -.0013435
30   2.1254720    **********     .0092200     .0101338     -.0009138
31   2.1254720    **********     .0091500     .0099460     -.0007960
32   2.1254720    **********     .0089500     .0095959     -.0006459
33   2.1254720    **********     .0090400     .0095991     -.0005591
34   2.1254720    **********     .0089300     .0092263     -.0002963
35   2.1254720    **********     .0090600     .0090430      .0000170
```

<div align="center">P1T2.OUT</div>

```
 1
     4            1            1           40          419            0            0


     V.....    D.....      R.....    PULSE.     BETA..     OMEGA.
0.000011  0.0000002       1.0      600.0        0.5        1.0
     1   1            1            0           1           1           1
         0.0       0.0        0.0        0.0        0.0        0.0
         0.0       0.0        0.0        0.0        0.0        0.0
   0.00000      1.0         1
   0.00142  2.208022      207
   0.00149  2.208022      807
   0.00140  2.208022     1407
   0.00150  2.208022     2007
   0.00141  2.208022     2607
   0.00143  2.208022     3207
   0.00145  2.208022     3807
   0.00155  2.208022     4407
   0.00150  2.208022     5007
   0.00143  2.208022     5607
   0.00141  2.208022     6207
   0.00138  2.208022     6807
   0.00153  2.208022     7407
   0.00143  2.208022     8007
   0.00158  2.208022     8607
   0.00158  2.208022     9207
   0.00161  2.208022     9807
   0.00163  2.208022    10407
   0.00171  2.208022    11007
   0.00176  2.208022    11607
   0.00184  2.208022    12207
   0.00198  2.208022    12807
   0.00197  2.208022    13407
   0.00228  2.208022    14007
   0.00247  2.208022    14607
   0.00262  2.208022    15207
   0.00256  2.208022    15807
   0.00268  2.208022    16407
   0.00286  2.208022    17007
   0.00346  2.208022    17607
   0.00365  2.208022    18207
   0.00370  2.208022    18807
   0.00407  2.208022    19407
   0.00427  2.208022    20007
   0.00443  2.208022    20607
   0.00459  2.208022    21207
   0.00472  2.208022    21807
   0.00485  2.208022    22407
   0.00487  2.208022    23007
   0.00463  2.208022    23607
   0.00502  2.208022    24207
   0.00523  2.208022    24807
   0.00533  2.208022    25407
   0.00498  2.208022    26007
   0.00573  2.208022    26607
   0.00575  2.208022    27207
   0.00579  2.208022    27807
   0.00566  2.208022    28407
   0.00573  2.208022    29007
   0.00544  2.208022    29607
```

P2T1.DAT

```
**********************************************************************
*
*          ONE-DIMENSIONAL CONVECTION-DISPERSION EQ. SOLUTION
*          NON-LINEAR LEAST-SQUARES ANALYSIS
*
*          DETERMINISTIC TWO-SITE/TWO-REGION NONEQUILIBRIUM MODEL FOR
*          PULSE-TYPE INJECTION WITH NO PRODUCTION OR DECAY
*          SOLUTION FOR FLUX CONCENTRATIONS
*          REDUCED CONCENTRATION DATA
*
*
*
*
**********************************************************************
```

INITIAL VALUES OF COEFFICIENTS
================================

NAME	INITIAL VALUE
V.........	.0000
D.........	.0000
R.........	1.0000
PULSE.....	600.0000
BETA......	.1000
OMEGA.....	1.0000
CI........	.0000
CO........	1.0000

ITERATION	SSQ	V.....	D.....	PULSE.	BETA..
0	.010438	.00001	.00000	600.00000	.10000
1	.002111	.00001	.00000	1206.72716	.09955
2	.001546	.00002	.00000	608.84479	.15760
3	.000185	.00003	.00000	710.91825	.25128
4	.000126	.00003	.00000	747.57503	.25280
5	.000112	.00003	.00000	761.14426	.26530
6	.000106	.00003	.00000	765.01742	.27584
7	.000104	.00003	.00000	765.73953	.28105
8	.000102	.00003	.00000	766.50339	.28527
9	.000101	.00003	.00000	767.80339	.29238
10	.000099	.00003	.00000	768.95284	.31073
11	.000092	.00002	.00001	780.82109	.42144
12	.000090	.00002	.00001	783.00821	.42242
13	.000090	.00002	.00001	785.49633	.42223
14	.000090	.00002	.00001	785.47537	.42227
15	.000090	.00002	.00001	785.50514	.42235
16	.000090	.00002	.00001	785.50894	.42235

CORRELATION MATRIX
==================

	1	2	3	4	5
1	1.0000				
2	-.4058	1.0000			
3	-.6534	.3990	1.0000		
4	-.0547	.2099	.0687	1.0000	

P2T1.OUT

```
  5    -.0037      .0243       -.0161      -.4293      1.0000
```

RSQUARE FOR REGRESSION = .96012642

NON-LINEAR LEAST SQUARES ANALYSIS, FINAL RESULTS
==

```
                                                        95% CONFIDENCE LIM
VARIABLE    NAME      VALUE        S.E.COEFF.   T-VALUE     LOWER        UP
    1       V.....   .242338E-04   .203687E-06   118.98   .238334E-04   .246
    2       D.....   .869556E-05   .166600E-06    52.19   .836806E-05   .902
    3       PULSE.   .785509E+03   .630894E+01   124.51   .773107E+03   .797
    4       BETA..   .422354E+00   .138032E-02   305.98   .419641E+00   .425
    5       OMEGA.   .538018E+01   .225323E-01   238.78   .533589E+01   .542
```


```
-------------------------ORDERED BY COMPUTER INPUT-----------------------
                                       CONCENTRATION            RESI-
NO    DISTANCE        TIME         OBS         FITTED           DUAL
 1    2.2080220   207.0000000   .0014200     .0000000       .0014200
 2    2.2080220   807.0000000   .0014900     .0000000       .0014900
 3    2.2080220   **********    .0014000     .0000000       .0014000
 4    2.2080220   **********    .0015000     .0000000       .0015000
 5    2.2080220   **********    .0014100     .0000000       .0014100
 6    2.2080220   **********    .0014300     .0000000       .0014300
 7    2.2080220   **********    .0014500     .0000003       .0014497
 8    2.2080220   **********    .0015500     .0000020       .0015480
 9    2.2080220   **********    .0015000     .0000093       .0014907
10    2.2080220   **********    .0014300     .0000293       .0014007
11    2.2080220   **********    .0014100     .0000711       .0013389
12    2.2080220   **********    .0013800     .0001433       .0012367
13    2.2080220   **********    .0015300     .0002507       .0012793
14    2.2080220   **********    .0014300     .0003943       .0010357
15    2.2080220   **********    .0015800     .0005712       .0010088
16    2.2080220   **********    .0015800     .0007755       .0008045
17    2.2080220   **********    .0016100     .0010003       .0006097
18    2.2080220   **********    .0016300     .0012383       .0003917
19    2.2080220   **********    .0017100     .0014828       .0002272
20    2.2080220   **********    .0017600     .0014842       .0002758
21    2.2080220   **********    .0018400     .0019157      -.0000757
22    2.2080220   **********    .0019800     .0021519      -.0001719
23    2.2080220   **********    .0019700     .0023806      -.0004106
24    2.2080220   **********    .0022800     .0026002      -.0003202
25    2.2080220   **********    .0024700     .0028100      -.0003400
26    2.2080220   **********    .0026200     .0030096      -.0003896
27    2.2080220   **********    .0025600     .0031990      -.0006390
28    2.2080220   **********    .0026800     .0033786      -.0006986
29    2.2080220   **********    .0028600     .0035488      -.0006888
30    2.2080220   **********    .0034600     .0037103      -.0002503
31    2.2080220   **********    .0036500     .0038636      -.0002136
32    2.2080220   **********    .0037000     .0040093      -.0003093
33    2.2080220   **********    .0040700     .0041481      -.0000781
34    2.2080220   **********    .0042700     .0042805      -.0000105
35    2.2080220   **********    .0044300     .0044069       .0000231
36    2.2080220   **********    .0045900     .0045280       .0000620
37    2.2080220   **********    .0047200     .0046440       .0000760
38    2.2080220   **********    .0048500     .0047553       .0000947
39    2.2080220   **********    .0048700     .0048623       .0000077
```

<div align="center">P2T1.OUT</div>

```
1
        4           1           1          40         169          0           0


      V.....      D.....      R.....    PULSE.      BETA..      OMEGA.
    0.000041  0.0000002        1.0      600.0         0.2         1.0
       1    1           1           0           1           1           1
            0.0         0.0         0.0         0.0         0.0         0.0
            0.0         0.0         0.0         0.0         0.0         0.0
       0.00000         1.0           1
       0.00002    2.208022         585
       0.00002    2.208022        1185
       0.00001    2.208022        1785
       0.00001    2.208022        2385
       0.00001    2.208022        2985
       0.00005    2.208022        3628
       0.00028    2.208022        4223
       0.00084    2.208022        4828
       0.00192    2.208022        5423
       0.00373    2.208022        6028
       0.00559    2.208022        6623
       0.00746    2.208022        7228
       0.00841    2.208022        7828
       0.00967    2.208022        8428
       0.01091    2.208022        9028
       0.01164    2.208022        9628
       0.01288    2.208022       10228
       0.01252    2.208022       10828
       0.01291    2.208022       11428
       0.01314    2.208022       12028
       0.01314    2.208022       12628
       0.01321    2.208022       13228
       0.01324    2.208022       13828
       0.01325    2.208022       14428
       0.01310    2.208022       15028
       0.01312    2.208022       15628
       0.01301    2.208022       16228
       0.01291    2.208022       16828
       0.01280    2.208022       17428
       0.01274    2.208022       18028
       0.01260    2.208022       18628
       0.01254    2.208022       19228
       0.01252    2.208022       19828
       0.01245    2.208022       20428
       0.01244    2.208022       21028
       0.01237    2.208022       21628
       0.01239    2.208022       22228
       0.01237    2.208022       22828
       0.01235    2.208022       23428
       0.01241    2.208022       24028
       0.01230    2.208022       24628
       0.01253    2.208022       25228
       0.01243    2.208022       25828
       0.01236    2.208022       26428
       0.01235    2.208022       27028
       0.01229    2.208022       27628
       0.01218    2.208022       28228
       0.01220    2.208022       28828
       0.01203    2.208022       29428
       0.01189    2.208022       30028
```

P2T2.DAT

```
*******************************************************************************
*
*          ONE-DIMENSIONAL CONVECTION-DISPERSION EQ. SOLUTION
*          NON-LINEAR LEAST-SQUARES ANALYSIS
*
*          DETERMINISTIC TWO-SITE/TWO-REGION NONEQUILIBRIUM MODEL FOR
*          PULSE-TYPE INJECTION WITH NO PRODUCTION OR DECAY
*          SOLUTION FOR FLUX CONCENTRATIONS
*          REDUCED CONCENTRATION DATA
*
*
*
*
*******************************************************************************
```

INITIAL VALUES OF COEFFICIENTS
================================

NAME	INITIAL VALUE
V.........	.0000
D.........	.0000
R........	1.0000
PULSE.....	600.0000
BETA......	.2000
OMEGA.....	1.0000
CI........	.0000
CO........	1.0000

ITERATION	SSQ	V.....	D.....	PULSE.	BETA..
0	.026669	.00004	.00000	600.00000	.20000
1	.005193	.00004	.00000	611.43288	.20693
2	.003217	.00006	.00000	463.93940	.28279
3	.001312	.00006	.00000	501.84238	.28822
4	.001243	.00007	.00000	468.90994	.31644
5	.000857	.00007	.00000	471.66703	.32093
6	.000718	.00007	.00000	452.31334	.33773
7	.000654	.00007	.00000	446.10763	.35138
8	.000566	.00008	.00000	437.64124	.35354
9	.000394	.00007	.00000	457.62289	.34312
10	.000229	.00007	.00000	471.23445	.33708
11	.000120	.00008	.00000	478.97927	.34150
12	.000075	.00008	.00000	484.90532	.34047
13	.000070	.00008	.00000	485.42215	.31719
14	.000070	.00008	.00000	485.81023	.31668
15	.000070	.00008	.00000	485.62706	.31399
16	.000070	.00008	.00000	485.63529	.31398

CORRELATION MATRIX
===================

	1	2	3	4	5
1	1.0000				
2	-.1231	1.0000			
3	-.5165	.2162	1.0000		
4	-.1087	.9118	.1247	1.0000	

P2T2.OUT

```
    5      .3396      -.2358      -.1753      -.4954      1.0000
```

RSQUARE FOR REGRESSION = .98438985

NON-LINEAR LEAST SQUARES ANALYSIS, FINAL RESULTS
==

VARIABLE	NAME	VALUE	S.E.COEFF.	T-VALUE	95% CONFIDENCE LIM	
					LOWER	UP
1	V.....	.773786E-04	.579930E-06	133.43	.762335E-04	.785
2	D.....	.464459E-05	.913687E-06	5.08	.284042E-05	.644
3	PULSE.	.485635E+03	.433956E+01	111.91	.477066E+03	.494
4	BETA..	.313978E+00	.138911E-01	22.60	.286549E+00	.341
5	OMEGA.	.361284E+01	.821851E-01	43.96	.345055E+01	.377


```
----------------------ORDERED BY COMPUTER INPUT----------------------
                                  CONCENTRATION            RESI-
NO   DISTANCE        TIME        OBS        FITTED         DUAL
 1   2.2080220    585.0000000   .0000200    .0000000      .0000200
 2   2.2080220    **********    .0000200    .0000000      .0000200
 3   2.2080220    **********    .0000100    .0000000      .0000100
 4   2.2080220    **********    .0000100    .0000000      .0000100
 5   2.2080220    **********    .0000100    .0000002      .0000098
 6   2.2080220    **********    .0000500    .0000100      .0000400
 7   2.2080220    **********    .0002800    .0001168      .0001632
 8   2.2080220    **********    .0008400    .0005962      .0002438
 9   2.2080220    **********    .0019200    .0017634      .0001566
10   2.2080220    **********    .0037300    .0036001      .0001299
11   2.2080220    **********    .0055900    .0052015      .0003885
12   2.2080220    **********    .0074600    .0074785     -.0000185
13   2.2080220    **********    .0084100    .0089561     -.0005461
14   2.2080220    **********    .0096700    .0099530     -.0002830
15   2.2080220    **********    .0109100    .0105850      .0003250
16   2.2080220    **********    .0116400    .0110013      .0006387
17   2.2080220    **********    .0128800    .0113182      .0015618
18   2.2080220    **********    .0125200    .0116030      .0009170
19   2.2080220    **********    .0129100    .0118836      .0010264
20   2.2080220    **********    .0131400    .0121651      .0009749
21   2.2080220    **********    .0131400    .0124418      .0006982
22   2.2080220    **********    .0132100    .0127056      .0005044
23   2.2080220    **********    .0132400    .0129740      .0002660
24   2.2080220    **********    .0132500    .0131828      .0000672
25   2.2080220    **********    .0131000    .0133807     -.0002807
26   2.2080220    **********    .0131200    .0135196     -.0003996
27   2.2080220    **********    .0130100    .0136506     -.0006406
28   2.2080220    **********    .0129100    .0137520     -.0008420
29   2.2080220    **********    .0128000    .0138246     -.0010246
30   2.2080220    **********    .0127400    .0138696     -.0011296
31   2.2080220    **********    .0126000    .0138882     -.0012882
32   2.2080220    **********    .0125400    .0138818     -.0013418
33   2.2080220    **********    .0125200    .0138517     -.0013317
34   2.2080220    **********    .0124500    .0137992     -.0013492
35   2.2080220    **********    .0124400    .0137259     -.0012859
36   2.2080220    **********    .0123700    .0136330     -.0012630
37   2.2080220    **********    .0123900    .0135218     -.0011318
38   2.2080220    **********    .0123700    .0133939     -.0010239
39   2.2080220    **********    .0123500    .0132503     -.0009003
```
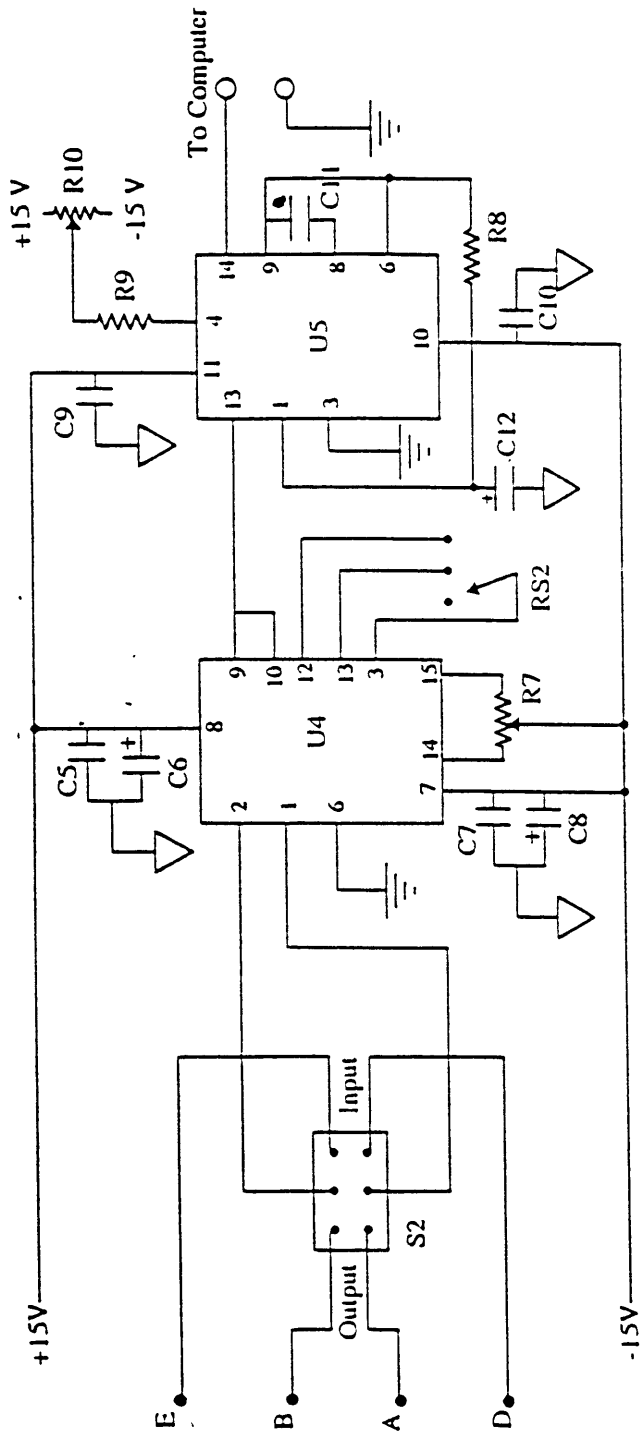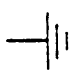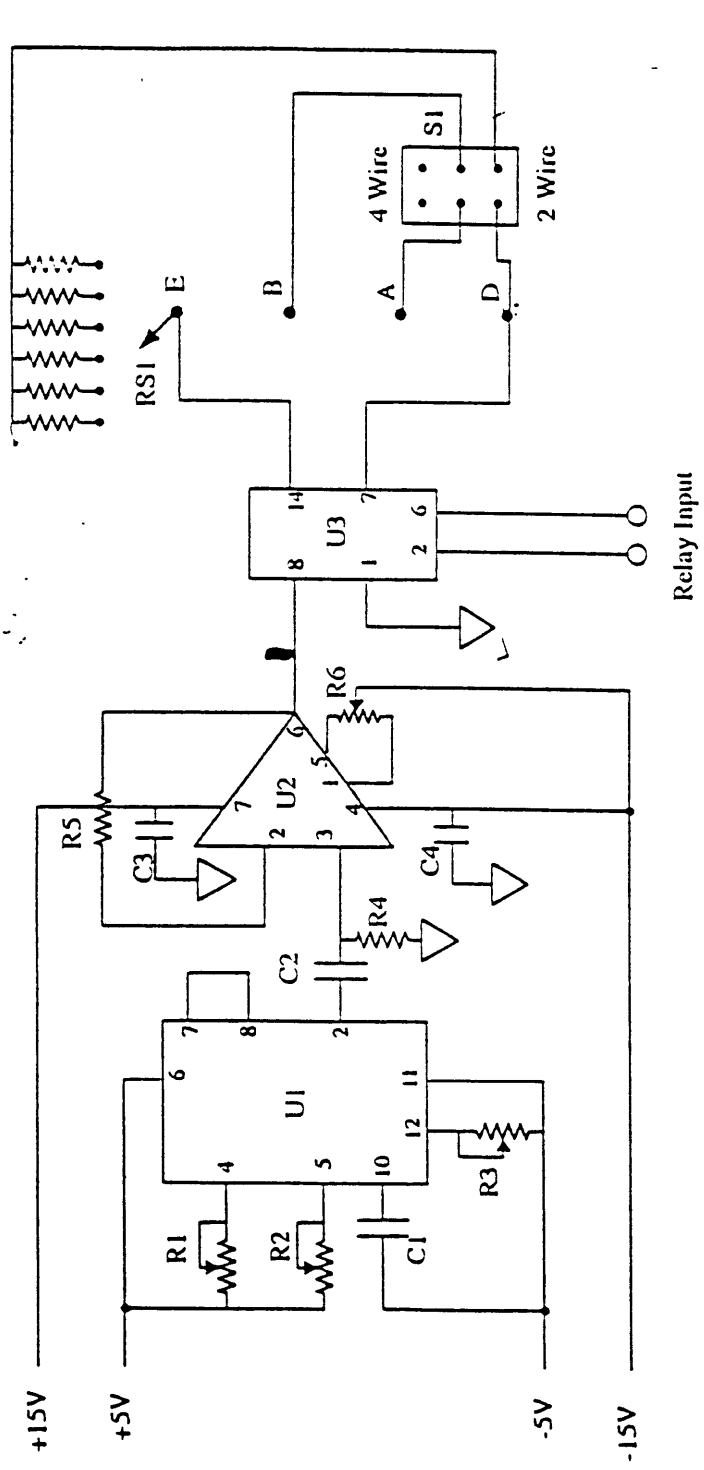
P2T2.OUT

APPENDIX F: CIRCUIT DIAGRAM AND PARTS LIST FOR
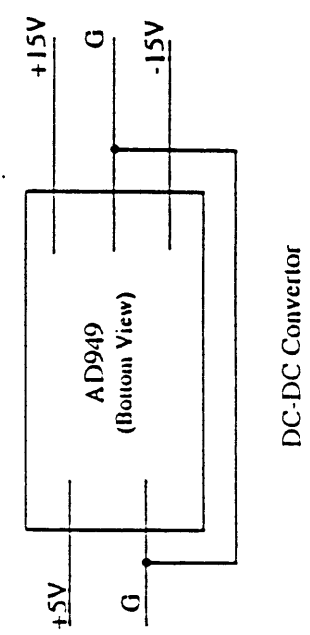MIT SINGLE CHANNEL ELECTRICAL CONDUCTIVITY
METER

Measurement Circuit

Note: Ground points indicated by ⏚ symbol should be directly connected to the system Star ground point.

218

Signal Generator Circuit

DC-DC Convertor

219

Symbol	Description	Comments
U1	ICL8038 Signal Generator	Made by Intersil Corporation.
U2	LF351 Op Amp	AD797 from Analog is a better choice. It is pin compatible if R6 is changed to 20 kΩ.
U3	W171DIP-21 Reed Relay	Double pole, Single throw. Made by Magnecraft.
U4	AD 524 Instrumen-tation Amplifier	Made by Analog Devices.
U5	AD 637 RMS-to-DC Convertor	Made by Analog Devices.
R1	10 kΩ Variable Resistor	Sets frequency of sine wave.
R2	10 kΩ Variable Resistor	Sets frequency of sine wave.
R3	81 kΩ Variable Resistor	
R4	1 MΩ Fixed Resistor	AC coupling resistor.
R5	1 kΩ Fixed Resistor	Feedback resistor for U2.
R6	10 kΩ Variable Resistor	Output offset trim for U2.
R7	10 kΩ Variable Resistor	Output offset trim for U4.
R8	22 kΩ Fixed Resistor	Low pass post filter resistor.
R9	500 kΩ Fixed Resistor	Offset trim network for U5.

R10	10 kΩ Variable Resistor	Offset trim network for U5.
C1	0.1 μF Ceramic Capacitor	Sets frequency of sine wave, f = 0.33/(RC1) where R = R1 = R2.
C2	0.1 μF Ceramic Capacitor	AC coupling capacitor. Sets cutoff frequency of high pass filter, f = 1/(2πRC2) where R = R4.
C3	0.1 μF Ceramic Capacitor	Decoupling Capacitor for U2.
C4	0.1 μF Ceramic Capacitor	Decoupling Capacitor for U2.
C5	0.1 μF Ceramic Capacitor	Decoupling Capacitor for U4.
C6	10 μF Tantlum Capacitor	Decoupling Capacitor for U4.
C7	0.1 μF Ceramic Capacitor	Decoupling Capacitor for U4.
C8	10 μF Tantlum Capacitor	Decoupling Capacitor for U4.
C9	0.1 μF Ceramic Capacitor	Decoupling Capacitor for U5.
C10	0.1 μF Ceramic Capacitor	Decoupling Capacitor for U5.
C11	0.1 μF Ceramic Capacitor	Integrating Capacitor for U5.
C12	4.7 μF Tantlum Capacitor	Low pass post filter capacitor.
RS1	6 Position Rotary Switch	Sets shunt resistor in two wire mode.

RS2	3 Position Rotary Switch	Sets gain of U4.
S1	Double pole, Single throw switch	Switches between 4 wire and 2 wire modes.
S2	Double pole, Double throw switch	Switches between input and output measurements.
	AD 949	60 mA, DC-DC stepup convertor